**University of Southampton**
Faculty of Medicine, Health & Life Sciences
School of Biological Sciences

# Characterising the *Drosophila* Extracellular Superoxide Dismutase Gene

**Michael James Blackney**

Submitted for the degree of Doctor of Philosophy

September 2010

UNIVERSITY OF SOUTHAMPTON
SCHOOL OF BIOLOGICAL SCIENCES

# ABSTRACT

Doctor of Philosophy

CHARACTERSING THE *DROSOPHILA* EXTRACELLULAR SUPEROXIDE DISMUTASE GENE

By Michael James Blackney

The indiscriminate action of reactive oxygen species (ROS), if left unregulated, has long been considered contributory to a range of disease processes within the animal kingdom and is also a factor associated with ageing. Consequently modifying the molecular mechanisms that regulate ROS levels may prove therapeutic and could also positively affect longevity. One of the key components of this machinery is the superoxide dismutase (SOD) family of enzymes which regulate ROS levels by scavenging the ROS superoxide. Mammals have three distinct SOD enzymes each responsible for managing superoxide levels in different cellular compartments. In *Drosophila* homologues of two of the mammalian SODs, the intracellular (SOD1) and mitochondrial (SOD2) SODs, have been identified and studied extensively demonstrating a clear link between SOD and oxidative protection and survival. Recently the sequence of a third *sod* gene, homologous to both the relatively poorly characterised mammalian (*sod3*) and *C. elegans* (*sod-4*) extracellular *sod*, was identified in *Drosophila* and is also predicted to locate extracellularly (*sod3*). To date, no (published) work has been carried out to assess the role of *sod3* within insects. This thesis reports the molecular and biochemical characteristics of *sod3* in *Drosophila*. Detailed within are the steps taken to clone the *sod3* gene which appears to be expressed as two gene products formed by alternative splicing. Furthermore, a combination of gene expression, proteomic and functional analysis of a number of *sod* mutants was used to: i) reveal sex specific *sod* gene expression; ii) validate a *sod3* hypomorph mutant; iii) indicate a functional role for *sod3* in protection against $H_2O_2$ induced oxidative stress; iv) suggest a SOD1-SOD3 co-dependency for maintaining Cu Zn SOD activity; v) demonstrate the appearance of genetic modifiers in the *sod3* hypomorph. The findings of this report and further studies on the *Drosophila sod3* gene should encourage the re-evaluation of the previous work concerning SOD's influence on disease states and lifespan regulation.

## TABLE OF CONTENTS

## DECLARATION

I, MICHAEL JAMES BLACKNEY

Declare that the thesis entitled CHARACTERISING THE *DROSOPHILA* EXTRACELLULAR SUPEROXIDE DISMUTASE GENE and the work presented in the thesis are my own, and have been generated by me as a result of my own original research. I confirm that:

- This work was done wholly or mainly while in candidature for a research degree at this University
- Where any part of the thesis has previously been submitted for a degree or any other qualification at this University or any other institution, this has been clearly stated
- Where I have consulted the published work of others, this is always clearly stated
- Where I have quoted from the work of others, the source is always given. With the exception of these quotations, this thesis is entirely my own work
- I have acknowledged all main sources of help
- Where the thesis is based on work done by myself jointly with others, I have made clear exactly what was done by others and what I have contributed myself

**Signed:**.....

**Date:**.....

## ACKNOWLEDGEMENTS

Firstly, my thanks go to the Gerald Kerkut Charitable Trust for kindly funding my project. I would also like to thanks John Phillips, John Tower, Bill Orr, Kiren Ubhi and Torsten Bossing for their generosity with fly lines. Thanks also to Nick Orsen for his technical assistance in maintaining my fly stocks.

I would also like to thank my supervisors Joel Parker and David Shepherd for their guidance, advice and expertise throughout my project. Huge thanks also go to Torsten Bossing for his invaluable advice with fly genetics and Neil Smyth for his guidance on the tissue culture work.

A big thank you also goes to Hazel Smith for her help, advice, understanding, support, cooking, lifts, distraction… while my stress levels rose. Finally, I would like to thank my parents, Corinne and Jonathan Blackney, who have supported me throughout my studies.

## ABBREVIATIONS

| | |
|---|---|
| 8-OH-G | 8-Hydroxyguanosine |
| Aβ | Amyloid beta |
| AD | Alzheimer's disease |
| ALS | Amyotrophic lateral sclerosis |
| Amp | Ampicillin |
| ANOVA | Analysis of variance |
| AP-1 | Activator protein 1 |
| APOE | Apolipoprotein E |
| APS | Ammonium persulfate |
| ATII | Angiotensin II |
| ATP | Adenosine triphosphate |
| BCS | Bathocuproine sulphonate |
| BDGDP | Berkley *Drosophila* Gene Disruption Project |
| BSA | Bovine serum albumin |
| CAT | Catalase |
| cDNA | Complimentary DNA |
| CGD | Chronic granulomatous disease |
| CIP | Calf intestinal alkaline phosphatase |
| DMEM | Dulbecco's modified eagle medium |
| DNA | Deoxyribonucleic acid |
| dNTP | Deoxynucleotide triphosphate |
| DTT | Dithiothreitol |
| ECL | Enhanced chemiluminescence |
| EDTA | Ethylenediaminetetraacetic acid |
| Eff | Efficiency |
| EGF | Epidermal growth factor |
| EGFP | Enhanced green fluorescent protein |
| EGFR | Epidermal growth factor receptor |
| EMS | Ethyl methanesulfonate |
| ER | Endoplasmic reticulum |
| Erk | Extracellular signal-related kinase |
| EST | Expressed sequence tag |
| ETC | Electron transport chain |
| FALS | Familial amyotrophic lateral sclerosis |
| FAM | 6-carboxyfluorescein |
| FAP | Familial adenomatous polyposis |
| FRET | Förster resonance energy transfer |
| GPX | Glutathione peroxidase |
| GSH | Glutathione |
| GSSG | Glutathione disulfide |
| GTP | Guanosine triphosphate |
| HEK293 | Human embryonic kidney 293 |
| HRE | $H_2O_2$-responsive element |
| HRP | Horse radish peroxidase |
| HSP | Heat shock protein |
| IL | Interleukin |
| IMS | Intermembrane space |
| INF-γ | Interferon gamma |

| | |
|---|---|
| IPTG | Isopropyl beta-D-1-thiogalactopyranoside |
| iTRAQ | Isobaric tag for relative and absolute quantitation |
| JNK | Jun N-terminal kinase |
| KCL | Potassium chloride |
| LB | Lysogeny broth |
| LBA | Lysogeny broth agar |
| MAPK | Mitogen-activated protein kinase |
| MDA | Malondialdehyde |
| miRNA | Micro RNA |
| M-MLV | Moloney murine leukaemia virus |
| MPO | Myeloperoxidase |
| mRNA | Messenger RNA |
| MS/MS | Tandem mass spectrometry |
| MSRA | Methionine sulfoxide reductase |
| mtDNA | Mitochondrial DNA |
| nano-LC | Nano-liquid chromatography |
| NBT | Nitro blue tetrazolium chloride |
| NFκB | Nuclear factor-kappa B |
| NFQ | Non-fluorescent quencher |
| NIH | National Institutes of Health |
| NOS | Nitric oxide synthase |
| NOX | NADPH oxidase |
| PAGE | Polyacrylamide gel electrophoresis |
| PBS | Phosphate buffered saline |
| PCR | Polymerase chain reaction |
| PD | Parkinson's disease |
| PDGF | Platelet derived growth factor |
| PDGFR | Platelet derived growth factor receptor |
| PI 3-K | Phosphoinositide 3-kinase |
| PKC | Protein kinase C |
| PLC | Phospholipase C |
| PP1 | Protein phosphatase 1 |
| PP2A | Protein phosphatase 2A |
| PTK | Protein tyrosine kinase |
| PTP | Protein tyrosine phosphatase |
| qPCR | Quantitative PCR |
| RLM-RACE | RNA liagse mediated-rapid amplification of cDNA ends |
| RNA | Ribonucleic acid |
| RNS | Reactive nitrogen species |
| ROS | Reactive oxygen species |
| rpm | Revolutions per minute |
| rRNA | Ribosomal ribonucleic acid |
| RT | Reverse transcriptase |
| RTK | Receptor tyrosine kinase |
| SCX | Strong cation exchange |
| SDS | Sodium dodecyl sulphate |
| SEM | Standard error of the mean |
| SOD | Superoxide dismutase |
| spec | Spectinomycin |
| TAE | Tris-acetate-EDTA |

| | |
|---|---|
| TAP | Tobacco acid pyrophosphatase |
| TE | Tris-EDTA |
| TEAB | Triethylammonium bicarbonate |
| TEMED | Tetramethylethylenediamine |
| TNFα | Tumour necrosis factor alpha |
| tPBS | Tween phosphate buffered saline |
| UAS | Upstream activation sequence |
| UTR | Untranslated region |
| VEGF | Vascular endothelial growth factor |
| *WT* | Wild type |
| XO | Xanthine oxidase |
| *Yw* | Yellow white |

# CHAPTER 1

# 1. Introduction

Organisms across all taxa routinely experience ‘stress’ of some variety. Dr Richard Carlson (1961–2006), an American author, psychotherapist and motivational speaker, wrote: “Stress is nothing more than a socially acceptable form of mental illness.” Although a witty one-liner, this statement highlights a key concept that defines ‘stress’, that is; rather than stress being something that happens to an individual (often termed the “stressor”), it is in fact the reaction or response to the thing that has happened.

Although the term ‘stress’ had a use within psychological terminology prior to the 1930’s, it is generally accepted that it was not until 1936 that renowned Austrian-born Canadian endocrinologist, Hans Selye (1907-1982), first described ‘stress’ as a biological occurrence (Selye 1936). Selye reported observing a conserved but non-specific condition in rats in response to a number of biological insults including, cold shock, muscle exertion and injection of sub-lethal doses of various drugs. He went on to term this non-specific damage the ‘General Adaptive Syndrome’ (GAS), with ‘stress’ being the manifestation of the GAS (Selye 1936;Viner 1999). The identification of ‘stress’ as a biological trait prompted much research into its link with disease states, with biological stresses of some variety being implicated in the pathology of numerous diseases including cardiovascular disease, cancer, ageing, neurodegenerative disorders, arthritis, diabetes, hypertension, anxiety, depression and AIDS.

Oxidative stress is a subtype of biological stress and refers to the cytotoxic effect of oxidation by reactive variants of oxygen, as will be discussed.

## 1.1 Oxidative Stress, Reactive Oxygen Species (ROS) and Reactive Nitrogen Species (RNS)

The ability of cells to produce energy through the reduction of molecular oxygen during aerobic respiration is fundamental to life. However a consequence of living in an oxygen rich environment is the production of intermediate reactive oxygen and nitrogen species (ROS and RNS, respectively). Although physiological levels of ROS/RNS are critical for maintaining cellular function, increased oxidant production can be destructive. Antioxidant systems are employed to regulate ROS/RNS levels, but when the equilibrium fails and the pro-oxidant capacity overwhelms the pro-antioxidant capability then free ROS/RNS can cause cellular macromolecular damage as well as disturbed redox signalling. A delicate balance must therefore be maintained between the oxidant and antioxidant systems in order to preserve cellular function, regulation and adaptation. Dysregulation of this ROS/RNS homeostasis has long been considered causative in the pathology of numerous human diseases and a factor associated with ageing. Oxidative stress (or nitrosative stress in reference to RNS) is the term used to describe the adverse consequences of the action of various ROS on an individual system.

### 1.1.1 Species of ROS/RNS and their sources

ROS encompass a range of radical (species with an unpaired electron in their outer electron shell) and non-radical molecules (Table 1.1), formed by the reduction of molecular oxygen. These molecules are usually highly unstable and, as their name suggests, will react rapidly with numerous cellular components as well as other ROS. Superoxide ($O_2^{-}\cdot$) is considered a primary ROS and is formed by the one electron reduction of oxygen ($O_2$) (eqn 1):

$$O_2 + e^- \rightarrow O_2^{-}\cdot \quad (1)$$

**Table 1.1. Examples of ROS and RNS.**

| Name | Formula | ROS/RNS | Species |
|---|---|---|---|
| Oxygen | $O_2$ | ROS | Non-radical |
| Superoxide anion | $O_2^{-}\cdot$ | ROS | Radical |
| Hydroxyl radical | $\cdot OH$ | ROS | Radical |
| Hydroxyl anion | $OH^-$ | ROS | Non-radical |
| Hydroperoxyl | $HO_2\cdot$ | ROS | Radical |
| Hydrogen peroxide | $H_2O_2$ | ROS | Non-radical |
| Hypochlorite anion | $ClO^-$ | ROS | Non-radical |
| Nitric oxide | $NO\cdot$ | RNS | Radical |
| Peroxynitrite anion | $ONOO^-$ | RNS | Non-radical |
| Nitrogen dioxide | $NO_2$ | RNS | Non-radical |

The majority of $O_2^{-}\cdot$ and other ROS are produced through metabolic processes. One of the most well studied sources of $O_2^{-}\cdot$ is as a by product of mitochondrial aerobic respiration where the reduction of $O_2$ can result in the formation of $H_2O$ and $O_2^{-}\cdot$ as electrons leak out of the electron transport chain (ETC) (Loschen et al. 1974;Nohl and Hegner 1978). For example, in the ETC there is a propensity for a single electron to directly reduce molecular $O_2$ to $O_2^{-}\cdot$ as coenzyme Q (ubiquinone) cycles between its fully oxidised (quinine) and fully reduced (quinol) states (Cadenas and Davies 2000) (Figure 1.1). It has been estimated that 1-2% of total daily $O_2$ consumed by the mitochondrial respiratory chain is converted to $O_2^{-}\cdot$ (Cadenas & Davies 2000), leading to suggestion that aerobic respiration may be a primary intracellular source of $O_2^{-}\cdot$. However the true rate of $O_2^{-}\cdot$ production is likely to be considerably less than this since most experiments measuring $O_2^{-}\cdot$ production are performed by exposing isolated mitochondria to room air, which is hyperoxic for the organelles (Halliwell and Gutteridge 2007). Furthermore, the *in vivo* mitochondrial $O_2^{-}\cdot$ leakage rate is minimised by a number of factors. Firstly, the actual intra-mitochondrial $O_2$ concentration is fairly low. Secondly, the electron transport carriers are complexed in such a way as to facilitate electron movement to the next component of the chain rather than allowing escape to react with $O_2$. Thirdly, the presence of uncoupling proteins within the inner mitochondrial membrane allows the passage of protons which lead to the collapse of the proton gradient, causing the energy derived from electron transfer to be released as heat rather than ATP. This proton leak is proposed to minimise $O_2^{-}\cdot$ production by preventing a 'back up' of electrons escaping to react with $O_2$ (Halliwell & Gutteridge 2007). The anionic nature of $O_2^{-}\cdot$ at neutral pH also

means that this radical is ineffective at permeating biological membranes (Gus'kova et al. 1984;Takahashi and Asada 1983). Thus, since the ETC is located on the inner mitochondrial membrane it is likely that the majority of $O_2^{-}\cdot$ produced by this means is retained within the mitochondrial matrix rather than being released into the cytosol or extracellularly.

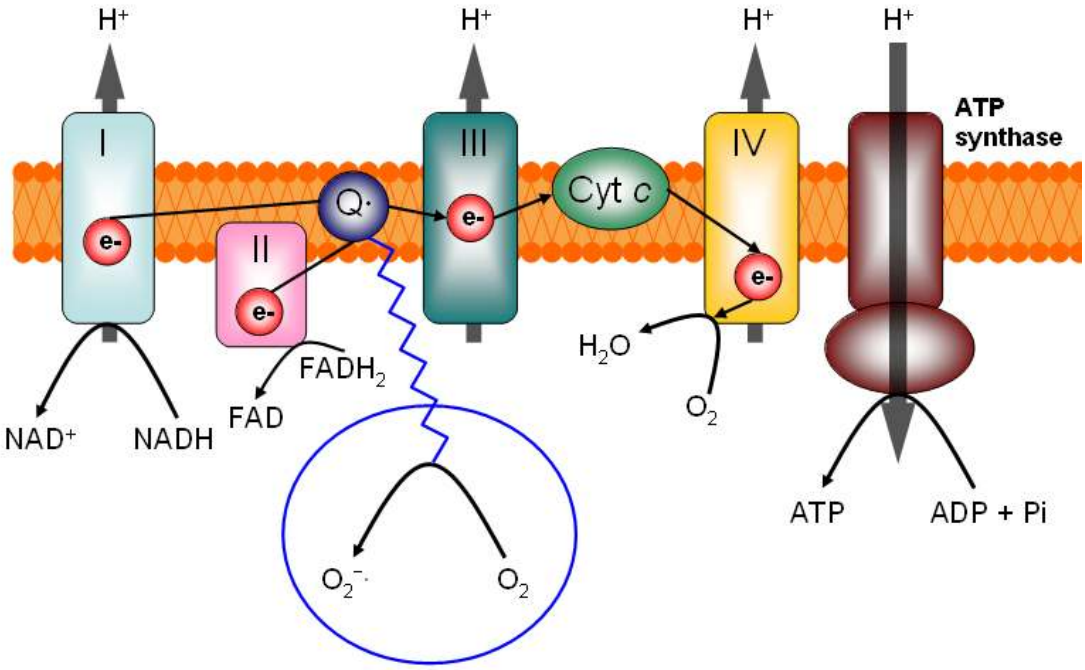


**Figure 1.1. Production of $O_2^{-}\cdot$ by the mitochondrial electron transport chain.** Complex I (NADH:ubiquinone oxidoreductase), catalyses the transfer of electrons from NADH, derived from cytosolic glucose oxidation or the mitochondrial citric acid cycle, to ubiquinone (Q). Ubiquinone is also reduced by electrons donated by $FADH_2$-containing dehydrogenases such as complex II (succinate:ubiquinone oxidoreductase). Complex III (ubiquinol:cytochrome *c* oxidoreductase) catalyses the reduction of cytochrome *c* by accepting electrons from the ubisemiquinone (Q·) radical-generating Q cycle. Complex IV finally catalyses the oxidation of cytochrome *c* by $O_2$. Electrons that are transferred through complexes I, III and IV are coupled to translocation of protons, with the resulting gradient able to drive ATP synthesis through the ATP synthase. Figure is adapted from (Brownlee 2001).

There are, however, a number of endogenous enzymes that use molecular $O_2$ as a substrate which generate $O_2^{-}\cdot$ in the cytosol and/or extracellular matrix. NADPH (nicotinamide adenine dinucleotide phosphate) oxidase (NOX) is an enzyme primarily present in the membrane of the phagocytotic vacuole of immune cells and generates $O_2^{-}\cdot$ in the cytosol and extracellularly through the removal of electrons from NADPH (Lambeth 2004) (eqn 2):

$$2O_2 + NADPH \rightarrow 2O_2^{-}\cdot + NADP^{+} + H^{+} \quad (2)$$

Although important for immune cell function (as will be discussed) components of NOX have also been found in non-phagocytic cell types, such as fibroblasts (Meier et al. 1991), endothelial cells (Jones et al. 1996) and neurons (Tammariello et al. 2000). Xanthine oxidase (XO), part of the xanthine oxidoreductase complex, is another endogenous enzyme which produces $O_2^{-}\cdot$ using $O_2$ as its oxidising substrate. Important for purine catabolism and innate immunity (Vorbach et al. 2003), XO catalyses the oxidative hydroxylation of hypoxanthine to xanthine and subsequently xanthine to uric acid with by products of $O_2^{-}\cdot$ and also $H_2O_2$. Interestingly, whilst $O_2^{-}\cdot$ and $H_2O_2$ are effective oxidant species, uric acid is a known potent antioxidant (Ames et al. 1981), thus XO appears to have both pro- and antioxidant properties. As well as a product of enzymatic function, $O_2^{-}\cdot$ and/or $H_2O_2$ are also produced by intracellular organelles such as the endoplasmic reticulum and the peroxisomes of the liver and kidney (Hool 2006). $O_2^{-}\cdot$ can either directly or through enzyme- or metal-catalysed reactions, interact with other molecules to generate 'secondary' ROS. For instance the antioxidant enzyme superoxide dismutase (SOD) will metabolise $O_2^{-}\cdot$ to $O_2$ and $H_2O_2$, as will be discussed later. A further example is in the generation of $OH^{-}$ and the highly reactive $\cdot OH$. Under stressful conditions an excess of $O_2^{-}\cdot$ can lead to iron ($Fe^{2+}$) release by oxidising [4Fe-4S] cluster-containing enzymes (Liochev and Fridovich 1994). This free $Fe^{2+}$ can react with $H_2O_2$ in the Fenton Reaction to generate these ROS (eqn 3).

$$\begin{aligned} Fe^{3+} + O_2^{-}\cdot &\rightarrow \underline{Fe^{2+}} + O_2 \\ \underline{Fe^{2+}} + H_2O_2 &\rightarrow Fe^{3+} + OH^{-} + \cdot OH \end{aligned} \quad (3)$$

The major RNS is the $NO\cdot$ radical which is a highly abundant oxidant species involved in diverse signalling processes. It is generated by the action of specific $Ca^{2+}$-calmodulin dependent nitric oxide synthases (NOSs) which metabolise L-arginine to citrulline (Ghafourifar and Cadenas 2005). As previously stated, cells of the immune system, as well as generating $O_2^{-}\cdot$, also contain the inducible form NOS (iNOS) and thus also produce $NO\cdot$ (Hevel et al. 1991;Tumurkhuu et al. 2009). These two ROS can subsequently readily react together to form the highly reactive $ONOO^{-}$ anion (eqn 4).

$$2NO\cdot + 2O_2^{-}\cdot \rightarrow 2ONOO^{-} \qquad (4)$$

Additionally, mitochondria contain another member of the NOS family (mtNOS) and are therefore also a site of NO· production (Bates et al. 1995;Elfering et al. 2002). Thus depending on the formation rates of $O_2^{-}\cdot$ and NO· mitochondria can also be a site of $ONOO^{-}$ synthesis (Packer et al. 1996). Under normal physiological conditions the $O_2^{-}\cdot$ scavenging enzyme SOD and NO· essentially compete for available $O_2^{-}\cdot$, however in situations where SOD activity is low (for example in tumour cells (Puscas et al. 1999)) or when high concentrations of NO· are generated (for example in ischemia/reperfusion injury (Lui et al. 1999;Zweier et al. 1995)), NO· out-competes SOD and generates $ONOO^{-}$. Since both $H_2O_2$ and $ONOO^{-}$ can easily cross biological membranes, it is believed that some of the reactions of these two ROS will promote $O_2^{-}\cdot$ generation outside of the mitochondria (Schoneich 1999). The common pathways by which ROS and RNS are produced are summarised in Figure 1.2.

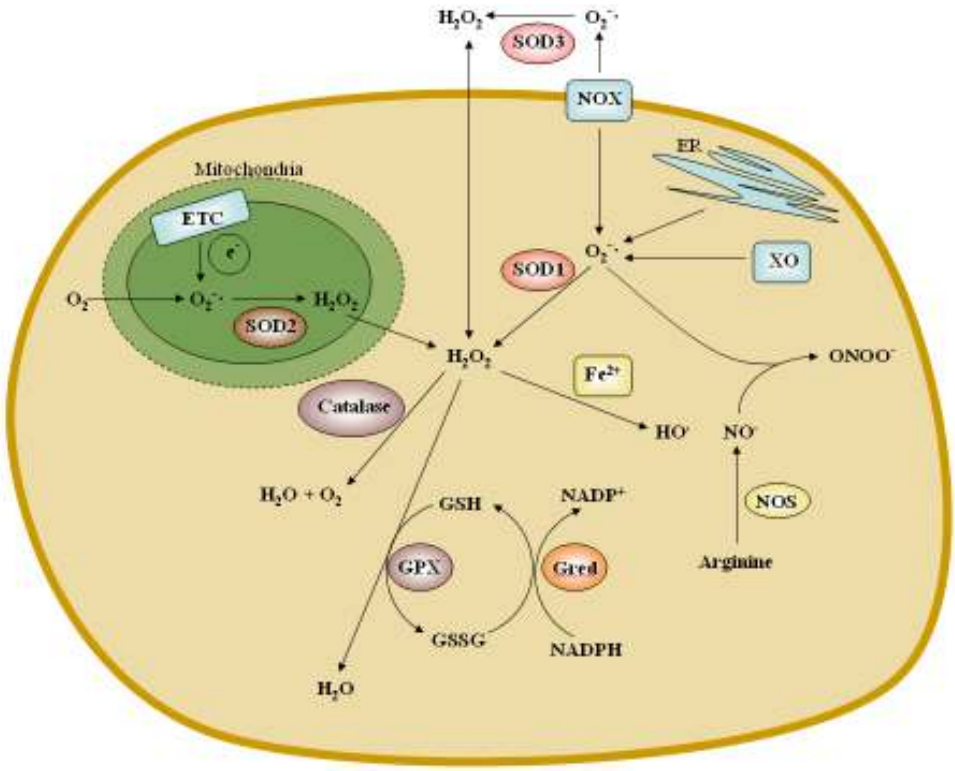


**Figure 1.2. The many sources of ROS/RNS generation in a cell.** The particular ROS/RNS described in the text are shown in the figure. Abbreviations: ER, endoplasmic reticulum; ETC, electron transport chain; GPX, glutathione peroxidase; Gred, glutathione reduced; NOS, nitric oxide synthase; NOX, NADPH oxidase; SOD1, 2 and 3, superoxide dismutase 1, 2 and 3; XO, xanthine oxidase. Figure adapted from (Trachootham et al. 2009).

Whilst the majority of $O_2^{-}\cdot$ and other ROS are produced through metabolic processes (as discussed) there are also a multitude of exogenous sources. Environmental factors including ultraviolet light and χ- and γ-radiation generate ROS, as do pollutants such as car exhaust emission and pesticides. Furthermore, behavioural activities such as cigarette smoking and chronic exercise are also known to elevate ROS levels (Gracy et al. 1999).

## 1.1.2 The importance of ROS and RNS in fundamental biological processes

Traditionally ROS and RNS production were considered unavoidable deleterious consequences of living in an oxygen rich environment. Consequently research on these molecules focused on the ways in which organisms protect themselves from oxidative damage. This changed in the late 1980's following the discovery of NO· as an "endothelium derived relaxing factor" which is critical in maintaining vascular tone (Palmer et al. 1987). Consequently considerable research has turned towards understanding the mechanisms by which ROSs/RNSs function to affect fundamental cellular process such as signal transduction and metabolism. Some roles of oxidant species under different physiological conditions are discussed below.

### 1.1.2.1 Maintenance of 'Redox Homeostasis' and 'Redox Signalling'

The term 'redox homeostasis' refers to the ability of cells to maintain a condition of oxidant/antioxidant equilibrium within their internal environment in order to preserve normal cellular function. ROS and other oxidant species exist in cells at low but measurable concentrations, however the comparatively high levels of intracellular antioxidants means there are substantial clearance mechanisms keeping ROS/RNS under tight cellular control. The main antioxidant species maintaining the cellular redox state include the enzymes superoxide dismutase (SOD), catalase (CAT) and glutathione peroxidase (GPx), whilst non-enzymatic regulators include glutathione (GSH), α-tocopherol (Vitamin E), ascorbate (Vitamin C) and free amino acids. Throughout its life cycle the redox homeostasis of a cell is constantly fluctuating in

response to changes in environment and metabolic needs and these changes in the redox balance occur through redox signalling. Redox signalling generally occurs during times of oxidative stress caused by either increased ROS formation or a decrease in the antioxidant capacity. For example, during times of enhanced oxidative stress GSSG (the oxidised form of GSH) levels rise causing an increase in the disulphide content of thiol residue containing proteins (Valko et al. 2007). These proteins include signalling mediators such as receptors, protein kinases and transcription factors. Consequently, the function of these proteins, and therefore also the pathways in which they are involved, becomes altered in response to changes in the thiol/disulphide redox state. Examples of thiol/disulphide sensitive signalling pathways include: Src family kinases, c-Jun N-terminal kinase (JNK), p38 mitogen-activated protein kinase (MAPK) and insulin receptor kinases (reviewed in (Droge 2002;Valko et al. 2007)). The GSH/GSSG couple are thus examples of redox signalling molecules.

#### 1.1.2.2 Oxidant signal transduction

It is perhaps unsurprising that ROS and RNS make attractive signalling molecules. Many are small, easily diffusible, highly reactive with short half lives and there are numerous systems in place, in the form of antioxidants, to terminate their production. Intracellular signalling cascades are typically initiated by the binding of extracellular ligands such as hormones, peptide growth factors, cytokines and neurotransmitters to specific cell surface receptors. Activation of a number of these receptors has been shown to initiate ROS mediate signal transduction in non-phagocytic cell types (Bae et al. 1997;Lo et al. 1996;Lo and Cruz 1995). The best characterised of the growth factor receptor (also known as the receptor tyrosine kinase (RTK)) class include the epidermal growth factor (EGF) receptor and platelet derived growth factor (PDGF) receptor. Both receptors are not only sensitive to ROS stimulation but have also been shown to promote $H_2O_2$ formation upon activation which consequently leads to downstream signalling effects (Bae et al. 1997;Catarzi et al. 2002). Likewise, stimulation of the cytokine tumour necrosis factor alpha (TNFα) receptor and also the interleukin 1-beta (IL-1β) receptor results in increased ROS formation (Sundaresan et al. 1996). ROS generated through this ligand/receptor interaction can function as

intracellular second messengers acting on downstream targets including: protein tyrosine phosphatases (PTPs), protein tyrosine kinases (PTKs), serine/threonine kinases, serine/threonine phosphatases, insulin receptor kinases, small G proteins, phospholipase-C (PLC), calcium ($Ca^{2+}$) and a variety of transcription factors (reviewed in Valko et al. 2006 and Droge 2002). Whilst elaborating on the details of individual ROSs interactions with different target molecules is beyond the scope of this chapter, Table 1.2 summarises the nature of ROSs effects on these signalling targets. ROS mediated signalling has been shown to be important in regulating cellular functions such as inflammatory responses (Millar et al. 2007), proliferation (Stone and Collins 2002) and apoptotic decisions (Kasahara et al. 1997).

**Table 1.2. ROS/RNS target signalling molecules. Table recreated from (Kamata and Hirata 1999).**

| ROS target signalling molecule | Oxidant effect |
|---|---|
| Protein tyrosine kinases<br>EGF and PDGF receptors, Src | Activation |
| Protein tyrosine phosphatases | Inactivation |
| Protein serine/threonine kinases<br>MAPK, JNK, p38, Akt, PKC | Activation/Inactivation |
| Protein serine/threonine phosphatases<br>PP1, PP2A | Inactivation |
| Small G proteins<br>Ras | Activation |
| Lipid signalling<br>PLC, PI 3-kinase | Activation |
| $Ca^{2+}$<br>Ins(1,4,5)P3 receptor, $Ca^{2+}$ ATPase | Activation |
| Transcription factors<br>AP-1, NFκB, p53 | Activation/Inactivation |

### 1.1.2.3 The immune response

ROS are also biologically important for the correct functioning of the host innate immune system in defence against pathogens, infectious agents and tumours. Macrophages and neutrophils are phagocytic immune cells and become activated

during the inflammatory response and generate ROS in order to carry out their phagocytotic defensive tasks.

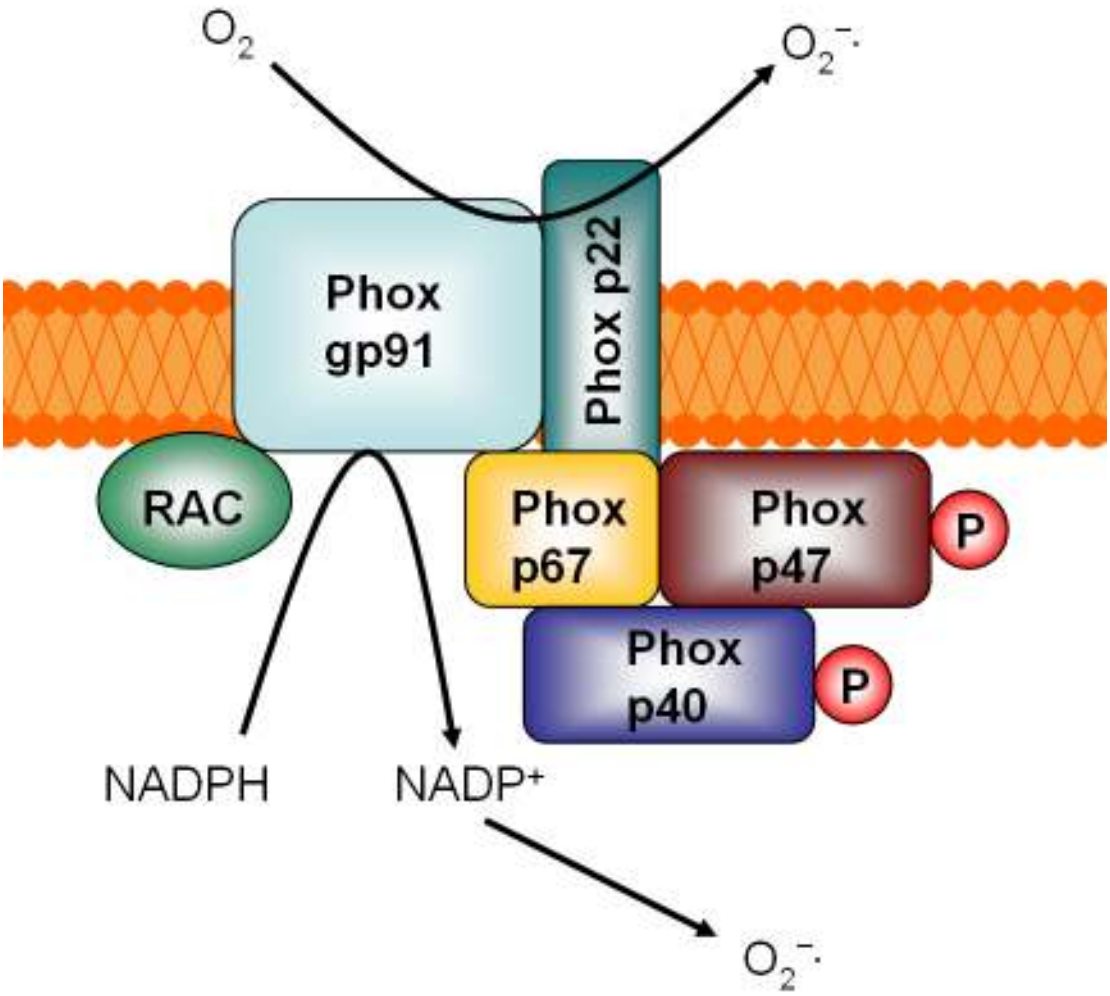


**Figure 1.3. The multicomponent NADPH oxidase (NOX) complex.** Unactivated the phox p22 and phox gp91 subunits reside unoccupied with the plasma membrane of phagocytic cells. Upon activation the cytosolic regulatory subunits phox p67 and phox p47, together with the phox p40 accessory protein and a RAC-GTP binding protein translocate to the cell membrane forming the NOX complex. During the respiratory burst, large amounts of $O_2$ are consumed which, coupled to NADPH oxidation, generates $O_2^{-}\cdot$. Figure adapted from (Rommel et al. 2007).

As mentioned previously, NOX present in the membrane of the phagocytotic vacuole of immune cells generate ROS to carry out their killing function. Upon infection, the cytosolic components of the NOX complex translocate to the membrane bound machinery to form the activated enzyme (Figure 1.3). Specific initiators of activation include microbial products such as endotoxin (Moore and MacKenzie 2009), as well as cytokine production (Kim et al. 2007) and IgG-binding (Shao et al. 2003). Once

activated the NOX complex consumes large amounts of $O_2$ and transports electrons out of the cell causing the reduction of $O_2$ to generate $O_2^{-}\cdot$ in the vacuole and extracellularly, a phenomenon known as the "respiratory burst". Whilst $O_2^{-}\cdot$ itself has been shown to be bactericidal *ex vivo* (Babior et al. 1973), its production can also give rise to further anti-microbial metabolites such as $\cdot OH$ and $OH^{-}$, via the iron catalysed Haber-Weiss reaction, and $H_2O_2$, via dismutation by SOD present within the phagocytic vacuole. Other ROSs/RNSs of the immune system include $NO\cdot$, which, as described previously, is generated by iNOS in macrophages and neutrophils upon activation and also the reactive $ClO^{-}$, generated in neutrophils (but not macrophages) containing the enzyme myeloperoxidase (MPO) which catalyses the reaction between $H_2O_2$ and $Cl^{-}$.

Currently, the anti-microbial mechanisms of NOX function are not clearly understood, however the discovery that NADPH oxidase dysfunction leads to chronic granulomatous disease (CGD) in which patients are prone to, and struggle to rid themselves of, bacterial and fungal infections (Segal 1996) suggests that at least $O_2^{-}\cdot$ may be critical. $NO\cdot$ has also been proposed to have cytotoxic immune effects due to the observation of highly elevated iNOS activities in neutrophils of patients with urinary tract infections (Wheeler et al. 1997). However, $NO\cdot$'s precise importance in microbial killing is uncertain since, whilst $NO\cdot$ scavengers have been shown to inhibit macrophage-induced cytostasis (Hibbs, Jr. et al. 1987), knocking out iNOS in highly expressing species such as mice has been shown to have little effect on the organisms anti-microbial ability (Segal 2005). The functioning of MPO, however, appears critical to maintaining efficient immunity, suggesting a key role for $ClO^{-}$, since it is observed that mice lacking MPO are significantly more susceptible to bacterial and fungal infection (Aratani et al. 1999;Aratani et al. 2000).

Traditionally it was believed that the reactive nature of ROS enabled them to carry out their immune function by directly attacking and destroying phagocytosed pathogens. However, it has recently been suggested that ROS alone are insufficient for microbial destruction, since microbial killing was found to be abolished in mice lacking major neutrophil proteases despite having a normal respiratory burst (Segal 2005). As such it is now proposed that ROS may not be directly responsible for microbial killing. The action of NOX pumping electrons out of the phagocytotic vacuole and the resulting

translocation of compensating ions and digestive enzymes into the vacuole, together with the abundance of ROS within the vacuole, have been suggested to create an environment ideal for microbe destruction (Segal 2005).

### 1.1.3 The damaging effects of ROS and RNS

Whilst physiological levels of ROS and RNS are required for efficient cellular functioning, maintenance and growth as discussed, higher levels, or decreased levels of protective antioxidant enzymes, can result in cellular damage and consequently are postulated to be causative of a number of diseases and ageing. The 3 main classes of biological macromolecules (DNA, lipids and proteins) can all be affected by ROS induced oxidation.

#### 1.1.3.1 Oxidative DNA damage

The hydroxyl radical (·OH) is perhaps the best characterised of all ROS known to attack DNA molecules, with this radical species able to damage both the purine and pyrimidine bases as well as the sugar moiety of the deoxyribose backbone (Dizdaroglu et al. 2002). The resulting strand breaks or erroneous cross links can cause the incorrect initiation or termination of transcription, the synthesis of abnormal proteins, replication errors and genomic instability, all of which are purported to be causative of carcinogenesis and other diseases (Valko et al. 2006). ·OH radicals transmit oxidative damage to DNA bases through addition reactions, generating OH-adduct radicals, whereas they attack carbon-centred sugars through abstraction reactions, producing carbon-centred radicals. Furthermore, if present, $O_2$ can also add to OH-adduct radicals and carbon-centred radicals to produce peroxyl radicals (Dizdaroglu et al. 2002). It is the downstream reactions of these base and sugar radicals that generate modified bases and sugars, strand breaks and DNA-protein cross-links. A recognised example of ·OH induced oxidative DNA damage is its reaction with guanosine to form the carcinogenic and mutagenic 8-hydroxyguanosine (8-OH-G). This oxidised species has been identified in human urine and therefore has been proposed as a useful biomarker for oxidative stress and also possibly cancer (Shigenaga et al. 1989). The RNSs $NO^{\cdot}$ and $ONOO^{-}$ can also cause DNA damage.

Oxidation of $NO^{\cdot}$ by $O_2$ generates the nitrosating agent $N_2O_3$ which can directly attack DNA by deaminating bases. Deamination of cytosine, for example, forms uracil which has the propensity to give rise to a G:C → T:A transversion mutations through mispairing (Burney et al. 1999). The intrinsically more reactive $ONOO^-$ exerts its damage in an oxidative manner, causing sugar fragmentation and DNA strand breaks, believed to be via a mechanism involving hydrogen abstraction leading to carbon-centred sugar radical formation (Burney et al. 1999). Along with nuclear DNA, mitochondrial DNA (mtDNA) is also believed to be susceptible to ROS induced damage. Indeed, the oxidised base 8-OH-G has been found to be far more prevalent in mtDNA than in nuclear DNA (Richter et al. 1988), suggesting that mtDNA may be more oxidatively susceptible under physiological conditions, possibly due to the limited mtDNA repair capacity and absence of mtDNA protection from histones (Valko et al. 2006).

### 1.1.3.2 Lipid peroxidation

The mechanism by which ROS cause lipid oxidation has been well characterised. The methylene groups of polyunsaturated fatty acid side chains of phospholipids, the key constituents of biological membranes, are highly susceptible to oxidation. Oxidant species such as $O_2^{-\cdot}$ and $\cdot OH$ can remove a hydrogen atom from the methylene group, generating carbon-centred fatty acid radicals. These in turn will readily react with $O_2$ to form peroxyl radicals. The fate of the peroxyl radical is dependent upon its position within the fatty acid chain. A peroxyl radical located at the end of a fatty acid chain will be reduced to hydroperoxide, by either another fatty acid or by vitamin E (Marnett 1999). Although relatively stable, hydroperoxide generation can propagate further fatty acid oxidation. Peroxyl radicals formed in internal positions within fatty acid chains have a number of fates. Firstly, they can react with another peroxyradical from a nearby fatty acid side chain, resulting in covalent cross-links that will cause significant reduction in membrane fluidity and consequently change the membrane's properties. However, typically the peroxyl radical will undergo a cyclisation reaction to an adjacent double bond producing a cyclic peroxide, which can undergo a second cyclisation to form a precursor of malondialdehyde (MDA) (Marnett 1999). MDA has be found to be mutagenic in bacterial and mammalian cells and also carcinogenic in

rats (Valko et al. 2007). Furthermore, MDA is known to form adducts with DNA bases, with guanine adducts shown to be particularly mutagenic in *E. coli* by causing mutations of guanine to adenine and thymine (Fink et al. 1997).

### 1.1.3.3 Protein oxidation

Similarly to lipid peroxidation, the polypeptide backbone of proteins is highly susceptible to oxidative damage. Both $O_2^{-}\cdot$ and ·OH are able to abstract a hydrogen atom from the peptide backbone forming a carbon-centred radical species which, under aerobic conditions, will generate the peroxyl radical mentioned previously. The peroxyl radical species has a number of fates, including: reacting with other carbon-centred peptides or lipid backbones to form stable crosslinks; abstracting a hydrogen atom from a neighbouring amino acid generating another carbon-centred radical or reacting with other reactive oxygen radical species to form further ROS derivatives such as the alkoxyl radical, which can undergo peptide bond cleavage (Stadtman 2004). The side chains of amino acids are also highly susceptible to oxidative attack. For instance, oxidation of cysteine residues can result in the formation of mixed disulphides between protein thiol groups and low molecular weight thiols such as glutathione (GSH) (Valko et al. 2007). Furthermore, direct oxidation of amino acid side chains by ROS can result in protein carbonyl formation leading to altered protein function. Additionally, amino acid residues located at metal binding sites, such as lysine, arginine, proline and histidine, readily undergo metal-catalysed oxidation to generate protein carbonyls (Amici et al. 1989). Carbonyls can be generated by a number of different mechanisms, of which only a couple have been touched on here. There are a variety of methods for assaying for carbonyl groups and since their concentration is significantly higher than any other product of protein oxidation, protein carbonyl content is typically used as a measure of oxidative protein damage (Stadtman 2004). Along with ROS, the RNS $ONOO^{-}$ can also mediate protein oxidation through nitrosation of cysteine sulfhydryl groups (Stubauer et al. 1999), nitration of tyrosine residues (Radi et al. 2001) and via oxidation of methionine residues (Squadrito and Pryor 1998), all in a $CO_2$ dependent manner. Nitration of tyrosine residues can be particularly harmful as it can prevent phosphorylation of tyrosine residues, a key step in many signalling pathways. Whilst protein oxidation

can be deleterious to correct cellular functioning, some of the oxidative lesions described are transiently reversible. For instance, methionine oxidation to methionine sulphoxide can be reversed by methionine sulphoxide reductases, which have been found to be present in mammalian cells (Dean et al. 1997). Those proteins in which oxidation is non-reversible however are usually marked for destruction, a process carried out by intracellular proteases (Stadtman 2004).

Whilst the mechanisms underlying the oxidation of proteins, lipids and nucleic acids can vary greatly, the oxidised products of each often interact. For example, the oxidation of DNA can lead to irregular transcription instruction and consequently abnormal proteins can result. These versions of native proteins may be particularly susceptible to oxidation and thus will be targeted for degradation (Figure 1.4).

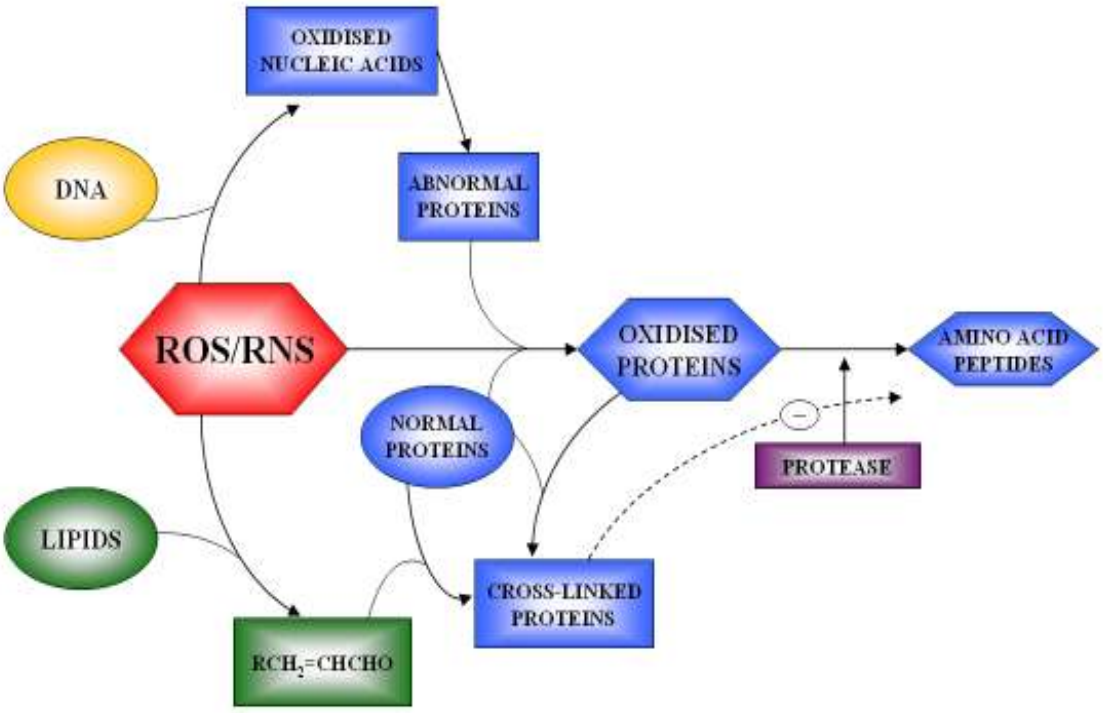


**Figure 1.4. The interaction of ROS/RNS, proteins, lipids and nucleic acids.** Figure re-created from (Stadtman 2004).

## 1.1.4 ROS associated disorders

As described above, the consequence of pathologically elevated, or insufficiently regulated, levels of ROS can be macromolecular destabilisation or even cell death,

however the downstream consequences of such events have yet to be addressed. Oxidative stress has been implicated in various conditions including cancer, cardiovascular disease, neurological disorders, diabetes, ageing and many other diseases. The following is an introduction to a selection of the disease states in which the action of ROS have been implicated.

#### 1.1.4.1 Cancer

The cells of a number of different cancer types present a redox imbalance (Valko et al. 2007) suggesting an intimate link between oxidative stress and cancer. Although it is not clear whether this redox imbalance is a cause or a result of the cancer, what is clear, is that DNA mutation is an essential primary step in the progression of carcinogenesis and oxidatively damaged DNA has been found in a number of tumour cells. For instance, as mentioned earlier, the oxidised base 8-OH-G is an established marker for oxidatively damaged DNA and has been found to be elevated in carcinomas such as lung (Vulimiri et al. 2000), gastric (Lee et al. 1998) and colon (Oliva et al. 1997). As discussed above, ROS can directly attack DNA with the oxidation products causing mutations through stand breaks, base transitions and replication errors. Furthermore, the lipid peroxidation product MDA is able to form adducts with DNA bases generating carcinogenic and mutagenic phenotypes. For example, MDA DNA base adducts have been found to be significantly elevated in breast cancer tissue (Wang et al. 1996). Both redox and non-redox metals have also been implicated in the mechanisms of carcinogenesis. For instance, iron catalysed ROS generation is proposed to be an oncogenic factor in the propagation of colon cancer (Valko et al. 2001) and cadmium (McElroy et al. 2006), chromium (Gibb et al. 2000) and arsenic (Smith et al. 1992) exposure have all been shown to be linked to carcinogenesis. Along with DNA damage, abnormal cellular signalling is proposed to be another critical ROS mediated factor associated with cancer, since cellular signalling is a key mediator of cell growth and proliferation, a fundamental attribute of cancer development. ROS sensitive signalling targets include: a number of growth factor receptors, such as epidermal growth factor receptor (EGFR) and platelet derived growth factor receptor (PDGFR), where expression of EGFR has been intimately linked to the progression of lung cancer (Hirsch et al. 2003) and high

PDGFR expression is observed in prostate cancer (Hagglof et al. 2010); the transcription factor NFκB, which has been found to be activated in breast tumours (Biswas et al. 2004); and the tumour suppressor protein p53, inactivation of which, possibly due to ROS induced DNA base modification, has been associated with a number of cancers (Hollstein et al. 1991).

### 1.1.4.2 Neurological disorders

Unsurprisingly the brain is particularly vulnerable to oxidative damage due to its high oxygen requirement, significant polyunsaturated fatty acid content and abundance of redox metals. Oxidative damage is coupled to age in the case of neurodegenerative disease, with age being the primary risk factor in the disorders subsequently described. Alzheimer's disease (AD) is characterised by the loss of neurones and synapses in the cerebral cortex caused by protein misfolding due to the accumulation of oligomeric amyloid-β peptide (Aβ) in senile plaques and the deposition of neurofibrillary tangles (Valko et al. 2007). There is a wealth of evidence supporting the notion of increased oxidative stress in the brains of AD sufferers including: increased transition metal abundance (Lovell et al. 1998); increased lipid peroxidation (Sayre et al. 1997); increased protein oxidation (Aksenov et al. 2001); increased DNA oxidation (Lovell et al. 1999) and elevated carbonyl levels (Aksenov et al. 2001). Furthermore, the lipid carrier, Apolipoprotein E (APOE), has been proposed as a risk factor for AD and its peroxidation by ROS damage or knockout by mutation correlates with AD progression and increases vulnerability to Aβ induced oxidative stress (Butterfield et al. 2002). Parkinson's disease (PD) is another neurodegenerative disease characterised by the loss of dopaminergic neurones in the substantia nigra, leading to impaired communication between nigral and striatum cells through dopamine depletion. As with AD, there exists significant evidence for the role of oxidative stress in PD etiology. For instance, oxidative stress has been shown to induce nigral cell death (Jenner 1998) and increased oxidative stress is observed in PD patients (reviewed in (Jenner 2003)). Furthermore, it appears that mitochondrial complex I dysfunction may be causative in PD, with this dysfunction suggested to be a result of nitration through $NO^{\cdot}$ and $ONOO^{-}$ action (Brown and Borutaite 2004;Good

et al. 1998;Swerdlow et al. 1996). Indeed treatment of cells with NOS inhibitors can prevent complex I inhibition (Frost et al. 2005).

### 1.1.4.3 Ageing

A role for ROS in determining lifespan was first proposed in the 1950's when Denham Harman proposed the "free radical theory" of ageing (Harman 1956). This theory suggested that endogenous free radicals were generated within cells and that they caused accumulative damage leading to ageing. The realisation that many ROS, which are not technically free radicals, can also cause oxidative damage in cells (as has been discussed) has led many to accept a modified version of the free radical theory – the oxidative damage theory of ageing (Muller et al. 2007).

Currently, support for the oxidative damage theory of ageing appears to fall into two classes of evidence. 'Weak' support is provided by evidence demonstrating that oxidative damage is 'associated' with ageing, whilst 'strong' support is given by evidence which clearly shows that oxidative damage determines lifespan (Muller et al. 2007;Beckman and Ames 1998). Presently, there exists a wealth of evidence supporting the 'weak' proposal. Such evidence includes:

- the observation of lowered oxygen consumption in both long lived queen bees compared to workers and larger longer lived animals compared to smaller short lived ones (Valko et al. 2007)
- the finding of accumulated levels of lipofuscin, a biomarker of lipid peroxidation, in aged tissues in a number of model species (Beckman and Ames 1998)
- the finding that the protein carbonyl content (a marker of oxidative protein damage) in aged tissue is 2- to 3-fold higher than the levels found in younger tissue (Beckman and Ames 1998)
- the observation that the activity of several oxygen-sensitive enzymes, such as glutamate synthase, decreases in mammalian models of ageing (Beckman and Ames 1998)

For a comprehensive overview of the evidence for the association of oxidative damage and ageing please see the review by Beckman and Ames (1998).

Whilst the evidence described above clearly demonstrates that there is a link between ageing and oxidative damage, evidence proving that oxidative damage mediates lifespan (i.e. 'strongly' supporting the oxidative damage theory of ageing) is not nearly so abundant. Generally such evidence comes from interventionist studies in which lifespan is assessed in models where genetic modifications, leading to increased or decreased oxidative stress resistance, have been applied. The most extensive research in this area has focused on knocking out and overexpressing the superoxide dismutase (SOD) family of enzymes which scavenge $O_2^{-}\cdot$ in various cellular locations. Whilst the results of these studies are explained in more details later in the chapter, the general trend in a number of organisms is that by knocking out the *sod* genes, the organisms become more sensitive to oxidative stress often with shortened lifespan, thus lending 'strong' support to the idea that increased oxidative damage mediates lifespan (Muller et al. 2007). It should be noted however that this increased oxidative stress sensitivity does not always correlate with reduced lifespan. For instance, in *C. elegans* knocking out the mitochondrial *sod* genes (*sod-2* and *sod-3)* was shown to have no effect on lifespan despite severe hypersensitivity to hyperoxia (Doonan et al. 2008). In terms of *sod* overexpression, lifespan extension can be achieved in *Drosophila*, dependent on the genetic background used, whilst in *C. elegans* and rodent models, overexpression of *sod* appears to have little effect on longevity (Muller et al. 2007). With regard to other enzymes involved in oxidative protection, knocking out of glutathione peroxidase 1 (GPx1), the enzyme responsible for degrading intracellular $H_2O_2$, in mice was, perhaps surprisingly, found to have no effect on lifespan (Muller et al. 2007). However, knocking out methionine sulfoxide reductase A (*MsrA*), the enzyme responsible for repairing oxidised methionine residues, was found to decrease the lifespan of mice significantly and overexpression of *MsrA* in the nervous system of *Drosophila* caused an increase in lifespan of ~70% compared to controls (Ruan et al. 2002). The current evidence therefore suggests that in some models and backgrounds the expression of genes required for oxidative protection can directly determine lifespan whilst in others it appears to have little effect. For a comprehensive overview of the evidence for oxidative damage determining lifespan please see the review by Muller and colleagues (2007).

Therefore, whilst lifespan and oxidative damage are linked, the free radical and oxidative damage theories of ageing appear too simplistic, since it is still unclear whether this oxidative damage causes or is a result of ageing. However, the relationship between oxidative damage and lifespan may become clear through emerging studies of ROS sensitive signalling pathways. Whilst it is clear that antioxidant levels must be sufficient to protect against ROS induced macromolecular damage, what effect modifying ROS levels might have on complex signalling pathways is still unclear. It is entirely possible that altered transcription factor activation and therefore altered gene expression, resulting from modified signalling cascades may prove as important in determining lifespan as the rate of macromolecular damage accumulation.

## 1.2 Antioxidants and the SOD gene family

In biology antioxidants can be considered any compound that serves to reduce or regulate the levels or effect of ROS. Typically they take the form of enzymes which metabolise various ROS molecules, however they can also be agents that decrease ROS formation, such as mitochondrial uncoupling proteins which decrease ROS production through reducing the mitochondrial membrane potential and pH gradient (Lambert and Brand 2004;Miwa et al. 2003), or proteins that protect molecules from oxidative damage through other means, such as the heat shock protein (HSP) family of molecular chaperones (Benjamin and McMillan 1998). The focus of this section is on antioxidant enzymes which are considered to be one of the primary means by which cells regulate ROS levels to ensure appropriate cellular function whilst simultaneously protecting themselves from oxidative damage.

The three most widely studied antioxidant enzymes are the superoxide dismutases (SODs), catalase (CAT) and glutathione peroxidise (GPx). The SOD family of enzymes are critical to maintaining cellular viability by reducing toxic $O_2^{-}\cdot$ to $O_2$ and $H_2O_2$ (eqn 5). $H_2O_2$ itself is a toxic ROS and can be metabolised by both CAT, which degrades $H_2O_2$ to $H_2O$ and $O_2$ (eqn 6), and GPx, which reduces $H_2O_2$ through glutathione (GSH) oxidation (eqn 7). Furthermore, GPx can also catalyse the GSH-

dependent reduction of fatty acid hydroperoxides, a product of lipid peroxidation, to an alcohol (eqn 8).

$$2O_2^{-}\cdot + 2H^{+} \rightarrow O_2 + H_2O_2 \quad (5)$$

$$2H_2O_2 \rightarrow 2H_2O + O_2 \quad (6)$$

$$2GSH + H_2O_2 \rightarrow 2H_2O + O_2 + GSSG \quad (7)$$

$$2GSH + LOOH \rightarrow H_2O + GSSG + LOH \quad (8)$$

## 1.2.1 Superoxide dismutase

The catalytic activity of a copper containing enzyme able to dismutate $O_2^{-}\cdot$ radicals was first identified in bovine erythrocytes in 1969 by Joe McCord and Irwin Fridovich (McCord and Fridovich 1969). McCord and Fridovich called this enzyme superoxide dismutase (SOD). In the proceeding years following its original discovery a number of different SODs have been discovered which are characterised by their catalytic metal prosthetic group and/or cellular location, and are abundant in both prokaryotic and eukaryotic cells. To date, the SOD family of enzymes have been found to be copper/zinc- (Cu Zn), manganese- (Mn), iron- (Fe) or nickel-binding (Ni) enzymes. Despite the distinction in metal groups all SODs are believed to dismutate $O_2^{-}\cdot$ via a metal ion-catalysed cyclic redox pathway (eqn 9) (Johnson and Giulivi 2005).

$$\begin{aligned} Metal^{ox} + O_2^{-}\cdot &\rightarrow Metal^{red} + O_2 \\ Metal^{red} + O_2^{-}\cdot + 2H^{+} &\rightarrow Metal^{ox} + H_2O_2 \end{aligned} \quad (9)$$

### 1.2.1.1 Structure and compartmentalisation of eukaryotic SODs

Cu Zn-SOD, or SOD1, encoded by the *sod1* gene in mammals, was the first isoform to be characterised and was identified as a copper and zinc-binding homodimer with a molecular mass of approximately 32 kDa (Richardson et al. 1975). While zinc is not

required for catalytic purposes, it is needed to maintain protein structure (Johnson & Giulivi 2005). Cu Zn-SOD is primarily found intracellularly within the cytoplasm, nucleus and lysosomes (Chang et al. 1988;Crapo et al. 1992), however, fractionation of mitochondria from chicken liver identified a small amount also localising in the intermembrane space (IMS) of mitochondria (Weisiger and Fridovich 1973).

Mn-SOD, or SOD2, encoded by the *sod2* gene in mammals, binds manganese as the metal co-factor and is located within the mitochondrial matrix (Weisiger & Fridovich 1973). The enzyme is a homotetramer with a molecular weight of approximately 92 kDa (Barra et al. 1984), although it has been suggested that it is the dimeric form that is required for function (Jackson and Cooper 1998). Since one of the main sources of $O_2^{-}\cdot$ is as a by product of mitochondrial aerobic respiration, Mn-SOD is likely one of the first lines of defence against intracellular sources of ROS.

Extracellular SOD, or SOD3, encoded by the *sod3* gene in mammals, is also a copper and zinc binding protein found as a homotetramer with a molecular mass of approximately 135 kDa (Marklund 1982). SOD3 was first discovered in extracellular fluids including plasma, serum, lymph, ascites and cerebrospinal fluid (Marklund et al. 1982), however it is far more abundant in tissues than in plasma (Marklund 1984a;Marklund 1984b). Despite being predominantly an extracellular enzyme, immunohistochemical analysis of mouse tissue also demonstrated that the gene product can be secreted and transported back into the cell nucleus where it protects genomic DNA (Ookawara et al. 2002). Upon its discovery, extracellular SOD was also found to have various degrees of affinity for heparin suggesting that the enzymes extracellular location is determined through its interactions with polyanions such as heparin-sulphate (Marklund 1982) (this is discussed in further detail in Chapter 2).

The genomic sequence and gene structures have been identified for each of the three SOD isoforms in human tissue (Folz and Crapo 1994;Levanon et al. 1985;Wan et al. 1994) and has revealed that, whilst there is reasonable homology (approximately 40-60%) between the human *sod1* and *sod3* genes, *sod2* shows no significant homology to the two Cu Zn-containing enzymes (Figure 1.5) (Zelko et al. 2002).

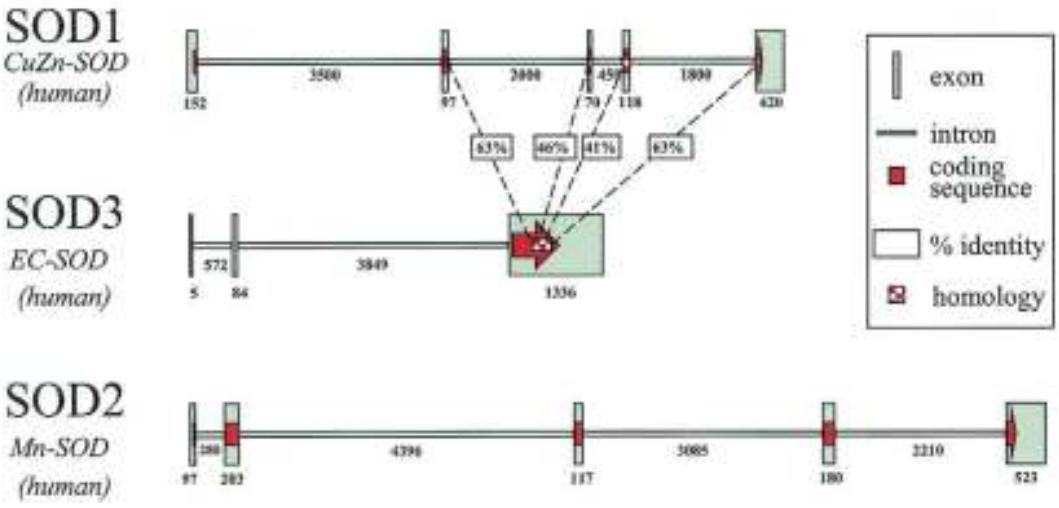


**Figure 1.5. Genomic arrangement of the 3 human SOD isoforms**. Whilst *sod1* and *sod3* show considerable sequence homology, *sod2* shows no significant homology with either *sod1* or *sod3*. Figure taken from (Zelko et al. 2002).

### 1.2.1.2 SODs in other organisms

Expression of the *sod* isoforms may vary greatly within eukaryotic species, however the cellular location of these antioxidants does not change across kingdoms. Whilst mammals boast all three of the SOD proteins, *Saccharomyces cerevisiae*, the unicellular eukaryotic yeast, unsurprisingly only contains the cytosolic Cu Zn SOD and mitochondrial Mn SOD subtypes. Cu Zn SOD has been found to account for 90-95% of the total SOD activity in *S. cerevisiae* (O'Brien et al. 2004), meaning mutations in the *Sod1* gene are likely to be far more damaging to the organism. Since $O_2^{-}\cdot$ does not easily cross biological membranes, this would also imply that non-mitochondrial derived sources of $O_2^{-}\cdot$ are the major contributor to oxidative damage in *S. cerevisiae*. Indeed, it has been shown that *sod1* null mutants grow more slowly and are less viable under normal conditions and normoxia, than *sod2* null mutants, which in fact grow like wild type cultures (Longo et al. 1996). This confirms the hypothesis of *sod1* mutant sensitivity in *S. cerevisiae*, and also that protection from endogenous sources of ROS is critical for *S. cerevisiae* survival.

Along with Cu Zn- and Mn-binding enzymes, SOD isoforms also exist that bind Fe and Ni. Fe SOD is primarily a prokaryotic protein although has also been found in some plant types (Salin and Bridges 1982). Fe SODs are found either as homodimers

or homotetramers and they show significant primary sequence and structural homology with prokaryotic Mn SODs (Parker et al. 1987). Moreover, Parker *et al.* reported that the two prokaryotic SOD isoforms are not easily distinguishable based on primary, secondary and tertiary structure and that differences between the two proteins likely arise from single amino acid substitutions. Due to this high level of homology it is perhaps unsurprising that cambialistic SODs within the Mn/Fe SOD family have been observed. A number of studies have shown that these enzymes in bacteria are capable of using either Fe- or Mn- catalytically (Gabbianelli et al. 1995;Lancaster et al. 2004). The level of significant homology between the Mn/Fe SOD isoforms also implies that both enzymes evolved from a common ancestor, thus supporting the notion that mitochondria originated from proteobacteria engulfed by eukaryotic cells (Wallin 1923). The tetra- or hexameric Ni SOD is restricted to prokaryotes too and has been purified in strains of *Streptomyces* (Youn et al. 1996). Whilst showing little sequence or amino acid homology to other SODs, Ni SOD retains a similar specific activity per metal to that of Cu Zn SOD and can thus is considered a novel SOD. The structure of the different SODs' catalytic active sites and their respective metal configurations were well summarised in a review by Anne-Francis Miller in 2004 (Miller 2004).

#### 1.2.1.3 Identification and evolution of invertebrate extracellular SOD

Whilst vertebrates have long been known to synthesise an extracellular form of SOD, until recently, invertebrates were assumed to only possess cytosolic Cu Zn SOD and Mn SOD. The nematode *C. elegans* contains a cytosolic Cu Zn SOD, but has two isoforms of the Mn SOD, (SOD-2 and SOD-3) which have been cloned and mapped to separate chromosomes (Suzuki et al. 1996). It was not until 1998 that Fujii *et al.* characterised an extracellular *sod* gene (*sod-4*) in *C. elegans* (Fujii et al. 1998). By cloning and sequencing the *sod-4* gene they identified two gene products (SOD4-1 and SOD4-2) formed from alternative splicing, with both containing an N-terminal signal cleavage sequence homologous to mammalian extracellular SOD. SOD4-2 also contained a C-terminal transmembrane domain and when expressed in mammalian cells, both protein isoforms were extracellularly located with SOD4-2 also membrane

bound. Thus at this point, *C. elegans* was considered to have 4 SODs, compared to the 3 found in mammals. Unfortunately, this makes for slightly confusing nomenclature since the mammalian extracellular SOD is referred to as SOD3, yet in *C. elegans* SOD-3 denotes one of the Mn SOD isoforms (Table 1.3). Despite the appearance of an extracellular SOD in *C. elegans*, it was still generally accepted that insects contained only a cytosolic Cu Zn SOD and a mitochondrial Mn SOD (Kirby et al. 2002). That changed in 2004 when Parker *et al.* cloned a novel Cu Zn SOD mRNA from the ant *L. niger* (Parker et al. 2004a). Sequence analysis with the SODs of other species, and in particular the well characterised extracellular SOD of *Mus musculus* and SOD-4 of *C. elegans*, revealed that this Cu Zn SOD was indeed a novel extracellular SOD expressed in insects. The sequence analysis also revealed a 5$^{th}$ *C. elegans* SOD which closely resembled *C. elegans* cytosolic Cu Zn SOD. This second cytosolic Cu Zn SOD (called SOD-5) is believed to have arisen from gene duplication (Parker et al. 2004a).

The SOD family of enzymes first appeared around 2 billion years ago following the emergence of oxygen producing photosynthetic organisms. Two separate types of SOD appeared, Cu Zn-containing and Fe/Mn-containing, with their distinct lack of homology suggesting they did not evolve from a common SOD ancestor (Zelko et al. 2002). Sequence and structural analysis have also revealed that the extracellular Cu Zn SODs appear to have diverged from the cytosolic Cu Zn SODs early on during evolution (Zelko et al. 2002). Phylogenetic analysis of the Cu Zn SOD gene in insects (Parker et al. 2004a) and of all the SOD genes and proteins in a wide range of species (including insects) (Landis and Tower 2005) have confirmed this diversion. However, Landis and Tower have proposed that the extracellular SODs in the species analysed have all evolved independently from the cytosolic SOD. Due to the significant lack of sequence homology between Cu Zn SOD and extracellular SOD, compared to a strong homology between the extracellular SODs in different insects (Parker et al. 2004a), it appears more reasonable to assume that extracellular SODs have evolved from a common ancestor.

**Table 1.3. Nomenclature of SODs across a variety of species.** Adapted from (Culotta et al. 2006).

| Species | Metal co-factor | Localisation | Protein Name |
|---|---|---|---|
| *E. coli* | Manganese | Intracellular | SodA |
| | Iron | Intracellular | SodB |
| | Copper-Zinc | Periplasmic | SodC |
| *S. cerevisiae* | Copper-Zinc | Cytoplasm and Mitochondrial IMS | SOD1 |
| | Manganese | Mitochondrial matrix | SOD2 |
| *Drosophila* | Copper-Zinc | Cytoplasm and Mitochondrial IMS | SOD1 |
| | Manganese | Mitochondrial matrix | SOD2 |
| | Copper-Zinc | Extracellular | SOD3 |
| *C. elegans* | Copper-Zinc | Cytoplasm and Mitochondrial IMS | SOD-1 |
| | Manganese | Mitochondrial matrix | SOD-2 |
| | Manganese | Mitochondrial matrix | SOD-3 |
| | Copper-Zinc | Extracellular | SOD-4 |
| | Copper-Zinc | Cytoplasm and Mitochondrial IMS | SOD-5 |
| Mammals | Copper-Zinc | Cytoplasm and Mitochondrial IMS | SOD1 |
| | Manganese | Mitochondrial matrix | SOD2 |
| | Copper-Zinc | Extracellular | SOD3 |

It should be noted that from this point on the SOD isoforms will be referred to by the names listed in the 'Name' column of Table 1.3.

## 1.2.2 Catalase

As described above, dismutation of $O_2^{-}\cdot$ generates $H_2O_2$, however so do a number of oxidase enzymes including xanthine oxidase, urate oxidase, glucose oxidase and D-amino acid oxidase. Whilst $H_2O_2$ is a ROS, and therefore is proposed to be cytotoxic if left unregulated, it actually has relatively poor reactivity with biological macromolecules, a feature which probably enables it to act as a common signalling molecule (Halliwell & Gutteridge 2007). Although some cellular damage by $H_2O_2$ can be direct, such as the oxidation of haem proteins (Rice et al. 1983), the primary cytotoxic effects mediated by $H_2O_2$ are proposed to occur through its reaction with intracellular copper and iron ions to generate the highly reactive and damaging ·OH species (Halliwell & Gutteridge 2007). Consequently, regulation of $H_2O_2$ levels is critical for maintaining cellular viability through minimised macromolecular damage and maintenance of appropriate signalling cascades.

Catalase (CAT) is a ubiquitous enzyme in animals which catalyses the direct composition of $H_2O_2$ to ground-state $O_2$ (see equation 6; section 1.2). In animals CAT is composed of four subunits, each with Fe(III)-haem bound at the active site along with one molecule of NADPH. The CAT activity of animal and plant cells is largely located in the peroxisomes (Chance et al. 1979), in which it colocalises with several $H_2O_2$ enzymes, such as glycollate oxidase, urate oxidase and flavoprotein dehydrogenases, possibly as a protective mechanism (Halliwell & Gutteridge 2007). Interestingly, mitochondria and the ER contain little CAT (Chance et al. 1979; Antunes et al. 2002), meaning any $H_2O_2$ produced by these organelles will be degraded by other means, unless diffusion to the peroxisomes occurs (Halliwell & Gutteridge 2007). Although enzymatic activities vary between cell types, in animals the highest concentrations of CAT are found in the liver and erythrocytes, whilst the brain, heart and skeletal muscles have been found to harbour considerably lower levels (Halliwell & Gutteridge 2007).

### 1.2.3 The glutathione peroxidases

The glutathione peroxidase (GPx) family of enzymes are widely distributed in animal tissues and degrade $H_2O_2$ by coupling its reduction to $H_2O$ with the oxidation of reduced glutathione (GSH) (see equation 7; section 1.2). A number of GPx exist, with the classical GPx (GPx1) being a cytosolic protein and thus is probably responsible for scavenging the majority of mitochondrially-derived $H_2O_2$ (Muller et al. 2007). Another GPx is found in cells lining the gastrointestinal tract (GPx2) which may metabolise peroxides within ingested food lipids (Halliwell & Gutteridge 2007). The third member of the GPx family (GPx3) is found at low levels in mammalian extracellular fluids such as plasma, milk, seminal fluid and amniotic fluid. As well as using GSH as a substrate GPx3 can also utilise thioredoxin (Halliwell & Gutteridge 2007). The final member of the GPx family (GPx4) is able to not only reduce $H_2O_2$ and synthetic organic peroxides but also fatty acid and cholesterol hydroperoxides which remain esterified (see equation 8; section 1.2) (Halliwell & Gutteridge 2007). GPx1, 2 and 3 are all tetrameric proteins with each subunit binding a selenium atom at their active site, whilst GPx4 is monomeric harbouring only a single selenium atom.

Consequently, traces of selenium are essential in the diet of animals to maintain GPx activity. This has been demonstrated in rodent models deprived of selenium which had lowered GPx activity (Rotruck et al. 1973).

## 1.3 Genetic and phenotypic studies of SOD manipulations in model systems

The precise role that the SOD family of enzymes play in regulating ROS/oxidative stress associated disorders has been the focus of much research for many decades. Traditionally this has been achieved through genetic manipulation and transgenic techniques to generate specific *sod* mutants or drive *sod* over-expression in a number of model organisms, with the results providing interesting insights into the functional role of the SODs within in a variety of organisms. The following will discuss some of the genetic studies of all three SOD isoforms, with the focus on oxidative stress, longevity and certain disease states.

### 1.3.1 SOD1

#### 1.3.1.1 Familial amyotrophic lateral sclerosis

One of the best characterised pathologies associated with SOD1 mutations is that of amyotrophic lateral sclerosis (ALS), also know as "Lou Gehrig's Disease". This is a neurodegenerative disease primarily affecting the motor neurones or the spinal cord and the brain, leading to muscle weakness, paralysis and ultimately death, usually within 5 years of onset (Potter and Valentine 2003). Whilst approximately 90% of ALS cases are sporadic, the remaining 10% are familial (FALS), with 20-25% of all FALS cases having been linked to mutations of the *sod1* gene (Rosen et al. 1993). To date over 100 different, and seemingly random, mutations (mainly point mutations) within this gene have been implicated in the pathology of FALS (Lindberg et al. 2005;Potter & Valentine 2003). The mechanisms of cytotoxicity are poorly understood, however it appears not to be due to accumulative ROS damage through SOD1 dysfunction, since histological analysis of *sod1* knockout mice reveals no signs

of spinal cord motor neurone pathology (Reaume et al. 1996). Thus FALS appears to be attributed to a toxic gain of function mutation within SOD1, possibly through the formation of protein aggregates. Indeed, numerous studies suggest that protein mis-folding, oligomerization and incorrect disulfide formation leads to SOD1 ALS-associated aggregate formation (Elam et al. 2003;Furukawa et al. 2006;Hough et al. 2004;Lindberg et al. 2005). Aggregate induced pathology is believed to be achieved through impairment of axonal transport, protein degradation and anti-apoptotic functions. For instance, Okado-Matsumoto and Fridovich propose that heat-shock proteins (HSPs) bind and inhibit mitochondrial uptake of the mutant SOD1 and that the hsps consequent occupation interferes with their anti-apoptotic function, with neuronal death then resulting (Okado-Matsumoto and Fridovich 2002). Alternatively, Turner and colleagues propose that mutant *sod1* pathogenesis is achieved by impairment of mutant SOD1 secretion due to golgi and endoplasmic reticulum breakdown (Turner et al. 2005). In fusing the SOD3 signal peptide to a number of *Sod1* mutant's pathogenesis could be attenuated through extracellular secretion of the mutant proteins. Interestingly, while toxic gain of function mutations in *sod1* expressed in transgenic mouse models leads to a FALS phenotype, a similar phenotype is not apparent in transgenic *Drosophila* models. For instance, expression of human FALS-SOD in *Drosophila* motorneurones can rescue the short lived phenotypes of SOD1-null mutants (Elia et al. 1999;Mockett et al. 2003), and the minimal SOD activity of FALS-SOD mutants is, in fact, sufficient to extend longevity in *Drosophila* (Elia et al. 1999). It would therefore seem that the mechanism, (or perhaps mechanisms) by which the many different point mutations within the *sod1* gene transfer toxicity, remains to be identified.

#### 1.3.1.2 Oxidative stress and lifespan

Due to the popularity of the 'free radical theory' of ageing much research has gone into understanding the role of the SODs in this fundamental process. Knocking out the *Sod1* gene has been found to result in conserved phenotypes of reduced lifespan and susceptibility to oxidative stress. This has been observed in yeast which show severe $O_2$ hypersensitivity and reduced viability, together with decreased sporulation and reduced amino acid biosynthesis and increased mitochondrial protein carbonylation

(Liu et al. 1992;Longo et al. 1996;O'Brien et al. 2004). *Drosophila sod1* nulls display similar traits of paraquat (a herbicide superoxide generator) sensitivity, adult infertility, reduced lifespan and DNA damage (Phillips et al. 1989;Rogina and Helfand 2000;Woodruff et al. 2004), with genetic studies suggesting that the reduced longevity of *sod* mutants is due to an accelerated rate of ageing rather than an acquired pathological process (Rogina & Helfand 2000). In *C. elegans*, deletion of the major Cu Zn SOD, *sod-1*, is found to increase paraquat sensitivity and reduce lifespan modestly, however no hypersensitivity to mild hyperoxia is observed. Additionally deletion of the *sod-5* gene has no effect on any of the test parameters (Doonan et al. 2008). Studies in mice, reveal that an absence of *Sod1* results in paraquat sensitivity, reduced female fecundity, an increase in oxidative stress markers and shortened lifespan (Elchuri et al. 2004;Ho et al. 1998;Sentman et al. 2006). Interestingly, like with *C. elegans*, *sod1* deficient mice also appear tolerant to hyperoxia (Ho et al. 1998;Ho 2002). Furthermore, the shortened lifespan associated with the null mutants may be a result of hepatocellular carcinoma development (Elchuri et al. 2004), likely due to the high rate of DNA mutations observed in *sod1* knockout mice (Busuttil et al. 2005).

It is apparent that *sod1* mutations confer a phenotype more susceptible to oxidative stress with reduced lifespan. However, with regards to lifespan, it is unknown whether this reduction is due to the absence of *sod1* affecting pathways or molecules essential for life (for instance as might be concluded by the appearance of carcinoma's in *sod1* deficient mice) rather than those directly involving ageing. Methods that extend lifespan, however, are believed to function by changing or retarding the ageing process in some way. Thus *sod1* expression patterns in long-lived model species and transgenic *Sod1* over-expression have both been utilised to assess exactly how or if *Sod1* and/or oxidative stress resistance regulate longevity.

Using artificial selection, through delayed reproduction, a number of long lived *Drosophila* strains have been generated (Arking 1987;Luckinbill et al. 1984). In these long lived lines enhanced paraquat resistance is observed (Arking et al. 1991) as well as enhanced *sod1* and *cat* expression (Dudas and Arking 1995;Hari et al. 1998). Reverse selection of the long-lived strain for the normal-lived strain abolished the extended longevity phenotype, decreased antioxidant mRNA levels, specifically *sod1*,

and reduced antioxidant defence capacity (Arking et al. 2000). These studies suggest a tight correlation between oxidative protection, through SOD1 activity, and lifespan, thus supporting the 'free radical theory' of ageing. However, studies in other long-lived models present a different picture. For instance, long lived queens of the ant species, *Lasius niger*, have been found to have significantly decreased *sod1* gene expression and protein activity levels compared to considerably shorter lived males and workers of the same species (Parker et al. 2004b). Furthermore, naked mole rats, which can live up to eight times longer than similar sized rodents, have only moderately higher levels of SOD1 and other antioxidants (Andziak et al. 2005), thus not satisfactorily explaining this extended lifespan and additionally no difference in *sod1* or *sod2* expression was observed in two rodent species of significantly differing lifespan (Csiszar et al. 2007). These results suggest that perhaps longer-lived species produce lower rates of ROS and therefore have reduced SOD1 activity (Perez-Campo et al. 1998).

A number of transgenic tools are available in *Drosophila* to promote ectopic gene expression, thus this model species has been extensively employed to research the effect of *sod1* over-expression on lifespan and oxidative stress resistance. Whilst several experiments in which transgenic flies over-expressing native *sod1* showed no additional resistance to oxidative stress and no extended lifespan (Orr et al. 2003;Orr and Sohal 1993;Seto et al. 1990), other groups have demonstrated the ability of *sod1* over-expression to increased fly longevity and oxidative stress resistance (Orr and Sohal 1994;Parkes et al. 1998;Sun and Tower 1999), whilst high levels of *sod1* over-expression has been shown to be toxic (Reveillaud et al. 1991). This variable ability of *sod1* over-expression to extend lifespan has been proposed to be dependent upon the genetic background of the test strains of *Drosophila* and the method of over-expression used (Orr and Sohal 2003;Spencer et al. 2003). Studies in other organisms also suggest that *sod1* over-expression is insufficient to extend lifespan. For instance, mice show a marginal decrease in lifespan with *sod1* over-expression (Huang et al. 2000), with no enhanced paraquat resistance in whole animals despite elevated resistance in embryonic fibroblasts (Mele et al. 2006). Interestingly, over-expression of human *sod1* in mice has been found to cause a number of neurodegenerative phenotypes and motor abnormalities (Jaarsma et al. 2000) akin to FALS symptoms, as well as muscle wastage (Rando et al. 1998a). Conversely, in *C. elegans*, *sod1* over-

expression is found to promote modest lifespan extension (Doonan et al. 2008), and whilst supplementation with SOD mimetics has been found to extend longevity in some instances (Melov et al. 2000), in others no effect on lifespan is seen despite oxidative protection being observed (Keaney et al. 2004).

Whilst its role in lifespan regulation appears complex at best, manipulative studies of SOD1 to date at least demonstrate this antioxidant's importance in oxidative protection.

## 1.3.2 SOD2

### 1.3.2.1 Oxidative stress and lifespan

As stated previously, mitochondrial aerobic respiration is proposed to be one of the major sources of intracellular $O_2^{-}\cdot$ production. Additionally, since $O_2^{-}\cdot$ does not easily penetrate biological membranes SOD2 dysfunction can be predicted to result in serve phenotypes. Indeed, mice lacking *sod2* suffer a range of pathologies including, neo-natal lethality coupled with multiple organ complications (Li et al. 1995), progressive neurodegeneration (Lebovitz et al. 1996;Melov et al. 1998), significant hyperoxia sensitivity (Asikainen et al. 2002), together with mitochondrial respiratory chain enzyme dysfunction and increased oxidative DNA damage (Melov et al. 1999). *Sod2* also appears vital for survival in *Drosophila* with null mutants displaying severely reduced mortality and enhanced oxidative stress sensitivity, as well as mitochondrial respiratory chain enzymes defects, such as seen in mice (Duttaroy et al. 2003;Kirby et al. 2002). In other model species, however, the requirement of SOD2 is less well defined. For example, in yeast, knocking out *sod2* is found to dramatically increase ageing in an environmental oxygen dependent manner in the stationary phase of life, but have no effect during the logarithmic growth phase (Longo et al. 1996;Longo et al. 1999). In *C. elegans*, *sod-2* null strains are found to be hypersensitive to oxidative stress but show no change in lifespan (Doonan et al. 2008;Honda et al. 2008) or are found to have increased oxidative damaged but increased lifespan (Van Raamsdonk and Hekimi 2009).

*Sod2* over-expression, particularly in *Drosophila*, reveals contradictory results with regard to lifespan extension, similar to as is seen for *sod1* over-expression. For instance, evidence has been presented that *sod2* over-expression can extend lifespan in *Drosophila* (Phillips et al. 2000;Sun et al. 2002;Sun et al. 2004), however work from other labs suggests *sod2* over-expression is insufficient to influence longevity (Mockett et al. 1999;Orr et al. 2003), although oxidative protection can be conveyed (Bayne et al. 2005). Interestingly, while Bayne and colleagues observed increased resistance to oxidative stress, they found flies showed a decrease in lifespan of up to 43% with over-expression of *sod2* and *cat*. To my knowledge only one study has assessed the influence of *sod2* over-expression on lifespan in mice, revealing over-expression in hippocampal neurones to indeed increase longevity, together with reducing mitochondrial superoxide levels, but with no effect on memory (Hu et al. 2007). However, over-expression of *sod2* has been found to make animals no more resistant to hyperoxia induced oxidative stress (Ho 2002).

#### 1.3.2.2 Disease states

The severe phenotype observed in *sod2* deficient mice and *Drosophila* suggests that *sod2* is in some way crucial for survival in these organisms. In many cases the pathology underlying the neo-natal causes of death in these models is unknown, however it is likely the mechanisms involved will be the same as those found in many disease states. As described *sod2* null mice present a range of complications including neurodegeneration, and mutations in the *sod2* gene have been associated with the progression of both Parkinson's disease (PD) (Shimoda-Matsubayashi et al. 1996) and Alzheimer's disease (AD) (Wiener et al. 2007). Furthermore, increased *sod2* protein and activity levels have been found in ALS patients (Liu et al. 1998;McEachern et al. 2000), suggesting a casual link with the disease, whilst *sod2* over-expression has been found to protective against neurotoxic agents (Callio et al. 2005;Maragos et al. 2000). The observation of DNA damage in *sod2* null mice also suggests a link between *sod2* and cancer (Melov et al. 1999). Indeed decreased *sod2* expression has been observed in a number of carcinomas including pancreatic (Cullen et al. 2003), prostate (Best et al. 2005) and breast (Soini et al. 2001). Furthermore, whilst heterozygous *sod2* knockout mice show no accelerated ageing they do have increased tumour

development (Van et al. 2003) and *sod2* over-expression is shown to increase resistance to chemical carcinogens (Zhao et al. 2001) as well as reduce tumour proliferation (Cullen et al. 2003;Venkataraman et al. 2005).

## 1.3.3 SOD3

### 1.3.3.1 Oxidative stress and lifespan

In comparison with SOD1 and SOD2, relatively little is known about the ability of SOD3 to regulate lifespan in model systems, however there is evidence that this isoform protects against oxidative stress. For instance mice lacking *sod3* have relatively mild phenotypes, developing normally with no reduction in lifespan (Sentman et al. 2006), however they are found to die prematurely under hyperoxia (Carlsson et al. 1995), a feature not observed with *sod1* deficient mice (Ho et al. 1998). Furthermore, it is unclear whether *sod3* knockout mice suffer increased oxidative stress since one marker of oxidative stress (urinary isoprostane levels) has been found not to be elevated, whilst another marker (plasma thiobarbituric acid-reactive substances) has in this model (Sentman et al. 2006). Interestingly, in *C. elegans* extracellular Cu Zn SOD removal (*sod-4*) alone was also found to have no effect on lifespan and also no effect on oxidative stress sensitivity (Doonan et al. 2008;Van Raamsdonk & Hekimi 2009). However, surprisingly, *sod-4* knockout was found to increase the lifespan of longer lived *daf-2* mutants. The *daf-2* gene encodes a member of the insulin receptor family, mutations of which have been show to increase *C. elegans* lifespan through reduced insulin signalling (Gems et al. 1998;Houthoofd et al. 2003;Kimura et al. 1997). Furthermore, *daf-2* regulates whether *C. elegans* arrests at the dauer larvae stage of development (a quiescent state with extend longevity and high stress resistance (Larsen 1993)) or whether it proceeds into a reproductive lifecycle (Kimura et al. 1997). Doonan *et al*. suggest that an absence of *sod-4* reduces $H_2O_2$ production, which would normally function to promote insulin signalling by inhibiting redox-sensitive, signal-suppressing phosphatases, thus reducing insulin signalling and promoting longevity (Doonan et al. 2008). This proposal of reduced insulin signalling is supported by the authors' observation of increased dauer larva formation in *daf-2; sod-4* mutants.

*Sod3* expression is particularly high in the lungs (Folz et al. 1997), probably due to the level of direct exposure to oxygen encountered within airways, thus SOD3's dysfunction or over-expression in this organ can be critical for managing lung disease and injury. For instance, *sod3* knockout mice are significantly more vulnerable to hyperoxic lung injury (Carlsson et al. 1995) which is attenuated by transgenic *sod3* over-expression (Auten et al. 2006;Folz et al. 1999) which also protects against hyperoxia induced pulmonary hypertension (Nozik-Grayck et al. 2008). Furthermore, under hyperoxic conditions, SOD3 levels are found to decrease in lung tissue of mice in an mRNA independent manner by apparent proteolytic cleavage of the heparin-binding domain (Oury et al. 2002). This may further propagate pulmonary injury by disturbing the oxidant/antioxidant redox state of the lungs.

#### 1.3.3.2 Disease states

Since SOD3 is the only known enzymatic extracellular scavenger of $O_2^{-}\cdot$ it has been proposed to play a role in the pathology of a number of diseases. Along with the lungs, *sod3* expression is also high in blood vessels (Oury et al. 1996;Stralin et al. 1995), and thus has been suggested as important in the pathophysiology of many vascular-related diseases. Atherosclerosis is one such disease and is associated with increased ROS secretion, particularly $O_2^{-}\cdot$, from cells within the atherosclerotic lesion (Fukai et al. 1998;Mugge et al. 1994;Ohara et al. 1993). A number of atherosclerotic-promoting growth factors have been found to down-regulate *sod3* in vascular smooth muscle cells (Stralin and Marklund 2001), whilst over-expression of *sod3* has been found to inhibit low-density lipoprotein oxidation (Takatsu et al. 2001), an important factor in atherosclerosis development (Kita et al. 2001). Furthermore, Fukai and colleagues discovered a novel, mutated SOD3 which increased with the progression of atherosclerosis (Fukai et al. 1998). Increased $O_2^{-}\cdot$ levels due to reduced SOD3 are also proposed to exacerbate atherosclerotic lesion formation by reacting with NO·, to form $ONOO^{-}$ which is a potent mediator of lipoprotein oxidation (White et al. 1994). Furthermore, NO· occupation will interfere with its ability to regulate vascular tone. Other vascular diseases in which *sod3* plays a role include diabetes, where glycation of SOD3 is associated with reduced heparin affinity leading to an accumulation of glycated SOD3 in diabetes patients (Adachi et al. 1994), and ischemia/reperfusion

injury, in which transgenic mice over-expressing *sod3* show increased cardiac protection following injury (Chen et al. 1998).

*Sod3* has also been proposed to play a role in neurological functioning and disease. For example, both knockout and over-expression of *sod3* has been shown to impair long term potentiation (Levin et al. 1998;Levin et al. 2000;Thiels et al. 2000), however improved memory has been observed in ageing mice over-expressing SOD3 (Levin et al. 2005). These results suggest that, rather than being neurotoxic, extracellular sources of $O_2^{-}\cdot$ in the brain may in fact function as important signalling molecules. Furthermore, SOD3 has been shown to be important in regulating cerebral vascular tone by preventing $NO\cdot$ inactivation (Demchenko et al. 2010). Additionally, after traumatic brain injury transgenic *sod3* over-expressing mice show more rapid neurological recovery (Pineda et al. 2001), while increased heparin-dissociated mutant SOD3 levels have been found in patients suffering from familial amyloidotic polyneuropathy type 1 (FAP), an autosomal dominant disease characterised by amyloid deposition around blood vessels (Sakashita et al. 1998).

## 1.4 Conclusions about the biological significance of the SODs

The importance of the SOD isoforms in a variety of disease processes has been well documented (see above). However, there does not seem to be a common mechanism by which disease pathology is propagated in relation to SOD dysfunction. The most attractive theory would seem to suggest that an absence of SOD results in disease states through the accumulation of oxidative damage by unscavenged ROS. Whilst this may be the case in many cancer types, characterised by oxidative DNA damage in *sod2* null mice (Melov et al. 1999), or in hyperoxic lung injury in *sod3* mutants (Carlsson et al. 1995), the neurodegenerative disease FALS results from *sod1* mutants acquiring toxic, pro-oxidant, gain of function properties (Mockett et al. 2003), while both under- and over-expression of *sod3* have been shown to impair neurological function (Levin et al. 1998), suggesting a pathology characterised by disturbed redox signalling, most likely through altered $H_2O_2$ production. Furthermore, excessive *sod* over-expression has been associated with a number of disorders including muscular

dystrophy (Rando et al. 1998b) and Down's syndrome (Groner et al. 1994). Thus the SOD enzymes role in disease pathology, while crucial, appears complex. While enzymatic levels must be high enough to prevent oxidative damage occurring, they must, at the same time, be sufficient to regulate, but not disturb, critical signalling cascades.

### 1.4.1 Oxidative stress and lifespan

To date, evidence suggests that while SOD levels are important in regulating oxidative sensitivity, their influence on lifespan and ageing is contentious. While *sod1* mutations are found to reduce lifespan only modestly in mice and *C. elegans* (Doonan et al. 2008;Sentman et al. 2006), they dramatically reduce the lifespan of *Drosophila* (Phillips et al. 1989;Rogina & Helfand 2000;Woodruff et al. 2004) and yeast (Liu et al. 1992;Longo et al. 1996;O'Brien et al. 2004). Over-expression of *sod1* is found to have no effect on mice lifespan (Huang et al. 2000), marginally increase *C. elegans* lifespan (Doonan et al. 2008) but can significantly increase the lifespan of *Drosophila* (Orr & Sohal 1994;Parkes et al. 1998;Sun & Tower 1999), dependent on genetic background. In the case of *sod2* deficient mutants, early life mortality is observed in mice (Li et al. 1995) and *Drosophila* (Duttaroy et al. 2003;Kirby et al. 2002), but no effect is seen on the lifespan of *C. elegans* (Doonan et al. 2008;Honda et al. 2008). *sod2* over-expression can extend the lifespan of both *Drosophila* (Phillips et al. 2000;Sun et al. 2002;Sun et al. 2004), again dependent upon genetic background, and mice (Hu et al. 2007). *Sod3* dysfunction is found to have no effect on mice lifespan (Sentman et al. 2006), but is found to extend *C. elegans* lifespan in conjunction with mutants promoting decreased insulin signalling (Doonan et al. 2008). Thus it appears that whilst SOD can regulate longevity in some organisms, and in certain genetic backgrounds, it does not appear to be a common mechanism by which organisms control ageing. As scavengers of ROS, the SODs are important in protection against macromolecular oxidative damage, however the observation of $O_2^{-}\cdot$ and particularly $H_2O_2$ as important cellular signalling molecules means that the downstream consequences of altered SOD levels in response to ROS are complex and significant work is still required to unravel how these signalling cascades function to regulate disease, ageing and lifespan.

## 1.5 Aims of this thesis

As has been described previously, compared with *sod1* and *sod2*, relatively little is known about the *in vivo* function of the extracellular *sod3* gene. This has been primarily due to the absence of short lived model systems, particularly insect species, in which initial genetic and phenotypic studies would usually be carried out. As has been discussed, the *Drosophila sod3* gene was only recently discovered, and to date there has been no published work detailing any aspects of this gene in this model species. Furthermore, presently all oxidative stress and longevity data from *Drosophila* in which SOD1 and/or SOD2 activity has either been removed (using null-mutants) or increased (by transgenic overexpression), has been interpreted based on the assumption that no SOD3 existed. Therefore the aim of this study was to use genetic and biochemical approaches to characterise the molecular features of the *sod3* gene in *Drosophila*. Results of this work will not only provide important information about a gene that was previously thought to be absent in insect species, but it will also provide the foundations upon which further *sod3* characterisation work in mammalian models can be carried out.

Furthermore, it is thought that characterising the *Drosophila sod3* gene will resolve a number of concerns surrounding the SOD family. For instance, why was SOD3 never detected in *Drosophila* before Parker *et al*. (2004) discovered it? Phillips *et al.* (1989) used adult fly homogenates and gel electrophoresis to analyse Cu Zn SOD levels in his *Sod1* mutational studies and picked up no SOD activity. Since there is currently no means of distinguishing between SOD1 and SOD3 activity if the two are not separated during isolation (Parker et al. 2004a), the observation of no Cu Zn SOD activity in *Sod1* mutants is somewhat surprising given the knowledge that a *sod3* gene is present. It is also thought that characterising the *sod3* gene may encourage re-interpreting of the previous transgenic data with *sod1* and *sod2* and might help to explain the conflicting longevity results described with transgenic *sod1* and *sod2* overexpression.

The following chapters detail the experimental work carried out and results obtained to characterise the *Drosophila sod3* gene.

# CHAPTER 2

# 2. Cloning and sequencing of the *Drosophila sod3* transcript

## 2.1 Aim

This chapter details the steps taken to experimentally verify the presence of the extracellular *sod* gene in *Drosophila*.

## 2.2 Introduction

SOD3 is the least well characterised and most recently discovered of the SOD family. The human form of SOD3 was first identified in extracellular fluids and lung tissue around 30 years ago (Marklund et al. 1982;Marklund 1982), while the first invertebrate extracellular *Sod* gene was not identified until 1998 in *C. elegans* (called *sod-4*) (Fujii et al. 1998). The discovery of insect genes apparently belonging to the extracellular *sod* family were only discovered more recently through molecular phylogenetic analysis of insect gene sequences following cloning and sequencing of a *sod* mRNA in the ant species *Lasius niger* (Parker et al. 2004a).

Mammalian SOD3 is composed of three distinct domains: an N-terminal hydrophobic secretion peptide, a Cu Zn SOD like domain, and a C-terminal heparin-binding domain (Folz et al. 1997). Although sharing significant homology with SOD1, the copper co-factor loading pathway of SOD3 is dissimilar to that of SOD1. The metal co-factor is not inserted by the CCS copper chaperone, but rather the secreted protein is loaded with copper within the secretory compartments (Culotta et al. 2006). The heparin-binding domain of mammalian SOD3 is formed by a cluster of positively charged amino acids within the C-terminal region. The proteoglycan heparan-sulfate is present on cell surfaces and within the extracellular matrix and the ability of SOD3's heparin-binding domain to electrostatically interact with heparan-sulfate is

key to maintaining SOD3 localisation (Karlsson et al. 1988). Three different forms of mammalian SOD3 have been characterised based on their affinity for heparin: A, B and C, with no affinity, low affinity and high affinity for heparin, respectively (Karlsson et al. 1988;Marklund 1982) (Figure 2.1). Most tissue SOD3 is found as the C form and this accounts for 90-99% of the total SOD3 in the body (Fattman et al. 2003;Marklund 1984b). Whilst the tissue distribution of SOD3 varies within mammalian species, highest concentrations are found in the lungs, kidneys and the uterus (Marklund 1984a;Marklund 1984b), where its activity can exceed that of SOD1 and SOD2 (Zelko et al. 2002).

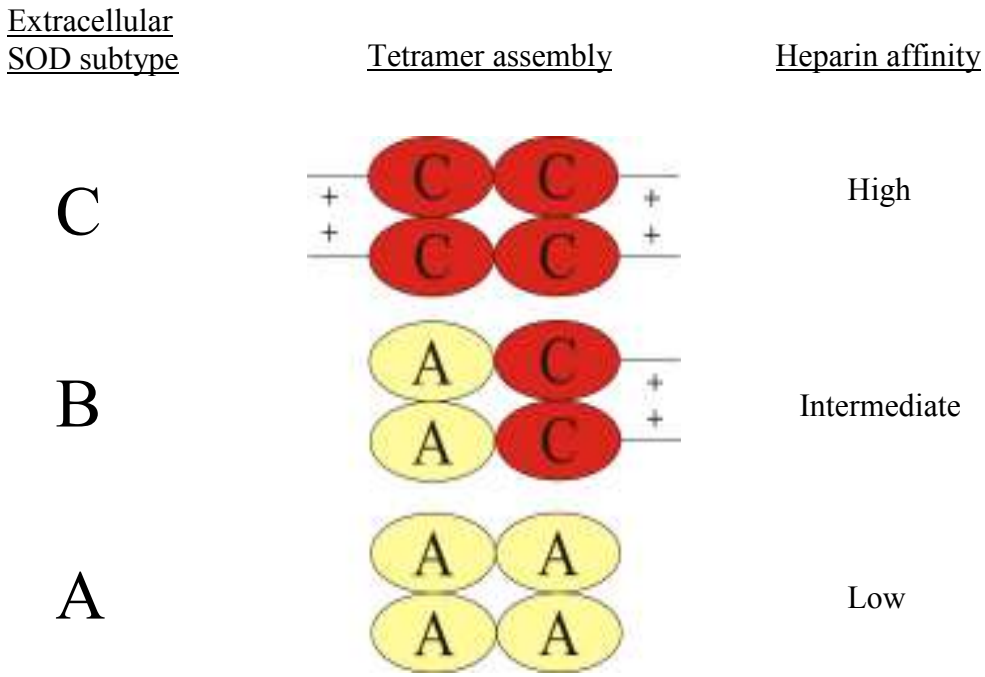


**Figure 2.1. Illustration of the tetrameric assembly of the heparin binding C-terminal domains of the 3 members of the mammalian SOD3 family.** The heparin binding domains are maintained by intersubunit disulfide bonds. Figure recreated from (Fattman et al. 2003).

In mammals, the A and B forms are believed to be circulating forms of SOD3 found in plasma, whilst the C form is thought to exist attached to endothelial cell surfaces, but has been shown to release into the plasma upon intravenous injection of heparin (Karlsson and Marklund 1988a;Karlsson and Marklund 1988b). Interestingly, the heparin-binding sequence has also been shown to act as a nuclear localisation signal in a number of cell types (Ookawara et al. 2002). Consequently, SOD3 is proposed to provide DNA and nuclear proteins with antioxidant protection, as well as being a

scavenger of exogenous ROS in mammals. It would, however, appear that this heparin-binding domain is not be present in invertebrates. Upon cloning *sod4-1* and *sod4-2* in *C. elegans*, Fujii *et al.* (1998) noted that there existed no positive cluster of amino acids in the C-terminus end corresponding to a conserved heparin-binding domain. Rather the membrane bound form of the protein was generated by inserting a hydrophobic region into the C-terminus (Fujii et al. 1998).

This chapter describes the work undertaken to clone and sequence the *sod3* gene in *Drosophila*, with the aims of experimentally verifying that the gene is expressed and identifying the mechanisms by which the gene is assembles.

## 2.3 Materials and methods

### 2.3.1 Genomic DNA preparations

Three adult *Oregon R* flies (a gift from Dr K Ubhi, University of California, San Diego) were anaesthetised by placing the tube containing them on ice. Each fly was then transferred into a separate 0.5mL microfuge tube containing 50µL of Squishing Buffer (10mM Tris-Cl (pH 8.2), 1mM EDTA, 25mM NaCl and 200µg/mL proteinase K). Using a pipette tip, each fly was homogenised in the Squishing Buffer and then each tube was incubated at 37°C for 20 mins. Each tube was then subjected to a further incubation at 95°C for 2 mins in order to inactivate the proteinase K. Genomic preparations were stored at 4°C until required.

### 2.3.2 Primer design

Nested gene specific primers were designed based on the alignment of the GenBank (http://www.ncbi.nlm.nih.gov/genbank/) nucleotide sequences of four *Drosophila sod3* variants, predicted from expressed sequence tag (EST) data (GenBank accession numbers: NM_165829 (transcript variant A); NM_136838 (transcript variant B); NM_001038850 (transcript variant C); NM_001043071 (transcript variant D)) with the complete *Drosophila* chromosome 2R genomic sequence (GenBank accession number AE013599) (Table 2.1). All sequence alignments were performed using the BioEdit Sequence Alignment Editor programme. Primers were designed such that: the C:G content was ~50%; the length was no longer than 24 nucleotides; primers had minimal propensity to form secondary structures; primers did not form dimers; and the melting temperatures were within approximately 1°C of each other.

**Table 2.1. *Sod3* gene specific primer sequences**

| Primer name | Primer sequences |
|---|---|
| 3' outer nested | 5'-TTGCCTATCTGATTGGACCCGT-3' |
| 3' inner nested | 5'-ACGGCTTCCACATTCACGAGAA-3' |
| 5' outer nested | 5'-CCAATAACACCACACAGGCAATGC-3' |
| 5' inner nested | 5'-CAACAACTCCCCTGCCAATGAT-3' |

All primers were reconstituted in nuclease-free $H_2O$ (Ambion, Inc.) to a concentration of 100μM according to the manufacturer's instructions (Sigma Genosys), and used at a concentration of 10μM in polymerase chain reactions (PCRs).

### 2.3.3 RNA

Adult, larval and embryo poly(A)$^+$ RNA (5μg) were purchased from Clontech Laboratories, Inc. and used in the subsequent RLM-RACE experiments.

### 2.3.4 RNA Ligase Mediated – Rapid Amplification of cDNA ends (RLM-RACE)

#### 2.3.4.1 RLM-RACE theory

The *Drosophila sod3* gene was cloned by RNA Ligase Mediated Rapid Amplification of cDNA Ends (RLM-RACE). Traditional Rapid Amplification of cDNA Ends (RACE) is a technique employing polymerase chain reaction (PCR) to clone full-length cDNA sequences, often from low abundance or complex DNA mixtures (Frohman et al. 1988;Schaefer 1995). Typically, first strand cDNA is synthesized from either total or poly(A) RNA in a reverse transcription reaction. The 5' and 3' ends of the cDNA are then amplified following attachment of oligonucleotide adapters to each end of the cDNA to which specific primers can attach. The principal inadequacy of conventional RACE stems from the lack of specificity for fragments corresponding to the actual 5' ends of mRNA. Reverse transcriptases are often prematurely terminated resulting in stunted cDNAs and since all cDNAs make suitable templates, the RACE PCR steps will preferentially produce smaller, non-full length amplicons, resulting in a heterogeneous population of products.

With RLM-RACE, oligonucleotide adapters are ligated directly to the 5' and 3' ends of mRNA species prior to cDNA synthesis, thus improving on conventional RACE techniques by amplifying only cDNA from full-length, capped mRNA (Liu and

Gorovsky 1993). cDNA sequences are then amplified using a combination of adapter specific and gene specific primers (Figure 2.2).

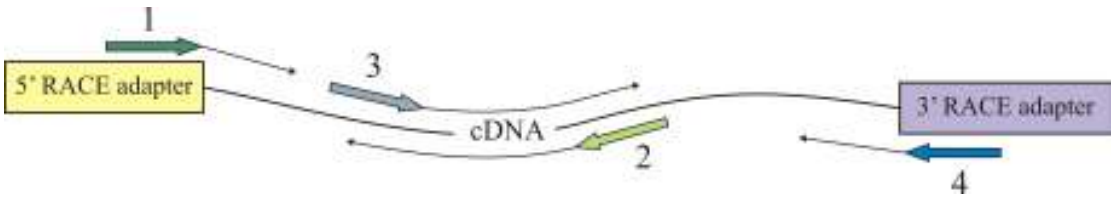


**Figure 2.2. Illustration of the RLM-RACE theory.** Following adapter ligation to full length mRNA species, first strand cDNA is synthesised and adapter specific and gene specific primers are employed to amplify overlapping portions of the target cDNA. 1 = 5' RACE specific primer; 2 = 5' gene specific primer; 3 = 3' gene specific primer; 4 = 3' RACE specific primer.

### 2.3.4.2 5' RNA processing

Each RNA sample (adult, larval and embryo) underwent RNA processing to attach an adapter to the 5' end of the capped mRNA, according to the RLM-RACE manufactures protocol (Ambion, Inc.). Firstly, the RNA samples were treated with Calf Intestine Alkaline Phosphatase (CIP) to remove 5'-phosphates from contaminating and fragmented RNA and DNA, as follows: 250ng of the poly(A)$^+$ RNA sample (adult, larval or embryo) was added to 2µL 10X CIP buffer (Ambion, Inc), 2µL CIP (Ambion, Inc.) and made up to 20µL with nuclease-free $H_2O$. The mixture was mixed, spun briefly and then incubated at 37°C for 1 hour. The CIP reaction was terminated by the addition to the mixture of 15µL ammonium acetate solution (Ambion, Inc.), 115µL nuclease free $H_2O$ and 150µL acid phenol:chloroform (Ambion, Inc.). This mixture was vortexed and centrifuged at 13,200 rpm for 5 mins at room temperature. The aqueous layer was then transferred to a new 1.5mL microfuge tube and 150µL of chloroform (Ambion, Inc.) was added to this. This mixture was vortexed, centrifuged at 13,200 rpm for 5 mins at room temperature and again the aqueous phase was transferred to a new tube. To this, 150µL of isopropanol (Sigma) was added and the mixture was chilled on ice for 10 mins. The mixture was then centrifuged at 13,200 rpm for 20 mins and the pellet was rinsed in 0.5mL cold 70% ethanol. After another 5 mins centrifugation at 13,200 rpm at room temperature the ethanol was removed and the pellet allowed to air dry. The pellet was resuspended in 11µL of nuclease free $H_2O$ and placed on ice for use in the following de-capping

step. The cap structure which is present on full length mRNA molecules required removing. This was achieved through treatment of the CIP treated RNA with Tobacco Acid Pyrophosphate (TAP) as follows: 5µL CIP'd RNA was combined with 1µL 10X TAP buffer (Ambion, Inc.), 2µL TAP (Ambion, Inc.) and 2µL nuclease-free $H_2O$. This was mixed, spun briefly and incubated at 37°C for 1 hour. This mixture was then used in the flowing ligation step. Treatment with TAP leaves a 5'-monophosphate exposed to which a 5'-adapter can be ligated as follows: 2µL CIP/TAP-treated RNA is mixed with 1µL 5'RACE adapter, 1µL 10X ligase buffer, 2µL T4 RNA ligase (2.5U/µL) and 4µL nuclease-free $H_2O$. This was mixed, spun briefly and incubated at 37°C for 1 hour to complete adapter ligation. This 5' adapter provides the region to which the 5'RACE inner and outer primers can bind in subsequent PCR reactions.

#### 2.3.4.3 3' RNA processing

Unlike RNA to be used in 5' RLM-RACE, RNA molecules for 3' RACE do not require any processing since the adapter can ligate directly to the poly(A) tail present at the 3' end of RNA molecules.

#### 2.3.4.4 Reverse transcription

First strand complementary DNA (cDNA) was prepared from the 5' ligated RNA according to the RLM-RACE handbook (product of the ***RLM-RACE: 5' RNA processing*** step) as follows: 2µL of ligated RNA was mixed with 4µL dNTP mix (Ambion, Inc.), 2µL random decamers (Ambion, Inc.), 2µL 10X RT buffer (Ambion, Inc.), 1µL RNase inhibitor (Ambion, Inc.), 1µL M-MLV reverse transcriptase (Ambion, Inc.) and 8µL nuclease-free $H_2O$. The mixture was mixed, spun briefly and incubated at 42°C for 1 hour. This mixture was used in subsequent PCR reactions.

3' reverse transcription was achieved by mixing 2µL of 50ng poly(A)$^+$ RNA (adult, larval or embryo) with 4µL dNTP mix, 2µL 3'RACE adapter, 2µL 10X RT buffer, 1µL RNase inhibitor, 1µL M-MLV reverse transcriptase and 8µL nuclease-free $H_2O$. This was mixed, spun briefly and incubated at 42°C for 1 hour. This mixture was used in subsequent PCR reactions. The resulting cDNA had a 3' adapter ligated to the

poly(A) tail and it is to this adapter that the 3'RACE inner and outer primers can bind in the subsequent PCR reactions.

## 2.3.5 Polymerase Chain Reactions (PCRs)

### 2.3.5.1 PCR of genomic DNA preparations

PCRs were initially performed on the 3 genomic DNA samples in order to validate the nested gene specific primers designed. Different combinations of the 5' and 3' inner and outer nested primers were tested in order to confirm the presence of PCR products of the predicted size with genomic DNA (Table 2.2). PCR reactions were prepared in 200µL thin walled PCR reaction tubes (Abgene) as follows: 1µL genomic DNA was mixed with 2µL 10X PCR Buffer (Qiagen), 0.4µL 10mM dNTP mix (10mM each of dATP, dGTP, dCTP and dTTP) (Qiagen), 0.4µL 10µM 5' inner or outer nested primer, 0.4µL 10µM 3' inner or outer nested primer, 0.1µL of 5U/µL Taq DNA polymerase (Qiagen) and made up to 20µL with nuclease-free $H_2O$. The mixture was mixed, spun briefly and then subjected to PCR using the DNA Engine tetrad 2® thermocycler (MJ Research). Thermocycling conditions used are shown in Table 2.3.

**Table 2.2. Predicted PCR product size with different combinations of gene specific primers using genomic DNA as the template.**

| Primer Combination | Predicted PCR product size (bp) |
|---|---|
| 5' outer nested* + 3' outer nested | no product |
| 5' inner nested + 3' inner nested | 290 |
| 5' outer nested* + 3' inner nested | no product |
| 5' inner nested + 3' outer nested | 419 |

*5' outer nested primer spans an intron thus produces no product when genomic DNA is used as the template.

**Table 2.3. Thermocycling conditions for PCR amplification of genomic DNA preparations.**

| Steps | Incubation time | Temperature (°C) |
|---|---|---|
| **1. Hot start** | - | 94 |
| **2. Initial denaturation** | 3 mins | 94 |
| **3. 3 step cycling** | - | - |
| Denaturation | 45 sec | 94 |
| Annealing | 45 sec | 63 |
| Extension | 1 min | 72 |
| **4. 29 more cycles to step 3** | - | - |
| **5. Final extension** | 10 mins | 72 |

### 2.3.5.2 RLM-RACE PCR

cDNA produced by the RLM-RACE steps were subjected to PCR using different combinations of either:

i) one of the 5' gene specific primers (outer nested or inner nested) designed above with one of the 5'RACE adapter specific primers (outer or inner)
ii) one of the 3' gene specific primers (outer nested or inner nested) with either of the 3'RACE adapter specific primers (outer or inner) supplied.
iii) either of the 5' gene specific primers with one of the 3' gene specific primers.

Using different combinations of these primers in our PCR reaction generated different length products of predicted sizes (Table 2.4).

PCR reactions were set up according to the RLM-RACE protocol. That is: 1µL of cDNA (product of the **2.3.4.4 Reverse transcription** step) was mixed in a 200µL thin walled PCR tube (Abgene) with 5µL 10X PCR buffer, 4µL dNTP mix, 2µL of the gene specific primer (10µM), 2µL RACE primer or 2µL alternative gene specific primer (10µM), 0.25µL of 5U/µL Taq DNA polymerase (Qiagen) and made to 50µL with nuclease-free $H_2O$. The reaction was mixed, spun briefly and then subjected to PCR using a DNA Engine tetrad 2® thermocycler. Typical thermocycling conditions used are shown in Table 2.5, however annealing temperatures and extension times were often varied to optimise the desired PCR products.

**Table 2.4. Predicted PCR product size for each GenBank variant for different combinations of RACE and gene specific primers using cDNA as the template.**

| GenBank® variant | Primer combination | Predicted PCR product size (bp) |
|---|---|---|
| A | 5' RACE outer + 5' outer nested | 679 |
| | 5' RACE inner + 5' inner nested | 576 |
| | 5' RACE outer + 5' inner nested | 583 |
| | 5' RACE inner + 5' outer nested | 672 |
| | 3' RACE outer + 3' outer nested | 759 |
| | 3' RACE inner + 3' inner nested | 630 |
| | 3' RACE outer + 3' inner nested | 630 |
| | 3' RACE inner + 3' outer nested | 759 |
| B | 5' RACE outer + 5' outer nested | 824 |
| | 5' RACE inner + 5' inner nested | 720 |
| | 5' RACE outer + 5' inner nested | 727 |
| | 5' RACE inner + 5' outer nested | 817 |
| | 3' RACE outer + 3' outer nested | 759 |
| | 3' RACE inner + 3' inner nested | 630 |
| | 3' RACE outer + 3' inner nested | 630 |
| | 3' RACE inner + 3' outer nested | 759 |
| C | 5' RACE outer + 5' outer nested | 2357 |
| | 5' RACE inner + 5' inner nested | 2256 |
| | 5' RACE outer + 5' inner nested | 2263 |
| | 5' RACE inner + 5' outer nested | 2350 |
| | 3' RACE outer + 3' outer nested | 754 |
| | 3' RACE inner + 3' inner nested | 625 |
| | 3' RACE outer + 3' inner nested | 625 |
| | 3' RACE inner + 3' outer nested | 754 |
| D | 5' RACE outer + 5' outer nested | 680 |
| | 5' RACE inner + 5' inner nested | 576 |
| | 5' RACE outer + 5' inner nested | 583 |
| | 5' RACE inner + 5' outer nested | 673 |
| | 3' RACE outer + 3' outer nested | 953 |
| | 3' RACE inner + 3' inner nested | 824 |
| | 3' RACE outer + 3' inner nested | 824 |
| | 3' RACE inner + 3' outer nested | 953 |
| A, B, C and D | 5' outer nested + 3' outer nested | 450 |
| | 5’ outer nested + 3’ inner nested | 321 |
| | 5’ inner nested + 3’ outer nested | 356 |
| | 5’ inner nested + 3’ inner nested | 227 |

**Table 2.5. Thermocycling conditions for PCR amplification of RLM-RACE PCR products.**

| Steps | Incubation time | Temperature (°C) |
|---|---|---|
| **1. Hot start** | - | 94 |
| **2. Initial denaturation** | 3 mins | 94 |
| **3. 3 step cycling** | - | - |
| Denaturation | 30 sec | 94 |
| Annealing | 30 sec | 55 – 65* |
| Extension | 30 sec | 72 |
| **4. 34 more cycles to step 3** | - | - |
| **5. Final extension** | 7 mins | 72 |

*annealing temperature varied depending on the primer pairs but was usually tested at ~5°C below the Tm of the primers.

### 2.3.5.3 Gradient PCR of RLM-RACE cDNA

In instances where the Tm of the primer pairs differed dramatically gradient PCRs of the RLM-RACE cDNAs were performed to determine the optimum annealing temperatures for PCR product production. PCR reactions were assembled according to the methods detailed in section **2.3.5.2 RLM-RACE PCR**, and carried out with thermocycling conditions as listed in Table 2.6, in the DNA Engine tetrad 2® thermocycler.

**Table 2.6. Gradient PCR thermocycling conditions of RLM-RACE PCR products.**

| Steps | Incubation time | Temperature (°C) |
|---|---|---|
| **1. Hot start** | - | 94 |
| **2. Initial denaturation** | 3 mins | 94 |
| **3. 3 step cycling** | - | - |
| Denaturation | 30 sec | 94 |
| Annealing gradient | 30 sec | 55 – 65 |
| Extension | 30 sec | 72 |
| **4. 34 more cycles to step 3** | - | - |
| **5. Final extension** | 7 mins | 72 |

## 2.3.6 Gel electrophoresis

PCR products were revealed on 1-2% (depending on the size of the product expected) (w/v) agarose (Sigma)/TAE (40mM Tris/acetate (pH 8.0), 1mM EDTA) gels containing 1µL Ethidium Bromide (Fisher Scientific). Following gel setting, 10µL of PCR amplified DNA was mixed with 2µL of 6X type III gel loading buffer (0.25%

bromophenol blue, 0.25% xylene cyanol FF and 30% glycerol in $H_2O$), and the whole 12µL was loaded onto the gel. Additionally, 5µL of either 100 bp low ladder (Sigma) or 1 kb ladder (Sigma), depending on the size of product expected, was mixed with 5µL $dH_2O$ and 2µL 6X type III gel loading buffer and loaded onto the gel to assess PCR product size. The gel tank was filled with 1X TAE buffer and run at 110 volts for 45 mins with a Powerpac 300 (Bio-Rad), before visualising under UV light.

## 2.3.7 Subcloning

Candidate PCR products to be sequenced were run on large 100mL 1-2% agarose/TAE gels. Appropriate PCR bands were cut from the gels with a scalpel and transferred to a 1.5mL microfuge tube. After weighing the gel slice the DNA was purified on spin columns according to the Qiagen QIAquick spin protocol (Qiagen). Purified DNA was quantified spectrophotometrically by applying 1µL to a NanoDrop ND-1000 spectrophotometer (NanoDrop Technologies). Isolation of correct bands was also reconfirmed by running 5µL of the purified DNA sample on a 2% agarose/TAE gel.

### 2.3.7.1 Ligations and transformations of pGEM®-T Easy Vectors

The purified DNA was then subcloned by ligation into pGEM®-T Easy Vectors (Promega) (Figure 2.3) as follows: 3µL of purified DNA (PCR product) was added to 5µL 2X rapid ligation buffer, 1µL pGEM®-T Easy Vector (50ng) and 1µL T4 DNA ligase (3 Weiss units/µL). The reaction was mixed by pipetting and incubated for 1 hour at room temperature. High-efficiency competent cells (JM109) ($\geq 1 \times 10^8$cfu/µg DNA) were then transformed with the ligated vectors. 50µL of cells was mixed with 2µL of ligation reaction, placed on ice for 20 mins, heat-shocked at 42°C for 45-50 secs and placed back on ice again for 2 mins. Nine hundred and fifty microlitres of SOC medium (Invitrogen) was added to the reaction and the mixture was incubated for 1.5 hours at 37°C with constant shaking. One hundred microlitres of transformation culture was transferred on to pre-made duplicate LB Agar (1% Tryptone, 0.5% yeast extract, 1% NaCl and 1.5% Agar in $dH_2O$, adjusted pH to 7.0 and autoclaved) culture plates supplemented with 100µg/ml ampicillin (Sigma)

(hereafter referred to as LBA/amp plates) and with 100µL of 100mM IPTG (Promega) and 20µL of 50mg/ml X-Gal (Promega) spread on the plate surface (hereafter referred to as LBA/amp/IPTG/X-Gal plates). Plates were incubated overnight at 37°C. White colonies observed were assumed to contain PCR inserts.

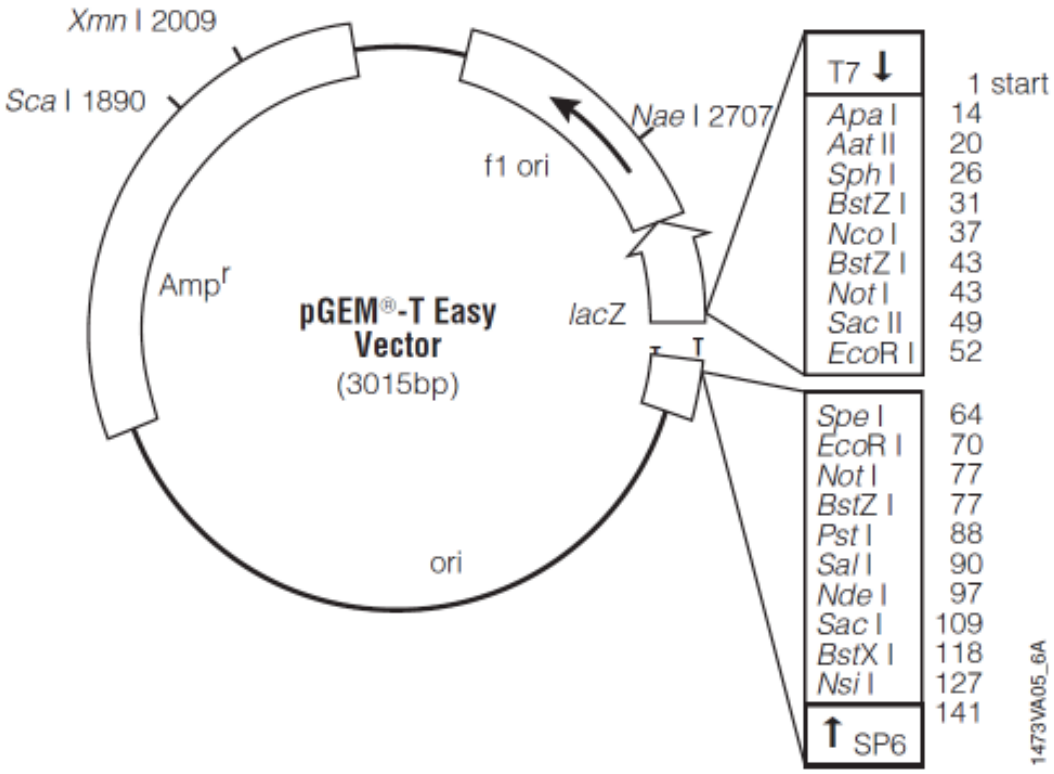


**Figure 2.3. pGEM®-T Easy Vector circle map.** Taken from the Promega pGEM®-T and pGEM®-T Easy Vector System technical manual.

Selected single white colonies were cultured by smearing onto a new LBA/amp plate and incubated overnight at 37°C. PCR reactions were run of each colony to confirm the presence of inserts. After overnight incubation white colonies were grown up in 4mL LB medium with ampillicin added to a final concentration of 100µg/mL. The bacterial cells were harvested by centrifugation at 10,000 rpm for 3 mins at room temperature. The DNA plasmids were purified according to the QIAprep spin mini prep protocol (Qiagen). One microlitre of the resulting purified plasmid DNA was quantified on the NanoDrop spectrophotometer and PCRs were run again to confirm the presence of the correct inserts following purification. A minimum concentration of 100ng/µL DNA was required for sequencing of the PCR inserts.

### 2.3.8 DNA sequencing

Sequencing of the DNA inserts was carried out by Microsynth AG, Switzerland. Thirty microlitres of purified DNA plasmid was supplied at a concentration of 100ng/µL. The plasmids were sequenced in both directions from the T4 and SP6 promoters present on the pGEM®-T Easy Vector.

## 2.4 Results

### 2.4.1 Validation of primers

The nested gene specific primers listed in Table 2.2 were first verified against adult *Drosophila* genomic DNA, which also served to corroborate preliminary working PCR conditions. Figure 2.4 illustrates PCR products produced with 3 biological replicates of adult flies when either the 5' and 3' inner nested primer sets were tested together (lanes 1 – 4) or when the outer nested primers were used (lanes 5 – 8) (lanes 4 and 8 are no DNA controls with respective primer pairs). As predicted, each fly sample tested with the 5' and 3' inner gene specific primers produced a single band at 290 bp, whereas no product was found when the 5' and 3' outer gene specific primers, due to the 5' primer lying across an intron/exon junction.

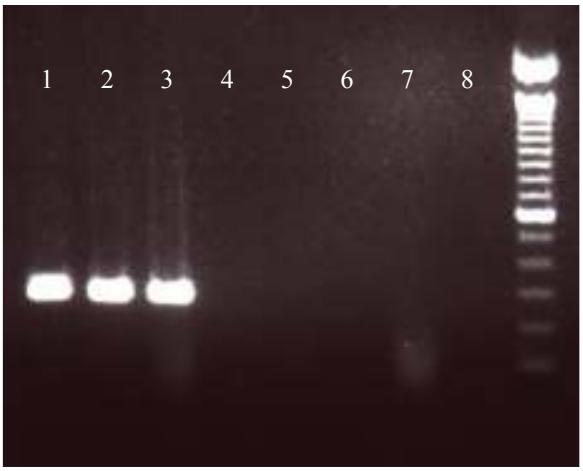


**Figure 2.4. PCR products of adult fly genomic DNA preparations.** Lanes 1 – 3 = adult fly samples, lane 4 = no DNA control – all with 5' inner gene specific and 3' inner gene specific primers; Lanes 5 – 7 adult fly samples, lane 8 = no DNA control – all with 5' outer gene specific and 3' outer gene specific primers. Samples are run against a 100bp ladder.

### 2.4.2 RLM-RACE: PCR products

Since the nucleotide sequence of the four *Drosophila sod3* variants is available through GenBank it was possible to predict the size of the expected PCR products (Table 2.4). Alignment of the available sequences with the genomic *Drosophila*

sequence also meant PCR product size could be predicted if the primers bound to any genomic DNA present through contamination. Figure 2.5 illustrates PCR products (on agarose gels) produced through RLM RACE. 5' RLM-RACE PCR with inner gene specific and inner RACE primers produced products at 581 bp for each cDNA sample (adult, larval and embryo) (Figure 2.5A). More interesting were the products of the 3' RLM-RACE PCR. For each cDNA, when tested with outer gene specific and RACE primers, a prominent band was visible at 848 bp; however a second band at 720 bp was also visible, most prominently in the embryonic cDNA sample (Figure 2.5B). The bright bands at ~160 bp are likely due to primer dimer formation. To confirm that the 720 bp product was definitely present in adult cDNA samples, a gradient PCR was performed to find the optimal primer annealing temperature (55–65°C) that could help amplify this particular PCR product (Figure 2.5C). At an annealing temperature of 65°C this second band became clearly discernable from the 848 bp product with the adult cDNA. Products to be subcloned and sequenced were re-run on large agarose gels and excised and purified as specified in the methods. Figure 2.5D is an example of a gel run with 5μL of amplified adult cDNA products from 3' RLM RACE, following gel extraction and purification. Lanes 1 and 2 are replicates of products when adult cDNA was amplified with 5' and 3' gene specific outer primers. Lanes 3 and 4 show adult cDNA products following the successful separation of the two bands (at 848 bp and at 720 bp) found in previous 3' RLM RACE PCR reactions.

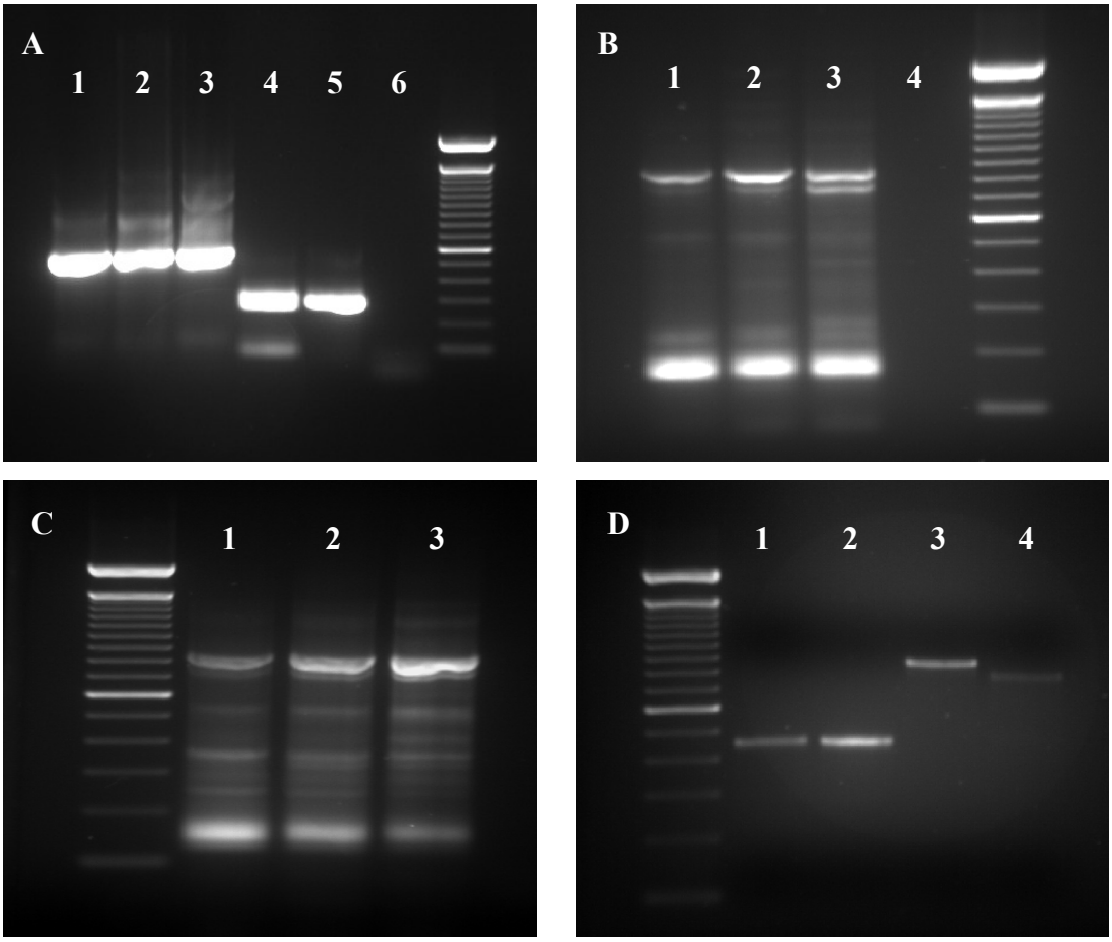


**Figure 2.5. PCR products resulting from RLM-RACE.** (**A**) PCR products from 5' RLM RACE. Lane 1 = adult cDNA, lane 2 = larval cDNA, lane 3 = embryo cDNA, lane 4 = internal control, lane 5 = internal control, lane 6 = no template control. Samples run against a 100bp ladder. Single PCR products are seen at 581 bp and represent the distance from the 5' inner gene specific primer to the 5' inner RACE primer. (**B**) PCR products from 3' RLM RACE. Lane 1 = adult cDNA, lane 2 = larval cDNA, lane 3 = embryo RNA, lane 4 = no template control. A prominent product is found in each cDNA sample at 848 bp. A second band is also found at 720 bp, most prominently in the embryonic cDNA sample. PCR products represent the distance from the outer gene specific primer to the outer RACE primer. (**C**) Gradient PCR products of 3' RLM RACE of adult cDNA samples. Lane 1 = 55°C annealing temperature; lane 2 = 60°C annealing temperature; lane 3 = 65°C annealing temperature. The two bands at 720 bp and 848bp become more visible at the 65°C annealing temperature. (**D**) Gel extracted and purified adult cDNA 3' RLM-RACE PCR products. Lanes 1 and 2 = products with 5' and 3' gene specific outer primers. Lane 3 = the larger product (848 bp) from Figure 2.5C and lane 4 = the smaller band (720 bp) from Figure 2.5C. This gel confirms that these two bands were separated and purified successfully.

## 2.4.3 cDNA sequencing

Following ligation of a variety of PCR products into pGEM®-T Easy Vectors and subsequent subcloning, the purified DNA samples were sequenced. The T7 and SP6 promoters present on the plasmids flanked the DNA inserts and thus were used as primer sites for sequencing. Using both promoters meant sequencing was performed in both directions on the DNA inserts. The raw nucleotide sequences produced from each PCR fragment were aligned and edited using BioEdit and revealed two related *sod3* cDNA sequences of 859 bp and 988 bp, respectively. Alignment of the two sequences with the *Drosophila* genomic sequence for chromosome 2R (Appendix 1) revealed that the two cDNA species differ in their final exon. The short form of *sod3*, termed *sod3v1*, is composed of 5 exons whereas the long species, *sod3v2*, is made up of 6 exons (Figure 2.6), indicating that *sod3v1* and *sod3v2* are encoded by alternative splicing of the *sod3* gene. The coding sequence (shown in orange in Figure 2.6) was determined from the predicted start and stop codons in GenBank, and the sequencing has included the 5' and 3' untranslated regions (shown in white in Figure 2.6).

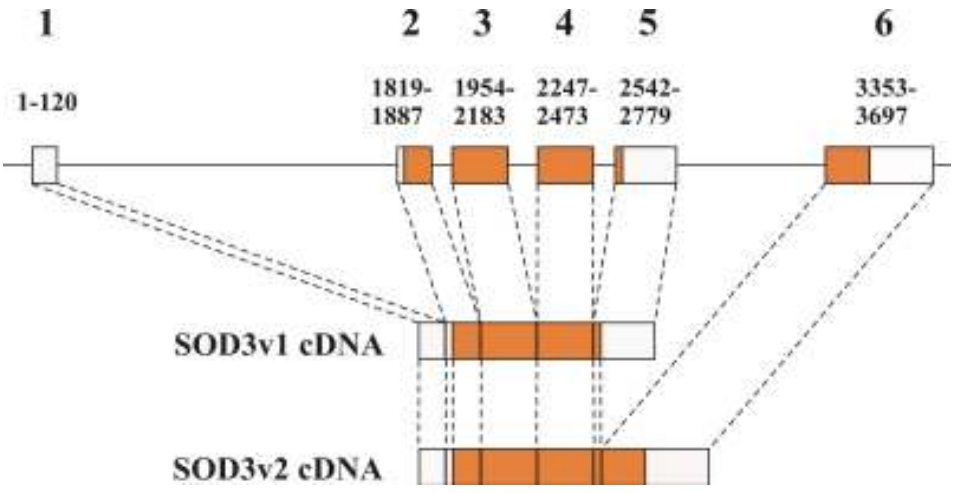


**Figure 2.6. Exon arrangement of the *Drosophila sod3* gene.** The genomic sequence is symbolized as the solid horizontal line. Open boxes represent the non-coding regions and filled orange boxes are the coding regions of the *sod3* gene. Number 1–6 represent the appropriate exon for each transcript. The numbers below these represent the start and end of the *sod3* nucleotide sequence and include the 5' and 3' untranslated regions (UTRs). Diagram is not drawn to scale.

### 2.4.4 Translation analysis

Utilising the translation tools available through the online proteomics site ExPASy (**Ex**pert **P**rotein **A**nalysis **Sy**stem http://expasy.org/), the two *sod3* nucleotide sequences were translated using the start codons predicted in GenBank. Translation of the *sod3v1* and *sod3v2* cDNA sequences predicts peptides of 181 amino acids and 19.2 kDa molecular weight, and 217 amino acids and 23.1 kDa molecular weight, respectively. These two translated sequences were then aligned against the *Drosophila* cytoplasmic Cu Zn SOD, SOD1 (GenBank accession number NP_476735), amino acid sequence, again using BioEdit (Figure 2.7). SOD3v1 and SOD3v2 were found to have identical amino acid compositions except SOD3v2 contains an additional 3' flanking region of 36 amino acids. Furthermore, upon comparison with SOD1, SOD3v1 and SOD3v2 were both found to contain the key metal binding residues and SOD signature sequences previously identified by Parker and colleagues for *Drosophila* SOD1 and *L. niger* SOD3 (Parker et al. 2004a). A Kyte and Doolittle hydropathy plot (Kyte and Doolittle 1982) of SOD3v1 (Figure 2.8A) and SOD3v2 (Figure 2.8B) revealed the amino acids located at the N- terminus of each peptide sequence to be particularly hydrophobic, however the C-terminal residues of SOD3v2 were found to be even more so.

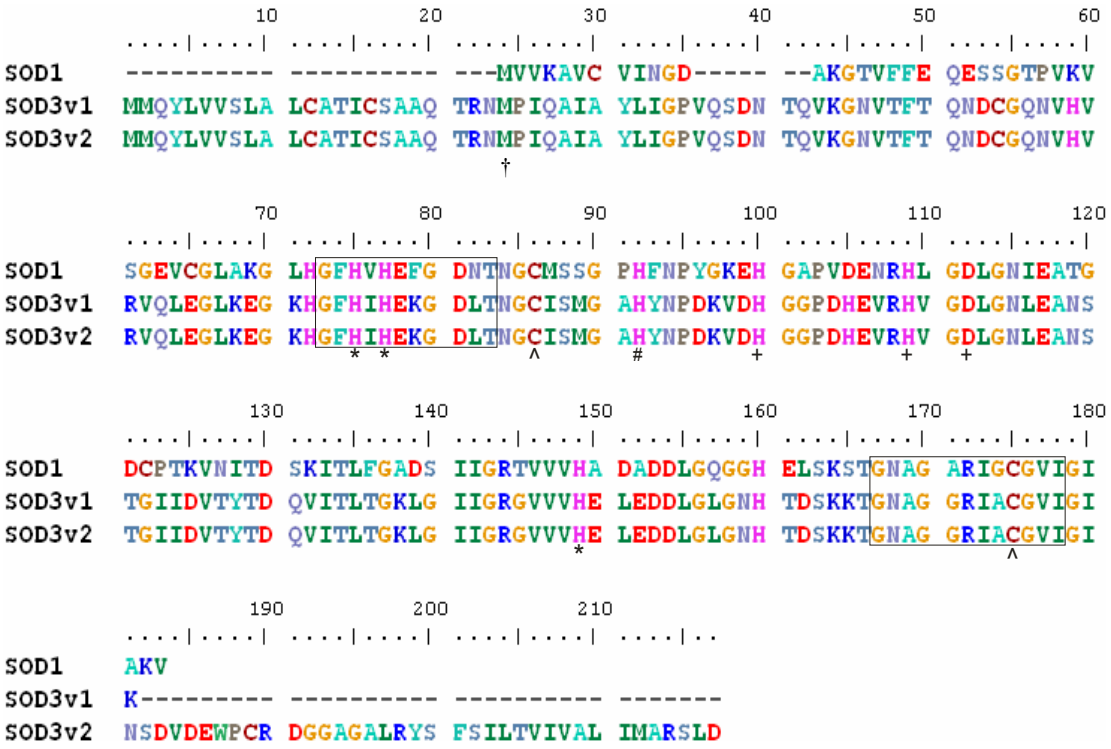


**Figure 2.7. Alignment of *Drosophila* SOD3v1 and SOD3v2 translated peptide sequences with SOD1.** *, Cu binding sites; ^, disulphide bond sites; #, Cu and Zn binding site; +, Zn binding sites; †, possible alternative translation start site; boxed regions are the SOD signature sequences.

**A**

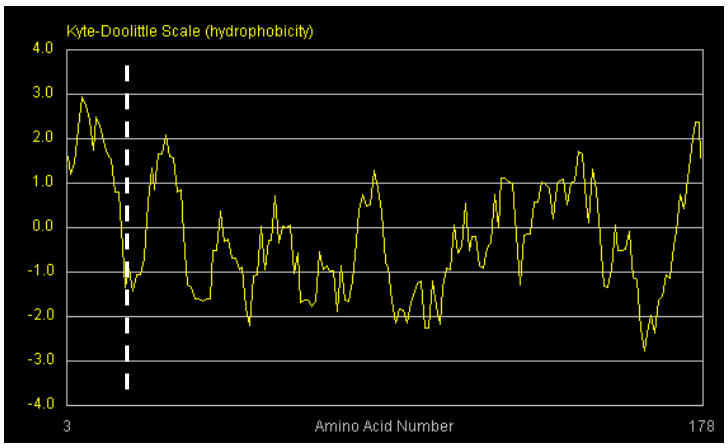


**B**

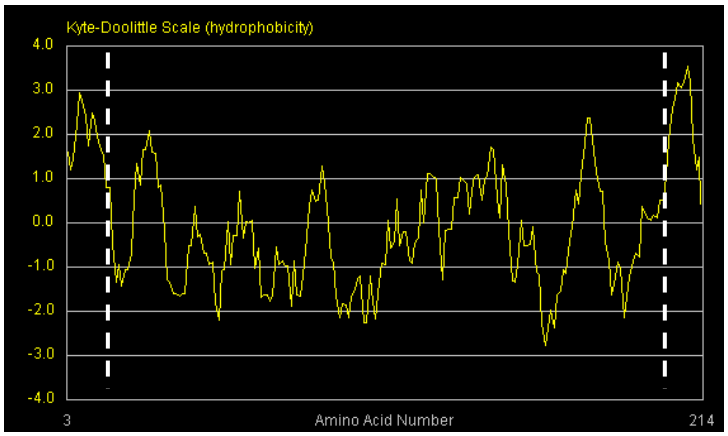


**Figure 2.8. Hydropathy plots of SOD3v1 and SOD3v2.** (**A**) Plot of the 181 amino acids of SOD3v1. Dashed white line indicates the hydrophobic N-terminal region predicted to encode the signal peptide. (**B**) Plot of the 217 amino acids of SOD3v2. Dashed white lines indicate both the hydrophobic N-terminal region predicted to encode the signal peptide, as well as the more hydrophobic extra 36 amino acids located at the C-terminal.

## 2.5 Discussion

### 2.5.1 *Sod3* cDNA cloning and discrepancies with GenBank predictions

Using the RLM-RACE PCR technique the *Drosophila sod3* transcript was cloned from adult poly(A)$^+$ RNA. Sequencing of a variety of the PCR products produced revealed that there are two forms of the *sod3* gene formed by alternative splicing. There is a short variant, termed *sod3v1*, and a long variant, *sod3v2*. Both variants contain the important catalytic metal binding residues as well as the Cu Zn SOD signature sequence, consequently *sod3v1* and *sod3v2* can be considered splice variants of a novel *sod* gene. To my knowledge this is the first experimental evidence of alternative splicing in *Drosophila sod* genes.

As stated in the methods, the NIH genetic sequence database GenBank predicts four transcripts of the *sod3* gene (transcripts A–D). These transcripts were identified from EST data taken from the sequenced *Drosophila* genome (Adams et al. 2000). ESTs are short nucleotide sequences (up to 500 nucleotides) sequenced at the ends of cDNA of genes predicted to be expressed and then are used to pull out a complete gene sequences from chromosomal DNA. mRNA sequence analysis of these four predicted *sod3* variants, together with their alignment with *sod3v1* and *sod3v2* cloned here (data not shown), reveals subtle differences in the proposed genomic construction of the *sod3* gene. The nucleotide sequence of transcript A and *sod3v1* are identical, and likewise with transcript D and *sod3v2*, however the predicted transcripts B and C, whilst predominantly also identical to *sod3v1*, show important dissimilarities. Transcript B has a small additional exon inserted within what is the large first intron of *sod3v1*, whilst transcript C is predicted not to have the first intron present in *sod3v1* (i.e. exons 1 and 2 of *sod3v1* are joined). Furthermore, transcript C is slightly truncated compared to the other three predicted transcripts, with the first 20 bases of the 5' untranslated region apparently missing. Analysis of the peptide sequences of each *sod3* variant reveals that transcripts A and B are identical to SOD3v1 and transcript D is identical to SOD3v2. The peptide sequence of transcript C, however,

has an additional 7 amino acids at the N-terminal end, suggesting that this predicted variant has an alternative transcription start site than variants A, B and D and therefore may possibly be functionally altered compared to the other variants. Whilst ESTs are essential tools for gene discovery, unless the gene is physically cloned and sequenced EST data is limited to predicting gene sequences and expression by computational processing, analysis and database mapping. Furthermore, since ESTs are derived from cDNA they preclude the influence of introns in gene affects. As such, this might explain why four separate transcripts are listed in GenBank whereas only two were cloned, *sod3v1* and *sod3v2*, from adult cDNA.

### 2.5.2 *Sod3* sequence analysis

The distinction between the two *sod3* variants lies in their final exons, where the shorter variant has five exons and the longer variant has six. Consequently the difference in the translated peptide sequence lies in the C-terminal end, with SOD3v2 containing an additional C-terminal flanking sequence. Comparison with *Drosophila* SOD1 (Figure 2.7) revealed that both the SOD3 variants contain an additional N-terminal sequence of amino acids.

Although the scope of this chapter does not extend to determine protein localisation, sequence analysis suggests that the SOD3 enzyme will localise extracellularly (Landis & Tower 2005;Parker et al. 2004a). Both SOD3 isoforms have the N-terminal sequence (first 23 amino acids) that was previously identified as a likely signal cleavage sequence for routing of the SOD3 protein extracellularly (Parker et al. 2004a). Another potentially important observation from the sequence data is the existence of ATG sites corresponding with the cytoplasmic *sod* (*sod1*) gene which could act as an alternative start site for transcription initiation (site 24 in the translated sequence, Figure 2.7). Such conserved sites are present in several insects and even mice (see figure 1 in (Parker et al. 2004a)) suggesting that extracellular SOD protein may not always have the routing sequence and might be cytoplasmic in some instances.

Extracellular binding of the mammalian SOD3 enzyme is governed by post-translational modification. The mature protein is synthesised with a unique C-terminal domain containing a cluster of nine positively charged amino acids (3 lysines and 6 arginines) which have been found to have a strong affinity for heparin and heparan-sulfate (Fattman et al. 2003). It is through this C-terminal interaction with heparan-sulfate proteoglycans on cell surfaces and in the extracellular matrix that the extracellular localisation of SOD3 is maintained in mammals (Fattman et al. 2003). Upon targeted extracellular secretion (dictated by a cleaved N-terminal signal sequence), this C-terminal region may be cleaved producing a heterogeneous mixture of extracellular SOD3s which have both low and high affinities for heparin. As illustrated in figure 2.1, three SOD3 fractions have been separated which have low (fraction A), weak (fraction B) and strong (fraction C) affinities for heparin. Fraction A has been found to be composed of homotetramers in which all subunits have been found to be lacking the positively charged C-terminal domain. Fraction B is made up of heterotetramers of subunits that contain intact heparin binding domains but also subunits lacking this domain. Finally, fraction C is composed entirely of homotetramers of subunits with intact heparin binding domains (Fattman et al. 2003). Fractions A and B are generally found to be circulating forms of the SOD3 protein, while fraction C exists primarily in tissues where it binds heparan-sulfate proteoglycans on cell surfaces and haparan-sulfate located within the extracellular matrix (Fattman et al. 2003).

The observation that insects lack heparin, and furthermore the finding by Parker and colleagues of no positively charged C-terminal region in insect extracellular SODs, suggests that invertebrates have alternative mechanisms for managing extracellular SOD localisation (Parker et al. 2004a). This is further supported by the findings of Fujii and colleagues that the secreted and membrane bound forms of the *C. elegans* extracellular SODs (SOD4-1 and SOD4-2, respectively) are encoded by alternative splicing (Fujii et al. 1998). Both SOD4 peptides were found to contain a putative signal sequence at their N-terminus while SOD4-2 also contains a hydrophobic membrane-binding domain at its C-terminal (Figure 2.9). Interestingly, the hydropathy plots of *Drosophila* SOD3v2 (Figure 2.8B) reveals a particularly hydrophobic area present at the C-terminus (the region missing from SOD3v1) and, furthermore, an alignment of the *Drosophila* SOD3v2 translated sequence with the *C.*

*elegans* SOD4-2 sequence reveals strong homology between the two sequences that extends into the C-terminal region of both peptides (Figure 2.10). This suggests SOD3v2 in *Drosophila* is analogous to SOD4-2 in *C. elegans* and may well be a secreted membrane associated protein, whereas SOD3v1 is analogous to SOD4-1 in *C. elegans* and is likely extracellular.

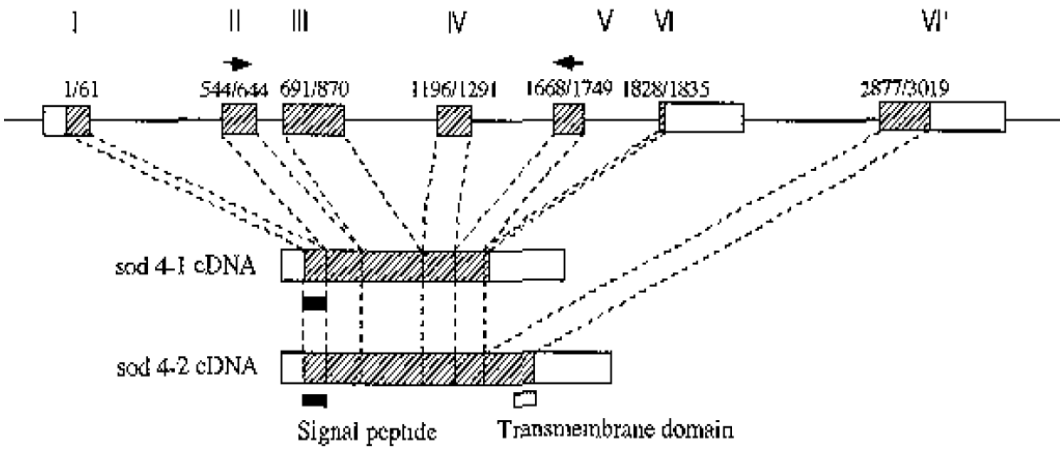


**Figure 2.9. Exon arrangement of the *sod-4* gene in *C. elegans*.** The horizontal line denoted the genomic sequence. The coding region is shown by the shaded boxes and the non-coding region by open boxes. The numbers represent the beginnings and ends of the coding regions. The arrows denote primer positions used to amplify the DNA. The bars represent the position of the signal peptide and transmembrane domains. Figure is not drawn to scale (Fujii et al. 1998).

```
                    10        20        30        40        50        60
SOD3v2    MMQYLVVSLALCATICSAAQTRNMPIQAIAYLIGPVQSDN-TQVKGNVTFTQNDCGQNVH
SOD4-2    MKTRVVLILALSVCIEAASEV----IRARAYIFKAEAGKIPTELIGTIDFDQ--SGSFLK
Consensus seq.  *   : * :  *** . .  *  : * : : .    * : *  * * : :  .  . .  * : :  * .:  *  *   . * .  : :

                    70        80        90        100       110       120
SOD3v2    VRVQLEGLKEGKHGFHIHEKGDLTNGCISMGAHYNPDKVDHGGPDHEVRHVGDLGNLEAN
SOD4-2    LNGSVSGLAAGKHGFHIHEKGDTGNGCLSAGGHYNPHKLSHGAPDDSNRHIGDLGNIESP
Consensus seq.  : .  . : . * *   * * * * * * * * * * * * * * : *  * . * * * * . * : . * * . * * . .  * * : * * * * * : * :

                    130       140       150       160       170       180
SOD3v2    STGIIDVTYTDQVITLTGKLGIIGRGVVVHELEDDLGLGNHTDSKKTGNAGGRIACGVIG
SOD4-2    ASGDTLISVSDSLASLSGQYSIIGRSVVIHEKTDDLGRGTSDQSKTTGNAGSRLACGTIG
Consensus seq.  : : *     : :  : * . :  : * : * :  . * * * * . * * : * *    * * * *  * .    : * * . * * * * * . * : * * * . * *

                    190       200       210       220
SOD3v2    INSD------VDEWP----CRDGGAGALRYSFSILTVIVALIMARSLD
SOD4-2    IVEERILETTTASLPPVTQSQPIGSSSSYYYSTFYLPIILYFLLSRIL-
Consensus seq.  *  . :         .  .  *      . :    * : . :   * *     * . : * :  : : : : *  *
```

**Figure 2.10. Alignment of *Drosophila* SOD3v2 with *C. elegans* SOD4-2.** A considerable degree of homology is observed between the peptide sequences of the two extracellular proteins, with 41% of amino acids being identical (*), 19% being conserved (:) and 14% being semi-conserved (.).

### 2.5.3 Clues to *sod3* evolution

Identification of the *sod3* gene in *Drosophila* may help our understanding of the evolution of the gene within the animal kingdom. Sequence and structural analysis has revealed that the extracellular Cu Zn *sods* diverged from the cytosolic *sods* at an early stage of evolution (Zelko et al. 2002). Phylogenetic analysis of the *sod1* gene in insects (Parker et al. 2004a) and of all the *sod* genes and proteins in a wide range of species (including insects) (Landis & Tower 2005) have confirmed this divergence. However, Landis and Tower have suggested that an organism's extracellular *sod* has derived directly from its individual cytoplasmic *sod* through addition of a signal peptide (Landis & Tower 2005). However, the striking similarities in the exon arrangement of the *C. elegans* (Figure 2.9) and *Drosophila* extracellular *sod* (Figure 2.6) along with the significant lack of sequence homology between *sod1* and *sod3* in *Drosophila*, compared to a strong homology between the *sods* in different insects (Parker et al. 2004a) supports the notion of extracellular SOD having a single ancestor.

# CHAPTER 3

# 3. Analysis of *sod* mRNA expression levels in diverse fly backgrounds and in response to oxidative insults

## 3.1 Aim

The aim of the present chapter is to measure the relative expression profiles of each of the *sod* genes in various fly backgrounds using real-time PCR techniques. Whilst the previous chapter detailed the steps taken to experimentally confirm transcription of the *sod3* gene, and additionally presented evidence that the *sod3* gene may be expressed in two splice forms, it is unknown how highly expressed the *sod* gene is, particularly in relation to the other members of the *sod* family. Furthermore, the affect of application of oxidative stress on *sod* gene expression profiles was also assessed to ascertain whether the *sod* isoforms act as oxidant responsive ROS scavenging species.

## 3.2 Introduction

Regulation of gene expression is fundamental for an organism's development, homeostasis and adaptation to environmental change. The mechanisms underlying gene expression are well established and almost every step involved in the synthesis of gene products (typically proteins, but also ribosomal RNA (rRNA) and transfer RNA (tRNA)) is subject to dynamic control. Such steps include: structural changes in chromatin domains, transcription initiation, RNA splicing, mRNA covalent modifications and transport, translation and also post-translational modifications (Nestler and Hyman 2002).

The expression of *Cu Zn sod*, *Mn sod* and *extracellular sod* varies greatly within the eukaryotic kingdom. Expression of mammalian *sods* is vital to cell survival and the

expression profiles of the *sod* isoforms have been characterised. *Sod1* is constitutively expressed in a wide range of metabolically active mammalian cells, such as the liver and kidneys (Marklund 1984a). Crapo and colleagues used immunocytochemistry to confirm its ubiquitous distribution in the nucleus and cytosol of human HepG2 cells, as well as other mammalian tissues (Crapo et al. 1992). Transcriptional regulation of *sod1* appears to be tightly regulated and can be affected by extra- and intracellular messengers and stimuli. Elevated *sod1* expression has been found to occur in response to heat shock (Hass and Massaro 1988;Yoo et al. 1999b), heavy metals (Yoo et al. 1999a), NO· (Frank et al. 2000) and $H_2O_2$ (Yoo et al. 1999b), whereas decreased *sod1* mRNA levels were found in both alveolar type II epithelial (ATII) cells and lung fibroblasts in response to hypoxia (Jackson et al. 1996). Like *sod1*, *sod2* is widely expressed in metabolically active cells where respiration is high, such as the liver and kidneys (Marklund 1984a). Inflammatory cytokines such as interleukin-1α (IL-1α) and IL-6 have be shown to increase *sod2* mRNA levels in the rat liver by 2- and 15-fold respectively, suggesting a role for *sod2* as an antioxidant in the inflammatory process (Dougall and Nick 1991). It is well established that *sod2* expression is suppressed in many cancer types, however more recently it has been suggested that this decreased expression may be due to epigenetic regulation. Human breast carcinoma cell lines have been shown to have significantly reduced *sod2* levels caused by DNA methylation, histone acetylation and a repressive chromatin structure(Hitchler et al. 2006;Hitchler et al. 2008). Whereas *sod1* and *sod2* levels are fairly similar, *Sod3* is less abundant, with tissue analysis revealing the highest levels to be found in the plasma and also the lungs of a variety of mammalian species such as humans, pigs, rabbits and mice (Marklund 1984a). Like *sod2*, *sod3* up-regulation can be achieved through cytokine exposure (Marklund 1992), although this is only achieved by interferon-γ (INF-γ) and IL-1α in human fibroblasts. *Sod3* is also up-regulated in response to NO· levels (Fukai et al. 2000). Human aortic smooth muscle cells exposed to an NO· donor showed increased *sod3* expression and Fukai *et al.* also demonstrated that increased exercise in wild type mice enhanced NO· production resulting in elevated *sod3* expression. *Sod3* expression is down-regulated by a number of growth factors including growth factor-β (Marklund 1992), platelet-derived growth factors, fibroblast growth factors and epidermal growth factor (Stralin & Marklund 2001).

Reported in this chapter are the gene expression results of a number of fly backgrounds. Along with gene expression quantification in a number of *sod* mutant lines also detailed are the efforts taken to generate a *sod3* knockout fly and the lethal effect such a knockout may have. Also raised is the issue of genetic background as a biological control and furthermore the effect oxidative stress on *sod* gene expression was also investigated.

## 3.3 Materials and Methods

### 3.3.1 Fly strains

The fly strains used in subsequent experiments are listed in Table 3.1 and include the source of the flies as well as the abbreviated name by which the strains are referred to in the text. All flies were maintained on standard *Drosophila* medium (Appendix 2) at 23°C in a 12 hour light/dark cycle.

### 3.3.2 Transposon excision from the *Sod*$^{06029}$ strain

The *sod3* mutant (*Sod3*$^{06029}$) strain was generated by the Berkley *Drosophila* Gene Disruption Project (BDGDP) and contains a stable single transposon insertion (*P*-element, *P{SUPorP}KG06029*) located on the second chromosome, 1,798 nucleotides upstream of the *Sod3* translation start site (Bellen et al. 2004b) (Figure 3.1).

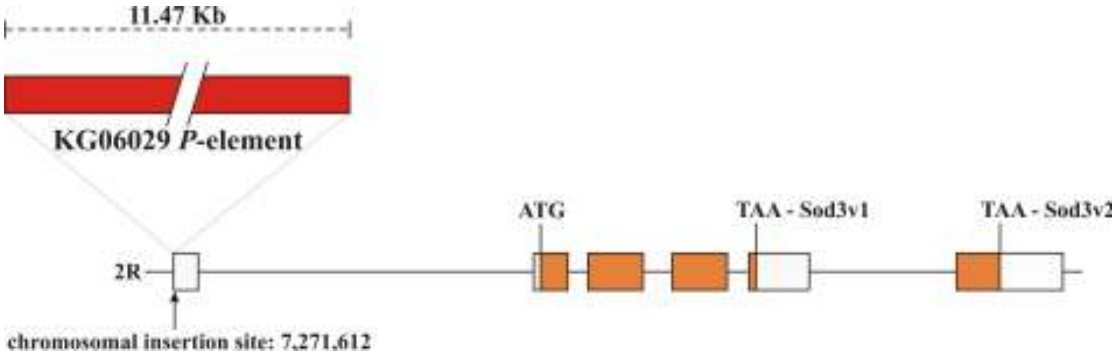


**Figure 3.1. Illustration of the *P*-element genomic insertion site.** Diagram is not drawn to scale.

The *P*-element was excised using standard crossing techniques (Duttaroy et al. 2003) as illustrated in Figure 3.2. Initially male *Sod3*$^{06029}$ flies were mass mated with females of the transposase strain *P(Δ2-3), sb/TM6, Ubx*. Single males, heterozygous for the transposon insertion and for the *(Δ2-3)* transposase, were identified by the *stubble* marker (stubbly bristles) associated with the *Δ2-3 P*-element and

**Table 3.1. Fly lines used including in text abbreviations and sources from where flies were obtained.**

| Genotype | In text abbreviation | Description | Source |
|---|---|---|---|
| *$y^1$ $w^{67c23}$; P{SUPor-P}CG9027$^{KG06029}$* | *Sod3$^{06029}$* | Homozygous *sod3* hypomorph | Bloomington *Drosophila* Stock Center |
| *sod1.n108 red/TM3* | *n108/TM3* | Heterozygous *sod1* null | Phillips Lab, University of Guelph |
| *sod1.n108 red* | *n108* | Homozygous *sod1* null | Phillips Lab, University of Guelph |
| *Red* | *Red* | Isogenic control line for *n108* strains | Phillips Lab, University of Guelph |
| *sod1x39/TM3* | *x39/TM3* | Heterozygous *sod1* knockout | Phillips Lab, University of Guelph |
| *$y^1$ $w^*$; $ry^{506}$ $Sb^1$ P{Delta2-3}99B/TM6,Ubx1* | *P(Δ2-3), sb/TM6, Ubx* | Heterozygous transposase | T. Bossing, University of Bangor |
| *$w^{1118}$; In(2LR)Gla, $wg^{Gla-1}$/CyO, P{GAL4-twi.G}2.2, P{UAS-2xEGFP}AH2.2* | *Gla, $wg^{Gla-1}$/CyO, twi, EGFP* | EGFP under the *twist* promotor | T. Bossing, University of Bangor |
| *y w; CyO/Sco* | *CyO/Sco* | Balancer | T. Bossing, University of Bangor |
| *Oregon R* | *WT* | Wild-type | K. Ubhi, University of California, San Diego |
| *y $w^c$* | *yw $^c$* | Yellow White non-backcrossed control | T. Bossing, University of Bangor |
| *y $w^{c\text{-}iso}$* | *yw $^{c\text{-}iso}$* | Yellow White backcrossed control | Generated from *$yw^c$* strain (see methods section 3.3.7) |

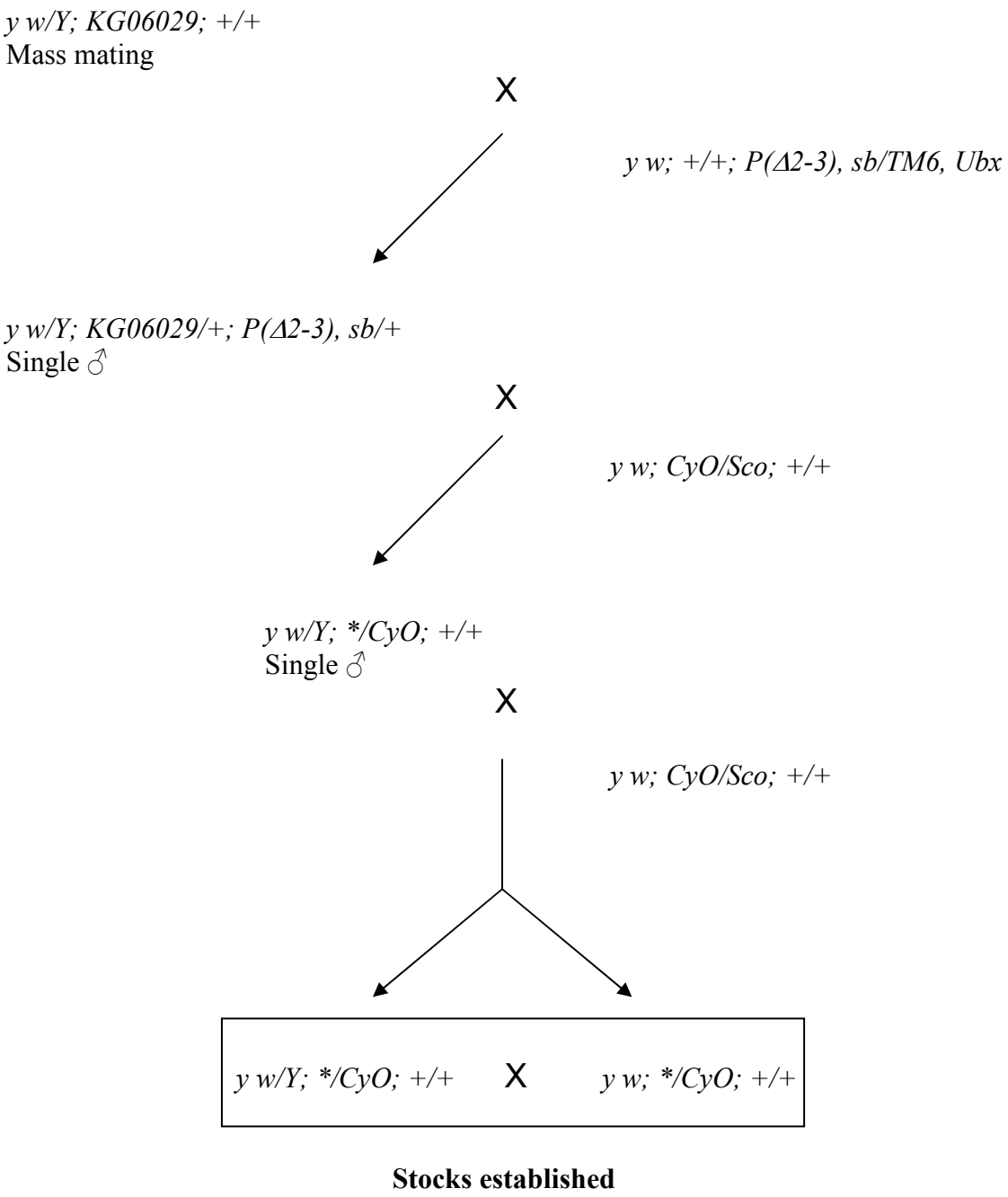


**Figure 3.2. The crossing scheme used to generate KG06029 *P*-element excision lines.** Excision events (*) were identified by loss of the white$^{+}$ phenotype associated with the *P*-element insertion.

were subsequently crossed with 3-5 females of the *CyO/Sco* balancer stock. Excision events in the progeny were identified by loss of the white$^{+}$ phenotype associated with the KG06029 *P*-element transposon. Appropriate single white eyed males containing the *CyO* marker (curly wings) and normal bristles were then crossed with 3-5 *CyO/Sco* virgin females to generate sister excision flies. Brother and sister excision

flies were then crossed to establish excision lines. In total 236 individual excision lines were generated.

### 3.3.3 Genomic DNA preparations of excision lines

Approximately 15 anaesthetised male flies of each excision line were homogenised with a sterile Pellet Mixer (Treff Lab) in a 1.5mL eppendorf tube containing 200µL of Buffer A (100mM Tris-HCl, pH 7.5, 100mM EDTA, 100mM NaCl and 0.5% SDS). A further 200µL of Buffer A was added and the sample incubated at 65°C for 30 mins. 800µL LiCl/KAc solution (1 part 5M KAc : 2.5 parts 6M LiCl) was added and the mixture was incubated on ice for a minimum of 10 mins. Following centrifugation at 13,200 rpm for 15 mins at room temperature, 1mL of the supernatant was transferred to a new tube. Six hundred microlitres of isopropanol was added, the mixture was vortexed and then re-centrifuged at 13,200 rpm for 15 mins. The supernatant was aspirated away, the pellet was washed with 70% ethanol, allowed to dry and then resuspended in 150µL TE (10mM Tris-Cl (pH 7.5) and 1mM EDTA) buffer. Preparations were stored at -20°C until required.

### 3.3.4 Excision primers

As stated previously, *P*-element excision events were assumed to occur in white eyed individuals. However, to confirm this and to also assess whether excision events occurred cleanly (i.e. without disrupting genomic DNA adjacent to the transposon insertion site) primers were designed which localised about the insertion site (KG P2, Sod3 del F and Sod3 del R) and also that bind internally to the transposon *P*-element (KG ins F) (Table 3.2).

**Table 3.2. Primers used to test transposon excision.**

| Primer name | Primer sequences |
|---|---|
| KG ins F | 5'-CACGGACATGCTAAGGGTTAATC-3' |
| KG P2 | 5'-ATGCGTGCATTCGATCCGAT-3' |
| Sod3 del F | 5'-CTGAACAATTTGATCGCAGGGC-3' |
| Sod3 del R | 5'-GGTGGCGCTCTCAATTCTCAAT-3' |

## 3.3.5 PCR of excision lines

PCRs were run with male genomic DNA of each of the 236 *Sod3*$^{06029}$ excision lines using the primer combinations shown in Table 3.3 and illustrated in Figure 3.3. Predicted PCR product sizes are listed.

**Table 3.3. *P*-element excision primer combinations and predicted product sizes.**

| Primer combinations | Primer numbers in Figure 3.3 | Predicted product size |
|---|---|---|
| KG ins F + KG P2 | 1 → 2 | 3.618 Kb |
| Sod3 del F + Sod3 del R | 3 → 4 | 0.779 Kb |

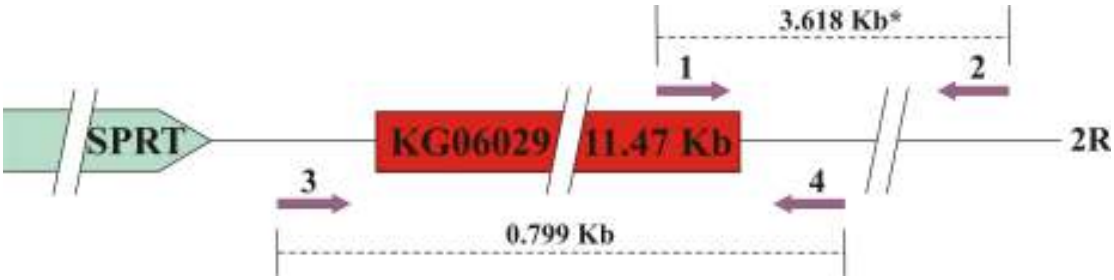


**Figure 3.3. Illustration of the binding regions of each of the excision primers in relation to the inserted *P*-element.** * Primer 1 will only bind if the *P*-element remains within the genome. Primers 3 and 4 will only produce a 0.799 Kb product if the *P*-element is precisely excised. Diagram is not drawn to scale.

PCR reactions were prepared in 200µL thin walled PCR reaction tubes as follows. For KG ins F + KG P2 primer pair – 2µL genomic DNA was mixed with 4µL 5X Phusion® HF Buffer (NEB), 1µL 10µM primer 1, 1µL 10µM primer 2, 0.1µL 10mM dNTP mix (Qiagen), 0.4µL 25mM $MgCl_2$ (Qiagen), 0.2µL 2U/µL Phusion® DNA polymerase (NEB) and made up to 20µL with nuclease-free $H_2O$. The reaction was

mixed, spun briefly and then subjected to PCR using the DNA Engine tetrad 2® thermocycler (MJ Research). Thermocycling conditions used are shown in Table 3.4. For Sod3 del F + Sod3 del R primer pair – 2µL genomic DNA was mixed with 2µL 10X PCR Buffer (Qiagen), 1µL 10µM primer 1, 1µL 10µM primer 2, 0.1µL 10mM dNTP mix (Qiagen), 0.4µL 25mM $MgCl_2$ (Qiagen), 0.1µL 5U/µL Taq DNA polymerase (Qiagen) and made up to 20µL with nuclease-free $H_2O$. The reaction was mixed, spun briefly and then subjected to PCR using the DNA Engine tetrad 2® thermocycler (MJ Research). Thermocycling conditions used are shown in Table 3.5.

**Table 3.4. Thermocycling conditions for the KG ins F + KG P2 primer pair.**

| Steps | Incubation time | Temperature (°C) |
|---|---|---|
| **1. Hot start** | - | 94 |
| **2. Initial denaturation** | 3 mins | 94 |
| **3. 3 step cycling** | - | - |
| Denaturation | 1 min | 94 |
| Annealing | 45 sec | 63 |
| Extension | 3 min (+ 5 sec each cycle) | 72 |
| **4. 34 more cycles to step 3** | - | - |
| **5. Final extension** | 7 mins | 72 |

**Table 3.5. Thermocycling conditions for the Sod3 del F + Sod3 del R primer pair.**

| Steps | Incubation time | Temperature (°C) |
|---|---|---|
| **1. Hot start** | - | 94 |
| **2. Initial denaturation** | 3 mins | 94 |
| **3. 3 step cycling** | - | - |
| Denaturation | 1 min | 94 |
| Annealing | 45 sec | 64 |
| Extension | 2 min | 72 |
| **4. 34 more cycles to step 3** | - | - |
| **5. Final extension** | 7 mins | 72 |

PCR products were revealed on 1-2% (w/v) agarose/TAE gels as detailed in Section 2.3.6.

### 3.3.6 Assessing development of excision lines

A number of transposon excision lines were tested for viability and developmental changes by utilising the reporter properties of the 'enhanced' derivative of *Aequorea victoria* green fluorescent protein (EGFP) under the control of the GAL4/UAS expression system (Brand and Perrimon 1993).

The GAL4/UAS system is a biochemical tool that allows for temporal control of ectopic gene expression in a cell- or tissue-specific manner. It has two components: GAL4, a transcription factor derived from *S. cerevisiae* maintained under the control of an endogenous promoter, and a gene of interest under the control of a GAL4 response promoter called the upstream activating sequence (UAS). Under conditions, or in cells or tissues, where the endogenous GAL4 promoter is activated, GAL4 will be expressed which in turn will bind to the UAS sequence, initiating target gene transcription. This is illustrated in Figure 3.4.

In the case of the *Gla, wg*$^{Gla\text{-}1}$*/CyO, twi, EGFP* line, two *P*-element insertions have been introduced into the second chromosome (Halfon et al. 2002). The first contains GAL4 under the endogenous *twist* (*twi*) promoter. The *twi* gene is a transcription factor predominantly involved in embryonic mesoderm development (Thisse et al. 1987). The second insertion contains two copies of the *EGFP* gene downstream of a UAS promoter. Thus, pronounced EGFP can be visualised in the embryos of this fly strain. Adults of this strain are characterised by small eyes with reduced colour, transferred by the *glazed* (*Gla*) marker and curly wings (*CyO*).

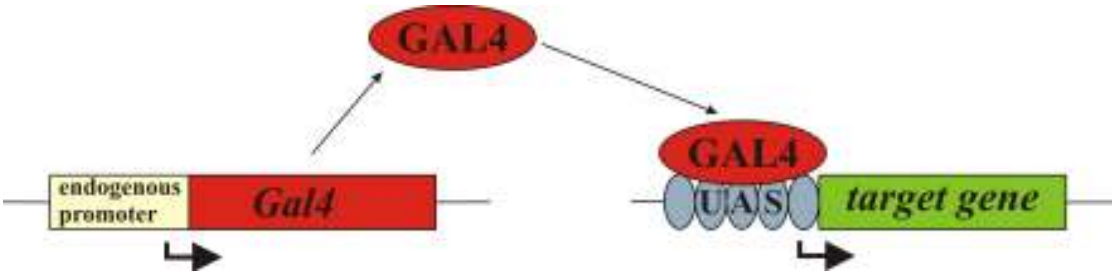


**Figure 3.4. The GAL4/UAS binary system.** GAL4 is expressed in cells or tissues in which the endogenous promoter is active. GAL4 drives cell/tissue specific target gene expression by binding to the UAS fused to the target gene initiating transcription.

To assess changes in development in the excision lines, male heterozygotes were crossed with virgin females of the *Gla, wg*$^{Gla\text{-}1}$*/CyO, twi, EGFP* strain, according to the crossing scheme in Figure 3.5. In the resulting progeny, males and females with normal eyes but curly wings were selected and crossed together on an egg lay plate (Appendix 2) supplemented with semi-dry yeast for 12 – 24 hours. After this time, flies were repeatedly transferred to fresh egg lay plates. Following fly withdrawal, egg lay plates were visualised under a Leica MZ 16F fluorescence stereomicroscope with

an EGFP filter set (488 nm excitation and 530 nm emission wavelengths). Non-fluorescent embryos were assumed to be homozygous for the transposon excision and were placed on a food plate of standard *Drosophila* medium (Appendix 2). Plates were incubated at 23°C in a 12 hour light/dark cycle. Development of embryos was monitored by daily visual inspection.

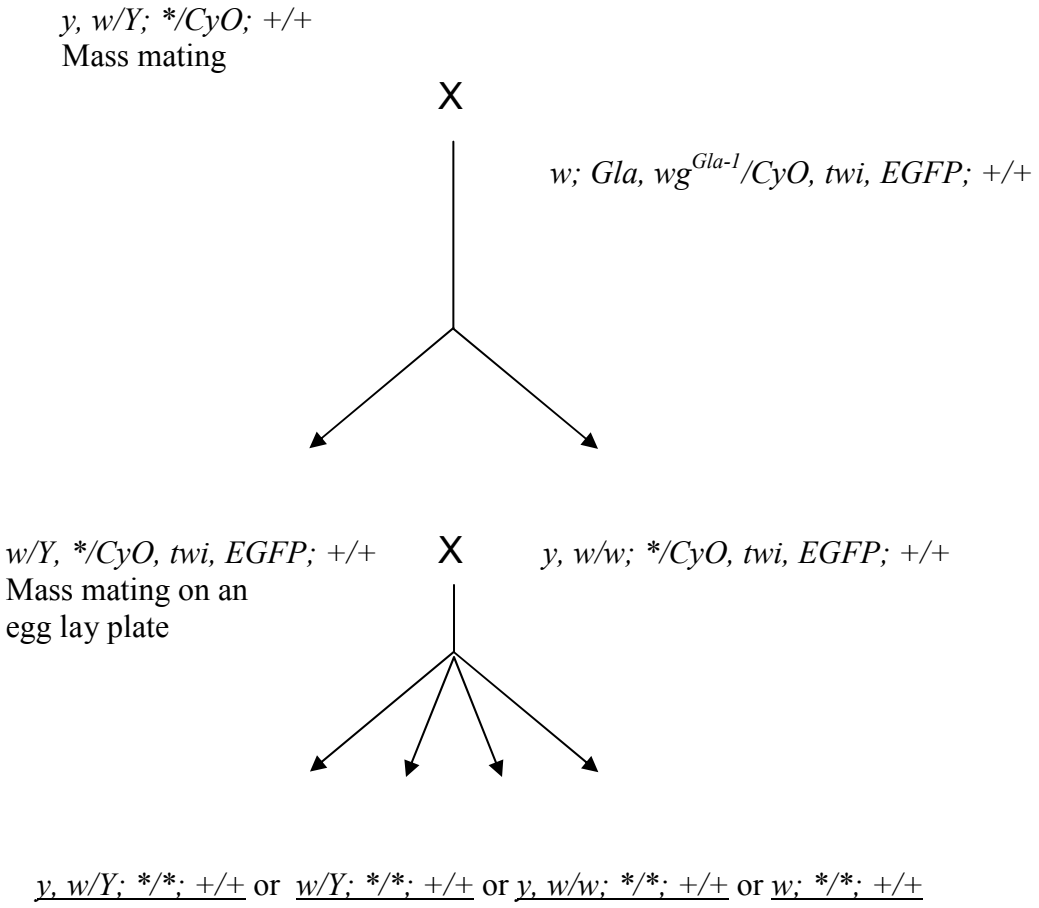


**Figure 3.5. The genetic crossing for selection of homozygous excision lines.** Non-EGFP embryos were selected and transferred to a food plate. Development was observed.

### 3.3.7 Backcrossing of *yw* $^{c}$

To investigate the effects of genetic background in gene expression measurements with *Sod3*$^{06029}$ flies, the *yw* $^{c}$ strain was backcrossed with the *Sod3* mutant background as illustrated in Figure 3.6. Initially three virgin female *yw* $^{c}$ flies were mated with one male *Sod3*$^{06029}$ fly. Single pair matings of the F1 generation were made and 10 further single pair matings were made of resulting progeny that had white eyes and yellow bodies to generate the backcrossed control stock *yw* $^{c\text{-}iso}$.

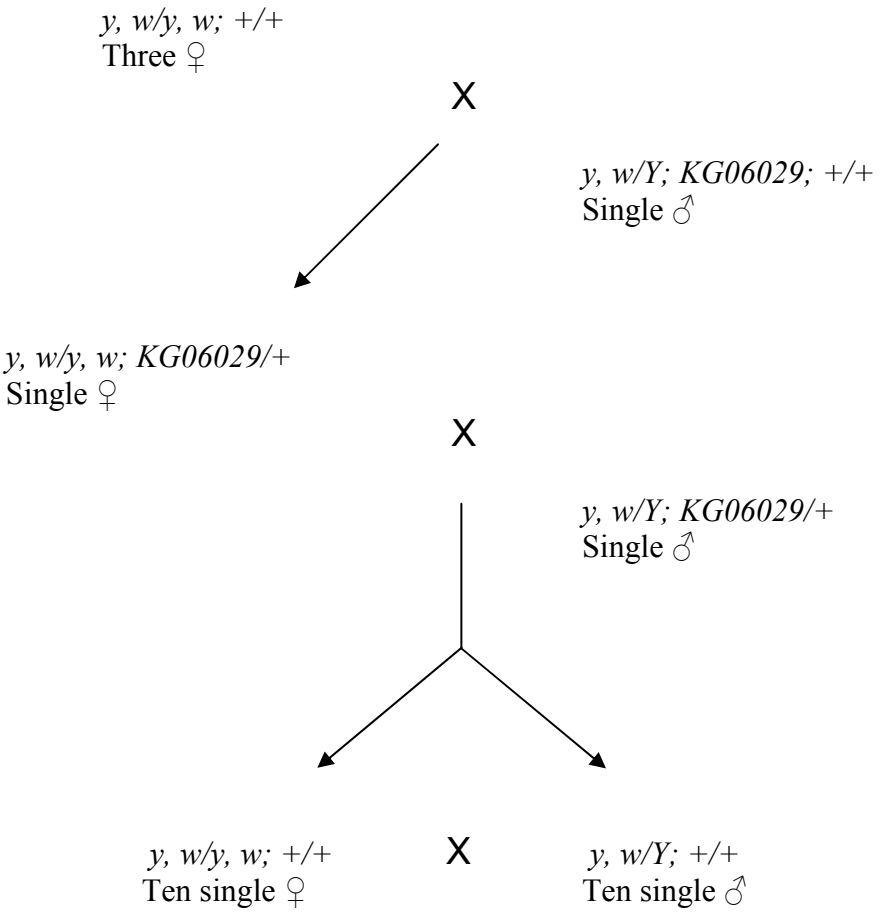


**Figure 3.6. The genetic cross for generation of the backcrossed *Sod3*$^{06029}$ control line (*yw* $^{c\text{-}iso}$).**

### 3.3.8 RNA isolation

Approximately 10 flies of appropriate genotype were briefly anesthetised and snap frozen in liquid nitrogen ($LN_2$) and RNA was prepared using the RNeasy mini kit (Qiagen). The concentration and purity of isolated RNA was determined by analysing 1µL of each RNA sample on the NanoDrop spectrophotometer.

### 3.3.9 First strand cDNA synthesis

The reverse transcription reaction was assembled in a 200µL thin walled PCR tube as follows: 0.565µg/µL RNA was added to 5µL 10X TaqMan® reverse transcription buffer (Applied Biosystems, California, USA), 5.5µL 25mM $MgCl_2$ solution (Applied Biosystems), 10µL 10mM dNTPs (2.5mM each of dATP, dCTP, dGTP and dTTP) (Applied Biosystems), 2.5µL 50µM random hexamers (Applied Biosystems), 1µL 20U/µL RNase inhibitor (Applied Biosystems) and 1.25µL 50U/µL MultiScribe® reverse transcriptase. The reaction was made up to 50µL with nuclease-free $H_2O$. The reverse transcription reaction was initiated by incubation at 25°C for 10 mins, followed by a 30 minute incubation at 48°C. The reaction was terminated by incubating at 95°C for 5 mins. The resulting cDNA was diluted 1:10 in nuclease-free $H_2O$, verified by PCR and stored at -20°C until required for subsequent real-time PCR reactions.

### 3.3.10 Oxidative stress treatments

#### 3.3.10.1 Paraquat

*WT* mixed sex adult flies up to seven days old were briefly anesthetised and transferred from standard plastic food vials to empty plastic vials for a maximum of one hour (~30 flies per vial), as previously described (Arking et al. 1991). After one hour, and without anesthetisation, flies were transferred into plastic vials containing five pieces of Whatman filter paper soaked in 500µL of 30mM paraquat (methyl viologen dichloride hydrate) (SIGMA, Dorset, UK) dissolved in 5% sucrose. Control

flies were given 5% sucrose. The vials were incubated at 23˚C for 24 hours. After 24 hours, surviving flies exposed to paraquat were snap frozen in $LN_2$. RNA was extracted and cDNA was synthesised as described previously in preparation for gene expression analysis.

#### 3.3.10.2 $H_2O_2$

For $H_2O_2$ (SIGMA, Dorset, UK) application, the same procedure was followed as with paraquat administration above, except for test flies five pieces of Whatman filter paper were soaked in 500µL of 15% $H_2O_2$ dissolved in 5% sucrose.

### 3.3.11 TaqMan® real-time PCR

Real-time PCR (also know as quantitative PCR (qPCR)) employs DNA binding fluorophores to quantify DNA amplification in a 'real-time' manner. Here, the TaqMan® system (Applied Biosystems) was employed. TaqMan® gene expression assays comprise a sequence specific DNA probe and primer pair, with the DNA probe being labelled with a fluorescent reporter dye (in this case 6-carboxyfluorescein (FAM) and a non-fluorescent quencher (NFQ). When the probe is intact the energy from the reporter dye is transferred to the quencher by means of fluorescence (or Förster) energy transfer (FRET) preventing fluorescence emission. The sequence specific probes and primers will bind to template DNA and the 5' exonuclease activity of DNA polymerases means that, when added, the probe becomes digested, separating the reporter and quencher, allowing a quantifiable fluorescent signal at 518 nm to be measured.

#### 3.3.11.1 TaqMan® probe and primer design

Custom TaqMan® gene expression assays were created using the File Builder 3.1 software available from the Applied Biosystems website (https://www2.appliedbiosystems.com/support/software/filebuilder/). The GenBank sequences for the *GAPDH* (reference (or housekeeping) gene) (accession number M11254), *sod1* (accession number NM_057387) and *sod2* (accession number

NM_057577) were used to design gene specific reporter and primer sequences. For *sod3v1* and *sod3v2* the nucleotide sequences sequenced from cloning of the *sod3* transcript (Chapter 2) were used. In order to generate specificity between the *sod3v1* and *sod3v2* assays, the *sod3v2* reporter binds in the 6$^{th}$ exon of the *sod3v2* transcript (i.e. the exon unique to *sod3v2*) and thus will not cross-react with the *sod3v1*. Furthermore, the *sod3v1* reverse primer binds over the junction of the 5$^{th}$ exon and the 3' untranslated region that is specific for the *sod3v1* transcript and therefore cannot bind to *sod3v2* cDNA. The primer and reporter sequences designed are listed in Table 3.6.

**Table 3.6. Custom TaqMan® Gene Expression Assay reporter and primer sequences.**

| Gene | Primer/Reporter | Sequence |
|---|---|---|
| *GAPDH* | Forward primer | CGACATGAAGGTGGTCTCCAA |
| | Reverse primer | ACGATCTCGAAGTTGTCATTGATGA |
| | Reporter (forward strand) | CTGCCTGGCTCCCC |
| *sod1* | Forward primer | CCAAGGGCACGGTTTTCTTC |
| | Reverse primer | CCTCACCGGAGACCTTCAC |
| | Reporter (reverse strand) | CCGCTGCTCTCCTGTTC |
| *sod2* | Forward primer | GTGGCCCGTAAAATTTCGCAAA |
| | Reverse primer | GCTTCGGTAGGGTGTGCTT |
| | Reporter (reverse strand) | CCGCCAGGCTTGCAG |
| *sod3v1* | Forward primer | CCAAGAAGACCGGCAATGC |
| | Reverse primer | GCTGACACGTTGGAAGGGATATTTA |
| | Reporter (reverse strand) | ACCACAGGCAATGCG |
| *sod3v2* | Forward primer | CGCATTGCCTGTGGTGTTATTG |
| | Reverse primer | GCCACCATCGCGACATG |
| | Reporter (reverse strand) | CCACATCCGAGTTGATGC |

### 3.3.11.2 Real-time PCR reagents and conditions

Real-time PCR assays were carried out according to the Custom TaqMan® Gene Expression Assay manufacturer's instructions (Applied Biosystems). Each Custom TaqMan® Assay was supplied in a 20X scale and contained 18µM of each primer and 5µM of the probe. Real-time PCR reactions were made up in clear 96-well plates (Bio Rad) as follows: 9µL cDNA was mixed with 10µL 2X TaqMan® Universal PCR Master Mix, No AmpErase UNG and 1µL 20X Custom Assay Mix. Reactions were mixed by pipetting and plates were capped with clear strip caps (Applied Biosystems). Plates were then centrifuged at 3,000 x g for 3 mins and real-time PCR was run on a

Chromo4 Real-Time PCR Detection System (Bio-Rad) using the Opticon Monitor III program.

Real-time PCR thermocycling conditions are as listed in Table 3.7.

**Table 3.7. TaqMan® real-time PCR thermocycling conditions.**

| Steps | Incubation time | Temperature (°C) |
|---|---|---|
| **1. Hold** | 10 min | 95 |
| **2. 2 step cycling** | - | - |
| Denaturation | 15 sec | 95 |
| Annealing/extension | 1 min | 60 |
| **3. Fluorescence reading** | - | - |
| **4. 39 more cycles to step 2** | - | - |

### 3.3.11.3 Real-time PCR analysis

Real-time PCR analysis depends on obtaining a cycle threshold (C(t)) value. The C(t) itself is a user defined figure (0.025 in all experimental reactions) that lies significantly above the baseline fluorescence. Thus, the C(t) value is the cycle number at which fluorescent emissions from the exponential accumulation of PCR products during the log-linear phase exceed this predetermined threshold.

Initial experiments were carried out to validate the efficiency of the primer pairs designed above. Serial dilutions (1:1, 1:5, 1:25 and 1:125) of two of the fly strain cDNAs (*WT* and *n108/TM3*) were run according to the conditions stated above with each of the primer/probe sets. The mean C(t) value for each primer/probe set was then plotted against the Log cDNA dilution with the amplification efficiency (Eff) of the primer pairs being calculated from the slope of the log-linear phase according to the following equation:

$$\text{Eff} = 10^{(-1/\text{slope})}$$

Ideally the amplification efficiency of the primers should be 2, representing a doubling of the DNA product after each cycle, however values of 1.6 – 2.2 are acceptable.

For test samples, gene expression was quantified according to the relative expression model using the following formula:

$$\text{Relative expression ratio} = \frac{(\text{Eff}_{\text{target}})^{\Delta C(t)\text{target (control sample – test sample)}}}{(\text{Eff}_{\text{reference}})^{\Delta C(t)\text{reference (control sample – test sample)}}}$$

'Target' refers to the target gene being assayed (i.e. *Sod1*, *Sod2*, *Sod3v1* or *Sod3v2*) and 'reference' indicates the reference gene being assayed (i.e.*GAPDH*). Expression ratios for different fly strains or under various experimental conditions were then used to illustrate gene expression results as either a proportion of *GAPDH* expression or as a fold-change in gene expression compared to control *Sod* gene expression. Statistical analysis of the data was performed using unpaired t-tests and a minimum of four biological replicates were tested for each cDNA sample in triplicate for each gene.

# 3.4 Results

## 3.4.1 *Sod* gene expression in *WT* flies

Using real-time PCR analysis the expression of *sod1*, *sod2*, *sod3v1* and *sod3v2* in male and female *WT* flies was quantified (Figure 3.7). Measured as a proportion of *GAPDH* (housekeeping gene) expression, *sod1* appeared to be the most prevalent of all the *sod* gene species in both sexes. *Sod2* was less highly expressed and both *sod3v1* and *sod3v2* had lower expression still, with *sod3v1* having the lowest expression profile, in both sexes. Interestingly, while *sod1* and *sod2* expression was equivalent between sexes, females were shown to express significantly higher levels of both *sod3* variants than males (for *sod3v1* df = 8, P = <0.01 and for *sod3v2* df = 8. P = <0.001). Furthermore, whilst *sod3* expression levels were comparable between variants in males, in females *sod3v2* was found to be significantly more abundant than *sod3v1* (df = 8, P = <0.01).

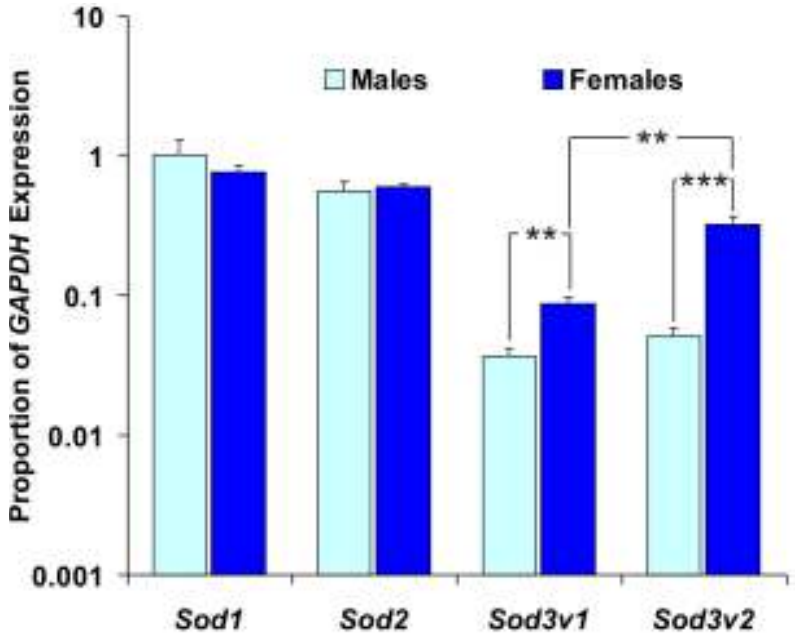


**Figure 3.7. *Sod* gene expression profiles in male and female *WT* flies as a proportion of *GAPDH* expression.** Five biological replicates of each sex were tested in triplicate for each gene. Error bars are standard error of the mean (SEM). **, P = <0.01; ***, P = <0.001.

### 3.4.2 *Sod* gene expression in *sod* mutant lines

Following quantification of *sod* expression levels in *WT* flies equivalent measurements were made in a number of *sod* mutant lines. Previous work by Phillips and colleagues reported that upon knocking out *sod1* in *Drosophila*, Cu Zn SOD activity was found to be completely abolished (Phillips et al. 1989). These findings now seem curious given that in the previous chapter it was demonstrated that *Drosophila* also contain a proposed extracellular Cu Zn SOD (*sod3*). Gene expression measurements were therefore taken in a number of *sod1* and *sod3* mutant lines to assess whether compensatory or co-transcriptional changes in *sod* gene expression occur in response to altered *sod1* and *sod3* expression, which may account for *sod3* being missed in the original *sod1*-null work.

*WT* cDNA was included as a non-isogenic control and the mutant lines tested were the *sod1* heterozygous mutants, *x39/TM3*, *n108/TM3*, the *sod1* homozygous *n108* line and the *sod3 P*-element insertion allele, $Sod3^{06029}$. As discussed, the *sod3* mutant line ($Sod3^{06029}$) is a product of the BDGDP gene disruption project and, until now, remained unexplored. However, homozygous $sod3^{06029}$ flies were observed to be both viable and fertile and therefore were tested as homozygotes. The two *sod1* mutant lines are well established. The *n108* allele was originally recovered as an ethylmethane sulfonate (EMS) induced recessive lethal mutation and results in a missense mutation, believed to be at the site of dimer interaction, which interferes with structural stability and leads to reduced lifespan and paraquat hypersensitivity (Campbell et al. 1986;Phillips et al. 1989;Phillips et al. 1995). The *x39* allele was generated by ionizing γ irradiation and results in a 395 bp deletion encompassing the transcription start site, all of the first exon and part of the single intron of *sod1* (Phillips et al. 1995). Whilst *x39* flies are only viable as heterozygotes, and are therefore tested as such, homozygous *n108* flies can be recovered meaning both heterozygous and homozygous *n108* flies were assayed for gene expression. It should be noted however that the *n108* line was assayed in a separate experiment.

*Sod* gene expression profiles for *WT* flies of each sex (Figures 3.8A and C for males; Figures 3.8B and D for females) matched that found previously, with *sod1* being most

highly expressed, followed by *sod2*, then *sod3v2* and finally *sod3v1*. However, in all the mutant strains tested, and in both sexes, *sod2* was found to be the most highly expressed. Additionally, both *sod3* variants were found to be more highly expressed in females than in males in all lines tested except for the female $Sod3^{06029}$ strain. Here we found reduced *sod3v1* expression in females compared to males whereas *sod3v2* was equally expressed between the sexes.

Analysis of the fold changes in gene expression compared to *WT* levels reveals more about the expression profiles of each *Sod* gene in each mutant strain:

#### 3.4.2.1 Males

Male *x39/TM3* flies showed statistically significant reduction of *sod1* mRNA levels (df = 8, P = <0.05) by greater than 2- fold (Figure 3.9A) compared to *WT*, whilst *sod2* and *sod3* (both variant) expression levels did not differ significantly. In contrast, no measurable change in *sod1* expression was observed in the other heterozygous *sod1* mutant line, *n108/TM3.* There was, however, significant down-regulation of both *sod3v1* (df = 8, P = <0.05) and *sod3v2* (df = 8, P = <0.05) in this strain, but no statistically measurable change in *sod2* expression. With the homozygous form of this strain (*n108*) however, whilst all *sod* genes were found to be down-regulated, none showed any statistically significant change in expression (Figure 3.9C). A significant reduction in expression of both *sod3v1* (df = 8, P = < 0.001) and *sod3v2* (df = 8, P = <0.01) (around 2-3 fold) in the $sod3^{06029}$ strain was also measured but little change in *sod1* or *sod2* was observed (Figure 3.9A).

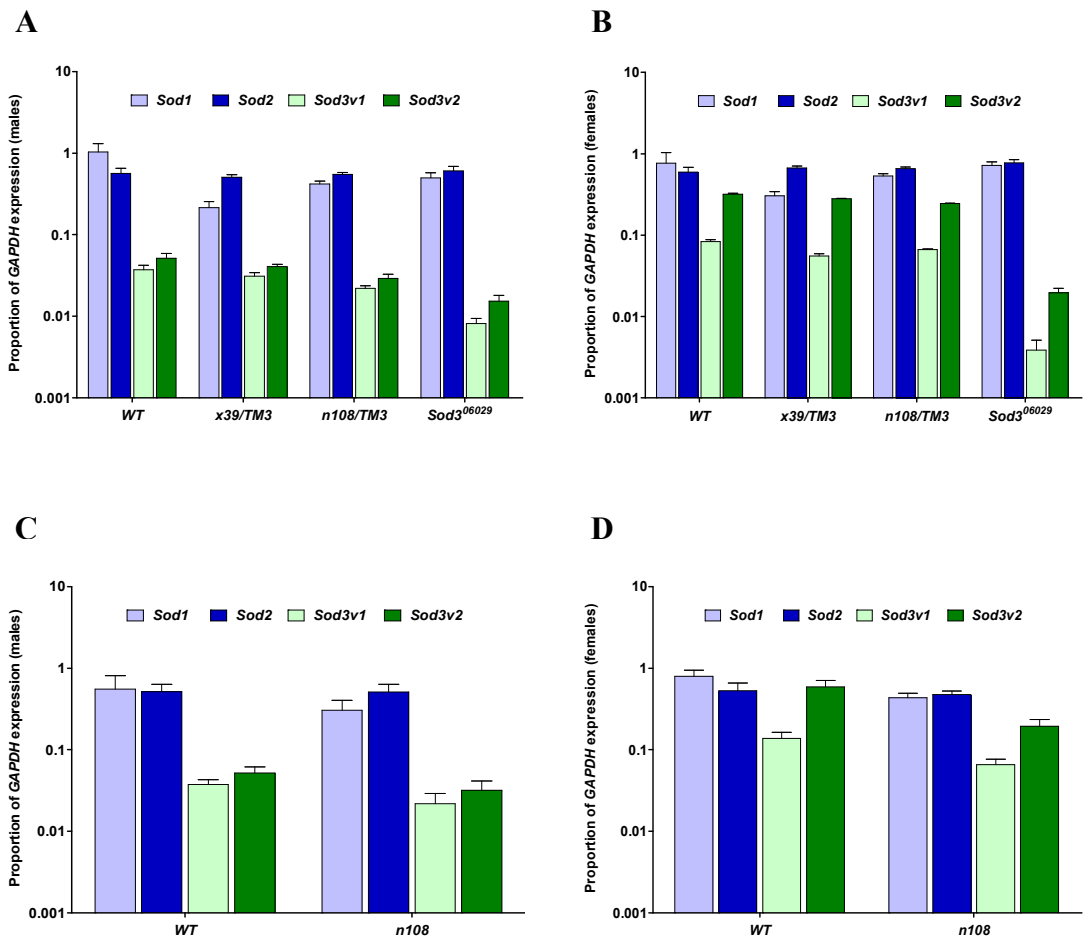


**Figure 3.8. *Sod* gene expression profiles in various *sod* mutant lines as a proportion of *GAPDH* expression. A**, expression in *WT*, *x39/TM3*, *n108/TM3* and $Sod3^{06029}$ male flies; **B**, expression in females of the same strain; **C**, expression in *WT* and *n108* males; **D**, expression in females of the same strain. All samples are tested at N = 5 and error bars are SEM.

### 3.4.2.2 Females

A similar trend was seen in female flies where *x39/TM3* flies showed ~2-fold down-regulation of *sod1* (df = 8, P = <0.001) but no significant difference in *sod2*, *sod3v1* or *sod3v2* expression compared to *WT* (Figure 3.9B). Unlike in males, a statistically significant down-regulation of *sod1* (df = 8, P = <0.05) was seen in *n108/TM3* flies. Also, unlike male flies, no significant down-regulation of *sod3v1* or *sod3v2* was observed in this strain. Once again, *sod2* levels did not vary significantly compared to *WT* in *n108/TM3* female flies. Interestingly, whilst no significant reduction in *sod1* expression was observed in the *n108* line, in this homozygous strain we did see a

significant down-regulation of *sod3v1* (df = 8, P = <0.05) and *sod3v2* (df = 8, P = <0.05) expression (Figure 3.9D). As expected $Sod3^{06029}$ females showed a considerable reduction in both *sod3v1* (df = 8, P = <0.001) and *sod3v2* (df = 8, P = <0.001) expression of 8- to 10-fold (Figure 3.9B). Whereas *sod1* levels did not differ compared to *WT* females, we also observed a significant up-regulation of *sod2* (df = 8, P = <0.01) in $Sod3^{06029}$ females.

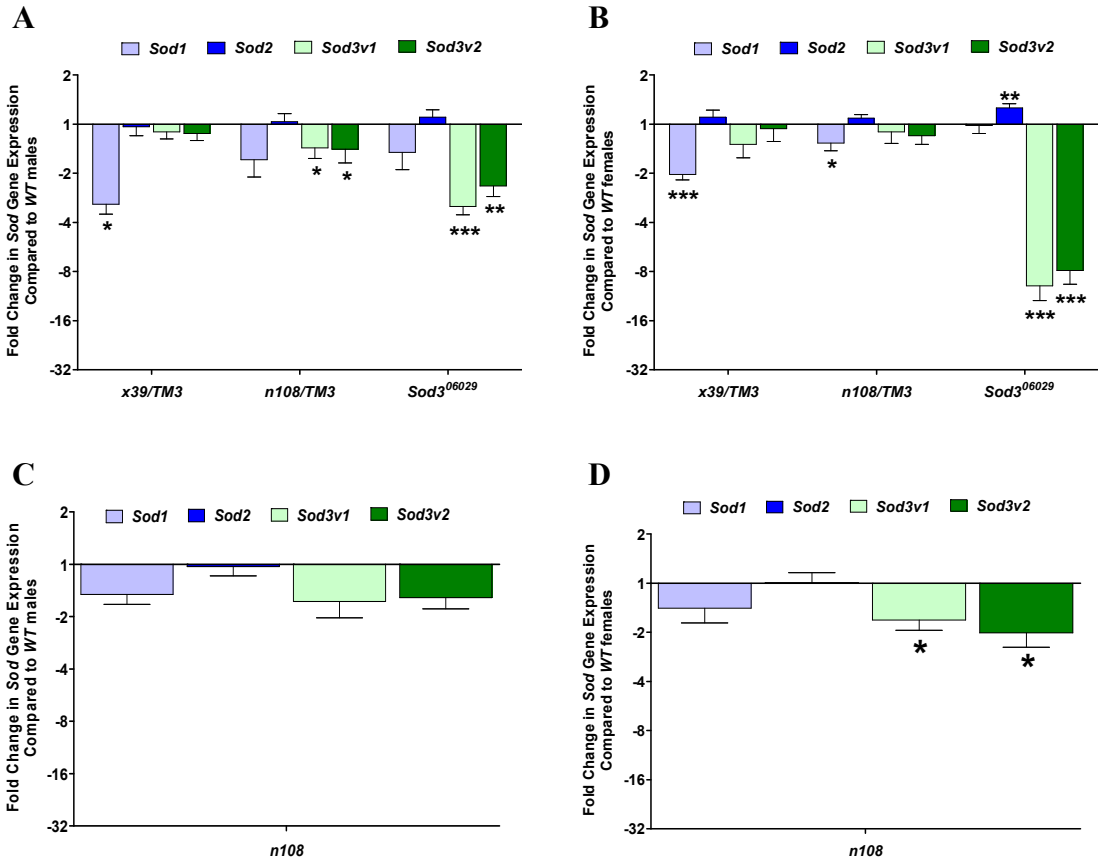


**Figure 3.9. Fold change in *Sod* gene expression in the *Sod* mutant lines compared to *WT* flies.** All samples are tested at N = 5 and error bars are SEM. *, P = <0.05; **, P = <0.01; ***, P = <0.001.

### 3.4.3 Transposon excision

The aim of excising the inserted *P*-element present in the promoter region of the *Sod3*$^{06029}$ strain was two fold. Firstly, generating revertant excision lines would allow for confirmation that any changes in gene expression found in the *sod3* mutant were indeed caused by transposon insertion. As such, revertant excision lines would be expected to have dramatically increased *sod3* transcript levels compared to *Sod3*$^{06029}$. Secondly, *P*-element excision can sometimes be imprecise (Robertson et al. 1988;Salz et al. 1987). In such circumstances removal of the element will also excise a portion of genomic DNA adjacent to the insertion site. When the *P*-element lies within a gene transcript region (as the KG06029 element does in *Sod3*$^{06029}$ hypomorph) this can lead to knockout mutants being generated, which would be useful to help characterise the function of the *sod3* gene in *Drosophila*.

By crossing homozygous *Sod3*$^{06029}$ flies with the transposase producer, *P(Δ2-3), sb/TM6, Ubx*, 236 individual transposon excision lines were generated. As described in the methods, to generate individual excision stocks a single male heterozygous for the excision over a *CyO* balancer (**/CyO*), was crossed with the *CyO/Sco* balancer stock. Resulting male and virgin female progeny of the **/CyO* genotype were then crossed together to propagate the stock. Typically, where *P*-element excision has occurred cleanly the ratio of straight wing (homozygous):curly wing (heterozygous) flies (i.e **/** : **/CyO*) would be 1:2. Should imprecise excision occur and disrupt genomic DNA encoding a gene critical for survival, the number of *CyO* flies may be expected to be higher or straight wing flies may be absent altogether if homozygous excision lines are lethal.

Of the 236 excision lines generated, 199 (84.3%) produced the expected 1:2 ratio of homozygous:heterozygous flies and 37 (15.7%) of the stocks only produced heterozygous offspring, suggesting lethal imprecise excision may have occurred in these stocks. Initially, excision events were assumed to have occurred in white eyed individuals as the white$^{+}$ phenotype (i.e. red eyes) is carried by the *P*-element. However, this was verified in all stocks (including heterozygotes) by PCR screening with a primer binding internally to the transposon (KG ins F) and a genome specific

primer (KG P2). Genomic DNA from the *Sod3*$^{06029}$ strain was used as a positive control. Despite all adults having white eyes, 10 of the 236 lines (*ex24*, *ex25*, *ex50*, *ex59*, *ex69*, *ex81*, *ex98*, *ex151*, *ex180* and *ex206*) gave rise to a 3.618 Kb product with the primer pair, indicating that the *P*-element was still present in these lines. Figure 3.10 shows the PCR products of the lines in which the *P*-element is still present. Results for all stocks are not shown as a positive result (i.e. transposon excision) is illustrated by no product.

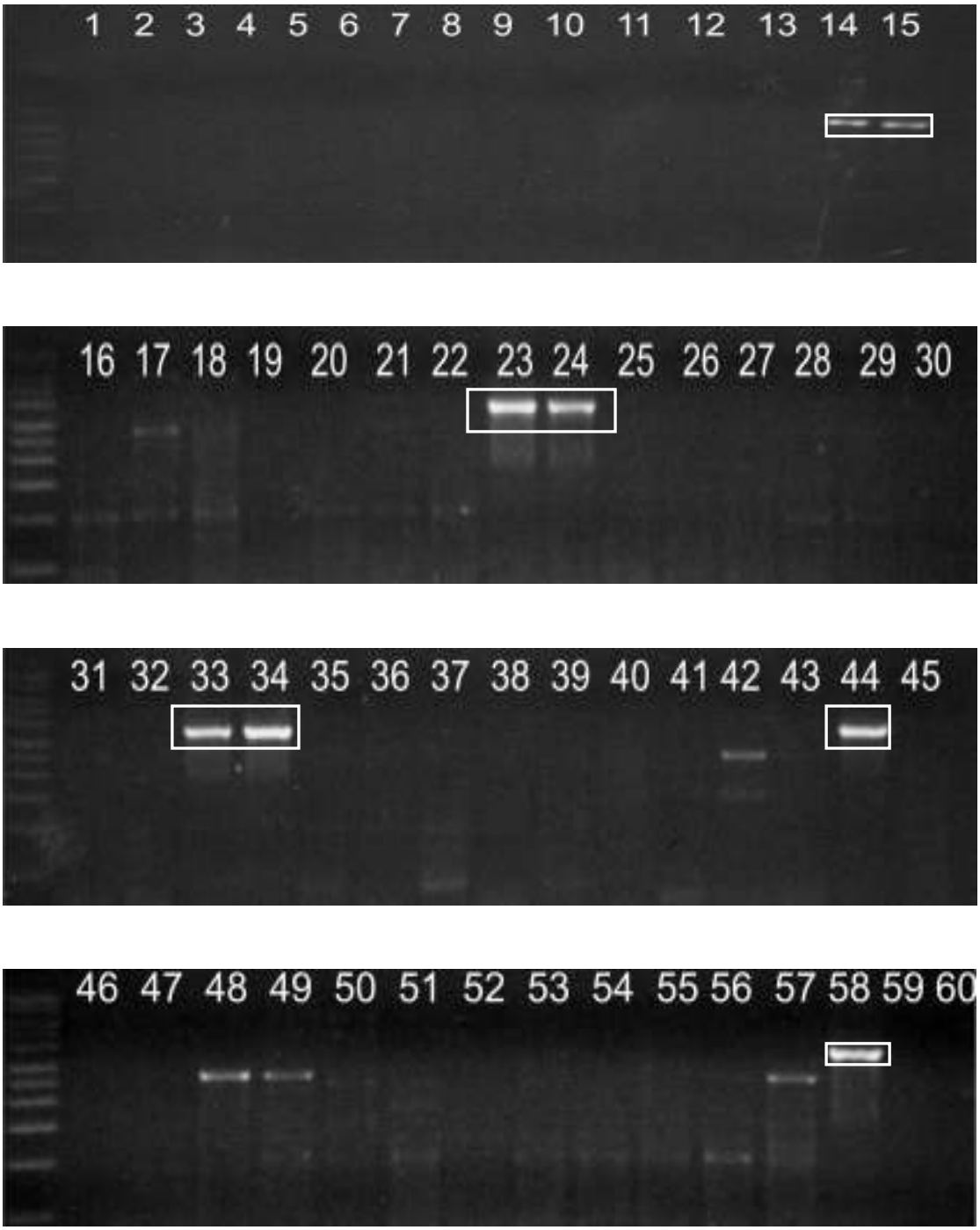

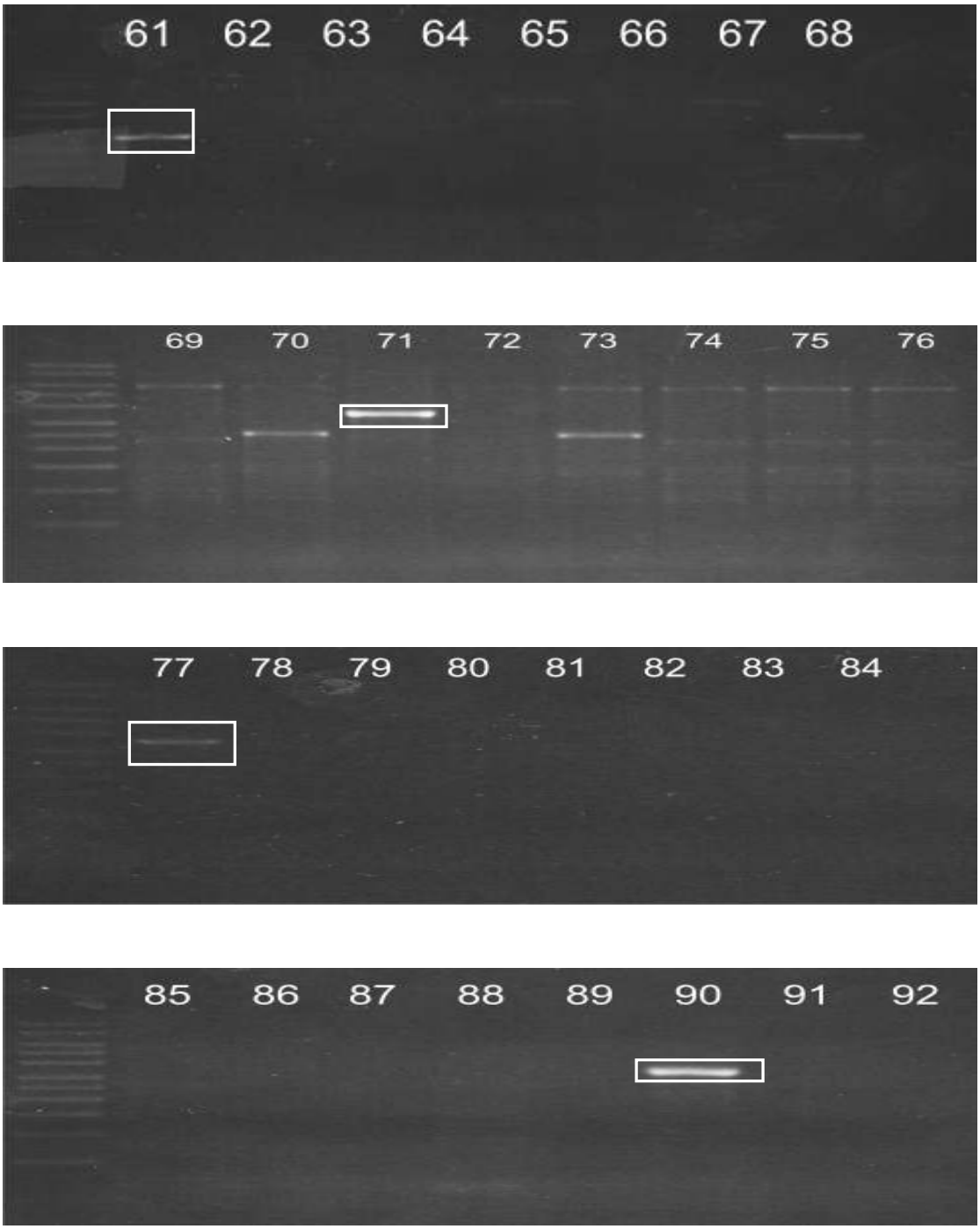


**Figure 3.10. PCRs of stocks in which the *P*-element remained inserted.** 3.618 Kb product indicates that the *P*-element is still inserted. The lanes in which a 3.618 Kb was found (white box) and the corresponding excision line are listed: lane 14 = *ex24*; 15 = *ex25*; 23 and 24 = duplicates of *ex53*; 33 and 34 = duplicates of *ex59*; 44 = *ex69*; 58 = *ex81*; 61 = *ex98*; 71 = *ex151*; 77 = *ex180*; 90 = *ex206*. Remaining lanes are excision lines in which the *P*-element was cleanly excised. PCR products other than those enclosed by a white box are due to non-specific primer binding.

Following confirmation of those stocks which had had the *P*-element insertion removed (and thus were now predicted to be like wild-type flies) each stock was screened for the presence of small genomic DNA deletions adjacent to the transposon insertion site. The Sod3 del F and Sod3 del R primers were used with the conditions detailed in the methods. Cleanly excised stocks were predicted to produce PCR products of 0.799 Kb, whereas in those stocks where imprecise excision has occurred an additional smaller product would be expected to be seen. Appendix 3 shows the PCR products of each of the excision lines tested with the Sod3 del primer pair. Of the 236 excision lines subjected to PCR, 217 produced products of 0.799 Kb, indicating clean transposon excision. Of the remaining 19 stocks; five gave products of greater than 0.779 Kb: *ex24*, *ex63*, *ex82*, *ex172* and *ex236*; four produced very faint bands in the 0.779 Kb region: *ex49*, *ex121*, *ex151* and *ex239*; nine gave no product at 0.779 Kb: *ex50*, *ex59*, *ex69*, *ex98*, *ex100*, *ex137*, *ex179*, *ex182* and *ex206*; and one stock gave a product that may be smaller than 0.779 Kb fragment: *ex233*.

All heterozygous excision lines, and lines in which a 0.799 Kb fragment was not found, were retained for future investigations. Additionally a number of lines in which the *P*-element was predicted to have been excised cleanly, therefore producing homozygous flies, were also retained. Table 3.8 summarises the nature of the excision lines generated.

**Table 3.8. Excision stocks (retained stocks shown in red).**

| Stock | Heterozygous stock | P-element excised | 0.799 Kb product |
|---|---|---|---|
| ***ex8*** | - | - | - |
| ***ex9*** | Yes | - | - |
| ***ex10*** | - | - | - |
| ex11 | - | - | - |
| ex13 | - | - | - |
| ex17 | - | - | - |
| ex17* | - | - | - |
| ex18 | - | - | - |
| ex19 | - | - | - |
| ***ex20*** | Yes | - | - |
| ex21 | - | - | - |
| ex22 | - | - | - |
| ex23 | - | - | - |
| ***ex24*** | - | No | No** |
| ex25 | - | No | - |
| ***ex26*** | Yes | - | - |
| ex29 | - | - | - |
| ex30* | Yes | - | - |
| ***ex30*** | Yes | - | - |
| ex31 | - | - | - |
| ex32 | - | - | - |
| ex33 | - | - | - |
| ex34 | - | - | - |
| ex35 | - | - | - |
| ex36 | - | - | - |
| ***ex37*** | Yes | - | - |
| ex38 | - | - | - |
| ex39 | - | - | - |
| ex40 | - | - | - |
| ex41 | - | - | - |
| ex42 | - | - | - |
| ex43 | - | - | - |
| ***ex44*** | Yes | - | - |
| ex45 | - | - | - |
| ***ex47*** | Yes | - | - |
| ***ex48*** | Yes | - | - |
| ***ex49*** | Yes | - | No^ |
| ex50* | - | No | No$^{+}$ |
| ***ex50*** | - | No | No$^{+}$ |
| ex51 | - | - | - |
| ex52 | - | - | - |
| ***ex53*** | Yes | - | - |
| ***ex54*** | Yes | - | - |
| ex55 | - | - | - |
| ***ex56*** | Yes | - | - |
| ex57 | - | - | - |
| ***ex58*** | Yes | - | - |
| ex59* | - | No | No$^{+}$ |
| ***ex59*** | - | No | No$^{+}$ |
| ex60 | - | - | - |
| ***ex61*** | - | - | - |
| ex62 | - | - | - |
| ***ex63*** | - | - | No** |
| ***ex64*** | - | - | - |
| ***ex65*** | Yes | - | - |
| ***ex66*** | Yes | - | - |
| ex67 | - | - | - |
| ex68 | - | - | - |
| ***ex69*** | - | No | No$^{+}$ |
| ***ex70*** | Yes | - | - |
| ex71 | - | - | - |
| ex72 | - | - | - |
| ex73* | - | - | - |
| ex73 | - | - | - |
| ***ex74*** | Yes | - | - |
| ex75 | - | - | - |
| ***ex76*** | Yes | - | - |
| ex77 | - | - | - |
| ex77* | - | - | - |
| ***ex78*** | Yes | - | - |
| ***ex79*** | Yes | - | - |
| ***ex80*** | Yes | - | - |
| ex81 | - | No | - |
| ***ex82*** | - | - | No** |
| ***ex84*** | Yes | - | - |
| ex85 | - | - | - |
| ex86 | - | - | - |
| ex87 | - | - | - |
| ex88 | - | - | - |
| ex89 | - | - | - |
| ex90 | - | - | - |
| ex91 | - | - | - |
| ex92 | - | - | - |
| ex93 | - | - | - |
| ***ex94*** | Yes | - | - |
| ex95 | - | - | - |
| ex97 | - | - | - |

| Stock | Heterozygous stock | P-element excised | 0.799 Kb product | Stock | Heterozygous stock | P-element excised | 0.799 Kb product | Stock | Heterozygous stock | P-element excised | 0.799 Kb product |
|---|---|---|---|---|---|---|---|---|---|---|---|
| ex97* | - | - | - | ex129 | - | - | - | ex161 | - | - | - |
| ***ex98*** | - | No | No$^{+}$ | ex130 | - | - | - | ex162 | - | - | - |
| ex99 | - | - | - | ***ex131*** | Yes | - | - | ex163 | - | - | - |
| ex100 | - | - | No$^{\#}$ | ex132 | - | - | - | ex164 | - | - | - |
| ex101 | - | - | - | ***ex134*** | Yes | - | - | ex165 | - | - | - |
| ex102 | - | - | - | ex135 | - | - | - | ex166 | - | - | - |
| ***ex104*** | Yes | - | - | ***ex136*** | - | - | - | ex167 | - | - | - |
| ex105 | - | - | - | ***ex137*** | - | - | No$^{+}$ | ex168 | - | - | - |
| ex106 | - | - | - | ex139 | - | - | - | ex169 | - | - | - |
| ***ex107*** | Yes | - | - | ***ex140*** | Yes | - | - | ex170 | - | - | - |
| ***ex108*** | Yes | - | - | ***ex141*** | - | - | - | ex171 | - | - | - |
| ex109 | - | - | - | ex142 | - | - | - | ***ex172*** | - | - | No** |
| ***ex110*** | Yes | - | - | ex143 | - | - | - | ex173 | - | - | - |
| ex111 | - | - | - | ***ex144*** | Yes | - | - | ex174 | - | - | - |
| ex112 | - | - | - | ***ex145*** | Yes | - | - | ex175 | - | - | - |
| ex113 | - | - | - | ex146 | - | - | - | ex176 | - | - | - |
| ***ex115*** | Yes | - | - | ex147 | - | - | - | ex178 | - | - | - |
| ex116 | - | - | - | ex148 | - | - | - | ***ex179*** | - | - | No$^{+}$ |
| ex117 | - | - | - | ***ex149*** | Yes | - | - | ex180 | - | No | - |
| ex118 | - | - | - | ex150 | - | - | - | ex181 | - | - | - |
| ex119 | - | - | - | ***ex151*** | - | No | No^ | ***ex182*** | - | - | No$^{\#}$ |
| ex120 | - | - | - | ex152 | - | - | - | ex184 | - | - | - |
| ***ex121*** | - | - | No^ | ex153 | - | - | - | ex185 | - | - | - |
| ***ex122*** | Yes | - | - | ex154 | - | - | - | ex186 | - | - | - |
| ***ex123*** | Yes | - | - | ***ex155*** | Yes | - | - | ex187 | - | - | - |
| ex124 | - | - | - | ex156 | - | - | - | ex188 | - | - | - |
| ex125 | - | - | - | ex157 | - | - | - | ex189 | - | - | - |
| ex126 | - | - | - | ***ex158*** | - | - | - | ex190 | - | - | - |
| ex127 | - | - | - | ex159 | - | - | - | ex191 | - | - | - |
| ex128 | - | - | - | ex160 | - | - | - | ex192 | - | - | - |

| Stock | Heterozygous stock | P-element excised | 0.799 Kb product |
|---|---|---|---|
| ex193 | - | - | - |
| ex194 | - | - | - |
| ex196 | - | - | - |
| ex197 | - | - | - |
| ex198 | - | - | - |
| ex200 | - | - | - |
| ex201 | - | - | - |
| ex202 | - | - | - |
| ex203 | - | - | - |
| ex204 | - | - | - |
| ex205 | - | - | - |
| ***ex206*** | - | No | No[+] |
| ex207 | - | - | - |
| ex208 | - | - | - |
| ex209 | - | - | - |
| ex210 | - | - | - |
| ex211 | - | - | - |
| ex213 | - | - | - |
| ex214 | - | - | - |
| ex215 | - | - | - |
| ex216 | - | - | - |
| ex217 | - | - | - |
| ex218 | - | - | - |
| ex219 | - | - | - |
| ex220 | - | - | - |
| ex221 | - | - | - |
| ex222 | - | - | - |
| ex224 | - | - | - |
| ex225 | - | - | - |
| ex226 | - | - | - |
| ex227 | - | - | - |

| Stock | Heterozygous stock | P-element excised | 0.799 Kb product |
|---|---|---|---|
| ex228 | - | - | - |
| ex229 | - | - | - |
| ex230 | - | - | - |
| ex231 | - | - | - |
| ex232 | - | - | - |
| ***ex233*** | - | - | - |
| ex234 | - | - | - |
| ex235 | - | - | - |
| ***ex236*** | - | - | No** |
| ex237 | - | - | - |
| ex238 | - | - | - |
| ***ex239*** | - | - | No^ |
| ex240 | - | - | - |
| ex241 | - | - | - |
| ex242 | - | - | - |
| ex243 | - | - | - |
| ex244 | - | - | - |
| ex245 | - | - | - |
| ex246 | - | - | - |
| ex247 | - | - | - |
| ex249 | - | - | - |
| ex250 | - | - | - |
| ex251 | - | - | - |
| ex252 | - | - | - |
| ex254 | - | - | - |
| ex255 | - | - | - |
| ex256 | - | - | - |
| ex261 | - | - | - |

* duplicate stock
** larger PCR product
[+] no PCR product
[#] PCR evaporated
^ very faint product

### 3.4.4 *Sod* gene expression in transposon excision lines

Three of the retained homozygous excision lines (*ex136*, *ex141* and *ex158*) were separated by sex and subjected to real-time PCR analysis in order to verify that removal of the *P*-element would increase *sod3* gene expression. Analysis of expression data for each excision line as a proportion of *GAPDH* (housekeeping gene) expression showed that removal of the *P*-element in both sexes served to increase *sod3* gene expression compared to the *sod3* mutant line (Figure 3.11A (males) and 3.11B (females)). However, whilst in both sexes the increase in *sod3v1* was similar, the increase in *sod3v2* expression in females was far more dramatic with the expression matching that of *sod1* and *sod2*. We previously showed that in both male and female *WT* flies *sod1* was the most highly expressed of the *sod* isoforms. However, in the $sod3^{06029}$ strain *sod2* expression predominated (see Figure 3.8A and 3.8B). In each of the male excision lines tested, *sod1* reverted to be the most highly expressed (Figure 3.11A) however this reversal was not found to occur in female excision strains (Figure 3.11B).

Analysis of the fold-change in gene expression compared to $Sod3^{06029}$ reveals the degree to which *sod* expression changes upon transposon removal. For all 3 male excision stocks, removal of the transposon resulted in an increase in the expression of *sod3v1* of 3.5 – 5.5-fold and of *sod3v2* of 2.5 – 3.5-fold (Figure 3.12A). Interestingly, a concurrent rise in *sod1* (1.5 – 3-fold) and, to a lesser extent, *sod2* (1 – 2-fold) transcript expression was also found. Female excision lines exhibited greater upregulation of both *sod3v1* (9 – 13-fold) and *sod3v2* (9 – 21.5-fold) (Figure 3.12B) in each excision line, supporting the notion that *sod3* gene expression is higher in females. Increased *sod1* (1 – 2-fold) and *sod2* (1 – 2-fold) expression was also observed in female excision stocks. The P values for appropriate results are listed in the figure legend.

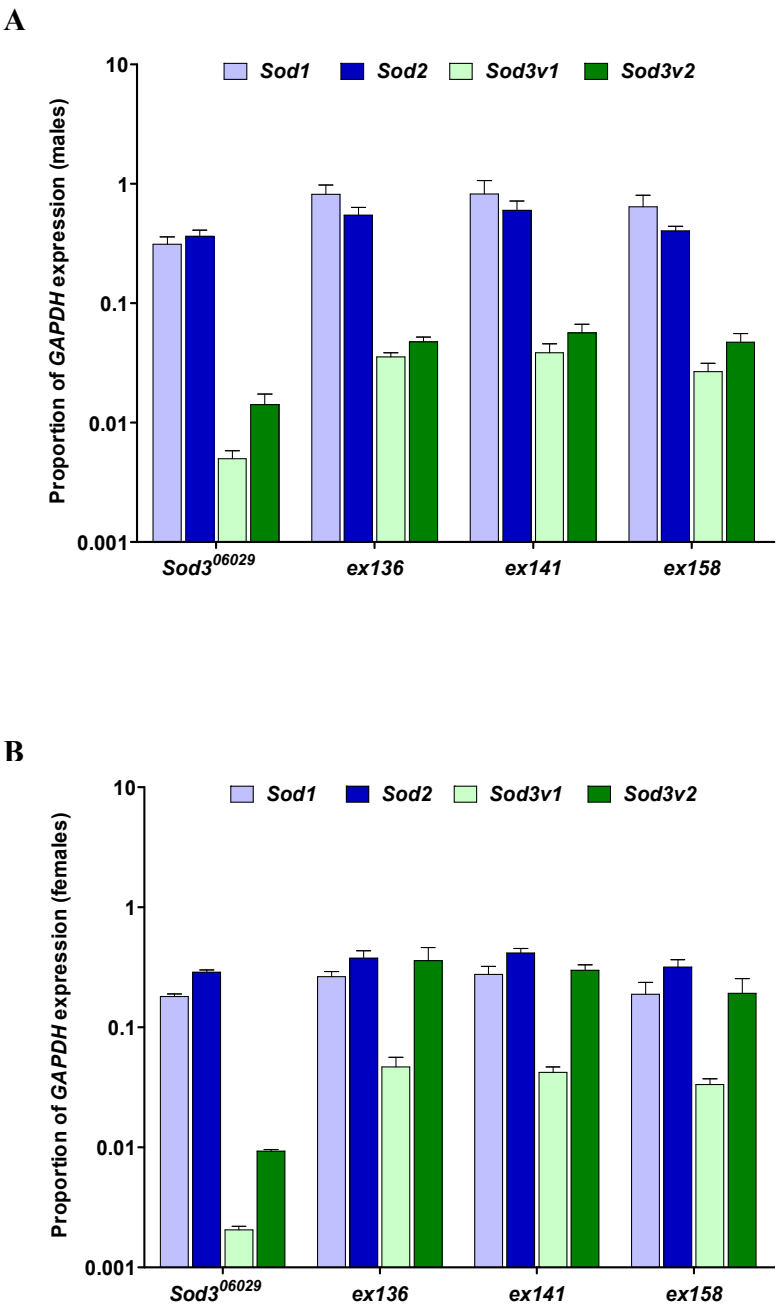


**Figure 3.11. *Sod* gene expression profiles in excision lines.** *Sod* gene expression was quantified in male (**A**) and female (**B**) excision lines as a proportion of *GAPDH* expression. All samples are tested at N = 4 and error bars are SEM.

**A**

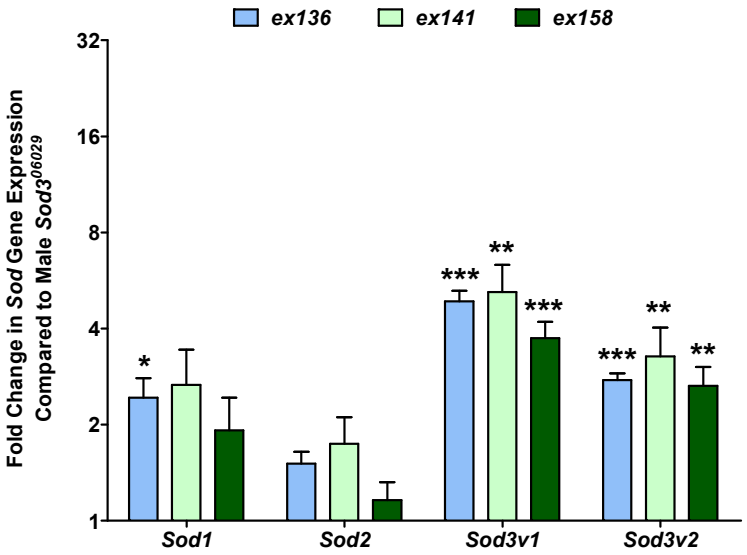


**B**

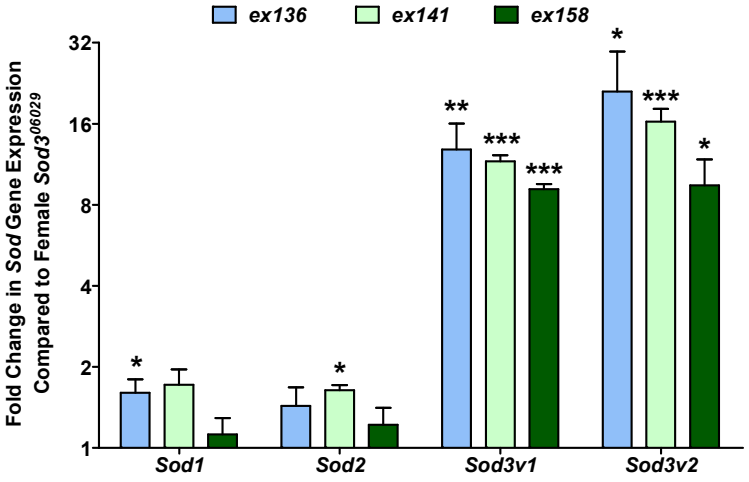


**Figure 3.12. Fold change in *Sod* gene expression in excision lines compared to the *Sod3*$^{06029}$ mutant line**. (**A**) Male excision lines and (**B**) female excision lines were tested at N = 4 and error bars are SEM. *, P = <0.05; **, P = <0.01; ***, P = <0.001.

### 3.4.5 Development of excision lines

Two of the excision lines in which only heterozygous progeny are generated (*ex110* and *ex155*) were crossed to the embryonic EGFP strain, *Gla, wg*$^{Gla\text{-}1}$*/CyO, twi, EGFP*, as detailed in the methods. Non-EGFP embryos were selected and their development monitored. Non-EGFP embryos of both excision strains successfully underwent organogenesis and cytodifferentiation, maturing to first instar larvae stage around 24 hours post embryo picking. First instar larvae underwent the two molts to second and third instar larvae by day 8 and two days later pupae were seen. Pupae appeared to undergo normal development with adult structures such as the head, abdomen and thorax being formed. Furthermore, later pupal developmental features such as bristles were also seen. However, none of the homozygous excision pupae, for either stock, were able to eclose as adults. Figure 3.13A and B show homozygous pupae from the *ex110* stock and Figure 3.13C and D are of those from the *ex155* stock. The lack of eye pigmentation indicates that only homozygous embryos were picked initially.

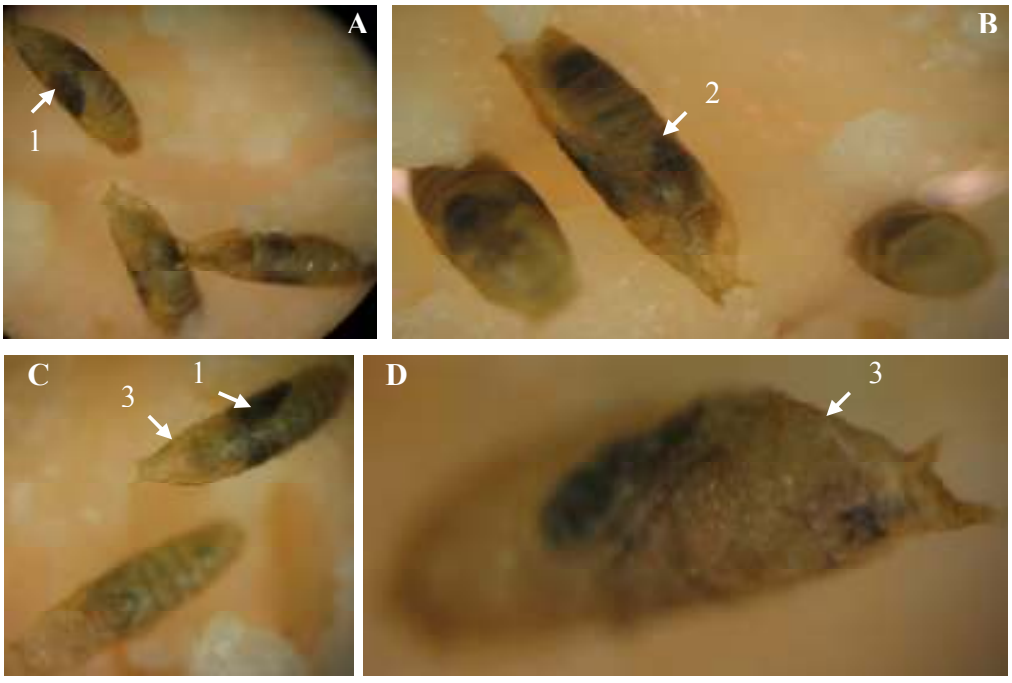


**Figure 3.13. Phenotypes of lethal homozygous excision lines**. **A** and **B** are *ex110* pupae and **C** and **D** are *ex155* pupae. Flies develop normally until the late pupal stage but then fail to eclose. Characteristic structures are shown which allowed development to be assessed. 1 = dark wings; 2 = bristles; 3 = lack of eye pigmentation.

### 3.4.6 *Sod* gene expression vs the backcrossed control strain

As detailed in the methods, a backcrossed control for the $Sod3^{06029}$ strain ($yw^{c\text{-}iso}$) was generated by backcrossing of the parental $yw^{c}$ line with the *sod3* mutant. Analysis of the change in expression of each *sod* gene in $Sod3^{06029}$ compared to $yw^{c\text{-}iso}$, revealed that in males there was variable change in *sod3* expression, with *sod3v1* showing no measurable change in expression whilst *sod3v2* was significantly up-regulated (df = 6, P = <0.05) (Figure 3.14A). A statistically significant rise in the expression of both *sod1* (df = 6, P = <0.01) and *sod 2* (df = 6, P = <0.01) of around 2-fold was also found. In female $Sod3^{06029}$ flies *sod3v1* expression was highly significantly suppressed ~3-fold (df = 6, P = <0.001) whereas *sod3v2* was down-regulated ~2-fold (df = 6, P = <0.01) (Figure 3.14B). As was found with males, *sod1* and *sod2* were found to be up-regulated although only marginally.

### 3.4.7 *Sod* gene expression vs the non-backcrossed control strain

*Sod* gene expression in the non-backcrossed male and female $Sod3^{06029}$ flies was also compared to the parental line, $yw^{c}$. Both *sod3v1* and *sod3v2* were found to be significantly down-regulated in male flies approximately 2-fold (df = 6, P = <0.01 and df = 6, P = <0.05, respectively) (Figure 3.15A), whilst no measurable change in *sod1* and *sod2* expression was observed. In females, down-regulation of *sod3v1* and *sod3v2* was significantly more pronounced at around 8-fold for both variants (both df = 6, P = <0.01) (Figure 3.15B). *Sod1* expression was also found to be significantly repressed in female flies (df = 6, P = <0.05) whereas *sod2* expression remained unchanged.

A

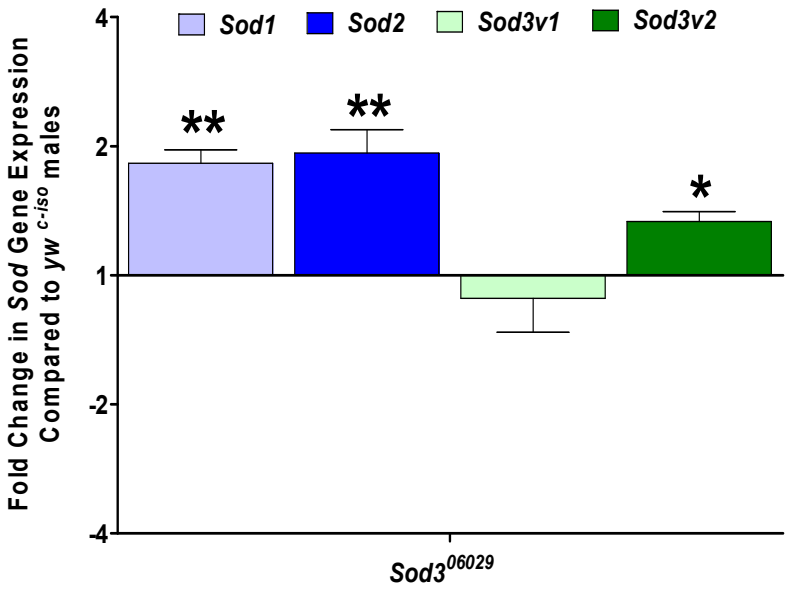


B

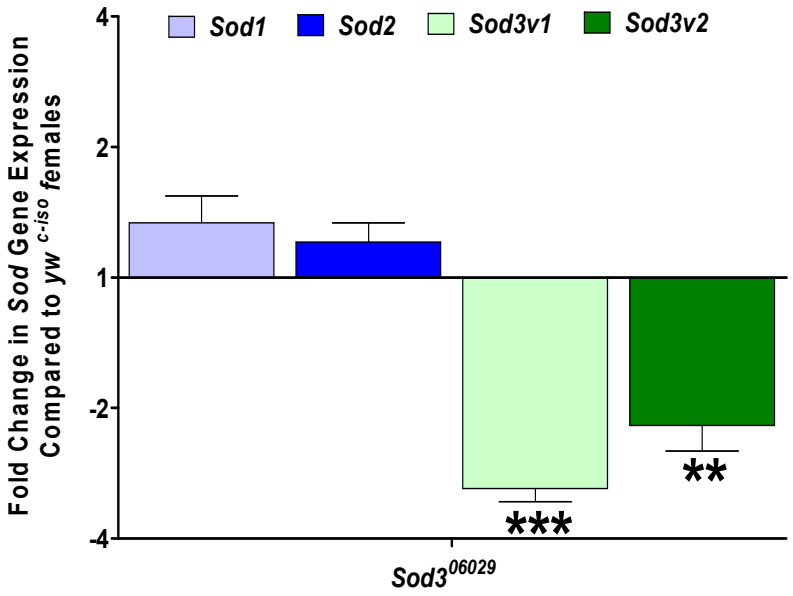


**Figure 3.14. Fold change in *Sod* gene expression in male (A) and female (B) *Sod3*$^{06029}$ flies compared to the backcrossed control line, *yw* $^{c\text{-}iso}$.** Samples are tested at N = 4 and error bars are SEM. *, P = <0.05; **, P = <0.01; ***, P = <0.001.

A

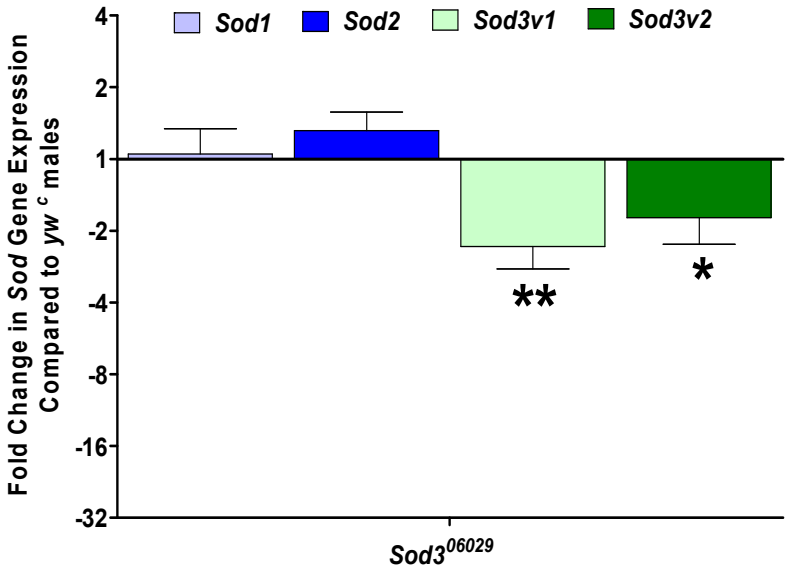


B

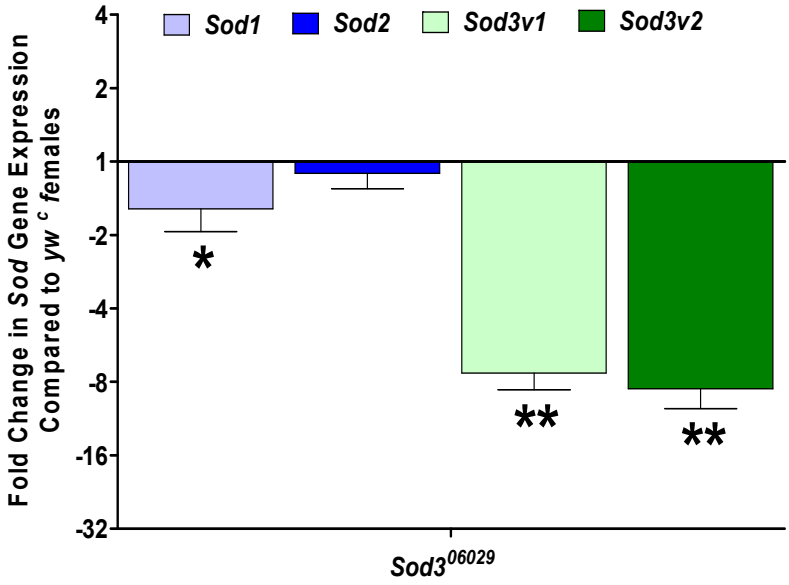


**Figure 3.15. Fold change in *Sod* gene expression in male (A) and female (B) *Sod3*$^{06029}$ flies compared to the non-backcrossed control line, *yw* $^{c}$.** Samples are tested at N = 4 and error bars are SEM. *, P = <0.05; **, P = <0.01.

## 3.4.8 *Sod* gene expression in response to oxidative stress

### 3.4.8.1 Paraquat

*Sod* gene expression profiles were also quantified in mixed sex *WT* adults in response to oxidative insults. After 24 hours of exposure to 30mM paraquat *WT* flies had ~50% mortality whereas control flies exposed to 5% sucrose showed 0% mortality (data not shown). Quantification of *sod* gene expression revealed all *sod* genes to be marginally down-regulated in surviving flies exposed to paraquat with *sod1* (df = 8, P = <0.05) and *sod3v2* (df = 8, P = <0.05) showing statistically significant reductions in expression (Figure 3.16).

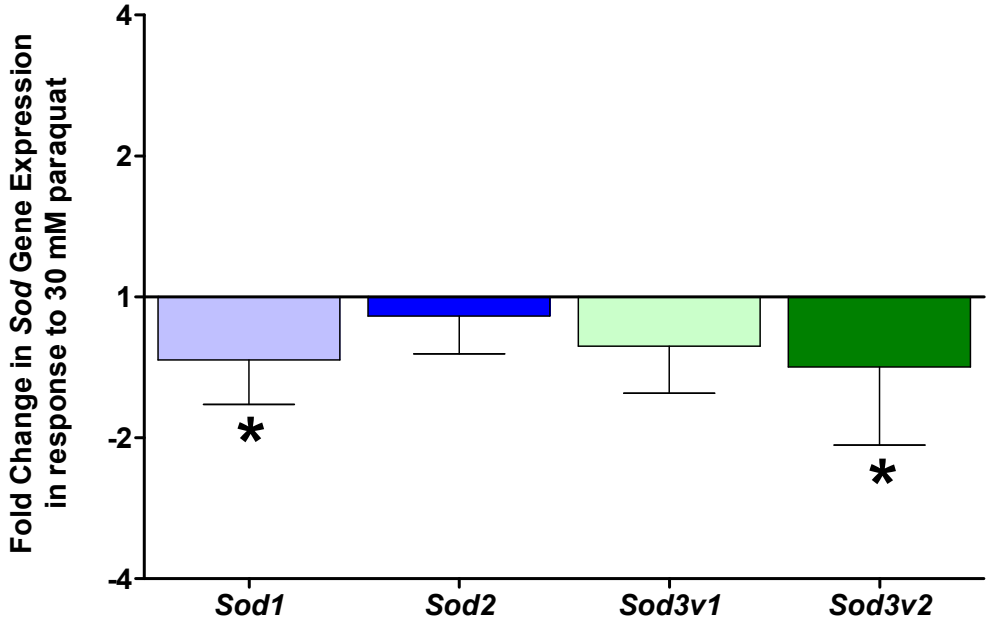


**Figure 3.16. Fold change in *Sod* gene expression in mixed sex *WT* flies in response to exposure to 30mM paraquat for 24 hours.** *, P = <0.05. Samples are tested at N = 5 and error bars are SEM.

### 3.4.8.2 $H_2O_2$

After 24 hours of exposure to 15% $H_2O_2$ *WT* flies had ~50% mortality whereas control flies exposed to 5% sucrose showed 0% mortality (data not shown). As with paraquat experiments, quantification of *sod* gene expression revealed all *sod* genes to be marginally down-regulated in surviving flies exposed to $H_2O_2$ with *sod1* (df = 6, P = <0.05) and *sod2* (df = 6, P = <0.05) showing statistically measurable down-regulation of expression (Figure 3.17).

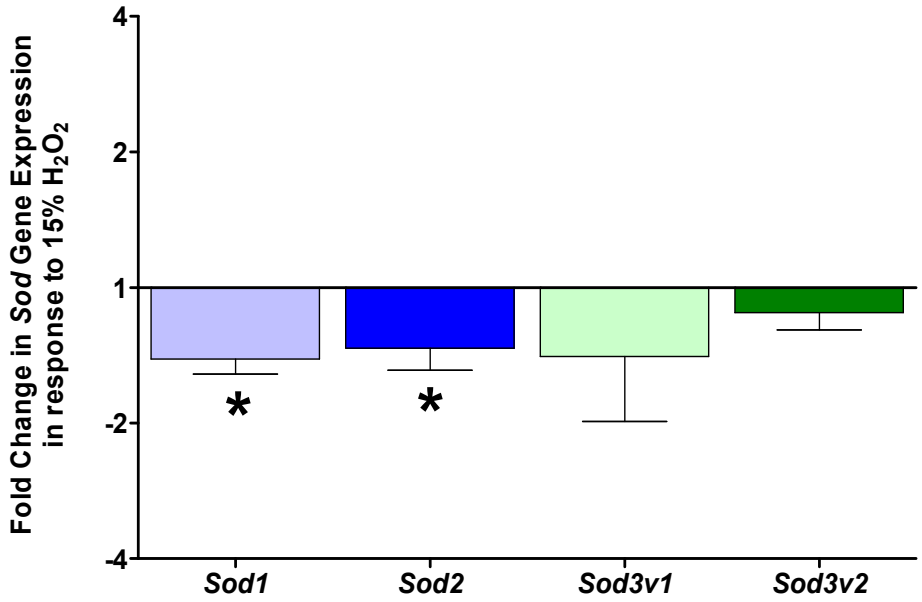


**Figure 3.17. Fold change in *Sod* gene expression in mixed sex *WT* flies in response to exposure to 15% $H_2O_2$ for 24 hours.** *, P = <0.05. Samples are tested at N = 5 and error bars are SEM.

## 3.5 Discussion

The main aims of the work presented in this chapter was to quantify the gene expression profiles of the *sod* isoforms in a number of *Cu Zn sod* mutants and to generate new *sod3* loss of function alleles. The *sod3* hypomorph strain used was generated by the Berkley *Drosophila* Gene Disruption Project (BDGDP) which aims to perturb each *Drosophila* gene through insertion of a single transposable element (*P*-element) (Bellen et al. 2004a). This sequence based screening project does not explore the consequence of disrupting individual genes and as such the *P*-element was excised, firstly to confirm that its insertion causes disturbed *sod3* transcription and secondly to try and generate *sod3* knockout mutants. Further work included exploring both the influence of genetic background and oxidative stress on *sod* gene transcription.

### 3.5.1 *Sod g*ene expression in *WT* flies reveals sex specific variation

Initial real time PCR experiments quantifying gene expression levels was carried out in *WT* adult flies and revealed differences in *sod3* expression between sexes. Whilst *Sod1* and *sod2* expression was comparable within sexes and between sexes, *sod3* expression was found to be lower in both genders. However, compared to males, females showed considerably higher expression of both *sod3* variants and furthermore *WT* females appear to express considerably higher levels of *sod3v2* than *sod3v1*, whereas males showed similar levels of expression of each. This higher level of antioxidant in females parallels the finding in honey bees that vitellogenin acts as an antioxidant which is highly expressed in egg-laying queens (Corona et al. 2007;Seehuus et al. 2006). Further support of higher antioxidant gene expression in females is given by developmental time-course microarray data showing *sod3* expression to be higher in females (Gauhar et al. 2008). Interestingly, the same study also revealed that *sod3* expression was found to be elevated in early embryos, during larval development and during metamorphosis. As illustrated in Figure 2.5B (Chapter 2), we also suggested that *Drosophila* embryos may express both *sod3*

variants more highly than larvae or adults thus supporting this notion. The scope of this study did not extend to determine the reason behind this sex specific genetic variation and thus the reasons for it can only be hypothesised. The most likely explanation is that females may contain tissues that have a higher abundance of *sod3*, possibly as a reproductive requirement, thus paralleling the findings of Corona and colleagues and Seehuus and colleagues (Corona et al. 2007;Seehuus et al. 2006). Alternatively, increased *sod3* expression may occur as an adaptive change in response to females being subjected to higher levels of extracellular $O_2^{-}\cdot$ than males. This again could be due to a reproductive requirement, however this finding of sex specific *sod* expression requires further work to explain.

### 3.5.2 *Sod g*ene expression in a *sod3* mutant line suggests compensatory changes in expression

*WT* cDNA was employed as the control in comparative real time PCR experiments with the *Sod* mutant lines. As found previously, in *WT* flies, in both sexes, *sod3v1* and *sod3v2* were less highly expressed than *sod1* and *sod2*, however females showed considerably higher expression of both *sod3* variant than males. As well as expressing higher levels of *sod3v1* and *sod3v2*, the degree to which expression is down-regulated in $Sod3^{06029}$ flies is much greater in female flies than males. It is important to note, however, that there is still a degree of *sod3* expression in the $Sod3^{06029}$ strain so this fly line must be considered a hypomorph rather than a null mutant. This is not entirely unexpected since the *P*-element insertion is upstream of the *sod3* coding sequence thus would likely only disrupt transcription. Interestingly, there was a general trend of *sod* gene suppression in all mutant lines tested and in both sexes. In the *x39/TM3* line *sod1* transcription was down-regulated around 2-fold in both sexes. This was to be expected since the *x39* allele is a deletion allele and as such heterozygous flies would be expected to exhibit at least half the expression of *sod1* compared to *WT* flies. *Sod1* gene expression in this particular fly strain could therefore be considered a control. However, in other lines compensatory changes in transcription were observed in response to the specific mutation. For instance, in male *n108/TM3* flies reduced expression of both the *sod3v1* and *sod3v2* transcripts almost 2-

fold was found, in female *Sod3*$^{06029}$ flies a significant increase *sod2* expression was observed and male *n108* flies had significantly suppressed *sod3v1* and *sod3v2* expression. These results imply that the *sod* genes are not entirely independent of each other and have either direct or indirect effects on each others' transcription. Studies in *C. elegans* support the notion of compensatory changes in *sod* expression in response to removing alternative members of the *sod* gene family, with a general trend of compensatory *sod* upregulation being observed (Back et al. 2010;Van Raamsdonk & Hekimi 2009).

### 3.5.3 Limitations of using *WT* flies as a control

As described, the control strain used for the comparative real-time PCR experiments was the wild-type *Oregon R* strain (*WT*). The major drawback of employing this strain is the lack of control for the influence of genetic background, or genetic variation, in each of the mutant fly strains. For instance, the transposon used to generate the *sod3* mutant line was inserted in to the *yellow white* (*yw*) background, not *Oregon R*. *yw* flies contain mutations in the *yellow* (*y*) and *white* (*w*) genes which cause phenotypic pigmentation deficiencies. The downstream effects or epistatic interactions of these mutations with the genetic background may be unknown but are likely to result in quantitative genetic variation that will not be present in *Oregon R* flies. Furthermore, inbred laboratory strains of *Drosophila* can accumulate alleles in a strain-specific manner. This has been shown in respect to lifespan, where strain specific accumulation of deleterious alleles has identified alleles which extend lifespan by suppressing the short-lived phenotype (Linnen et al. 2001;Spencer et al. 2003). Another consideration is the maternally inherited intracellular proteobacterium, *Wolbachia*. *Wolbachia* has been shown to have unpredictable effects on host fitness associated traits which is dependent upon genetic background in *Drosophila* strains (Dean 2006). Around 30% of stocks present at the Bloomington *Drosophila* Stock Centre are thought to contain *Wolbachia* (Clark et al. 2005), however it is unknown whether any of the strains used in this report are infected and even if they are what affect *Wolbachia* may be contributing to gene transcription. A number of recent studies have highlighted this need to control for genetic background in *Drosophila* genetics (Dworkin et al. 2009;Toivonen et al. 2007). Toivonen and colleagues suggest that, after correcting

for genetic background, *Indy* (*I'm not dead yet*) mutants, which have been shown to have long lived phenotypes (Rogina et al. 2000), actually show no increase in lifespan. Furthermore, Dworkin *et al*. determined the importance of genetic background in determining the phenotypic effect of a mutation in the *scalloped* (*sd*) gene in two wild type strains. *Oregon R* and *Samarkand* flies both have normal oval wings which differ only subtly, however whereas a *sd* mutation in *Oregon R* flies resulted in severely reduced wing size throughout the wing blade, the same *sd* mutation in *Samarkand* flies caused wings to remain elongated but with substantial tissue loss. The role that genetic background may play in influencing gene transcription must therefore be considered when interpreting the comparative real-time PCR results where *WT* flies were used as the control (see section 3.5.6).

### 3.5.4 Transposon excision restores gene expression but a knockout *sod3* mutant is not immediately obvious

Of the 236 independent excision lines generated, three homozygous precise excision lines (*ex136*, *ex141* and *ex158*) of each sex were analysed for *sod* gene expression. The purpose of measuring *sod* gene expression in these lines was to confirm that the reduction in *sod* expression found in the $Sod3^{06029}$ line was indeed due to transposon insertion. As a result precise excision of the *P*-element would be expected to return *sod* gene expression to *WT* levels. In each case *sod3* gene transcript levels were found to increase substantially in both sexes. The increase in expression was more dramatic in females (9 – 21.5-fold) than in males (2.5 – 5.5-fold), supporting our *WT* gene expression data which showed females to express higher levels of both *sod3* species. Interestingly, subtle differences in gene expression between sexes in our excision lines were also observed. Whilst in male lines *sod1* was found to be the most highly expressed isoform, in females it was *sod2*. Furthermore, transposon excision was found to be coupled to increased *sod1* and *sod2* transcription in both sexes suggesting that *Sod3* may help to regulate the expression of *sod1* and *sod2*.

Attempts to generate a *sod3* knockout mutant through imprecise *P*-element excision revealed some interesting results, which require further work to fully explain. Each of the 236 lines were subjected to PCR with a variety of primer pairs to identify any deletions around the *P*-element insertion site. Genomic deletions can be uni- or bi-directional (Adams and Sekelsky 2002) therefore primers were designed such that they bound a given distance either side of the *P*-element insertion site. As detailed in the results, PCRs with a primer pair spanning 799 bp of genomic DNA across the *P*-element locus revealed no smaller products indicating no small genomic deletion upon excision. A number of other primer pairs (data not shown) with predicted genomic products of up to ~5.5 Kb were also tested, again with no smaller products being found. Although no deletions were immediately obvious by PCR, in 15.7% of the 236 excision lines only heterozygous flies ever eclose, suggesting a lethal deletion mutation has occurred upon *P*-element excision in these strains. It should be noted that typically imprecise excision events are proposed to occur at a frequency of 2-10% (Adams & Sekelsky 2002), making this value slightly above the average. A reasonable explanation for the lack of observed genomic DNA deletion in these heterozygous lines is due to the unpredictable size of deletions. Deletions can range from a few base pairs up to tens of Kb's (for examples see: (Cayirlioglu et al. 2001;Hiesinger and Bellen 2004;Mihaly et al. 1997;Suzanne et al. 1999)) therefore it is probable that in these heterozygous lines the deletions extend into regions past where the primers bind, thus the PCR products revealed are likely those produced from the corresponding balancer chromosome, giving a wild type genomic size product. This argument becomes more reasonable given the observation that a gene critical for larval heart development (flybase: communication), *sprite* (*sprt*), is located 645bp upstream from the 5' UTR of *sod3*. It therefore appears likely that the deletions arising from imprecise excision of the *P*-element remove DNA coding for *sprt* and it is the knocking out of this gene, rather than *sod3*, which generates lethality in the heterozygous excision lines. This explanation is supported by the observation that mice lacking *sod3* actually have relatively mild phenotypes (Sentman et al. 2006), meaning it would be surprising if an absence of *sod3* in *Drosophila* was lethal. It cannot be ruled out, however, that the lethality of the heterozygous excision lines could occur from the *P*-element actually being excised cleanly but then subsequently re-inserting elsewhere in the genome within a critical gene, disruption of which is lethal. This would seem unlikely however, and particularly at the

frequency observed, since all excision lines were observed to be lacking the white$^{+}$ phenotype associated with the *P*-element.

The excision lines produced are listed in Table 3.8. Those stocks *italicised* and in red have been retained for future work to determine the size of the individual deletions. All heterozygous lines have been retained as they likely are deletion alleles. Also retained are those strains in which aberrant PCR products were found and also a number of clean revertant excision lines have been kept.

### 3.5.5 Phenotypes of heterozygous excision lines

Whilst genomic DNA deletions were not confirmed by PCR, the appearance of only heterozygous offspring upon transposon excision indicates the generation of lethal imprecise excision mutants. As detailed in the results, two of the heterozygous lines (*ex110* and *ex158*) were crossed to an embryonic EGFP producing strain. This allowed for identification of homozygous offspring by selecting those non-EGFP embryos. While homozygous excision lines appear to develop normally, with structures associated with late metamorphosis visible, they fail to eclose from the pupal case. A likely explanation is that an absence of *sod3* leaves the homozygous strains unable to tolerate an increase in oxygen consumption that has been shown to be highest during the late stages of *Drosophila* pupal development (Clare 1925;Wolsky 1938). Interestingly, SOD levels have been found to show a U-shape trend during *Drosophila* development from egg to adult (Nickla et al. 1983), with a significant increase in SOD activity found between larval and one day adult stage (Massie et al. 1980). This increased oxygen consumption coupled with a rise in SOD activity around the pupal stage suggests that an absence of the *sod3* gene may be lethal for *Drosophila* development.

### 3.5.6 *Sod* gene expression in a *sod3* mutant line compared to a backcrossed and non-backcrossed control suggests the appearance of modifiers

As discussed above, there are a number of limitations of using the *WT* line as the control in which to assess the contribution of *sod* mutations to gene transcription. Therefore, a backcrossed control line was generated (*yw* $^{c\text{-}iso}$) with which to compare the *Sod3* mutant. *sod* gene expression was quantified in our *Sod3* mutant line against both the backcrossed control and also the non-backcrossed *yw* $^{c}$ parental line. *yw* $^{c}$ was considered an appropriate control since *P*-element insertions are made into the *yw* background ($y^{1}$ $w^{67c23}$; *P{SUPor-P}CG9027*$^{KG06029}$). Female *Sod3*$^{06029}$ flies compared to the backcrossed control showed down-regulation of *sod3* expression of around 2-fold, whereas in comparison with *yw* $^{c}$ flies a more dramatic down-regulation of around 8-fold was observed. Equivalent measurements in male flies revealed relatively little change in expression of the *sod3* transcript when compared to *yw* $^{c\text{-}iso}$ flies, but when *yw* $^{c}$ was the control *sod3* expression was suppressed ~2-fold. Males did however show an upregulation of *sod1* and *sod2* of around 2-fold with the *yw* $^{c\text{-}iso}$ control, but this up-regulation was shown to be noticeably reduced with the *yw* $^{c}$ control strain. *Sod1* and *sod2* expression were moderately up-regulated in female *Sod3*$^{06029}$ flies in comparison with the backcrossed *yw* $^{c\text{-}iso}$ line, however an equivalent down-regulation of expression was observed when *yw* $^{c}$ was the control strain. The opposing *sod1* and *sod2* gene expression trends in males and female *Sod3*$^{06029}$ flies when *yw* $^{c}$ was the control highlights the differential co-transcriptional *sod* gene expression dependencies among sexes. The most likely explanation for the variation in *sod* expression with the backcrossed and non-backcrossed lines is that in backcrossing the mutant line, *yw* $^{c\text{-}iso}$ flies are revealing the effects of genetic modifiers inherited from the *Sod3*$^{06029}$ line. Genetic modifiers (or modifier genes) are an established facet of biology and have been proposed to act to indirectly stabilise an organism's fitness (Karlin and McGregor 1972). Furthermore, there is evidence for the protective effect of modifier genes in a *sod1* mutation of an ALS mouse model (Al-Chalabi et al. 1998). It appears that the unknown modifiers inherited by the backcrossed control line are also having protective effects since increased *sod1* and *sod2* transcription as well as reduced *sod3* knockdown in

the *sod3* mutant was observed. This suggests that the hypomorph mutation is having a significant impact on fitness and survival in the $Sod3^{06029}$ flies, and this could explain why the homozygous *sod3* knockout strains, generated through *P*-element excision, are found to be lethal.

### 3.5.7 No responsive increase in *sod* expression in response to oxidative stress insults

Interestingly we found that subjecting *WT* flies to both paraquat and $H_2O_2$ resulted in decreased rather than increased, as might be expected, expression of each of the *sod* genes. It is perhaps surprising that increased *sod* gene expression is not driven since a link between paraquat resistance, in particular, and *sod* expression in *Drosophila* has been observed. Using artificial selection by delayed reproduction, several long lived *Drosophila* strains have been generated (Arking 1987;Luckinbill et al. 1984) that show enhanced paraquat resistance (Arking et al. 1991;Force et al. 1995). Gene expression analysis of these strains revealed that a significant increase in *sod1* expression accompanied this increased paraquat resistance and long life (Dudas & Arking 1995). Equally, when these long lived strains were reverse-selected for normal lifespan, antioxidant gene expression was found to drop back to normal levels (Arking et al. 2000). Thus it seems the *sod* genes are not responding to oxidative stress induced by paraquat implying that their main function is not as a responsive defence mechanism. Instead, the increase in paraquat resistance appears to be a by-product of increased SOD activity in *Drosophila*. However, studies in other model systems such as the honey bee (Choi et al. 2006), mouse lung (Tomita et al. 2007) and even maize (Matters and Scandalios 1986) has demonstrated paraquat's ability to increase some of the *sod*'s gene expression profiles. Furthermore, rat *sod1* mRNA levels have been observed to increase in response to paraquat, heat shock and also $H_2O_2$ treatment (Yoo et al. 1999b). $H_2O_2$ is a product of SOD catalysis not a substrate, and therefore it may seem a little odd that it should stimulate *sod* mRNA levels. However, a 3-5 fold increase in promoter activity was observed with each of the three treatments and functional analysis showed that $H_2O_2$ stimulates transcription through a $H_2O_2$-responsive element (HRE) within the promoter, whereas heat shock and paraquat function through a

heat shock element (HSE). If we simply consider the proposed extracellular location of both *sod3* variants it is perhaps less surprising that neither variant's expression increased in response to paraquat. *In vivo*, paraquat is believed to undergo a NADH-dependant reduction to form the paraquat radical ($Pa^{+}$) intracellularly at microsomal and/or mitochondrial sites (Farrington et al. 1973;Fukushima et al. 2002). $Pa^{+}$ will then rapidly react with oxygen to form the superoxide radical and $Pa^{2+}$. Our results therefore support the notion that *sod3* in *Drosophila* encodes extracellular proteins which, unlike *sod1*, do not function to protect against paraquat or $H_2O_2$ induced intracellular oxidative stress.

It should, however, be noted that the concentrations of the oxidative insults (30mM paraquat and 15% $H_2O_2$) applied in this study are severe. These concentrations were chosen to parallel those used in the functional assays described in chapter 5 in order to determine whether any functional changes in oxidative stress resistance conferred by *Cu Zn sod* mutations could be attributed to compensatory changes in *sod* expression (see chapter 5 discussion). Due to the nature of the highly acute oxidative insult applied to the mutant lines tested in this chapter it is possible that the trend of decreased *sod* expression observed, recorded after paraquat and $H_2O_2$ exposure, actually results from global adaptive changes occurring to promote survival in the grossly toxic experimental conditions rather than as a direct response to the oxidative insult. As such it would be useful to repeat these experiments with lower concentrations of paraquat and $H_2O_2$ which would exert a less severe and more chronic stress condition. Under such conditions a more appropriate evaluation could be made of whether the expression of the *sod* genes alters in response to oxidative stress.

# CHAPTER 4

# 4. Proteomic analysis of SOD levels in diverse fly backgrounds and in response to oxidative insults

## 4.1 Aim

The aim of the current chapter is to build on the previous chapters' work and link gene expression to protein levels by highlighting the efforts of proteomic studies of SOD levels in a variety of fly backgrounds and again in response to oxidative stress. Results will demonstrate whether post-transcriptional changes are occurring in response to both specific *sod* mutations and oxidative stress treatments.

## 4.2 Introduction

Whilst gene transcription is a useful measure for assessing genetic changes occurring in an organism in response to changes in, for example, environment, development, stress and nutritional needs, protein levels and activities may correlate independently of their genetic foundations. Logically it would seem inefficient for genes to be transcribed to specific levels to manage an organisms current or changing needs, thus post-transcriptional and/or post-translational control would seem at least as important as gene expression in modulating protein activities. Translational regulation is a conserved feature of cellular hemostasis and occurs in the form of alterations in the levels, activities or availability of translation factors (initiation, elongation and/or release factors) and through interactions with regulatory features in the untranslated regions (UTRs) of mRNA species, such as by microRNA (miRNA) binding. Post-translational regulation generally occurs in the form

modifications, such as glycosylation or phosphorylation, or irreversible actions such as proteolysis.

Whilst there are examples of post-transcriptional regulation events of SOD in diverse species (Dubrac and Touati 2002;Sunkar et al. 2006) including *Drosophila* (Gu and Hecht 1996), perhaps the most critical regulatory feature of the SOD isoforms is that of metal redox co-factor insertion, required for catalytic function. In the case of SOD1 the catalytic copper ion is usually post-translationally inserted into each SOD1 subunit through interactions with the CCS copper chaperone (Culotta et al. 1997;Rae et al. 2001). The apo-form of SOD1 is characterised by a disulfide bond between the 2 subunits making up the dimeric active protein. In aerobic conditions, or in the absence of CCS, this disulfide bond can become reduced allowing the CCS to dock with this reduced disulfide link to transfer the metal ion to the subunits. This is important for the fraction of SOD1 that localises within the mitochondrial intermembrane space (IMS), since only the reduced disulfide apo-form of SOD1 can enter the IMS (Culotta et al. 2006;Field et al. 2003). Using a yeast model it was shown that increased abundance of CCS in the mitochondrial IMS elevated SOD1 abundance within the IMS by increasing retention of the enzyme within the mitochondria through protein-protein interactions of SOD1 and CCS (Field et al. 2003). Whilst the co-factor insertion mechanism for SOD1 is well understood, for SOD2 the precise details are unknown. It is known, however, that manganese is inserted post-translationally within the mitochondrial matrix since a mutant SOD2 from *S. cerevisiae*, lacking the mitochondrial targeting sequence was shown to pool in the cytosol and have no enzymatic activity (Luk et al. 2005). Furthermore, the same SOD2 mutant was used to demonstrate that, unlike SOD1 metal insertion, manganese can only be inserted into newly translated proteins and not into existing SOD2-apo proteins (Luk et al. 2005). These findings, together with the observation that the ribosomes required for SOD2 translation are adjoined to the mitochondrial outer membrane, lead Culotta and colleagues to propose a model by which translation, mitochondrial import and co-factor insertion of SOD2 are coupled (Culotta et al. 2006). In spite of the homology between SOD3 and SOD1, the copper loading mechanisms appear to be somewhat different, with SOD3 co-factor insertion occurring independently of CCS within intracellular secretory departments, particularly in the trans-Golgi network. The copper chaperone Atox 1, is understood to

deliver copper to the trans-Golgi network and has been shown to be essential for SOD3 activity in fibroblasts by positively regulating *sod3* gene expression (Jeney et al. 2005). These differential co-factor insertion mechanisms highlight the importance of post-translational modifications in maintaining SOD activity.

The present chapter details the results of studies of the SOD isoforms at the protein level. Highlighted is the development of a 96-well microtitre plate based assay allowing for the measurement of SOD activity in mutant lines and in response to oxidative stress, thus expanding on the gene expression measurements of the previous chapter. Also presented are the efforts to validate a *Drosophila* SOD3 specific antibody, initially for use in western blotting and finally described are proteomic studies, using the iTRAQ (isobaric tag for relative and absolute quantitation) technique, to measure quantitative changes in protein levels in response to various *sod* gene mutations.

## 4.3 Materials and methods

### 4.3.1 Fly strains

The fly strains used in subsequent experiments are listed in Table 3.1 and were maintained on standard *Drosophila* medium (Appendix 2) at 23°C in a 12 hour light/dark cycle.

### 4.3.2 Oxidative stress treatments

Paraquat and $H_2O_2$ treatment methodology was as described in section 3.3.10.

### 4.3.3 Preparation of protein samples for SOD activity assays

Adult flies to be assayed for SOD activity were briefly anaesthetised with $CO_2$, separated by sex (if appropriate) into a 1.5mL microtube (Eppendorf, UK), flash frozen in $LN_2$ and stored at -20°C until required. Protein preparations were made by homogenisation of frozen flies in 50mM potassium phosphate buffer (pH 7.8) as follows: Flies were transferred to 2mL screw-cap microtubes (Greiner Bio One) containing 10 – 20 1.4mm zirconium silicate beads (Quackenbush) along with an appropriate amount of 50mM potassium phosphate (pH 7.8) buffer (usually ~30 flies in 300µL). Tubes were placed in a Mini-Beadbeater homogeniser (BioSpec) and homogenised for 30 secs at 4,800 rpm (this was the default speed at which the Mini-Beadbeater was used unless stated otherwise). Following homogenisation, tubes were centrifuged briefly and the buffer/debris solution was transferred to a fresh 1.5mL microfuge tube by pipetting. Tubes were then centrifuged for 10 min at 10,000 x g at 4°C and the supernatant was retained.

- For preparations to be analysed for <u>total SOD activity</u>: supernatants were diluted 8:11 in the same homogenisation buffer (80µL supernatant + 30µL buffer) and centrifuged for 10 mins at 20,000 x g at 4°C. The supernatant was retained for activity measurements.

- For preparations to be analysed for Cu Zn SOD activity: supernatants were diluted 8:10 with 10% (w/v) sodium dodecyl sulfate (SDS) (20µL SDS + 80µL supernatant), incubated for 30 mins at 37°C and chilled on ice for 5 mins. The mixture was subsequently treated with 3M KCl (10µL KCl per 100µL), chilled for 30 mins on ice and centrifuged for 10 mins at 20,000 x g at 4°C. The supernatant was retained for activity measurements.

### 4.3.4 Determination of protein concentration for SOD activity assays, western blots and iTRAQ analysis

The protein concentration of the samples prepared above was determined using the Bio-Rad *DC* protein assay (Bio-Rad). This assay uses the reaction between protein in the test samples and copper in an alkaline medium to reduce Folin reagent (Lowry et al. 1951). The protein concentration was then determined for each of the samples in duplicate at two dilutions by measuring the colorimetric change against a standard curve of bovine serum albumin (BSA) (Sigma) standards at concentrations of: 0.03, 0.06, 0.125, 0.25, 0.5, 1 and 2mg/mL. Assays were prepared according to the manufacturer's instructions in 96-well optical bottom plates (Nunc) and measured spectroscopically at 680 nm in a FLUOstar OPTIMA plate reader (BGM Labtech).

### 4.3.5 SOD activity assay

SOD activities were measured according to the principle of Beauchamp and Fridovich (Beauchamp and Fridovich 1971). This method uses the reaction of xanthine with xanthine oxidase to produce $O_2^{-}\cdot$ which reduce NBT (nitro blue tetrazolium chloride) to formazon, formation of which can be measured spectroscopically. SOD competes with NBT for $O_2^{-}\cdot$ and thus SOD activity can be determined by the degree of inhibition of formazon formation after the addition of protein homogenates. The protocol is a modified version of that designed by Mockett *et al*. in that it allows for measurements to be taken in 96-well

plates in volumes of 200µL (Mockett et al. 2002). Assays reactions were prepared in 96-well plates (Nunc) as follows:

Per well:

| | | |
|---|---|---|
| 10µL | assay buffer | |
| 10µL | protein sample of known concentration (homogenisation buffer for blanks and standards) | |
| ↓ | | |
| 132µL | assay buffer | Make up as master mix, enough for 160µL per well being used |
| 5µL | Catalase (40U/mL) | |
| 5µL | NBT (2.24mM) | |
| 17µL | Xanthine (1.8mM) | |
| 1µL | BCS (10mM) | |
| ↓ Mix | | |
| 20µL | Xanthine Oxidase (0.025U/mL) (buffer for blanks) | |

NOTE : Assay buffer: 50mM potassium phosphate buffer (pH 7.8), 1.33mM diethylenetriaminepentaacetic acid (DTPA), 0.2mg/mL bovine serum albumin (BSA). Homogenisation buffer: 50mM potassium phosphate buffer (pH 7.8). BCS: bathocuproinedisulfonic acid disodium salt. NBT: nitrotetrazolium blue chloride. All assay reagents were obtained from Sigma. 'Blanks' refer to wells where no protein sample or enzyme was added in order to give a baseline reading of absorbance. 'Standards' refer to wells where only protein sample is absent and therefore gives a maximal, uninhibited, absorbance reading.

The reaction was initiated following the addition of 20µL xanthine oxidase (0.025U/mL) and measured spectroscopically at 560 nm for 30 mins. Each protein sample concentration was tested in quadruplicate and a minimum of four concentrations were tested for each sample such that two were predicted to inhibit the reaction rate by more than 50% and two by less than 50%. One unit of SOD activity is described as the concentration of protein sample required to inhibit the reaction rate by 50% under the experimental conditions. Purified SOD from bovine erythrocytes (Sigma) was used as a positive control sample in each assay. Statistical analysis of the data was performed using an unpaired t-test.

### 4.3.6 Preparation of protein samples for SOD activity gels

Protein preparations were made by homogenisation of frozen mixed sex adult flies in 10mM dithiothreitol (DTT)/0.1% Triton-X100 (both Sigma) using the Mini-Beadbeater homogeniser as described above. Five microlitres of homogenisation buffer was required per fly and a minimum of 80 flies required homogenising. The homogenate was centrifuged at 10,000 x g for 10 mins at 4°C and the supernatant was retained for assaying.

### 4.3.7 SOD activity gels

In-gel SOD activity was determined using the NBT negative staining principle of Beauchamp and Fridovich (Beauchamp & Fridovich 1971). Protein samples were assayed by native (non-denaturing) polyacrylamide gel electrophoresis (PAGE). One point five millimetre gels were cast with a 5% separating gel (Table 4.1) and a 4% stacking gel (Table 4.2). Following gel polymerisation, gels were loaded into a gel tank, submerged in 1X gel running buffer (0.25M Tris and 1.92M glycine) (both Sigma) and left to equilibrate for 5 – 10 mins. Protein samples were mixed with an equal volume of 2X non-denaturing loading buffer (25% Tris-HCl (pH 6.8), 20% Glycerol, 0.02% Bromophenol blue) and a maximum volume of 40µL (20µL protein + 20µL loading buffer) was applied to the gels. A positive control of purified SOD from bovine erythrocytes was also loaded on each gel. Gels were run for 1 hour and 45 mins at 120 volts.

Following completion of the run, gels were removed from the gel plates, the top left corner was cut off (for orientation) and the gel was submerged in 10mL of gel stain solution (12.24mM NBT, 6.63M TEMED, 0.18mM riboflavin, 1M $K_2HPO_4$) in a light proof box. The box was gently agitated on a rotary shaker at 35 rpm for 20 mins. Following staining, gels were illuminated with white light to initiate the photochemical reaction. Exposure to light causes the riboflavin within the gel stain to generate $O_2^{-}\cdot$ in the presence of $O_2$ and TEMED. NBT soaked into the gels and SOD in the protein samples compete for the $O_2^{-}\cdot$ as explained earlier. Those areas of the gel without SOD become purple-blue due to NBT reduction, whereas regions of the gel where SOD is present remain transparent as SOD

scavenges $O_2^{-}\cdot$. Illumination was maintained for 10 – 15 mins or until there was maximum contrast between transparent gel and purple-blue areas. Gels were analysed using the ImageJ image processing program.

**Table 4.1. Components of a 5% separating gel.**

| | Volume of reagent (mL) for a total volume of: | | | |
|---|---|---|---|---|
| | **10mL** | **20mL** | **30mL** | **40mL** |
| Distilled water | 5.7 | 11.4 | 17.1 | 22.8 |
| 30% Bis acrylamide (Bio Rad) | 1.7 | 3.4 | 5.1 | 6.8 |
| 1.5M tris-HCL (pH 8.8) (Sigma) | 2.5 | 5 | 7.5 | 10 |
| 10% ammonium persulfate (APS) (Sigma) | 0.1 | 0.2 | 0.3 | 0.4 |
| TEMED (Sigma) | 0.016 | 0.024 | 0.032 | 0.040 |

**Table 4.2. Components of a 4% stacking gel.**

| | Volume of reagent (mL) for a total volume of: | | | |
|---|---|---|---|---|
| | **2mL** | **4mL** | **6mL** | **8mL** |
| Distilled water | 1.408 | 2.926 | 4.384 | 5.842 |
| 30% Bis acrylamide | 0.27 | 0.53 | 0.8 | 1.07 |
| 1.5 M tris-HCL (pH 6.8) | 0.3 | 0.5 | 0.75 | 1 |
| 10% APS | 0.02 | 0.04 | 0.06 | 0.08 |
| TEMED | 0.002 | 0.004 | 0.006 | 0.008 |

### 4.3.8 Antibody production

A polyclonal antipeptide antibody to *Drosophila* SOD3 was manufactured by Eurogentec Ltd. Through analysis of the translated *Drosophila* SOD3 sequence, a 12 amino acid region was chosen based on the prediction that none of the residues in the sequence were important for catalytic function but that they were believed to reside on the outside face of the native protein. The following peptide sequence was chosen:

*Drosophila* SOD3 (residues 156-167): GLGNHTDSKKTG

The peptide antigen was synthesised by Eurogentec Ltd. and used to generate a rabbit anti-peptide polyclonal SOD3 antibody. The antibody generation schedule involved a first immunisation with the antigen followed by a boost 2 weeks later. A second boost followed 2 weeks after that and a small bleed serum sample was taken from the animal

approximately 9 days following. One month after the second boost the animal received a third boost and 9 days after this a large serum bleed was taken. A final bleed was taken approximately 3 weeks after this. Each of the bleed serums were supplied as well as a stock of the affinity purified antibody, reconstituted in phosphate buffered saline (PBS) (+ 0.01% thimerosal, BSA 0.1%) supplied at a concentration of 160µg/mL. Also supplied was the free peptide to which the antibody was raised (1.85g).

### 4.3.9 Preparation of protein samples for western/dot blots

Whole fly protein samples were made by homogenising 40 mixed sex whole flies in 600µL homogenisation buffer (5% SDS plus a Complete Mini protease inhibitor tablet (Roche)) using the Mini-Beadbeater homogeniser. The homogenised protein samples were centrifuged at 13,000 rpm briefly to separate solid fly particles and the supernatant was retained for protein concentration determination and use in subsequent western blots.

### 4.3.10 Western blots

Western blots were carried out according to standard procedures (Sambrook et al. 1989), using a 10% or 12% separating gel (specific gel compositions are detailed in individual results). Protein samples were prepared by mixing with an equal volume of 2X sample buffer (125mM Tris-HCL pH 6.8, 4% SDS (w/v), 20% glycerol (v/v), 10% 2-mercaptoethanol (v/v) and 0.002% bromophenol blue (w/v)) and boiling at 95°C for 5 mins. Protein samples (maximum volume of 40µL (20µL protein + 20µL sample buffer)) were loaded on the gel along side either 5µL of a Broad-Range prestained SDS-PAGE standard (Bio Rad) or 10µL of a Dual Colour Precision Plus Protein Standard (Bio Rad) and run at 150V for 1hour. Samples were subsequently transferred to a nitrocellulose membrane (Hybond-C Extra, Amersham) at 15V for 1 hour using the Trans-blot SD semi dry transfer cell (Bio Rad) and, following transfer, the membrane was incubated in a blocking solution of either 3 – 5% BSA in 0.5% tween PBS (tPBS) buffer or 3 – 5% milk powder in 0.5% tPBS buffer for a minimum of 1 hour at room temperature with gentle agitation at 35 rpm. The membrane was subsequently incubated in a variety of primary

antibody dilutions (see Table 4.3 – specific dilutions for individual experiments are detailed in the results), diluted in blocking solution, and agitated at 35 rpm at 4°C, overnight. After washing the membrane in 0.5% tPBS for a total of 15 mins, the membrane was incubated with the secondary antibody (see Table 4.4 – specific dilutions for individual experiments are detailed in the results), again made up in blocking solution, for 1 hour at room temperature with agitation at 35 rpm. Two five minute washes in 0.5% tPBS buffer, plus a further five minute wash in PBS buffer followed, before the membrane was visualised either using the Li-Cor Odyssey Infrared Imaging System (Li-Cor Biosciences) or the enhanced chemiluminescence (ECL) detection technique (Supersignal® West Pico, Thermo Scientific).

**Table 4.3. Primary antibodies used in western blots.**

| Antibody name | Supplier | Dilution range |
|---|---|---|
| *Drosophila* SOD3 | Eurogentec Ltd. | 1 : 50 - 1 : 5000 |
| Murine SOD3 | T. Fukai, University of Illinois at Chicago | 1 : 500 - 1 : 2000 |

**Table 4.4. Secondary antibodies used in western blots.**

| Antibody name | Host/reactivity | Conjugate | Supplier | Dilution range | Detection method |
|---|---|---|---|---|---|
| Alexa Fluor 680 | Goat/rabbit | 680 nm fluorophore | Invitrogen | 1 : 2000 - 1 : 10000 | Li-Cor |
| Alexa Fluor 780 | Goat/rabbit | 780 nm fluorophore | Invitrogen | 1 : 2000 - 1 : 10000 | Li-Cor |
| HRP* anti-rabbit | Goat/rabbit | HRP | Abcam | 1 : 2000 - 1 : 10000 | ECL |

*horseradish peroxidase

## 4.3.11 Dot blots

1–1.5µL samples of whole fly protein homogenate were spotted on to a nitrocellulose membrane (Hybond-C Extra, Amersham) and allowed to air dry. Once dry, the membrane was placed in blocking solution (3 – 5% BSA 0.5% tPBS or 3 – 5% milk powder 0.5% tPBS) for 1 hour at room temperature and agitated at 35 rpm. Multiple dilutions of the primary antibody were made in blocking solution and following blocking, each dilution

was spotted on top of a homogenate sample (see results for individual dilutions). The blots were incubated at room temperature for 1 hour. Blots were rinsed for a total of 15 mins in 0.5% tPBS and then a 1:10,000 dilution of the Alexa Fluor 780 secondary antibody, made up in blocking solution, was applied. Blots were incubated at room temperature for 1 hour with agitation at 35 rpm and were then washed twice for five minutes in 0.5% tPBS buffer, plus a further five minute wash in PBS buffer. The membrane blot was visualised using the Li-Cor Odyssey Infrared Imaging System.

### 4.3.12 Competition assays

For competition reactions western blots were repeated but the primary antibody was first pre-incubated with an excess of the free peptide (as specified in the results) to which the antibody was raised (supplied by Eurogentec Ltd. along with the antibodies). Pre-incubation was for a minimum of 2 hours at room temperature up to overnight at 4°C with gentle mixing (35 rpm).

### 4.3.13 Preparation of protein samples for iTRAQ analysis

Using the Mini-Beadbeater homogeniser, mixed sex adult flies were homogenised in 0.5M TEAB buffer (0.5M triethylammonium bicarbonate, 0.1% SDS). Following homogenisation, samples were centrifuged at 10,000 x g for 10 mins at 4°C and the supernatants were retained for subsequent protein concentration analysis and iTRAQ analysis.

### 4.3.14 iTRAQ – Theory

iTRAQ technology allows for proteins from different samples to be identified and quantified in a single experiment. This technique employs the covalent N-terminal labelling of proteolytically digested peptides with specific isobaric (same mass) tags. Each tag contains a reporter group of a defined mass and a balancer group resulting in tagged

peptides of identical mass due to mass distribution within the isobaric tag. Samples are pooled, fractionated by strong cation exchange (SCX), peptides are separated by reverse phase nano liquid chromatography (nanoLC) and then analysed by tandem mass spectrometry (MS/MS). Collision induced dissociation of the peptides during MS results in fragmentation of the isobaric tag, releasing a low molecular mass reporter ion which is unique to the tag used to label each digest. Database searching of the fragmentation data of the peptides allows for the identification of labelled peptides and hence the corresponding proteins. Analysis of the intensity of the reporter ions, enables the simultaneous relative quantification of the peptides and hence proteins.

The iTRAQ technique was employed to identify quantitative proteomic changes resulting from a reduction in Cu Zn SOD activity using either the *sod1*-null line (*n108*) or the *sod3* hypomorph strain ($Sod3^{06029}$). As described previously, *n108* flies are characterised by severely reduced lifespan and paraquat hypersensitivity (Phillips et al. 1989), thus any proteomic changes observed in these flies compared to the isogenic control line (*red*) will likely be functioning either to promote survival in this species or are resulting from the reduced oxidative protection conferred by a lack of cytosolic Cu Zn SOD. Any proteomic changes observed in the $Sod3^{06029}$ line compared to the $yw^{c\text{-}iso}$ control however, are expected to be revealing proteins that are functioning to influence fitness as a result of the genetic modifications proposed to have been revealed by backcrossing the $sod3^{06029}$ line (see section 3.5.6 of chapter 3).

## 4.3.15 iTRAQ – Methodology

All subsequent procedures were carried out at the Centre for Proteomic Research at the University of Southampton.

### 4.3.15.1 Peptide labelling

iTRAQ labelling of protein samples was performed according to the manufacturer's instructions (Applied Biosystems, Warrington, UK). To each of 100µg of four duplicate

protein samples (*Sod3*$^{06029}$, *yw* $^{c\text{-}iso}$, *n108* and *red*) in ≤34µl of 0.5M TEAB 1µL of 2% SDS and 2µL of the reducing agent, 50mM (tris-(2-carboxyethyl) phosphine was added and mixed by brief vortexing. After reduced samples had been incubated at 60°C for 1 hour, methyl methane-thiosulfonate in isopropanol (1µL of 200mM) was added and incubated for a further 10 mins at room temperature. Proteins were digested by adding 10µL of 1mg/ml trypsin in 80mM $CaCl_2$ and incubated for 16 hours at 37°C. Tryptic peptides were labelled with iTRAQ 8-plex tags by mixing the appropriate iTRAQ labelling reagent with the relevant sample (*Sod3*$^{06029}$ 1 – reagent 113; *Sod3*$^{06029}$ 2 – reagent 114; *yw* $^{c\text{-}iso}$ 1 – reagent 115; *yw* $^{c\text{-}iso}$ 2 – reagent 116; *n108* 1 – reagent 117; *n108* 2 – reagent 118; *red* 1 – reagent 119 and *red* 2 – reagent 121) and incubating at room temperature for 2 hours. If required, up to 5µL of 0.5M TEAB was added to ensure the pH was < 7.5 for each sample. All samples were pooled and then lyophilised in a centrifugal vacuum concentrator (Thermo Scientific) for approximately 3 hours.

#### 4.3.15.2 Fractionation and mass spectrometry

The sample was resuspended in 1mL of buffer A (95% acetonitrile containing 0.1% formic acid) and the combined peptide mixture was fractionated on a C18 RP column (2.1 mm x 250 mm column, Phenomenex). Peptides were detected at 214 nm and fractions collected at 1 min intervals into a 96-well microtitre plate. To each sample fraction, 30µL of 10% acetonitrile containing 0.1% formic acid was added and peptide separation was achieved by loading individual fractions onto a reverse phase trap column (5 mm x 300 µm, id, Dionex, Camberley, UK) and eluting by analytical nano-LC separation using a Pepmap C18 Reverse phase column (3 µm, 150 mm x 75 µm, i.d., Dionex, Camberley, UK). Fractions were separated over 120 mins using a gradient of 0 to 80% Buffer B at 200nL/min and electrosprayed into the mass spectrometer. All data were acquired using a Q-tof Global Ultima (Waters Ltd, Manchester, UK) fitted with a nanoLockSpray™ source.

#### 4.3.15.3 Peak list generation and database searching

Peak lists were generated using the ProteinLynx Global Server 2.2.5 (Waters Ltd, Manchester, UK). The following parameters were used for processing the MS/MS spectra; normal background subtraction with a 25% background threshold and medium de-isotoping with a threshold of 1%, no smoothing was performed. Peak lists from the MS/MS analysis of were submitted to the MASCOT search engine version 2.2.1 (MatrixScience, London, UK) and the data searched against a protein translation of the drosophila genome. The corresponding quantitative information using the iTRAQ reporter ions was also obtained via MASCOT. Protein identifications required the assignment of ≥2 different peptides with a significance threshold for accepting a match of P = <0.05. The protein ratios were calculated using MASCOT version 2.2.1, where the peptide ratios were weighted and median normalisation was performed, automatic outlier removal was chosen and the peptide threshold was set to 'at least homology'. False discovery rates were calculated by running all spectra against a decoy database using the MASCOT software.

## 4.4 Results

### 4.4.1 SOD activity in mutant lines

To complement the gene transcription data presented in Chapter 3, SOD activity measurements were initially taken in the same mutant backgrounds. Compared with a *WT* control, total SOD activity was found to fall significantly in $Sod3^{06029}$, *x39/TM3* and *n108/TM3* flies (all df = 8, P = <0.05) to approximately half that of the control samples (Figure 4.1A). Total SOD activity was found to be reduced further in homozygous *n108* flies (df = 8, P = <0.01), however there was no statistically significant difference between the activities in homozygous and heterozygous *n108* flies. A similar trend was observed when Cu Zn SOD activities were measured in the same strains. Again SOD activities in $Sod3^{06029}$, *x39/TM3* and *n108/TM3* flies were comparable and found to be significantly reduced (all df = 8, P = <0.01) to around a third of the control activity level (Figure 4.1B). Furthermore, in *n108* flies, Cu Zn SOD activity was found to be suppressed even further compared to *WT* flies (df = 8, P = <0.001). A highly significant difference in Cu Zn SOD activity was also observed between the heterozygous (*n108/TM3*) and homozygous (*n108*) alleles of the *sod1* mutant line (df = 8, P = <0.001).

### 4.4.2 SOD activity gels

Along with quantitative activity assays, SOD activity was also assessed using on gel methods. *WT* samples were found to resolve two distinct bands on the gels, the upper being attributed to Mn SOD activity and the lower resulting for Cu Zn SOD activity (Figures 4.2A and B). With $Sod3^{06029}$ samples, a prominent band for Mn SOD was observed, however there was only a negligible amount of Cu Zn SOD detectable (Figures 4.2A and C), a trend which was also observed with *x39/TM3* flies (Figures 4.2A and D). With the heterozygous *n108/TM3* mutant line, bands corresponding to both Mn SOD and Cu Zn SOD were clearly visible (Figures 4.2A and E), however, with the homozygous *n108* strain there was no detectable Cu Zn SOD activity (Figures 4.2A and F). In the *WT*

line, Cu Zn SOD was more pronounced than the Mn SOD isoform, however in each of the mutant lines tested, Mn SOD predominated.

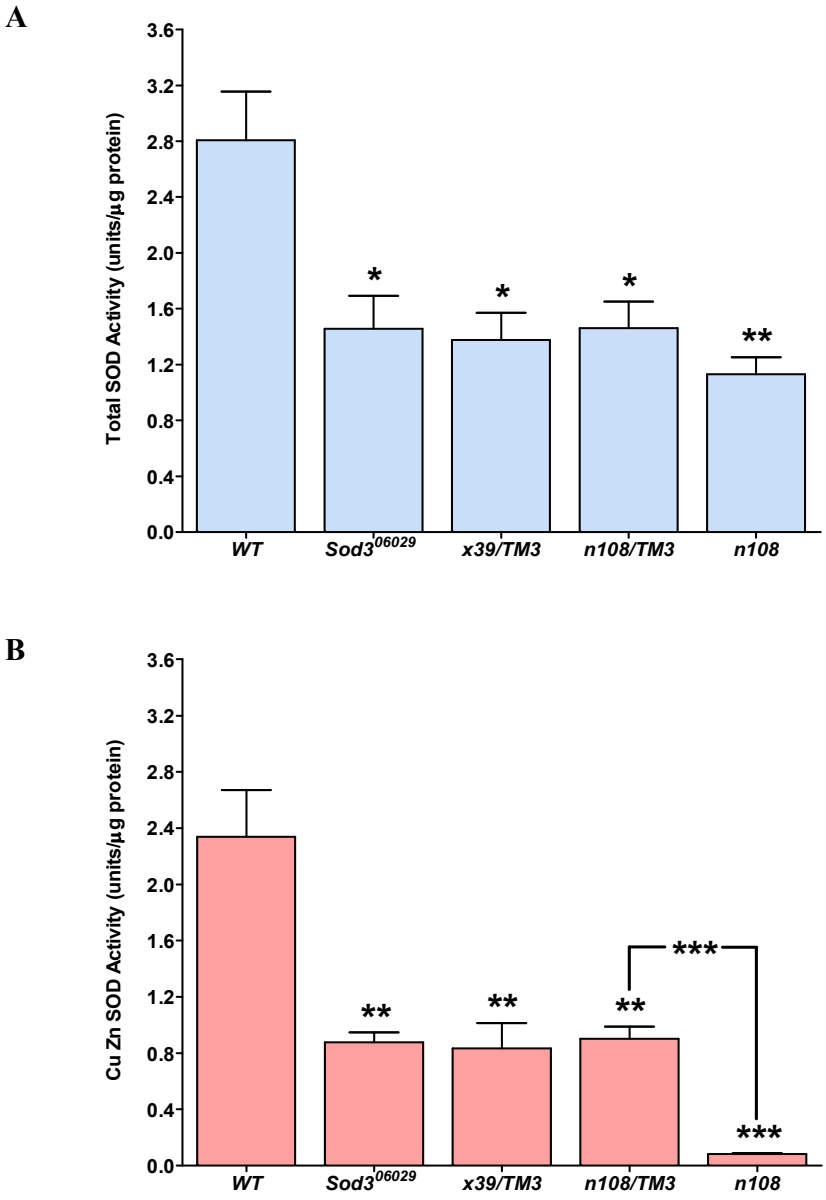


**Figure 4.1. SOD activity measurements in mutant fly lines.** (**A**) Total SOD activity was found to be significantly reduced in each of the mutant lines assayed compared to the *WT* control (all P = <0.05, df = 8, except *n108*, P = <0.01, df = 8) (**B**) Cu Zn SOD activities in the same mutant lines were also found to be significantly diminished compared to *WT* (all P = <0.01, df = 8, except *n108*, P = <0.001, df = 8), however, additionally, a highly significant decrease in activity was also observed between *n108/TM3* and *n108* flies (P = <0.001, df = 8). *WT* samples were tested at N=6 and all other samples were tested at N=4. Error bars are SEM.

**A**

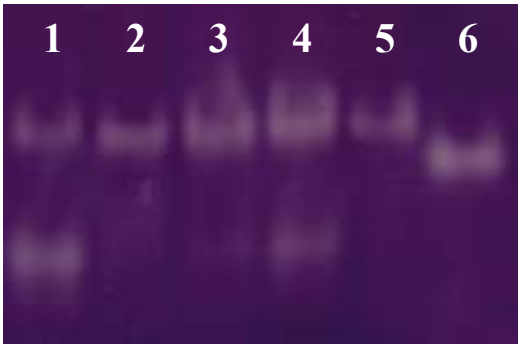


**B –** peak intensities of lane 1 (*WT*)

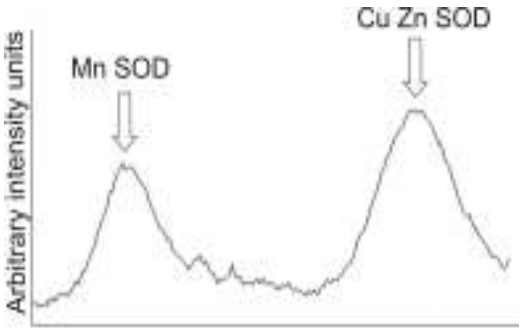


**C –** peak intensities of lane 2 (*Sod3*$^{06029}$)

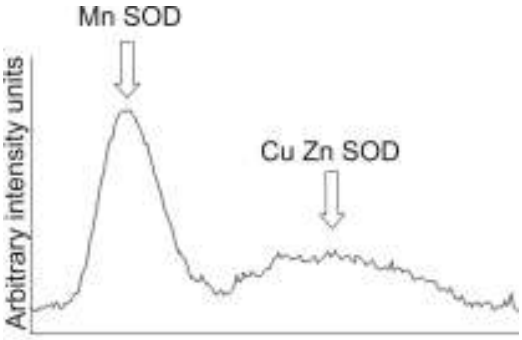


**D –** peak intensities of lane 3 (*x39/TM3*)

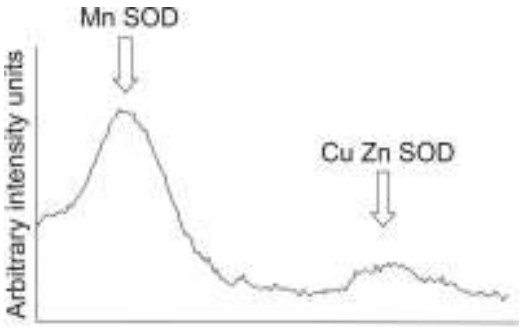


**E –** peak intensities of lane 4 (*n108/TM3*)

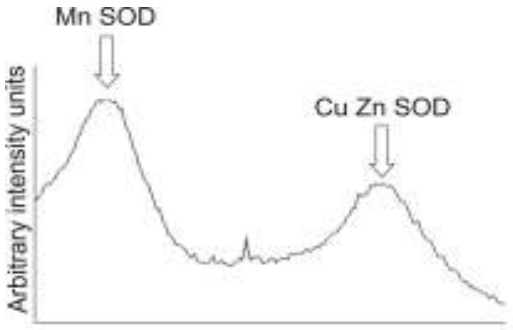


**F –** peak intensities of lane 5 (*n108*)

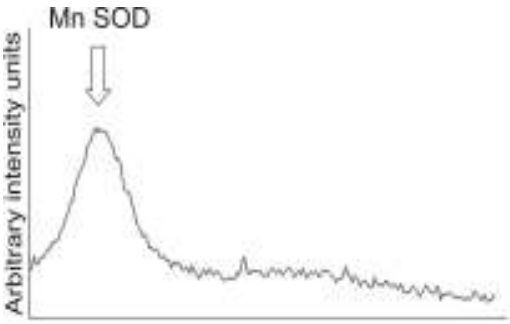


**Figure 4.2. In-gel analysis of SOD activity in mutant fly lines.** SOD activity gels were performed (**A**) on: *WT* (lane 1); *Sod3*$^{06029}$ (lane 2); *x39/TM3* (lane 3); *n108/TM3* (lane 4); *n108* (lane 5) and bovine Cu Zn SOD (lane 6) samples. Band peak intensities for each sample are also listed (**B-F**) and indicate a partial to complete absence of Cu Zn SOD activity in the *Sod3*$^{06029}$ and *n108* samples. All samples were tested at a minimum of N=3.

### 4.4.3 Cu Zn SOD activity in excision lines

As described in the previous chapter, the transposon insertion present in the *Sod3*$^{06029}$ lines was excised to assess its influence on gene expression. Here the same excision lines were assayed for Cu Zn SOD activity and compared to the *Sod3*$^{06029}$ line (Figure 4.3). Cu Zn SOD activities in all 3 excision lines (*ex136*, *ex141* and *ex158*) was higher than in the *Sod3*$^{06029}$ strain with *ex141* (df = 12, P = <0.05) and *ex158* (df = 12, P = <0.01) having statistically significantly elevated levels of Cu Zn SOD activity.

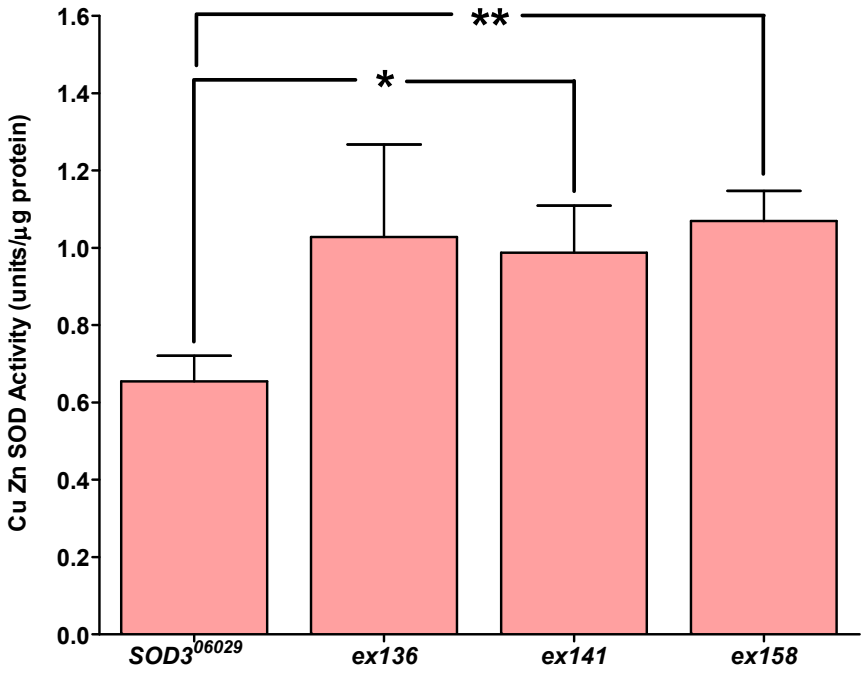


**Figure 4.3. Cu Zn SOD activities of excision lines.** Measurement of Cu Zn SOD activities in each of the three excision lines (*ex136*, *ex141* and *ex158*) revealed elevated activities compared to *Sod3*$^{06029}$ samples (P = <0.05, df = 12 for *ex141* and P = <0.01, df = 12 for *ex158*). All samples were tested at N=7 and error bars are SEM.

### 4.4.4 SOD activity vs the backcrossed control strain

Both total and Cu Zn SOD activities were measured in the *sod3* mutant line against the backcrossed control line, *yw* $^{c\text{-}iso}$, generation of which was described previously. Unexpectedly, total SOD activity was found to be highly elevated in male *Sod*$^{06029}$ flies compared to the *yw* $^{c\text{-}iso}$ strain (df = 6, P = <0.001) (Figure 4.4A). So too was Cu Zn SOD activity in the same strains, although the difference in activity was not so distinct (df = 6, P = <0.05) (Figure 4.4B). In female flies, like males, *Sod3*$^{06029}$ was found to have elevated total SOD activity levels compared to *yw* $^{c\text{-}iso}$, however the difference was not found to be statistically significant (Figure 4.4C). There was, however, a significant increase in Cu Zn SOD activity in female *Sod3*$^{06029}$ flies compared to the backcrossed control line (df = 6, P = <0.05) (Figure 4.4D).

### 4.4.5 SOD activity vs the non-backcrossed control strain

Total and Cu Zn SOD activities were also quantified in *Sod3*$^{06029}$ flies in comparison with the non-backcrossed *yw* $^{c}$ line. Total SOD activity levels in male *Sod3*$^{06029}$ flies were found to be marginally reduced compared to *yw* $^{c}$ flies (Figure 4.5A), however there was a highly significant reduction in Cu Zn SOD activity in the *Sod3*$^{06029}$ line compared to the non-isogenic control line (df = 6, P = <0.001) (Figure 4.5B). The same trend was observed in female flies with only a marginal difference in total SOD activity being measured between the two fly strains (Figure 4.5C). Like with male flies, female *Sod3*$^{06029}$ flies were found to have considerably lower Cu Zn SOD activity levels as compared with the *yw* $^{c}$ line (df = 6, P = <0.01) (Figure 4.5D).

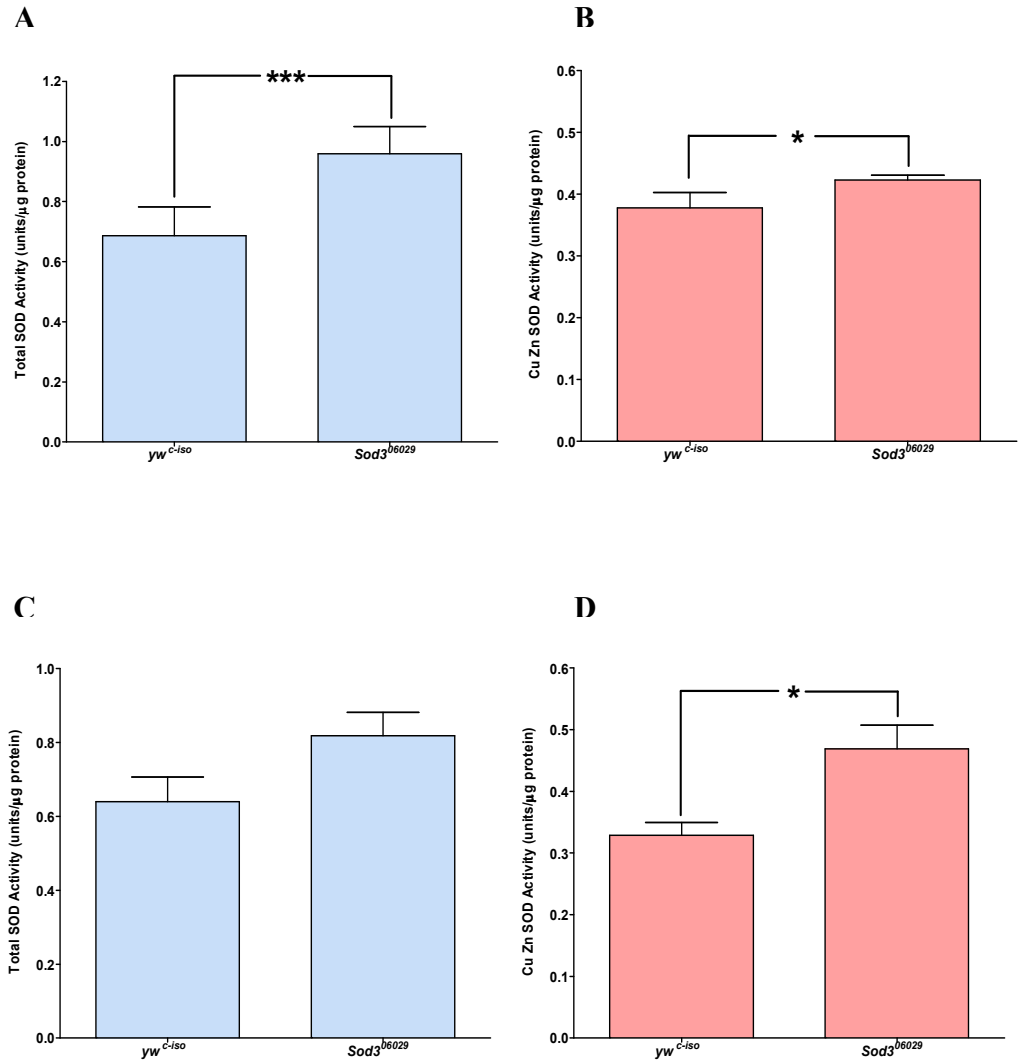


**Figure 4.4. SOD activity measurements of *Sod3*$^{06029}$ samples compared to the backcrossed *yw* $^{c\text{-}iso}$ line.** Male *Sod3*$^{06029}$ flies were found to have significantly elevated total (**A**) (P = <0.001, df = 6) and Cu Zn (**B**) (P = <0.05, df = 6) SOD activities. Whilst the increase in total SOD activity in female *Sod3*$^{06029}$ flies was not found to be statistically significant (**C**), the increase in Cu Zn SOD activity was found to be statistically measurable (**D**) (P = <0.05, df = 6). All samples were tested at N=4 and error bars are SEM.

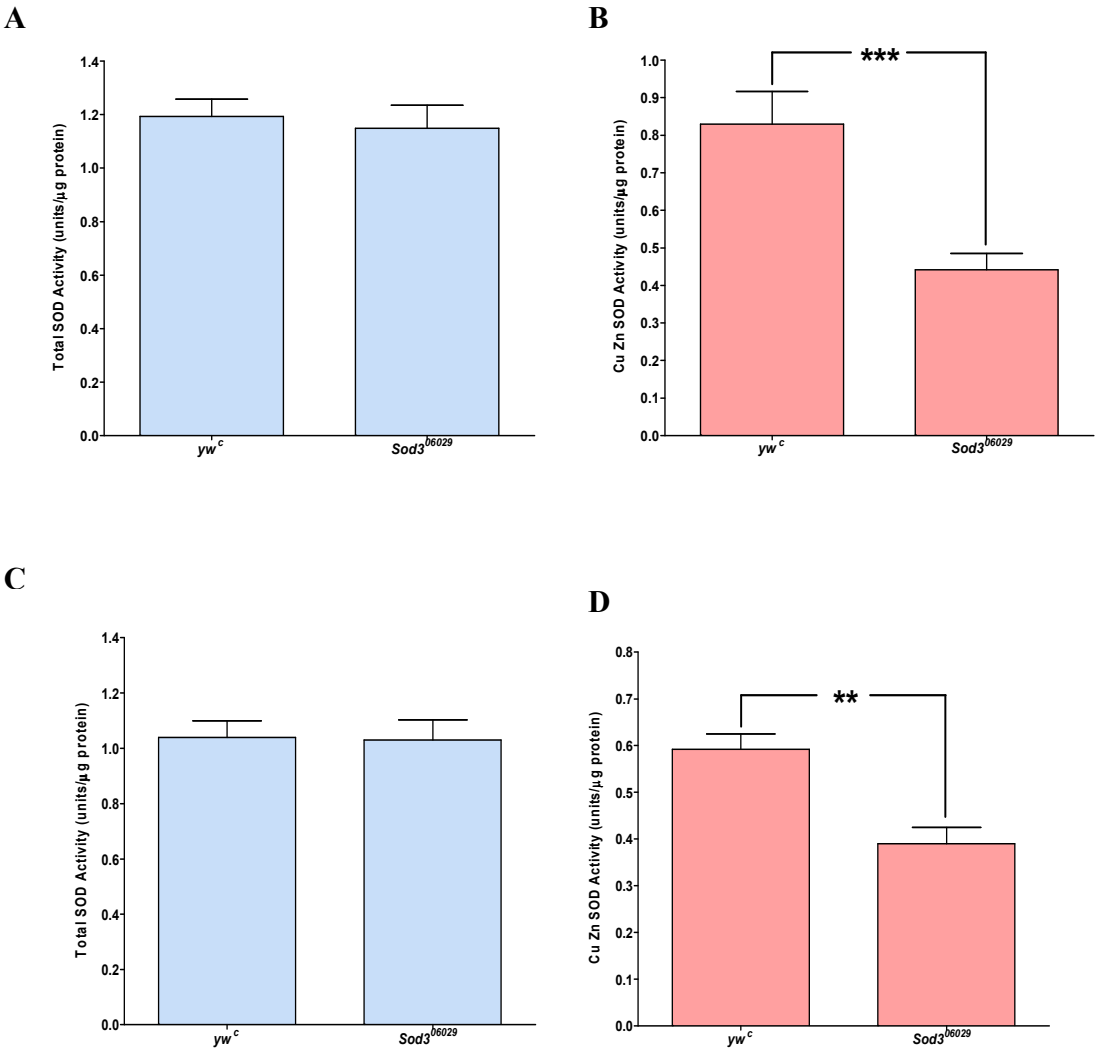


**Figure 4.5. SOD activity measurements of *Sod3*$^{06029}$ samples compared to the non-backcrossed *yw* $^{c}$ line.** Male *Sod3*$^{06029}$ and *yw* $^{c}$ flies were found to have indistinguishable total SOD activities (**A**), however Cu Zn activity was found to be significantly lower in the *sod3* hypomorph line (**B**) (P = <0.001, df = 6). A similar trend was observed in female flies where no difference in total SOD activity was found between genotypes (**C**), but a significant decrease in Cu Zn SOD activity of *Sod3*$^{06029}$ flies was observed (**D**) (P = <0.01, df = 6). All samples were tested at N=4 and error bars are SEM.

## 4.4.6 SOD activity in response to oxidative stress

### 4.4.6.1 Paraquat

SOD activity levels were quantified in *WT* flies in response to oxidative stress treatments. After 24 hours of 30mM paraquat exposure *WT* flies had ~50% mortality whereas control flies maintained on 5% sucrose showed 0% mortality. Total SOD activity analysis of surviving flies exposed to paraquat revealed there to be no statistical difference in activity with control flies, however a minor but measurable decrease in total SOD activity in test flies was observed (Figure 4.6A). Measurements of Cu Zn SOD activities in the same flies also revealed no difference in activity (Figure 4.6B).

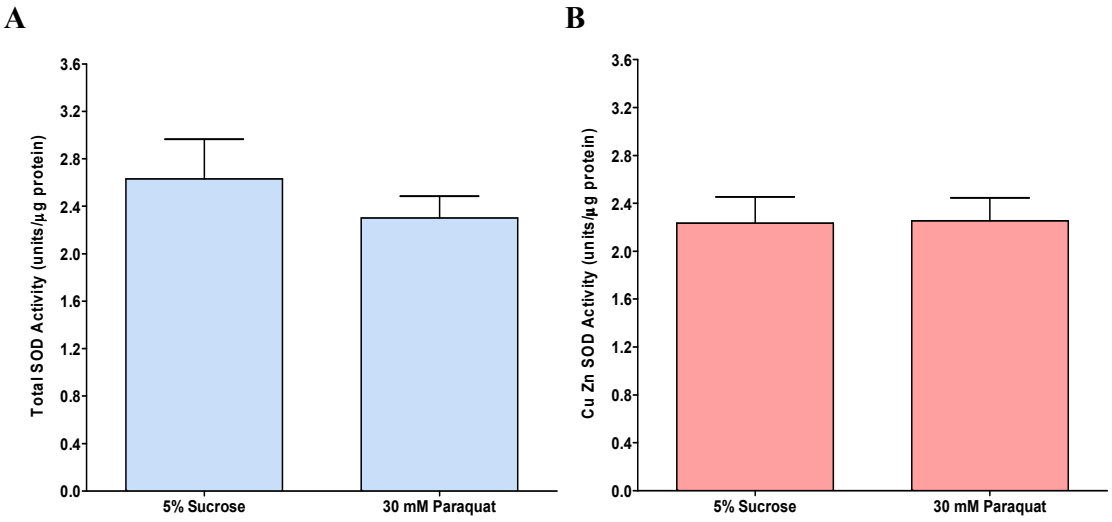


**Figure 4.6. SOD activity measurements in response to paraquat induced oxidative stress.** *WT* flies exposed to 30mM paraquat for 24 hours had both total (**A**) and Cu Zn SOD activities (**B**) comparable with flies maintained on control medium (5% sucrose). All samples were tested at N=4 and error bars are SEM.

### 4.4.6.2 $H_2O_2$

After 24 hours exposure to 15% $H_2O_2$ *WT* flies had ~50% mortality and control flies exposed to 5% sucrose had 0% mortality. As with the paraquat experiment, there was no statistical difference between the total SOD activity levels of flies exposed to $H_2O_2$ and those exposed to sucrose alone, although a minor suppression of total SOD activity was observed with $H_2O_2$ treatment (Figure 4.7A). Additionally, Cu Zn SOD activity measurements revealed no difference in activity between either treatment (Figure 4.7B).

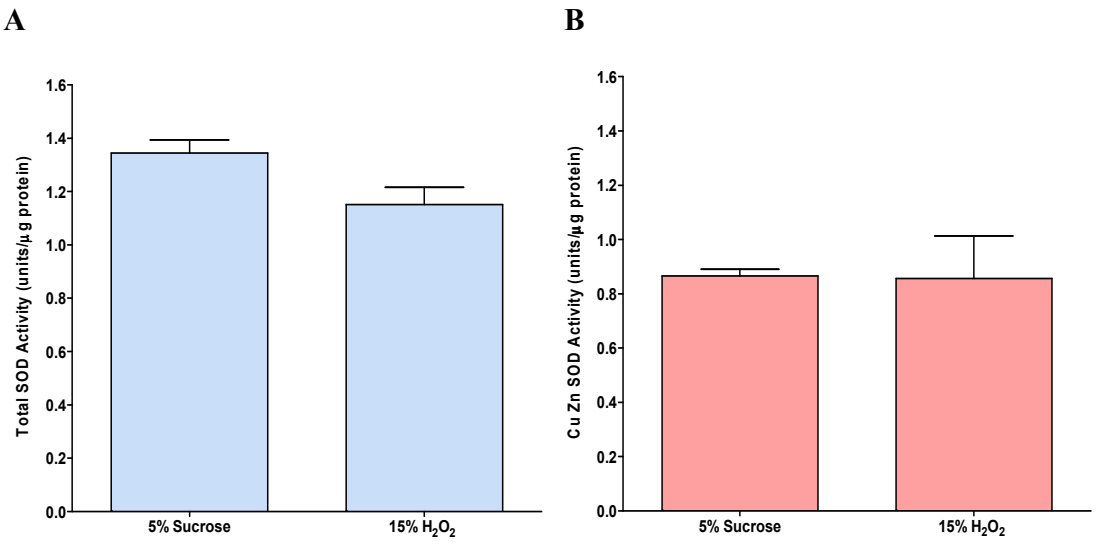


**Figure 4.7. SOD activity measurements in response to $H_2O_2$ induced oxidative stress.** *WT* flies exposed to 15% $H_2O_2$ for 24 hours had both total (**A**) and Cu Zn SOD activities (**B**) comparable with flies maintained on control medium (5% sucrose). All samples were tested at N=4 and error bars are SEM.

## 4.4.7 *Drosophila* SOD3 antibody validation

The antipeptide *Drosophila* SOD3 antibody generated was assessed for efficacy and specificity by a combination of dot blots, western blots and competition assays as will be discussed.

### 4.4.7.1 Dot blots

Initially dot blots were carried out with dilutions of the small bleed serum (taken 38 days post immunisation) to test for immunoreactivity with *WT* samples (Figure 4.8A). As a negative control the same dilutions were made with the pre-immune serum also supplied (Figure 4.8B). Both the small bleed serum and the pre-immune serum were tested at dilutions of 1:100 – 1:10,000. Immunoreactivity was observed at the highest dilution with the small bleed serum however reactivity was lost with the pre-immune sample after 1:1000 dilution, indicating that specific immunoreactivity can be observed at the highest dilutions of the small bleed serum.

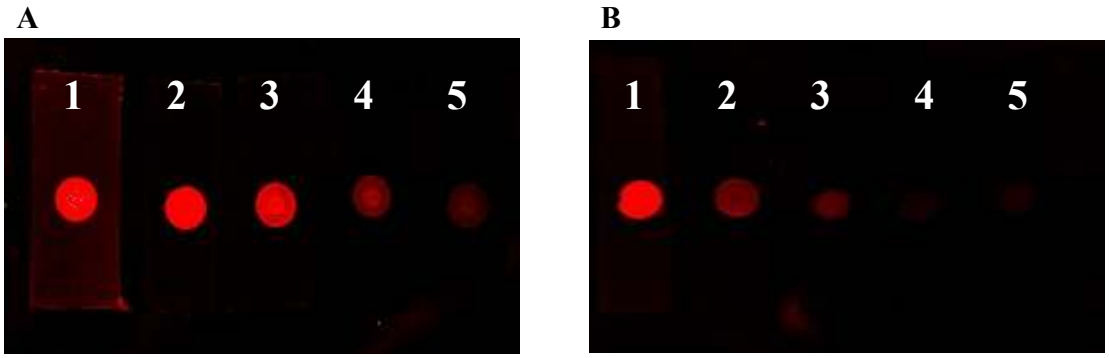


**Figure 4.8. Antibody screening by dot blots.** Both the small bleed serum (**A**) and the pre-immune serum (**B**) were assayed for immunoreactivity with *WT* protein homogenates. Each serum was tested at dilutions of 1:100 (lane 1), 1:500 (lane 2), 1:1,000 (lane 3), 1:5,000 (lane 4) and 1:10,000 (lane 5), blocked with 3% BSA tPBS and incubated with a 1:10,000 dilution of the Alex fluor 680 secondary antibody. Whilst immunoreactivity was lost after the 1:1,000 pre-immune serum dilution, immunoreactivity was still observable at all dilutions of the small bleed serum.

### 4.4.7.2 Western blots and competition assays

Having confirmed the presence of immunoreactivity through dot blots of the small bleed serum, western blots of whole fly homogenates were run with the purified *Drosophila* SOD3 antibody. Initial western blots were run to determine an appropriate primary antibody dilution with which subsequent western blots could be run (Figure 4.9A). This was achieved by loading 600µg of *WT* total protein on a 12% gel and titrating with increasing dilutions of the primary antibody (from the stock solution up to a 1/2000 dilution). A prominent band was seen above the fourth marker lane and estimated at ~30 kDa which remained detectable at all antibody dilutions. A primary antibody dilution of 1:1000 was chosen as a suitable initial working dilution based on this western blot since this dilution gave the greatest contrast between band intensity and background signal. Subsequently, further western blots were performed to determine an appropriate amount of protein to use in future studies (Figure 4.9B). In this instance 80µg, 40µg and 20µg of *WT* protein was probed with a 1:1000 dilution of the primary antibody. The prominent band at ~30 kDa seen previously was present in this blot at all protein quantities tested, however significant background reactivity was still observed suggesting that further dilutions of the primary antibody could still be tested for suitability in western blots. In order to assess which stained bands could be attributed to SOD3 immunoreactivity westerns were run with equal quantities of *WT, Sod3*$^{06029}$ and *n108/TM3* protein homogenates and probed with a 1:5000 dilution of the primary antibody (Figure 4.10). The prominent band at ~30 kDa observed previously was found in all 3 sample homogenates however the intensity of the stained band appeared diminished in the *Sod3*$^{06029}$ sample in comparison with the other two lines. To confirm that this ~30 kDa band was a result of SOD3 immunoreactivity western blot competition assays were performed in which the primary antibody (1:5000 dilution) was pre-incubated with an excess of the free peptide (20-fold – 10,000-fold excess) to which the SOD3 antibody was raised for 4 hours and 20 mins (Figure 4.11A). Probing 300µg of total *WT* protein homogenate with each primary antibody-peptide incubation revealed no abolition of the signal intensity of the ~30 kDa band at any of the peptide concentrations tested.

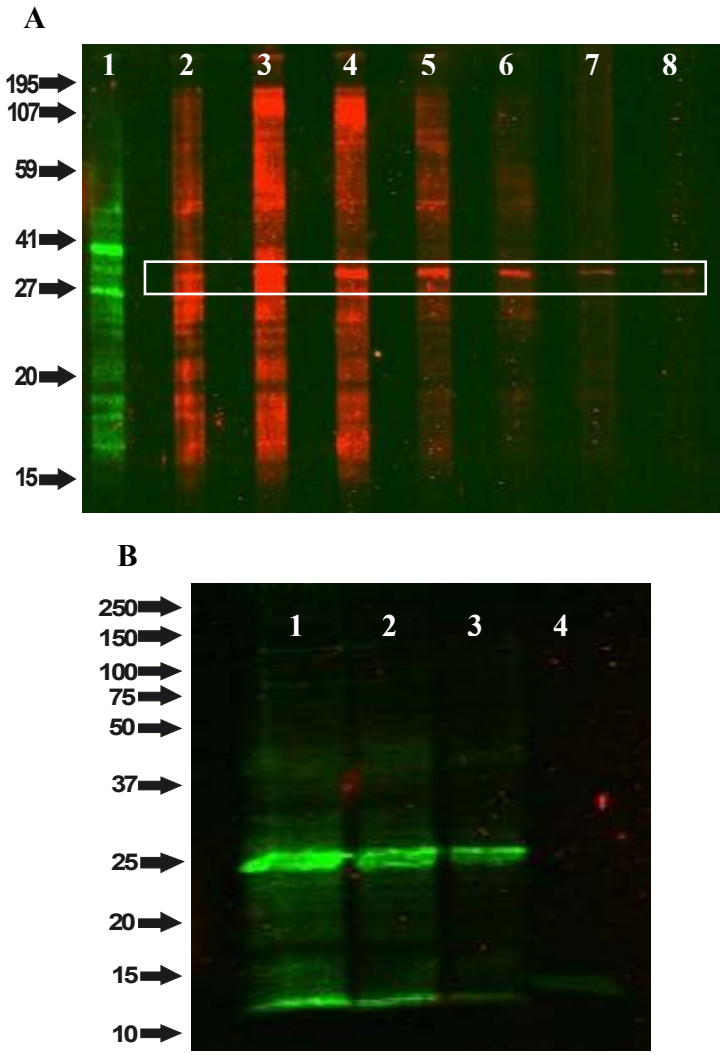


**Figure 4.9. Western blot. A**, western blot (12% gel) in which 600µg of Oregon R total protein was probed with increasing dilutions of the *Drosophila* SOD3 primary antibody. Lane 1 = 1:1000 syntaxin antibody (mAb602) control; lane 2 = primary antibody stock solution; lane 3 = 1:50 primary antibody dilution; lane 4 = 1:100 dilution; lane 5 = 1/250 dilution; lane 6 = 1/500 dilution; lane 7 = 1/1000 dilution; lane 8 = 1/2000 dilution. Blocking solution was 3% BSA tPBS. The secondary antibody used with the syntaxin primary antibody was 1:10,000 Alexa Fluor 680. The secondary antibody used with the SOD3 primary antibody was 1:10,000 Alexa Fluor 780. ~41 kDa band indicates syntaxin in lane 1. A prominent band of immunoreactivity was observed at ~30 kDa, observable at all antibody dilutions titrated (white box). **B**, western blots (10% gels) of decreasing amounts of *WT* total protein. *Drosophila* SOD3 primary antibody dilution = 1:1000. Blocking solution is 3% BSA tPBS. Lane 1 = 80µg protein; lane 2 = 40µg protein; lane 3 = 20µg protein; lane 4 = bovine Cu Zn SOD (3µL of 1mg/mL protein run on gel). Secondary antibody = 1:10,000 Alexa Fluor 680. Minimal cross reactivity with bovine Cu Zn SOD is observed. The ~30 kDa band is visible at each protein dilution, however band staining intensity decreases with decreasing concentration.

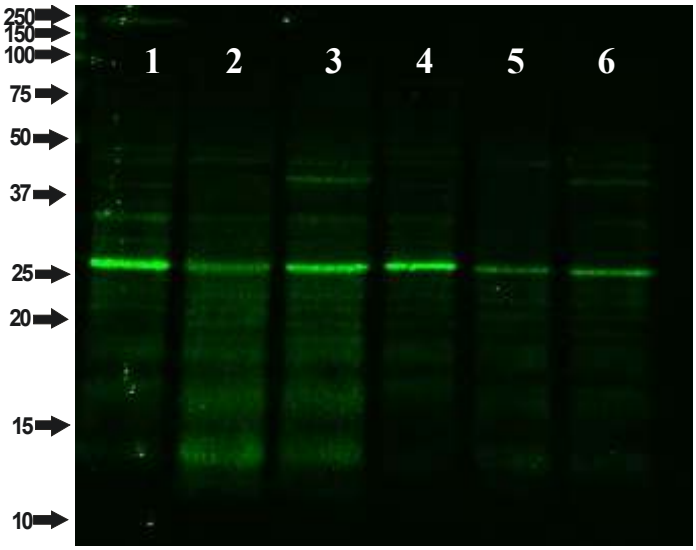


**Figure 4.10. Western blot.** Western blot (12% gel) probing 1:5000 primary antibody against mutant protein homogenates. Lane 1 = 40µg *WT* homogenate, lane 2 = 40µg *Sod3*$^{06029}$, lane 3 = 40µg *n108/TM3*, lane 4 = 20µg *WT* homogenate, lane 5 = 20µg *Sod3*$^{06029}$ and lane 6 = 20µg *n108/TM3*. Blocking solution = 3% BSA tPBS and secondary antibody = Alexa Fluor 680 at 1:10,000 dilution. A decrease in ~30 kDa band intensity can be seen in *Sod3*$^{06029}$ samples at both concentrations in comparison to *WT* and *n108/TM3* samples.

To assess the degree of non-specific binding occurring due to the primary and/or secondary antibody western blots were run with 250µg of *WT* total protein homogenate and probed with either:

i) primary antibody (1/5000 dilution) plus secondary antibody
ii) no primary antibody plus secondary antibody
iii) primary antibody (1/5000 dilution) plus 10µg/mL peptide (~20,000-fold excess) plus secondary antibody
iv) no primary antibody plus 10µg/mL peptide (~20,000-fold excess) plus secondary antibody.

All samples were pre-incubated for 5 hours and 30 mins with gentle agitation. The lanes probed with the samples containing the peptide showed no difference to those without

peptide as was seen previously (Figure 4.11B). However, those lanes probed with the samples containing the secondary antibody alone produced the same staining pattern as those that also contained the primary antibody, indicating that it is in fact the secondary antibody that is reacting non-specifically. In an attempt to reduce this non-specificity samples were incubated in an alternative blocking solution of 5% milk powder in tPBS. The staining intensity of the blots in these lanes was significantly diminished compared with those incubated in the standard blocking solution of 3% BSA in tPBS, indicating that the milk-based blocking solution was more effective at reducing non-specific binding. A horse radish peroxidise (HRP) conjugated anti-rabbit secondary antibody was employed to test whether non-specific background immunoreactivity could be reduced using the ECL detection method. Using 5% milk powder in tPBS as the blocking solution an optimum dilution of the primary antibody was found to be 1:500 (data not shown). Probing of *WT*, *Sod3*$^{06029}$ and *n108/TM3* protein samples with this primary antibody dilution produced a distinct band at ~30 kDa (as seen previously) with no background signal and showed a decrease in band intensity in the *Sod3*$^{06029}$ strain (Figure 4.11C).

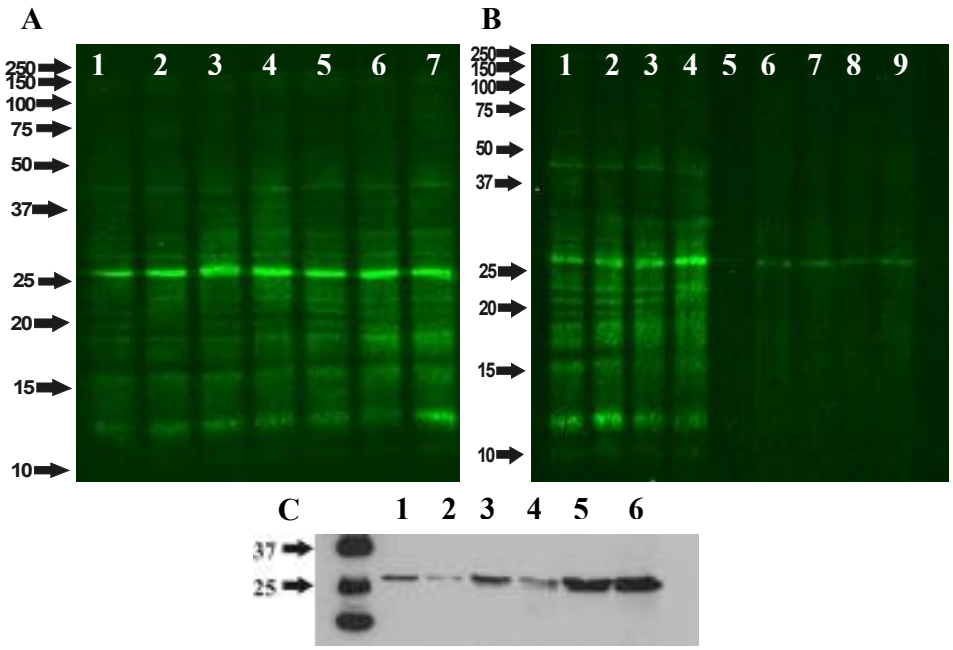


**Figure 4.11. Western blots. A**, western blot competition assay probed with a 1/5000 dilution of the primary antibody pre-incubated with increasing concentrations of the peptide for 4 hours and 20 mins. 300µg of *WT* total protein loaded onto the gel (12% gel). Lane 1 = primary antibody alone; lane 2 = antibody + 26ng/mL peptide (100-fold excess); lane 3 = antibody + 65.8ng/mL peptide (250-fold excess); lane 4 = antibody + 130ng/mL peptide (500-fold excess); lane 5 = antibody + 660ng/mL peptide (2,500-fold excess); lane 6 = antibody + 1.32µg/mL peptide (5,000-fold excess); lane 7 = antibody + 13µg/mL peptide (50,000-fold excess). Blocking solution = 3% BSA tPBS. Secondary antibody = Alexa Fluor 680 at 1:10,000 dilution. No abolishment of the ~30 kDa band was observed with any of the peptide pre-incubations. **B**, western blot investigating non-specific antibody binding and the effect of blocking solution. 250µg of *WT* total protein run on a 12% gel. All samples were pre-incubated for 5 hours and 30 mins. Lane 1 = primary antibody (1/5000) + secondary antibody (Alexa Fluor 680 at 1:10,000); lane 2 = no primary antibody + secondary antibody; lane 3 = primary antibody (1/5000) + 10µg/mL peptide (38,500-fold excess) + secondary antibody; lane 4 = no primary antibody + 10µg/mL peptide + secondary antibody; Lane 5 = empty; lanes 6-9 = as lanes 1-4. Samples used in lanes 1-4 were blocked with 3% BSA tPBS for 1 hour and 30 mins. Samples in lanes 6-9 were blocked with 5% milk powder tPBS for 1 hour and 30 mins. Whilst no decrease in ~30 kDa band intensity was observed in either blot, blocking with milk powder dramatically reduced the non-specific background signal. **C**, western blot (12% gel) probing 1:500 primary antibody against mutant protein homogenates. Lane 1 = 20µg *WT* homogenate, lane 2 = 20µg $Sod3^{06029}$, lane 3 = 40µg *WT*, lane 4 = 40µg $Sod3^{06029}$, lane 5 = 80µg *WT* and lane 6 = 80µg $Sod3^{06029}$. Blocking solution = 5% milk powder tPBS for 2 hours and secondary antibody = HRP anti-rabbit at 1:2,000 dilution. A decrease in ~30 kDa band intensity can be seen in $Sod3^{06029}$ samples at both 20µg and 40µg loaded compared to *WT* samples, with non-specific background noise eliminated.

### 4.4.8 iTRAQ analysis of proteomic changes in *sod* mutant lines

Duplicate *Sod3*$^{06029}$ and *n108* protein samples were assayed against respective controls (*yw* $^{c\text{-}iso}$ and *red*) for quantitative changes in protein levels by eight-plex iTRAQ analysis. With a false discovery rate of 1.69%, a total of 40 proteins were identified with a significance threshold of P = <0.05, of which 39 were identified by the assignment of ≥2 different peptides (Table 4.5). For *Sod3*$^{06029}$ samples, three proteins were found to be significantly differentially expressed (iTRAQ ratio ≥ ±1.4), with those being: ADP, ATP carrier protein (accession number: ADT_DROME); 14-3-3 protein zeta (accession number: 1433Z_DROME) and apolipophorins (accession number: APLP_DROME), all of which were down-regulated. For *n108* samples, four proteins were significantly differentially expressed: ATP synthase subunit alpha, mitochondria (accession number: ATPA_DROME); alcohol dehydrogenase (accession number: ADH_DROME); myosin regulatory light chain (accession number: 2 MLR_DROME), all of which were up-regulated, and cytochrome P450 4g1 (accession number: CP4G1_DROME) which was down-regulated. Gene ontology annotation of all proteins identified revealed a diversity of molecular functions, with the majority of proteins found to be involved in muscle formation and function (30%), ion transport (15%) and oxidoreductase enzyme function (12%) (Figure 4.12).

**Table 4.5. iTRAQ ratios for *Sod3*$^{06029}$ and *n108* flies.** The threshold index key below the table is used to illustrate the degree by which identified proteins are up- or down-regulated. Proteins with ratios ≤0.7 are considered significantly down-regulated and proteins with ratios ≥1.4 are considered significantly up-regulated.

| Protein name | Accession number | Protein MW (kDa) | Protein pI | Peptide count | Average iTRAQ ratio for *Sod3*$^{06029}$ flies | Average iTRAQ Ratio for *n108* flies |
|---|---|---|---|---|---|---|
| Myosin heavy chain, muscle | MYSA_DROME | 224.465 | 5.91 | 84 | 1.032 | 1.282 |
| Actin, larval muscle | ACT4_DROME | 41.787 | 5.30 | 17 | 0.995 | 1.073 |
| Actin-42A | ACT2_DROME | 41.824 | 5.30 | 17 | 0.962 | 1.174 |
| ATP synthase subunit alpha, mitochondria | ATPA_DROME | 59.422 | 9.09 | 19 | 1.026 | 1.662 |
| ATP synthase subunit beta, mitochondria | ATPB_DROME | 54.108 | 5.14 | 22 | 0.972 | 1.285 |
| Enolase | ENO_DROME | 54.31 | 8.68 | 12 | 1.005 | 1.393 |
| Tropomyosin 1, isoforms 9A/A/B | TPM1_DROME | 39.325 | 4.93 | 16 | 0.946 | 1.326 |
| Tropomyosin 2 | TPM2_DROME | 32.981 | 4.77 | 15 | 1.007 | 1.368 |
| Tropomyosin 1, isoforms 33/34 | TPM4_DROME | 54.585 | 4.39 | 17 | 0.953 | 1.335 |
| Calcium-transporting ATPase sarcolplasmic/endoplasmic reticulum type | ATC1_DROME | 111.701 | 5.28 | 14 | 0.951 | 1.385 |
| Alcohol dehydrogenase | ADH_DROME | 27.761 | 7.73 | 8 | 0.87 | 2.403 |
| Myosin regulatory light chain 2 | MLR_DROME | 23.714 | 4.67 | 9 | 1.035 | 1.411 |
| Troponin C, isoform 1 | TNNC1_DROME | 17.156 | 3.85 | 1 | 0.95 | 1.316 |
| Paramyosin, long form | MYSP1_DROME | 102.338 | 5.47 | 17 | 0.909 | 1.08 |
| Succinyl-CoA ligase [GDP-forming] subunit alpha, mitochondria | SUCA_DROME | 34.389 | 9.14 | 4 | 1.044 | 0.986 |
| Fructose-bisphosphate aldolase | ALF_DROME | 39.047 | 6.97 | 8 | 0.897 | 1.265 |
| ADP, ATP carrier protein | ADT_DROME | 34.215 | 9.82 | 4 | 0.486 | 1.097 |
| 60 kDa heat shock protein, mitochondrial | CH60_DROME | 60.809 | 5.38 | 6 | 0.901 | 1.055 |
| ATP synthase subunit gamma, mitochondrial | ATPG_DROME | 32.871 | 9.29 | 3 | 0.802 | 1.067 |
| Arginine kinase | KARG_DROME | 39.866 | 6.04 | 8 | 0.951 | 1.268 |
| V-type proton ATPase catalytic subunit A isoform 2 | VATA2_DROME | 68.302 | 5.23 | 3 | 0.86 | 1.304 |
| Voltage-dependent anion-selective channel | VDAC_DROME | 30.55 | 6.44 | 8 | 0.938 | 0.959 |
| Glycerol-3-phosphate dehydrogenase [NAD$^+$], cytoplasmic | GPDA_DROME | 39.684 | 6.17 | 10 | 0.702 | 0.987 |

| | | | | | | |
|---|---|---|---|---|---|---|
| 14-3-3 protein zeta | 1433Z_DROME | 28.228 | 4.77 | 5 | 0.69 | 0.944 |
| Apolipophorins | APLP_DROME | 372.677 | 8.13 | 16 | 0.623 | 0.88 |
| Alpha-actinin, sarcomeric | ACTN_DROME | 107.019 | 5.48 | 12 | 0.865 | 1.067 |
| Glucose-6-phosphate isomerase | G6PI_DROME | 62.339 | 6.63 | 3 | 0.908 | 1.125 |
| Probable isocitrate dehydrogenase [NAD] subunit alpha, mitochondrial | IDH3A_DROME | 40.844 | 6.96 | 4 | 0.95 | 1.081 |
| Fat-body protein 1 | FBP1_DROME | 119.663 | 6.06 | 8 | 0.943 | 1.161 |
| Catalase | CATA_DROME | 57.15 | 8.39 | 3 | 0.776 | 1.199 |
| Protein disulfide-isomerase | PDI_DROME | 55.781 | 4.72 | 3 | 0.869 | 1.179 |
| Troponin T, skeletal muscle | TNNT_DROME | 47.448 | 4.63 | 14 | 0.968 | 1.227 |
| Paramyosin, short form | MYSP2_DROME | 74.277 | 9.22 | 9 | 0.939 | 1.068 |
| Glyceraldehyde-3-phosphate dehydrogenase 1&2 | G3P1_DROME | 35.35 | 8.25 | 7 | 0.904 | 1.306 |
| Protein l(2)37Cc | L2CC_DROME | 30.384 | 5.55 | 3 | 0.956 | 0.991 |
| Cytochrome P450 4g1 | CP4G1_DROME | 62.971 | 6.98 | 5 | 0.777 | 0.637 |
| Glycogen phosphorylase | PYG_DROME | 96.997 | 6.09 | 6 | 0.796 | 1.232 |
| NADH-ubiquinone oxidoreductase 75 kDa subunit, mitochondrial | NDUS1_DROME | 78.63 | 6.43 | 2 | 0.784 | 0.998 |
| Larval serum protein 1 gamma chain | LSP1G_DROME | 93.408 | 5.27 | 3 | 0.771 | 0.947 |
| Elongation factor 2 | EF2_DROME | 94.459 | 6.17 | 3 | 0.841 | 0.782 |

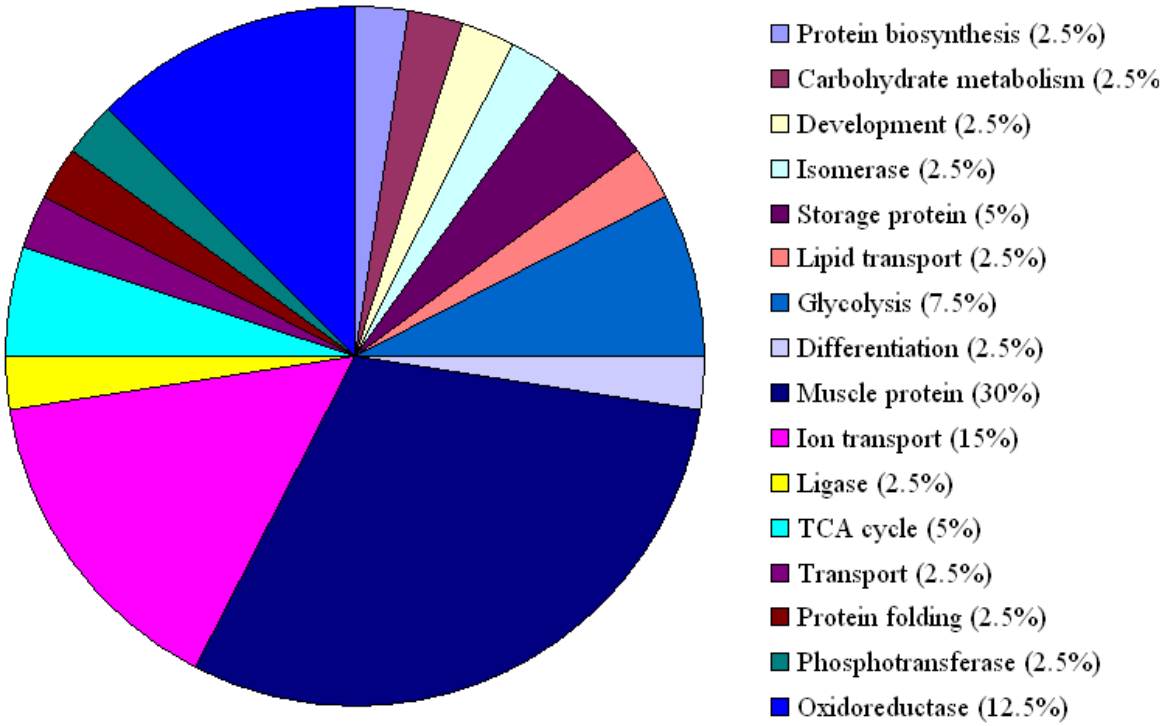


**Figure 4.12. Gene ontology classification of identified proteins according to cellular function.** Whilst the range of cellular functions is broad, the highest number of proteins were found to be muscle proteins.

## 4.5 Discussion

### 4.5.1 SOD activity in mutant lines implies compensatory changes in SOD activity in response to mutations and suggests a SOD1-SOD3 co-dependency

The previous chapter presented the results of gene expression analysis in *sod* mutant lines and suggested that compensatory changes in *sod* activity may be occurring. As will be discussed, enzymatic analysis of SOD activities in the same mutant lines supports this transcriptional compensatory theory and also suggests a co-dependency of the Cu Zn SOD isoforms.

Using *WT* samples for comparison, both *sod1* heterozygous mutants were found to have reduced total SOD activity to half the *WT* level, and reduced Cu Zn SOD activity to a third of *WT*. Interestingly, the *n108* line was found to reduce total SOD activity only a fraction more than the heterozygous *sod1* null sample but Cu Zn SOD activity was almost completely abolished in this strain. This suggests that in times of complete SOD1 absence SOD2 activity may increase in a compensatory manner. Indeed by calculating the difference in units/µg between total and Cu Zn SOD for each fly strain, the activity contributed by Mn SOD can be calculated. In the *WT*, *n108/TM3* and *x39/TM3* samples Mn SOD contributes 0.4 – 0.6 units/µg to total SOD activity, however over 1.0 unit/µg is found to be contributed to total SOD activity by Mn SOD in *n108/TM3* samples. Although a significant increase in *sod2* gene transcription in the *sod1* mutant lines was not observed, there was a significant upregulation in the $Sod3^{06029}$ flies and a positive trend in the *sod1* mutant lines (Figures 3.9A and B) suggesting that *sod2* might be both transcriptionally and translationally regulated in response to overall SOD activity. Given that *sod3* has been shown to be less highly expressed than *sod1* in adult flies one might assume that the residual Cu Zn SOD activity seen in the *n108* strains could be attributed to endogenous SOD3. However, $Sod3^{06029}$ flies were found to have total and Cu Zn SOD activities equivalent to that of the *sod1* heterozygous mutant strains. Thus the *P*-element insertion in the $Sod3^{06029}$

strain removes far more Cu Zn SOD activity than might be expected from the activity measurements.

There are two likely explanations for the discrepancies in the summation of the Cu Zn SOD activities in the Cu Zn SOD mutant lines. Firstly, the lack of control for genetic background by using *WT* flies as a control may lead to unpredictable quantitative changes in protein expression (discussed in Chapter 3 in relation to gene expression) and thus SOD activity. Alternatively, it is possible that SOD1 and SOD3 interact in some manner and are mutually dependent for Cu Zn SOD activity in *Drosophila*.

Analysis of *sod* mutant protein samples on SOD activity gels support the hypothesis that SOD1 and SOD3 may interact in some manner in *Drosophila*. In *n108* flies, no band of activity corresponding to Cu Zn SOD was found in the gels and the same band was also found to be absent with $Sod3^{06029}$ flies. This suggests that the reduction in total and Cu Zn SOD activity found by spectroscopic measurements of $Sod3^{06029}$ and all *Sod1* mutant lines appears in fact to be a result of global Cu Zn SOD inactivity, rather than due to SOD1 or SOD3 being independently absent. An explanation for the relationship between SOD1 and SOD3 could be that the endogenously active Cu Zn SOD measured in the assays results from heterodimers of SOD1 and SOD3 subunits, thus removing either would diminish the Cu Zn SOD activity proportionally. One more important caveat must be considered in interpreting these activity results. These assays were performed according to standard protocols where cellular debris was thrown away (Phillips et al. 1989). One would imagine that any extracellular SOD that is bound to membranes would be discarded with this fraction and therefore it was originally expected that no change in activity with the $Sod3^{06029}$ flies would be found. The fact that changes in activity were observed in this line perhaps supports the notion of SOD1-SOD3 interaction or alternatively suggests that one or both of the SOD3 variants is functioning in an intracellular location which would not be predicted by sequence analysis.

### 4.5.2 Transposon excision restores SOD activity

The primary aims of excising the transposon from the *Sod3*$^{06029}$ line were discussed in the previous chapter. Cu Zn SOD activity analysis of the three excision lines (*ex136*, *ex141* and *ex158*) found that activity levels increased in all three lines compared to *Sod3*$^{06029}$ flies. These results correlate with the gene expression data and provide further evidence that the *P*-element insertion causes decreased SOD activity.

### 4.5.3 SOD activity of *Sod3*$^{06029}$ flies in comparison with backcrossed and non-backcrossed controls provides further evidence for the influence of modifiers

Discussed in the previous chapter were the limitations to using *WT* samples as a control for mutant *sod* gene expression. Furthermore, mentioned above are the difficulties in interpreting some of the SOD activity data without controlling for genetic background. As such, SOD activity measurements were taken in individual sex *Sod3*$^{06029}$ lines against the same backcrossed (*yw* $^{c\text{-}iso}$) and non-backcrossed (*yw* $^{c}$) control strains described previously. As found with gene expression measurements of the same strains, differential activity measurements were observed with the backcrossed and non-backcrossed lines. In comparison with the *yw* $^{c\text{-}iso}$ line male and female flies showed similar trends with both total and Cu Zn SOD activities being found to be lower in the control line then in the *sod3* mutant line. Conversely, using *yw* $^{c}$ as the control, *sod3*$^{06029}$ flies were found to have marginally reduced total SOD activity levels in both sexes and significantly reduced Cu Zn SOD activity levels. These activity measurements support the gene expression data in the same strains and thus the concept of genetic modifiers influencing fitness in *Sod3*$^{06029}$ flies. *Sod1* and *sod2* were found to be upregulated in male and female *Sod3*$^{06029}$ flies compared to the *yw* $^{c\text{-}iso}$ line, whilst *sod3* knockdown was less pronounced than expected in female *Sod3*$^{06029}$ flies and mildly upregulated in males (Figures 3.14A and B). Since *sod1* and *sod2* are found to be expressed at higher levels than *sod3* this increase in SOD activity could be accounted for by alterations in gene expression. Compared to *yw* $^{c}$ controls *sod1* and *sod2* expression was found to remain unchanged in *Sod*$^{06029}$ flies whereas

*sod3* was significantly down-regulated in both sexes (Figures 3.15A and B), thus explaining the suppression in Cu Zn SOD activity in the mutant line. The similarity in total SOD activity in these lines also supports the notion of compensatory SOD2 changes occurring. It would therefore appear that in backcrossing the *sod3* mutant line modification of, at a minimum, *sod* gene expression has occurred, manifesting in a decrease in SOD activity in the isogenic *yw* $^{c\text{-}iso}$ line.

### 4.5.4 SOD activity shown not to alter in response to oxidative insults

As with the gene expression data, application of oxidative stress in the form of paraquat or $H_2O_2$ treatment resulted in no change in SOD activity indicating that post-translational modifications in response to oxidative insults are not occurring. Whilst the measurement of direct changes in SOD activities in response to paraquat and $H_2O_2$ insults in *Drosophila* appear not to have been carried out previously, similar studies in the adult house fly, *Musca domestica*, parallel these findings with no change in SOD activities being found in response to administration of paraquat (Allen et al. 1984) or $H_2O_2$ (Sohal 1988). Paraquat has, however, been found to elevate Cu Zn SOD activity in murine lymphoma cells (Jaworska and Rosiek 1991), whilst $H_2O_2$ was shown to increase total SOD in maize strains (Pastori and Trippi 1992). Whilst it appears that in some instances paraquat and $H_2O_2$ administration can elevate SOD activity levels, in *Drosophila* the SODs do not seem to function as oxidative stress responsive proteins. However, as was described in the analogous gene expression studies in chapter 3, it should considered that the oxidant concentrations (30mM paraquat and 15% $H_2O_2$) used in this study exerted a grossly hypertoxic acute stress. This means that the activity measurements made in this chapter may not reflect the true effect that oxidative stress has on SOD activity. As such, experiments should be reconsidered using oxidant concentrations that apply a less toxic, more chronic stress condition. Analysis of SOD activity under such conditions may give a truer reflection of the SOD's ability to act as oxidative stress proteins.

### 4.5.5 Validation of specificity of *Drosophila* SOD3 antibody is inconclusive

After some initial promise with the *Drosophila* SOD3 antibody it appears further work is required to determine whether the antibody can indeed detect SOD3 in western blots. Initial results revealed a prominent band of immunoreactivity at ~30 kDa, the intensity of which was found to diminish considerably with $Sod3^{06029}$ samples, thus suggesting the antibody may have SOD3 specificity. However, the predicted molecular weights of the monomeric forms of SOD3v1 and SOD3v2 are 19.2 kDa and 23.1 kDa, respectively, and since these masses are inclusive of the N-terminal signal sequence it might seem unlikely that ~30 kDa band found on the blots is due to SOD3 reactivity. This does not, however, exclude the possibility that this band arises from SOD3 immunoreactivity. It is possible that post-translational modifications such as glycosylation and phosphorylation are occurring or that the denaturation step in the western blot protocol is insufficient to separate the protein subunits. The occurrence of either of these would resolve protein products of a higher molecular weight than would be predicted by sequence analysis alone.

In an attempt to confirm that the ~30 kDa band is due to SOD3 immunoreactivity, competition assays were performed in which the primary *Drosophila* SOD3 antibody was pre-incubated with an excess of the free peptide to which the antibody was raised prior to probing protein samples. Any SOD3 specific bands would thus be expected to be abolished from subsequent western blots due to the primary antibody being coupled to the target peptide. However, competition assays in which the peptide excess went up to 50,000-fold failed to remove the ~30 kDa band, or any other protein band, suggesting that the primary antibody has limited or no immunoreactivity with SOD3. Furthermore, control assays in which the fluorescent secondary antibody alone was incubated with blots revealed that all protein bands could still be detected. Consequently, it appears the bands seen on these western blots were produced through unspecific binding of the secondary antibody and not through any binding of the primary antibody with SOD3. Coomassie stains of *WT* protein samples also revealed the major protein band of the homogenate samples to be located at the same mass as

the immunoreactive band seen previously supporting the notion of unspecific reactivity in the assays (Figure 4.13).

In order to remove as much unspecific binding as possible alternative blocking solutions were utilised, with 5% milk powder in tPBS being found to be the most stringent. Furthermore, HRP conjugated secondary antibodies visualised by ECL were also found to reduce unspecific binding. Whilst competition assays were not carried out with this blocking solution and secondary antibody due to insufficient amounts of the free peptide, *WT* and *Sod3*$^{06029}$ protein homogenates were tested and a single band of immunoreactivity was observed, as previously, at ~30 kDa, with the intensity of the band being diminished in the *sod3* hypomorph samples. The isolation of a knockout mutant, as attempted in Chapter 3, would allow for the confirmation of whether this band is indeed due to SOD3 reactivity.

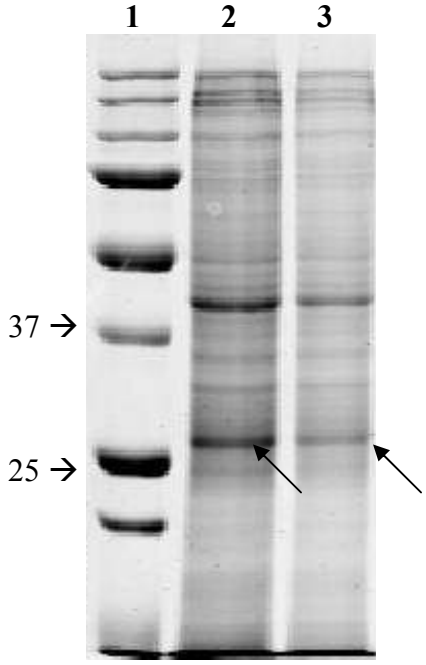


**Figure 4.13. Coomassie stain revealing the major protein bands in Oregon R homogenates.** Lane 1 = 5µL dual colour ladder; lane 2 = 40µg Oregon R total protein; lane 3 = 20µg Oregon R total protein. The major protein band seen resolves at ~30 kDa, exactly the same size at which the major band seen in our western blots is found.

Currently the ability of the SOD3 antibody to detect *Drosophila* SOD3 remains unknown. It is possible that the SOD3 protein is extremely stable and that current

denaturation steps are insufficient to separate the SOD3 monomers. Indeed this has been observed as a feature of SOD1, which still shows enzymatic activity in the face of harsh denaturants such as 10M urea and 4% SDS and at temperatures of 80°C (Culotta et al. 2006). Whilst the antigenic epitope sequence is predicted to lie on the external face of the SOD3 protein, it is possible that the sequence lies at the interface of dimer and/or tetramer formation and thus immunoreactivity may not be seen against the native form of the protein. It should also be noted that a murine SOD3 antibody (a kind gift from Professor T. Fukai, University of Illinois at Chicago) was tested for cross reactivity with *Drosophila* SOD3, however no such reactivity was observed (data not shown). The usefulness of having a *Drosophila* SOD3 antibody cannot be underestimated. In relation to the work presented in this thesis its primary use could be in confirming both the cellular location of the SOD3 proteins, through western blotting after cellular fractionation and/or immunocytochemistry of cells expressing SOD3 constructs, and furthermore any SOD3 interactions could be assessed through complex immunoprecipitation. It is possible that generation of an antibody to the total recombinant *Drosophila* SOD3 protein might prove more successful at producing a useful antibody and should be considered for future work.

### 4.5.6 Proteomic analysis of *sod* mutants hints at protein targets subject to quantitative changes

A preliminary screen to determine quantitative proteomic changes in $Sod3^{06029}$ and *n108* flies (compared to $yw^{c\text{-}iso}$ and *red* controls, respectively) was carried out by iTRAQ analysis. A total of 39 proteins were identified that satisfied the selection criteria detailed in the results, with just three of these proteins in $Sod3^{06029}$ samples and four in *n108* samples being observed to have a statistically significant change in expression. The variety of cellular processes in which the proteins are involved are diverse, with the majority of proteins found to be important for muscle formation and function, ion transport and oxidoreductase function. The observation of just 39 proteins represents a low proteome coverage, with typically a few hundred proteins often being identified in equivalent experiments with *Drosophila* samples (Pedersen et al. 2010;Xun et al. 2008). Such a low proteome coverage suggests that either the protein concentration of the samples tested (100μg) was too low or that only the most

highly abundant proteins are being detected by MS/MS. Alternatively, the use of whole adult extracts may cause high sample complexity leading to decreased peptide detection sensitivity (Pedersen et al. 2010;Paul Skipp, personal communication).

The three proteins found to be significantly repressed in *Sod3*$^{06029}$ flies are involved in cellular and ion transport (ADP, ATP carrier protein), differentiation (14-3-3 protein zeta) and lipid transport (apolipophorins), suggesting that the genetic modifications proposed to function in the *Sod3*$^{06029}$ line may be influencing fitness by decreasing the activity of one or more of these pathways. It should be noted, however, that the only control used in these experiments was the *yw* $^{c\text{-}iso}$ line, thus whether these decreases in protein expression occur as a result of inherited genetic modifiers can only be confirmed after assaying with the non-backcrossed *yw* $^{c}$ strain. In the *sod1* null strain, *n108*, the proteins: ATP synthase subunit alpha, mitochondria (important for ion transport); alcohol dehydrogenase (an oxidoreductase) and myosin regulatory light chain (involved in muscle formation and function) were found to be significantly up-regulated, whereas cytochrome P450 4g1 (an oxidoreductase) was significantly down-regulated. As stated previously, *n108* flies are characterised by significantly reduced mortality and paraquat hypersensitivity, suggesting that the proteomic changes observed either function as adaptive mechanisms promoting survival in this species or are as a result of the decreased oxidative protection in *n108* flies and thus maybe causative of the reduced lifespan phenotype observed.

The results of this study are preliminary since the proteome coverage revealed is so low. These experiments therefore need to be confirmed by repeating with either increased sample concentrations or with isolated *Drosophila* tissues, as well as with the non-backcrossed *yw* $^{c}$ strain. Furthermore, while just a few proteins were found to be significantly differentially expressed in this study, recently it has been suggested that current iTRAQ technology and analysis tends to underrepresent protein expression data, implying that proteins identified which fall outside of the significance threshold value may still be biologically relevant in comparative studies (Ow et al. 2009). It should also be noted that the iTRAQ technique only reveals quantitative changes occurring at the protein level, rather than at the genomic level which would be reported with techniques such as microarrays. It would be ideal to compare microarray data with the iTRAQ results presented in this chapter in order to

assess whether post-transcriptional events are occurring in response to the individual mutations tested. Whilst microarray analysis of these mutants was not carried out in this thesis, performing such experiments would be a useful addition to the study which could be carried out at a later date.

# CHAPTER 5

# 5. Functional phenotypic studies of *Drosophila* SOD3

## 5.1 Aim

To date the function of the *Drosophila sod3* gene can only be predicted from DNA sequence analysis which suggests the proteins primary role is as a scavenger of extracellular sources of $O_2^{-}\cdot$. This chapter presents the preliminary investigations into what might be the functional role of this protein in *Drosophila* by assaying *sod3* mutants for a functional phenotype.

## 5.2 Introduction

Compared to the number of intracellular sources, there are comparably few extracellular sources of ROS (see Figure 1.2). Furthermore, the anionic nature of certain ROS, including $O_2^{-}\cdot$, means that many species do not readily cross biological membranes leading to compartmentalised pools of ROS. The major producer of extracellular $O_2^{-}\cdot$ is the NADPH oxidase (NOX) complex of phagocytic and non-phagocytic cells (Lambeth 2004), however other extracellular sources of ROS include membrane bound xanthine oxidases and environmental factors such as ultraviolet light, χ- and γ-radiation and pesticides (Gracy et al. 1999). The extracellular SOD3 enzyme is thought to protect cells against these peripheral oxidants, however due to SOD3 remaining undiscovered in short lived insect models for so long, the majority of work concerning functional characterisation of the SOD3 protein has been in mammalian models. Mice lacking SOD3 (or with SOD3 mutations) in fact display relatively mild phenotypes. Unlike *sod1* and *sod2* null mice, which have impaired survival (Li et al. 1995;Sentman et al. 2006), an absence of *sod3* has no effect on lifespan, however there is evidence of increased oxidative damage (Sentman et al.

2006). Furthermore, *sod3* knockout mice are also significantly more vulnerable to hyperoxia (Carlsson et al. 1995), which correlates with the highest *sod3* expression levels being found in blood vessels and arterial cell walls (Oury et al. 1996;Stralin et al. 1995), particularly of the lung (Folz et al. 1997). *C. elegans* lifespan is also found to be unaffected upon removal of the extracellular Cu Zn SOD gene (*sod-4*), however in contrast with mice, *sod-4* deficient strains are no more susceptible to hyperoxia and additionally show no paraquat hypersensitivity (Doonan et al. 2008;Van Raamsdonk & Hekimi 2009).

Detailed in this chapter are the studies carried out on the Drosophila *sod3* hypomorph line to establish a functional phenotype for a *sod3* deficiency in this model system.

## 5.3 Materials and methods

### 5.3.1 Fly strains

The fly strains used in subsequent experiments are listed in Table 3.1 and were maintained on standard *Drosophila* medium (Appendix 2) at 23°C in a 12 hour light/dark cycle.

### 5.3.2 Oxidative stress tests

#### 5.3.2.1 Paraquat toxicity

The susceptibility of adult flies to paraquat toxicity and was assessed by comparing survival rates of $Sod3^{06029}$ and *n108/TM3* lines against control strains. Same sex adults up to 12 days old were briefly anesthetized with $CO_2$ and transferred from standard plastic food vials to empty plastic vials for a maximum of 1 hour (~10 flies per vial). After one hour, and without anesthetisation, flies were transferred into plastic vials containing 5 pieces of Whatman filter paper soaked in 500µL of 10mM paraquat dissolved in 5% sucrose. Flies were scored for survival at regular intervals and transferred onto fresh paraquat saturated filter paper every 24 hours. The experiment ran until all flies had died. Three replicates of each genotype were tested and the data was analysed by two-way analysis of variance (ANOVA).

#### 5.3.2.2 $H_2O_2$ toxicity

The same fly strains were also assessed for $H_2O_2$ sensitivity. Adult flies up to 12 days of age were prepared as detailed for the paraquat toxicity assays, but maintained on 15% $H_2O_2$, which was replaced every 24 hours until all flies has died. Three replicates of each genotype were tested and the data was analysed by two-way ANOVAs.

### 5.3.3 Climbing assays

Climbing assays were carried out on separate sex, individual flies to assess locomotor ability with increasing age. Flies were isolated at the pupae stage of development and identified by sex by the presence (males) or absence (females) of sex combs (a patch of black bristles) on the forelegs, visible from within the pupae case. Flies were isolated by taking a damp paint brush, lightly moistening the sides of the pupae case and then gently detaching the pupae from the side of the food vial. Single pupae were placed on the inside of a 2mL microtube (Greiner Bio One), containing approximately 0.5mL of standard *Drosophila* medium (Appendix 2), with a pin hole made in the lid to allow oxygen in. Flies were allowed to eclose and were transferred to fresh food microtubes every 2-3 days. Flies remained isolated throughout the duration of the experiment.

At time points of 2, 4 and 6 weeks of age, each fly was assayed for its climbing ability as follows: individual flies were transferred from their microtube, without anesthetisation, to a plastic climbing vial marked with a line at 7 cm up from the bottom of the vial. Flies were gently tapped to the bottom of the vial and the time taken for each fly to climb 7 cm was recorded. For those flies not reaching 7 cm within 30 secs, the maximum height climbed within 30 secs was recorded. Flies were tested three times at each age and the best result (quickest time climbed/maximum height climbed) was taken. Statistical analysis of the ability to climb between genotypes at each age time point was carried out by two-tailed Z-tests and analysis of climbing velocity was calculated by two-tailed student T-tests.

# 5.4 Results

## 5.4.1 Paraquat toxicity

### 5.4.1.1 *Sod3* mutant flies compared to the backcrossed control

A highly significant increase in resistance to 10mM paraquat was observed in both male (Figure 5.1A) and female (Figure 5.1B) $Sod3^{06029}$ flies compared to the backcrossed $yw^{c\text{-}iso}$ line (both P = <0.001). Survivorship curves for each sex were found to diverge after 10 hours and whilst they remained divergent throughout life in male genotypes, in females survival curves merged again between genotypes 100 hours into the experiment. Maximum lifespan was also found to be reduced in $yw^{c\text{-}iso}$ controls (105 hours) compared to $Sod3^{06029}$ flies (188 hours), under paraquat exposure.

### 5.4.1.2 *Sod3* mutant flies compared to the non-backcrossed control

Compared to non-backcrossed $yw^{c}$ flies, male $Sod3^{06029}$ flies were found to be significantly more sensitive to paraquat exposure (Figure 5.2A) (P = <0.001), surviving no more than 112 hours. Survival curves were found to diverge at 28 hours and $yw^{c}$ control flies survived up to 236 hours under paraquat exposure. No difference in survival was observed for females of the same genotype (Figure 5.2B).

### 5.4.1.3 *Sod1* mutant flies compared to an isogenic control

Male *n108/TM3* flies were found to be as susceptible to paraquat induced oxidative stress as isogenic *red* control flies (Figure 5.3A). Female *n108/TM3* flies, however, displayed a significant increase in paraquat resistance compared to the control strain (Figure 5.3B) (P = <0.001). Female survival curves diverged at 40 hours of oxidant exposure, with female control flies having a maximum lifespan of 166 hours compared to the 220 hours of *n108/TM3* flies.

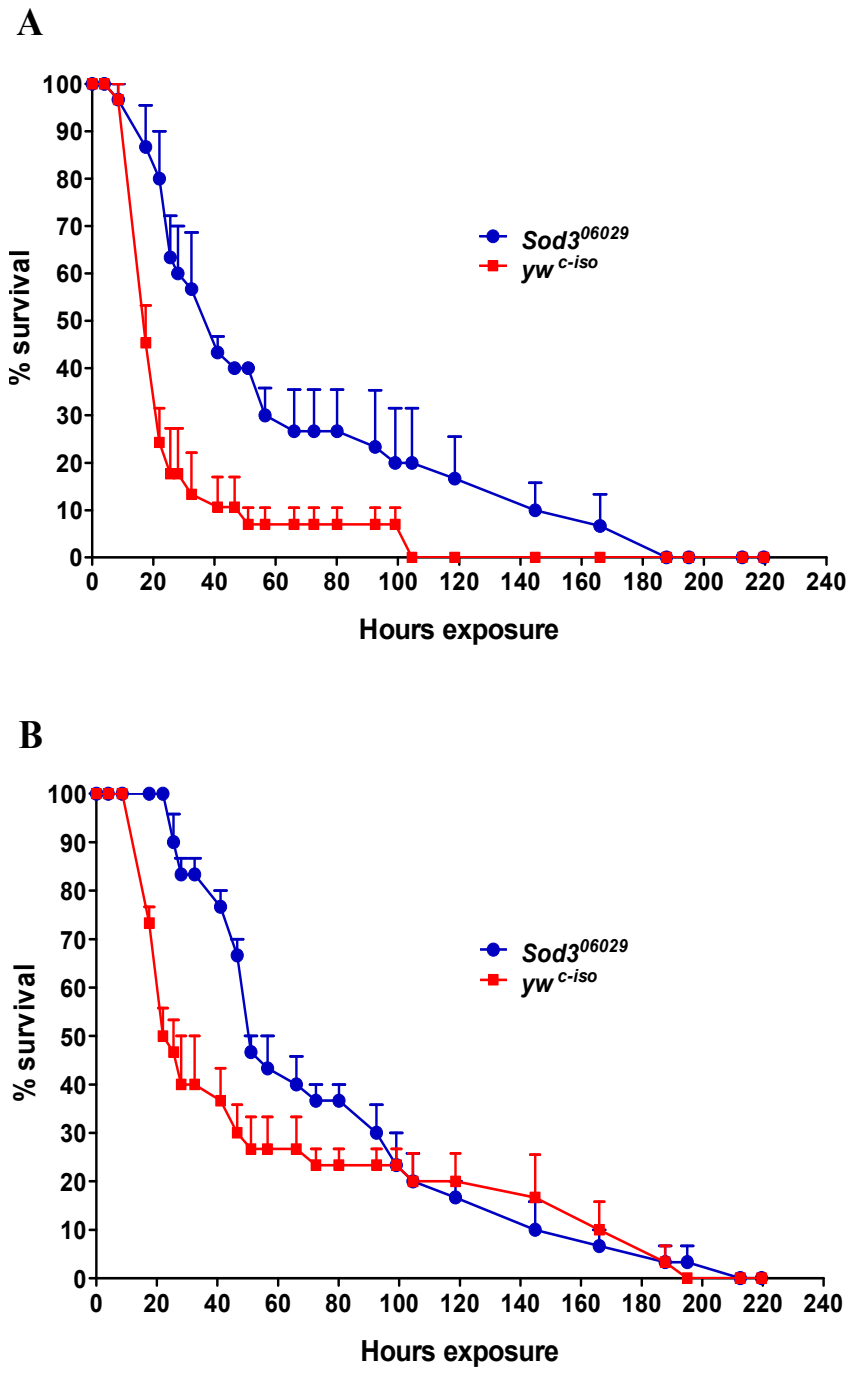


**Figure 5.1. Paraquat induced oxidative stress resistance of *Sod3*$^{06029}$ flies compared to the backcrossed control.** Male (**A**) and female (**B**) flies were exposed to 10mM paraquat and scored for survival until all flies had died (N = 3 for both sexes). A significant difference in survival was observed for both sexes (P = <0.001).

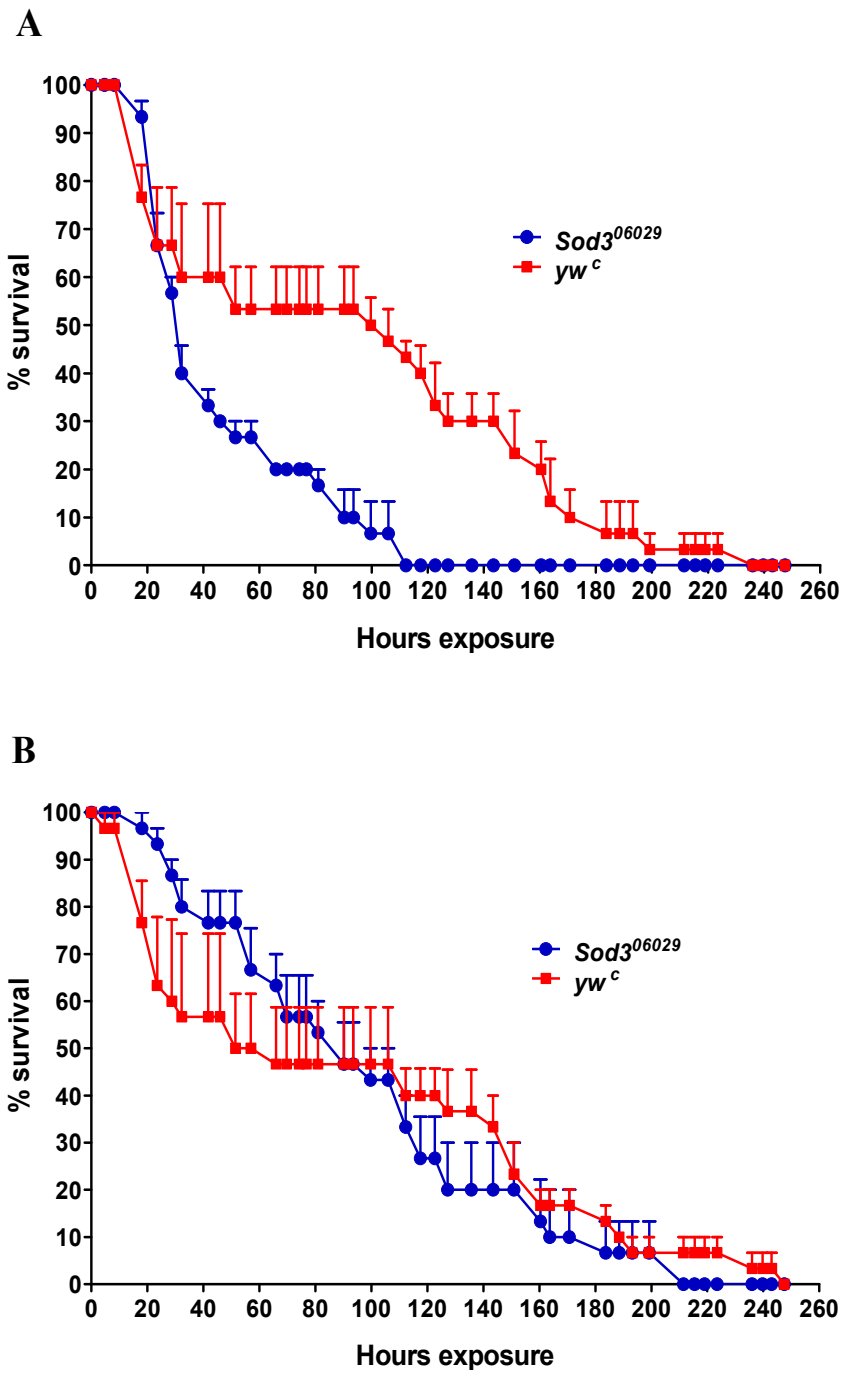


**Figure 5.2. Paraquat induced oxidative stress resistance of *Sod3*$^{06029}$ flies compared to the non-backcrossed control.** Male (**A**) and female (**B**) flies were exposed to 10mM paraquat and scored for survival until all flies has died (N = 3 for both sexes). A significant difference in survival was observed in male flies (P = <0.001) while no difference in survival was found for females.

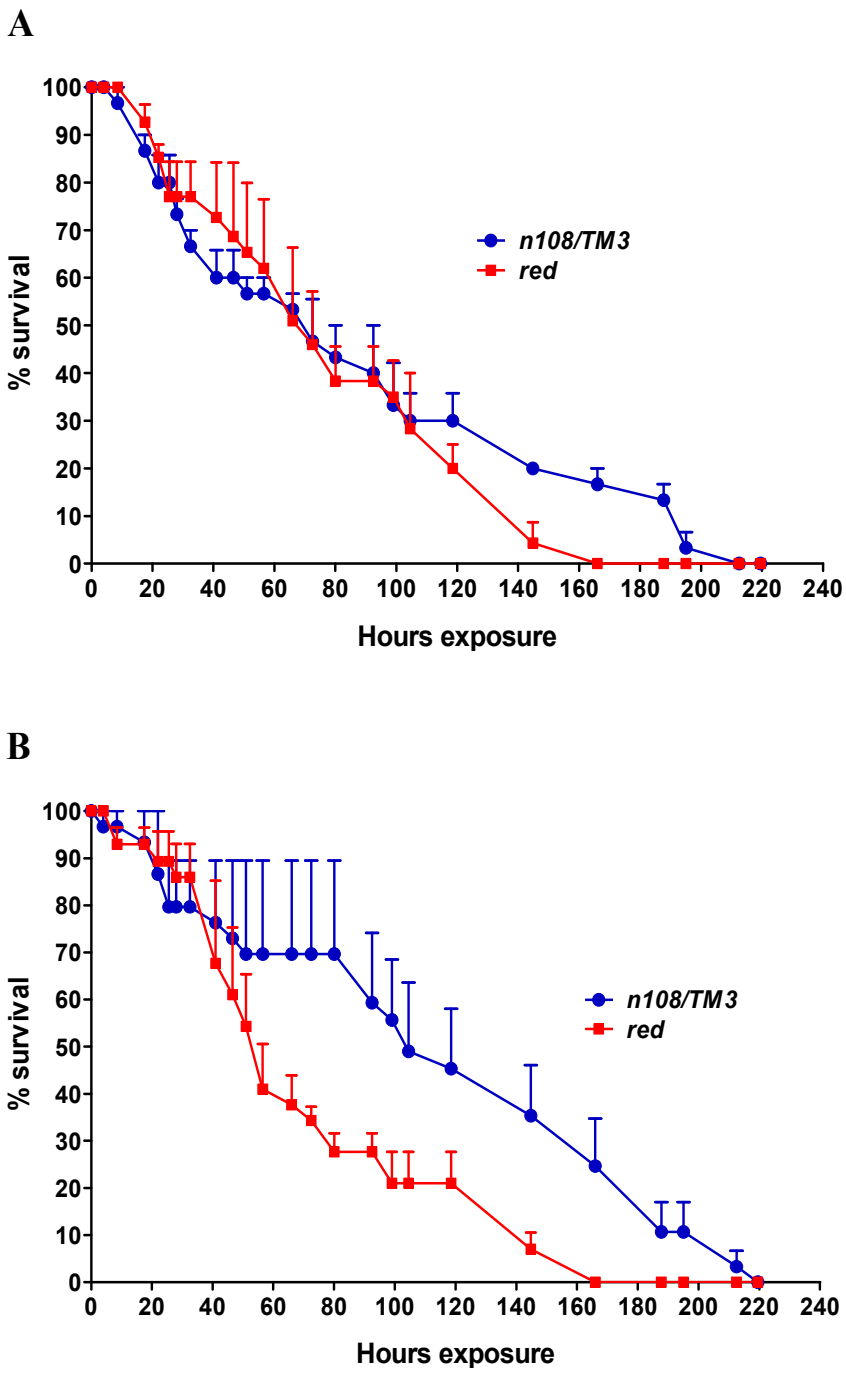


**Figure 5.3. Paraquat induced oxidative stress resistance of *n108/TM3* flies against an isogenic control.** Male (**A**) and female (**B**) flies were exposed to 10mM paraquat and scored for survival until all flies has died (N =3 for both sexes). While no difference in survival was observed in male flies a significant difference in survival was found for females (P = <0.001).

## 5.4.2 $H_2O_2$ toxicity

### 5.4.2.1 *Sod3* mutant flies compared to the backcrossed control

In response to 15% $H_2O_2$ exposure, both male (Figure 5.4A) and female (Figure 5.4B) $Sod3^{06029}$ flies were observed to be significantly more tolerant than the respective $yw^{c\text{-}iso}$ backcrossed controls (P = <0.001). Survivorship curves for each sex were found to diverge after 20 hours and remained divergent through out life. Maximum lifespan was found to be 47 hours in $yw^{c\text{-}iso}$ controls compared to 75 hours in $Sod3^{06029}$ flies under $H_2O_2$ exposure.

### 5.4.2.2 *Sod3* mutant flies compared to the non-backcrossed control

Both male (Figure 5.5A) and female (Figure 5.5B) $Sod3^{06029}$ flies were also found to be significantly more resistant to $H_2O_2$ induced oxidative stress than the non-backcrossed $yw^{c}$ line (P = <0.001). Survival curves diverged between genotypes in both sexes immediately upon $H_2O_2$ application, and while there was no difference in maximum lifespan between males of the two genotypes, maximum lifespan was found to be shortened in female controls at 81 hours, compared to 94 hours with $Sod3^{06029}$ flies.

### 5.4.2.3 *Sod1* mutant flies compared to an isogenic control

There was no measurable difference in susceptibility to $H_2O_2$ exposure of *n108/TM3* flies of either sex compared to the isogenic *red* control line (Figure 5.6A (male) and Figure 5.6B (female)). While there was no difference in the survival curves between genotypes and sexes, there was also only a negligible difference in the maximum lifespan of either genotype, with the isogenic *red* line being marginally longer lived than the *Sod1* mutant stain in both sexes.

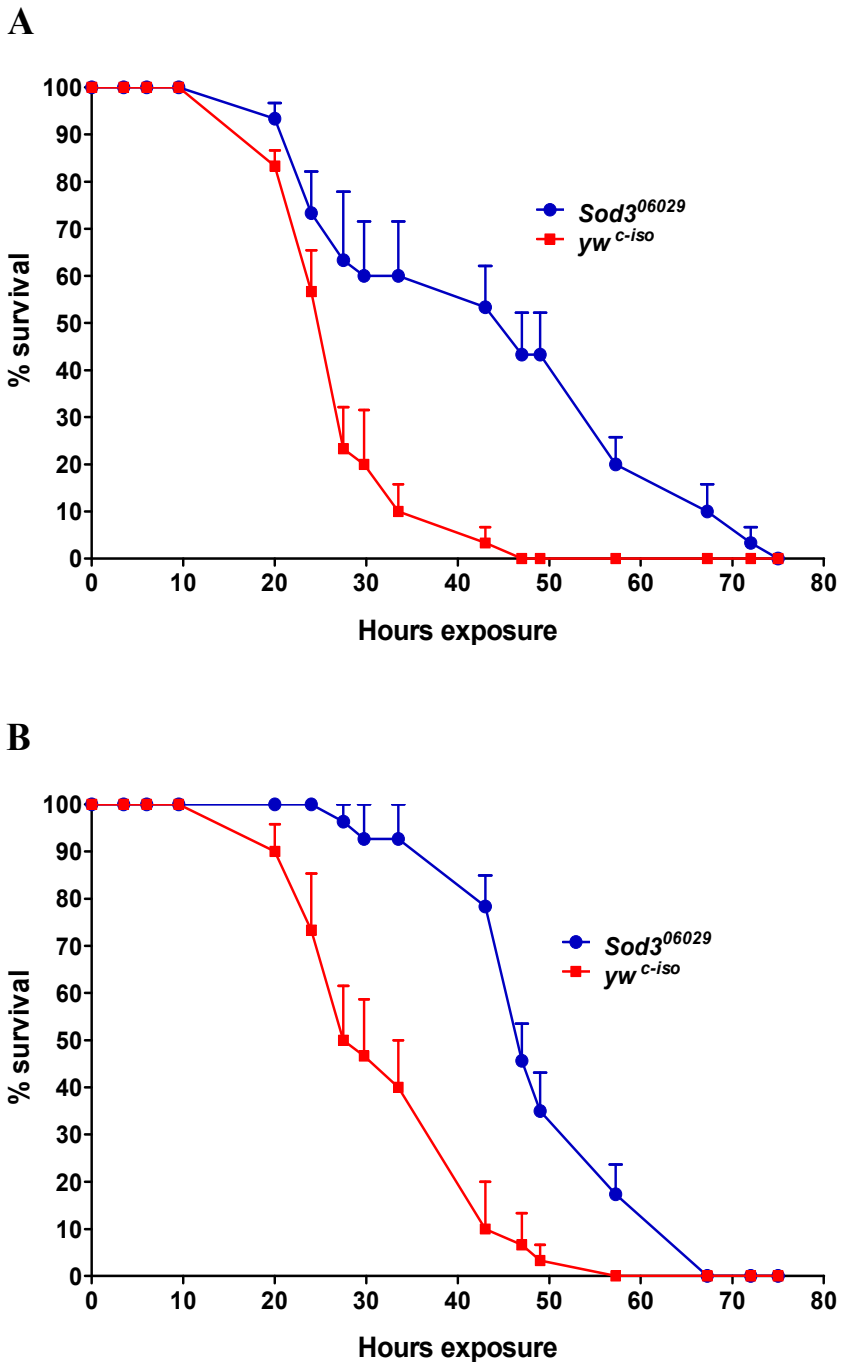


**Figure 5.4. $H_2O_2$ induced oxidative stress resistance of *Sod3*$^{06029}$ flies compared to the backcrossed control.** Male (**A**) and female (**B**) flies were exposed to 15% $H_2O_2$ and scored for survival until all flies has died (N = 3 for both sexes). A significant difference in survival was observed for both sexes (P = <0.001).

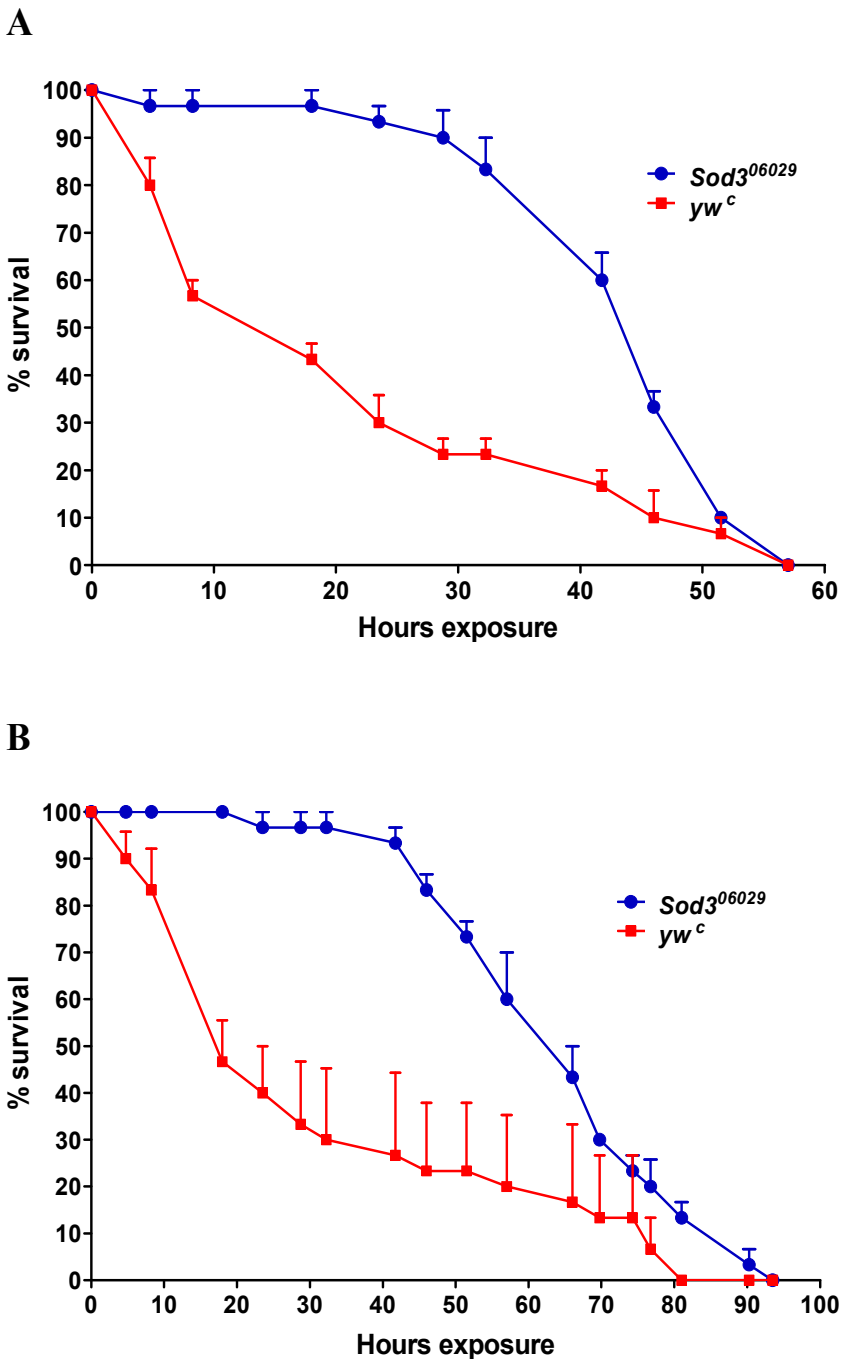


**Figure 5.5. $H_2O_2$ induced oxidative stress resistance of *Sod3*$^{06029}$ flies compared to the non-backcrossed control.** Male (**A**) and female (**B**) flies were exposed to 15% $H_2O_2$ and scored for survival until all flies has died (N = 3 for both sexes). A significant difference in survival was observed for both sexes (P = <0.001).

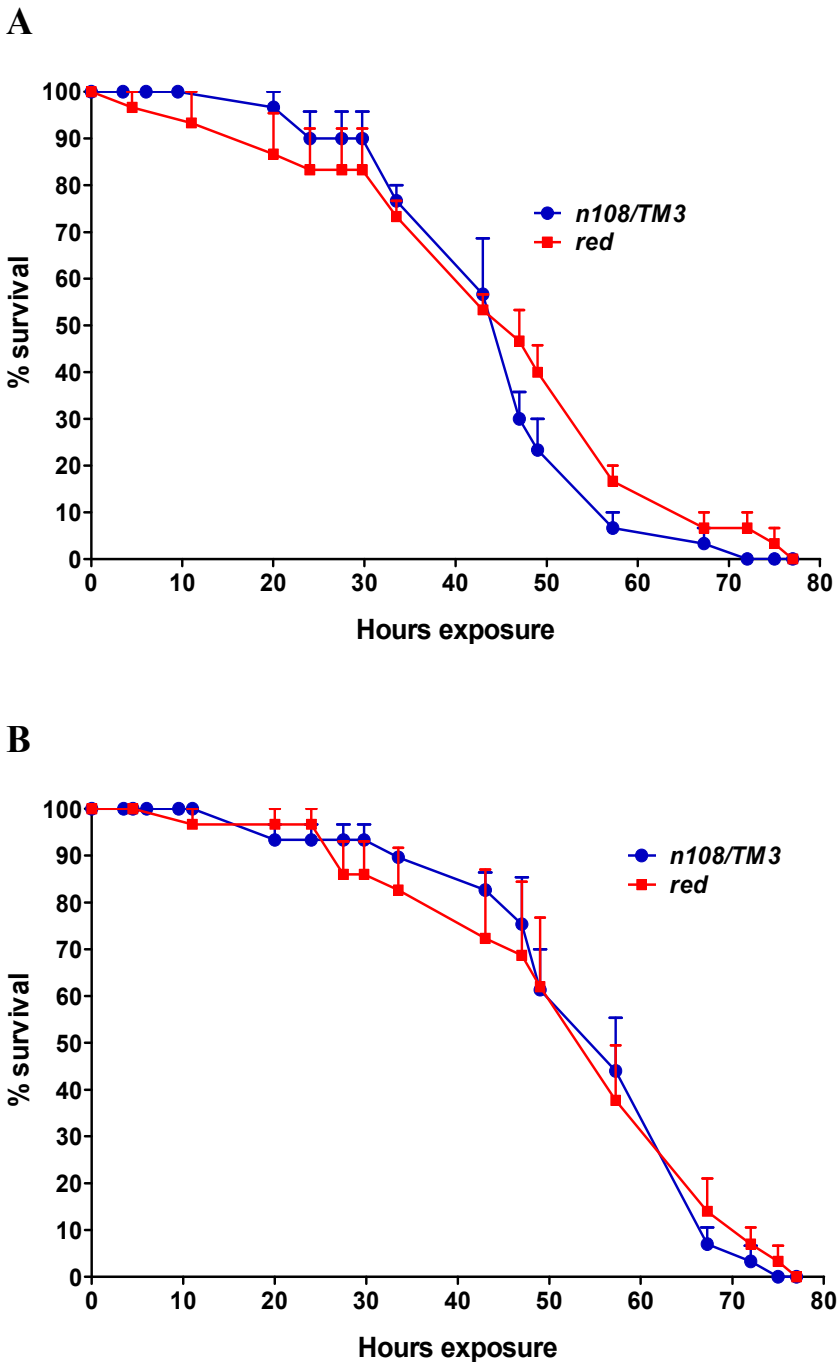


**Figure 5.6. $H_2O_2$ induced oxidative stress resistance of *n108/TM3* flies against an isogenic control.** Male (**A**) and female (**B**) flies were exposed to 15% $H_2O_2$ and scored for survival until all flies has died (N = 3 for both sexes). No difference in survival was observed in either sexes.

### 5.4.3 Climbing ability

The locomotor ability of *Sod3*$^{06029}$ flies with increasing age was compared against the backcrossed *yw* $^{c\text{-}iso}$ control line. Results for pooled sexes revealed no measurable difference in the ability of 2 week or 6 week old flies of either genotype to climb 7 cm within 30 secs (Figure 5.7A). There was, however, a slight increase in the number of successful *Sod3*$^{06029}$ climbers compared to control flies at 2 weeks of age. Furthermore, a highly significant reduction (P = <0.01) in the ability of *Sod3*$^{06029}$ flies to climb was observed at 4 weeks of age. The climbing velocity of those flies that reached 7 cm within 30 secs was also calculated (Figure 5.7B). Climbing velocity was found to decrease as a function of age in both genotypes and whilst there was no statistically significant difference in climbing speed between the genotypes at any of ages assayed, overall there was a trend of reduced climbing velocity in the *Sod3*$^{06029}$ line.

To assess whether reduced locomotor function is influenced by sex, the pooled data was reanalysed by sex. Both male (Figure 5.8A) and female (Figure 5.9A.) *Sod3*$^{06029}$ flies were found to have statistically significantly reduced climbing ability at 4 weeks of age (both P = <0.05), but no measurable difference at either 2 or 6 weeks of age. However, a slight increase in climbing ability was observed in *Sod3*$^{06029}$ flies of both sexes at 2 weeks of age, whereas 6 week old female *Sod3*$^{06029}$ flies were found to be unable to climb. The trend of reduced climbing velocity in the *Sod3*$^{06029}$ line was apparent between genotypes of both male (Fig 5.8B.) and female (Fig 5.9B.) flies, however, a statistically significant reduction in velocity was observed for females *Sod3*$^{06029}$ flies at 2 weeks of age (P = <0.05). Furthermore, females of both genotypes were also found to have dramatically reduced climbing velocities compared to their male counterparts at each of the ages tested.

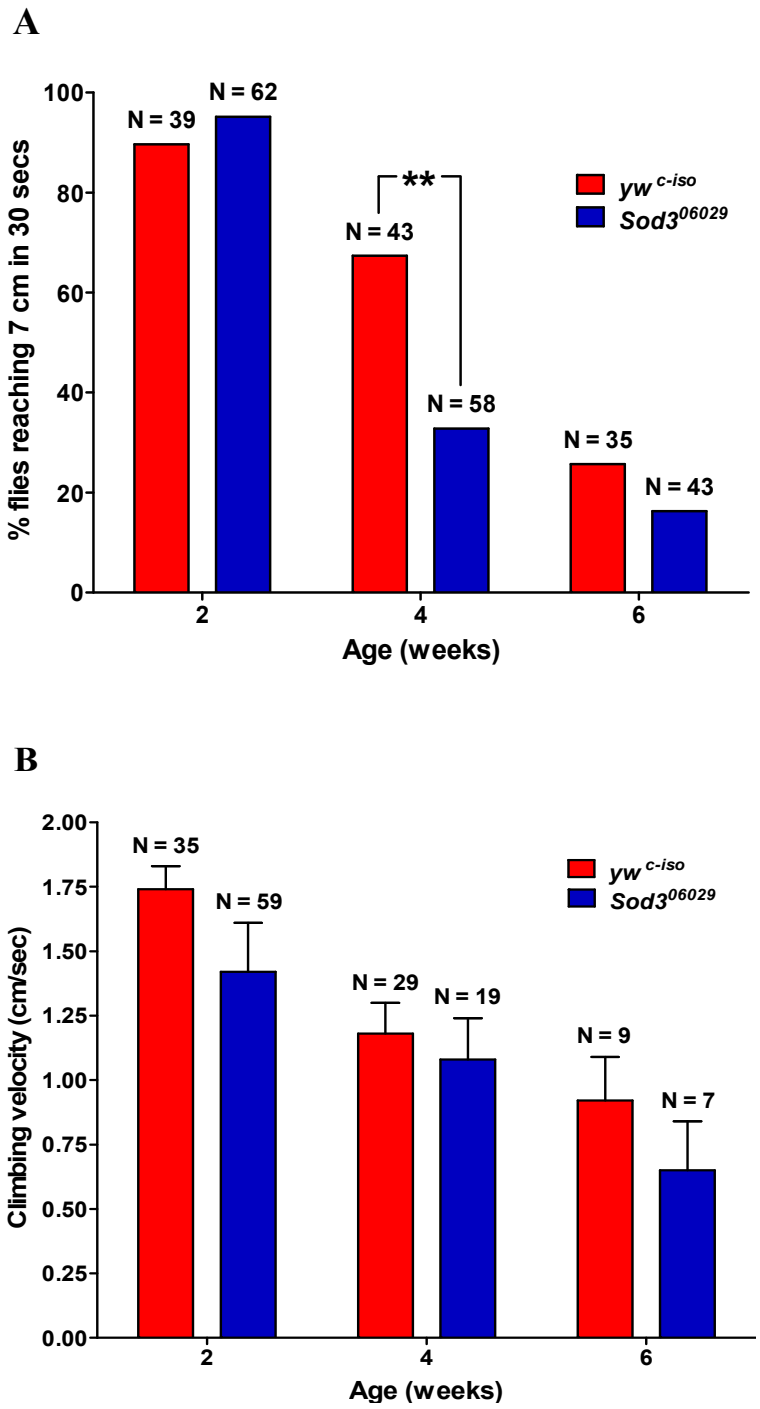


**Figure 5.7. Climbing ability of pooled sexes as a function of age.** Individual flies were assayed for their ability to climb 7 cm with 30 secs (**A**) and, of those flies successful, their climbing velocity was calculated (**B**). A significant reduction in climbing ability of *Sod3*$^{06029}$ flies was observed at 4 weeks of age (P = <0.01).

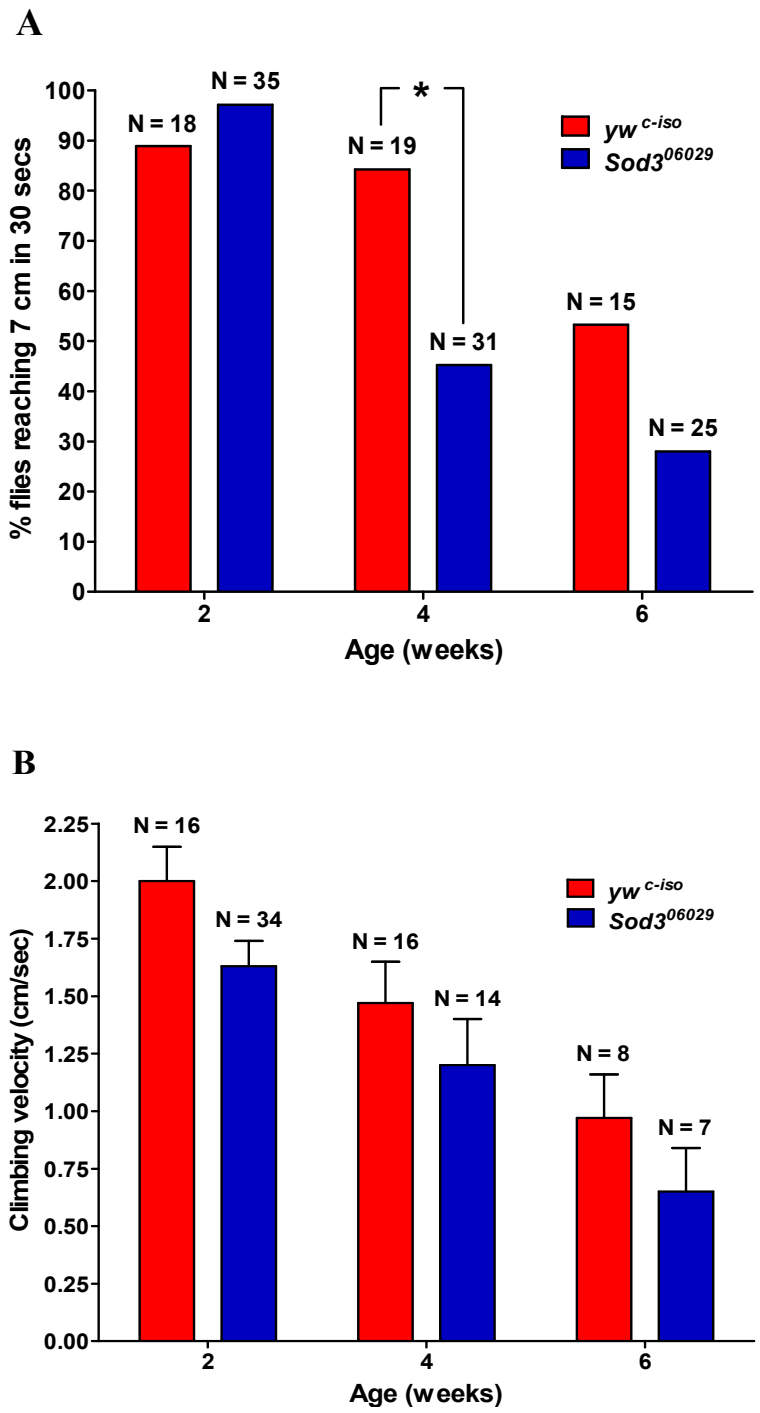


**Figure 5.8. Climbing ability of male flies as a function of age.** Individual flies were assayed for their ability to climb 7 cm with 30 secs (**A**) and, of those flies successful, their climbing velocity was calculated (**B**). A significant reduction in climbing ability of *Sod3*$^{06029}$ males was observed at 4 weeks of age (P = <0.05).

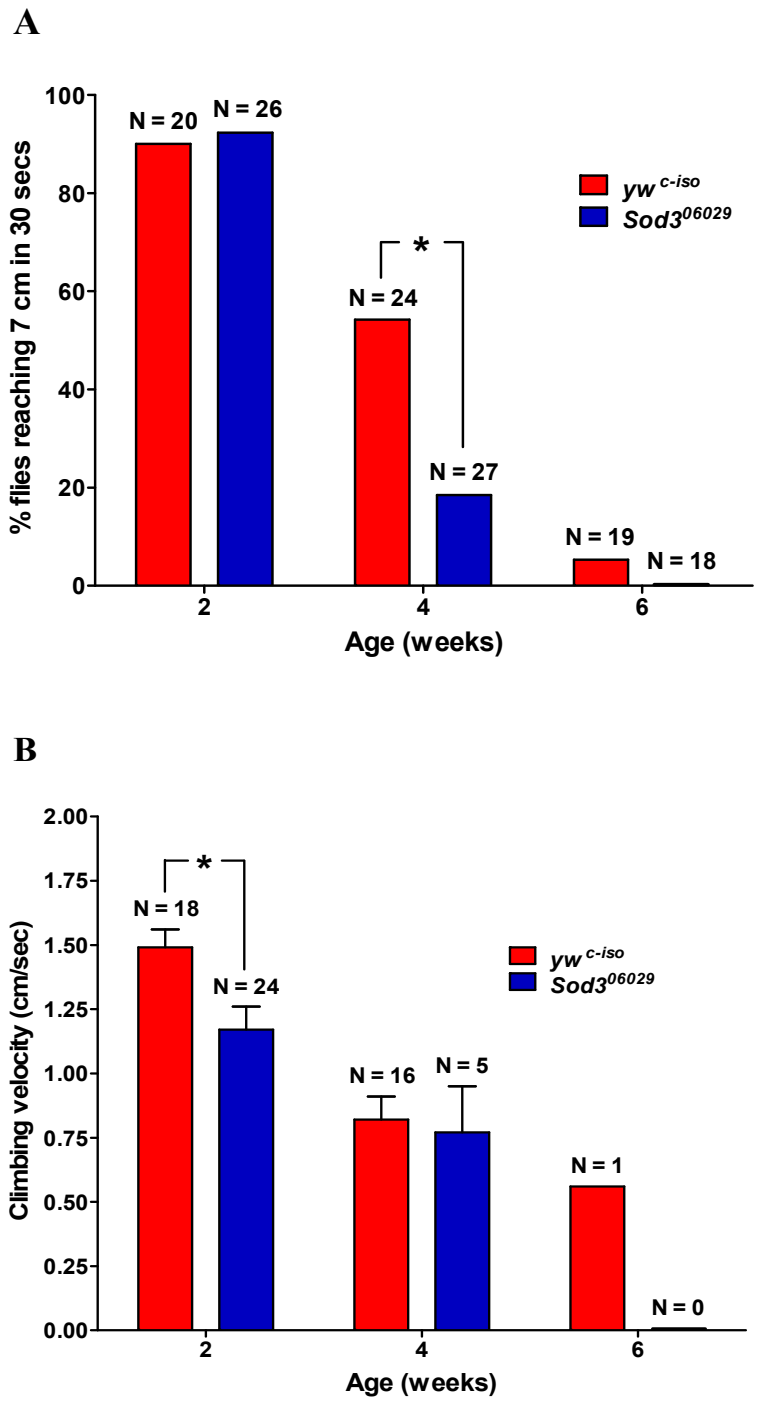


**Figure 5.9. Climbing ability of female flies as a function of age.** Individual flies were assayed for their ability to climb 7 cm with 30 secs (**A**) and, of those flies successful, their climbing velocity was calculated (**B**). A significant reduction in climbing ability of *Sod3*$^{06029}$ females was observed at 4 weeks of age (P = <0.05) and significantly reduced climbing velocity was calculated at 2 weeks of age (P = <0.05).

## 5.5 Discussion

### 5.5.1 Paraquat resistance in *sod* mutants reveals sex specific variation and also hints at the nature of the genetic modifiers transferred

As with previous assays, the *sod3* hypomorph mutant was assayed against both a backcrossed and non-backcrossed control, in this instance to assess the effect of oxidative stress on flies with reduced *sod3* expression. The key finding was differences in the patterns of survival upon 10mM paraquat exposure, dependent upon which control was used. Both male and female $Sod3^{06029}$ flies were found to be significantly more resistant to paraquat exposure than the backcrossed $yw^{c\text{-}iso}$ line. Previously it was shown that not only was *sod1* and *sod2* expression upregulated in $Sod3^{06029}$ flies of both sex in comparison to $yw^{c\text{-}iso}$ but not $yw^{c}$, but both total and Cu Zn SOD activity was also elevated. It therefore appears that this increase in intracellular antioxidant capacity may be sufficient to protect against paraquat induced toxicity, accounting for the increased survival observed. However, in comparison with the non-backcrossed $yw^{c}$ strain, female $Sod3^{06029}$ flies were found to be as susceptible paraquat induced toxicity as controls, while males were significantly more sensitive. The observation of no effect on paraquat toxicity in female *sod3* mutants replicates similar observations found after removal of the extracellular *sod* gene (*sod-4*) in *C. elegans* (Doonan et al. 2008). However the finding of decreased paraquat resistance in male $Sod3^{06029}$ flies is somewhat surprising for two reasons. Firstly, as stated previously, paraquat transfers toxicity intracellularly (Fukushima et al. 2002), whilst SOD3 is predicted to be an extracellular protein. This would either suggest that SOD3 can be intracellular in some instances, or that SOD1 and SOD3 do interact in some manner as proposed earlier. Secondly, in comparison with the non-backcrossed $yw^{c}$ strain, *sod3* knockdown was found to be far less pronounced in male $Sod3^{06029}$ flies than females and furthermore, *sod1* and *sod2* were up-regulated in males whereas they were down-regulated in females. Additionally Cu Zn SOD activities were found to be significantly reduced in both sexes of the *sod3* mutant line. This indicates that in fact female $Sod3^{06029}$ flies should be more oxidatively vulnerable and therefore sensitive to

paraquat. This data therefore suggest that females may have alternative mechanisms for coping with paraquat toxicity, which may become activated in response to decreased *sod* expression.

The findings of differential survival patterns with backcrossed and non-backcrossed controls support the notion that in backcrossing the *sod3* line, the *yw* $^{c\text{-}iso}$ control is revealing the effects of unknown genetic modifiers inherited from the *Sod3*$^{06029}$ flies, and these modifiers appear to be functioning to influence lifespan and survival under conditions of intracellular oxidative stress in *Sod3*$^{06029}$ flies. As mentioned previously, genetic modifiers have evolved to stabilise organisms' (in this case *Sod3*$^{06029}$ flies) fitness and survival (Karlin & McGregor 1972). The gene expression and SOD activity data presented earlier imply that these genetic modifications appear to function, at least in part, by increasing *sod1* and *sod2* expression in both sexes and this increased antioxidant status likely causes the elevated paraquat resistance observed. Whilst this explanation seems the most probable, it cannot be ruled out that increased survival under oxidative conditions occurs simply as a fortuitous by-product of the underlying evolved modifications in other unknown genes required for the survival of the *sod3* mutant line in normoxic conditions. Furthermore, the mechanisms by which genetic modifications in *Sod3*$^{06029}$ flies are manifested in reduced oxidative resistance in the *yw* $^{c\text{-}iso}$ line after backcrossing can only be hypothesised. Either the genetic alterations inherited, whilst promoting pro-survival effects in *Sod3*$^{06029}$ flies, function deleteriously in the *yw* $^{c\text{-}iso}$ line, or, in backcrossing, the *yw* $^{c\text{-}iso}$ line is acquiring the detrimental effects, possibly in the form of molecular damage, of having reduced *sod3* levels in the *sod3* mutant line, thus reducing fitness and survival.

*Sod1* homozygous null (*n108*) *Drosophila* have been shown to be highly susceptible to oxidative stress by paraquat exposure, whereas heterozygous (*n108/TM3*) flies retain wild type resistance (Phillips et al. 1989). The same phenotypes have also been observed in homozygous and heterozygous mice (Ho et al. 1998), while in *C. elegans* absence of *sod1* is crucial for maintaining viability under paraquat exposure (Doonan et al. 2008). Here, *sod1* null heterozygous flies were assayed for paraquat sensitivity by sex and whilst no difference in male *n108/TM3* and control lines (*red*) was found, females were observed to be significantly more resistant to paraquat toxicity. In the original *Drosophila* work by Phillips *et al*. it was not stated which sex was assayed in

their paraquat study, thus this observation of elevated paraquat resistance in female *sod1* null heterozygotes may represent a novel finding. The increase in survival in response to paraquat against an isogenic line in *sod1* null heterozygous females may suggest that modifiers are also functioning in this mutant line, however a lack of effect in male flies implies that perhaps females lacking partial *sod1* activity have alternative mechanisms for coping with paraquat toxicity than males. Shown previously was that the *sod* genes are primarily downregulated in both homozygous and heterozygous *n108* lines, therefore such mechanisms may become activated in response to decreased *sod* transcription, as has been proposed in *sod3* mutant females. Therefore, this finding also suggests that SOD1 and SOD3 may share some co-dependency or may interact in some manner.

### 5.5.2 A SOD3 deficiency confers $H_2O_2$ resistance but reduced SOD1 activity does not

Measurements of $H_2O_2$ toxicity in $Sod3^{06029}$ males and females revealed the mutant lines to be significantly more tolerant of $H_2O_2$, irrespective of the control used. The discovery of increased $H_2O_2$ resistance when SOD levels are reduced has been reported elsewhere (Magliaro and Saldanha 2009), however the mechanism by which the partial absence of *sod3* here increases $H_2O_2$ tolerance is unknown. An attractive theory is that, since the product of SOD activity is $H_2O_2$, the enzymes absence in the *sod3* mutant means that the addition of exogenous $H_2O_2$ serves only to restore $H_2O_2$ to physiologically normal levels. This reasoning is questionable however, since both male and female *n108/TM3* flies were found to be no more resistant to $H_2O_2$ than their isogenic controls. Since $H_2O_2$ resistance is conferred in $Sod3^{06029}$ flies, irrespective of the control line tested, the genetic modifiers present in the *sod3* mutant line, whilst they are able to protect against paraquat induced toxicity, appear not function to protect from $H_2O_2$.

These differential oxidative stress survival patterns found in the *sod3* hypomorph line may, however, stem from the different mechanisms by which $H_2O_2$ and paraquat are proposed to transfer toxicity. Whilst $H_2O_2$ is defined as a reactive oxygen species, the compound itself is actually poorly reactive. For instance, no oxidation occurs when

DNA, lipids or most proteins are incubated with $H_2O_2$ (Halliwell & Gutteridge 2007). $H_2O_2$ can, however, inactivate a few proteins, primarily by oxidising those with thiol groups, such a protein phosphatases. This ability, together with the ease with which $H_2O_2$ can permeate biological membranes makes this compound such an important signalling molecule. Despite its poor reactivity, $H_2O_2$ can still be cytotoxic (as has been shown in the results of this chapter), however it is believed that this toxicity is caused by its reaction with iron (in the Fenton reaction) and copper ions, forming the indiscriminately reactive ·OH radical (Halliwell & Gutteridge 2007). Indeed, it appears that it is ·OH that accounts for the majority of the damage caused to DNA in $H_2O_2$ treated cells (Halliwell & Gutteridge 2007). Paraquat, on the other hand, is thought to transfer toxicity through the production of $O_2^{-}\cdot$. Paraquat is believed to undergo a NADH-dependent reduction to form the paraquat radical ($Pa^{+}$) intracellularly at microsomal and /or mitochondrial sites (Farrington et al. 1973;Fukushima et al. 2002). $Pa^{+}$ then rapidly reacts with $O_2$ to form $O_2^{-}\cdot$ and $Pa^{2+}$. Whilst also considered relatively unreactive, $O_2^{-}\cdot$ does appear to be more reactive than $H_2O_2$. For instance, $O_2^{-}\cdot$ is highly reactive in organic solvents, meaning that any $O_2^{-}\cdot$ produced within the hydrophobic interior of biological membranes could be particularly damaging (Halliwell & Gutteridge 2007). Due to a number of sources of $O_2^{-}\cdot$ generation being membrane-bound systems (see chapter 1) it is likely $O_2^{-}\cdot$ is produced in these regions. However, currently there still exists no evidence that $O_2^{-}\cdot$ can cause membrane lipid damage *in vivo*. $O_2^{-}\cdot$ can be highly reactive with a number of proteins, in particular inactivating those containing iron-sulphur clusters at their active site, some of which are important for amino acid biosynthesis (Halliwell & Gutteridge 2007). Other enzymes reported to be inactivated by $O_2^{-}\cdot$ include creatine kinases and calcineurin, a protein involved in signal transduction (Halliwell & Gutteridge 2007). The different mechanisms by which the two oxidant species tested here are cytotoxic and cause molecular damage may explain the differing results found on survival in the mutant strains tested. However, further work is required to elucidate the mechanisms by which the genetic modifiers within the *Sod3*$^{06029}$ line function to promote paraquat resistance.

### 5.5.3 Assays of climbing ability indicate that *sod3* mutant flies have impaired locomotor function at an earlier age

The decline in negative geotaxis (climbing ability) with increasing age is an established facet of *Drosophila* physiology (Ganetzky and Flanagan 1978;Martinez et al. 2007;Toma et al. 2002). Here studies of the climbing ability of $Sod3^{06029}$ flies compared to the $yw^{c\text{-}iso}$ line confirmed these results by revealing both climbing ability and velocity to decrease as a function of age in both lines. Furthermore, a faster decline in climbing performance in females compared to males of both genotypes was found over the course of the experiment. The observation of a faster age dependent decrease in climbing ability in females compared to males has been reported elsewhere (Simon et al. 2006), and although the basis of this sex difference is unknown, functional declines in climbing performance are predicted to be caused by mechanisms of functional senescence rather than by a lack of selection for high performance at older ages due to a decline being seen throughout life (Simon et al. 2006). Comparisons between genotypes showed $Sod3^{06029}$ flies of both sexes to have marginally elevated climbing ability at 2 weeks of age, significantly reduced climbing abilities at 4 weeks of age and slightly reduced climbing function at 6 weeks of age. Other results included the finding of reduced climbing velocity of those flies able to climb at each time point in both sexes of the $Sod3^{06029}$ line compared to the control strain. The observation of a significant decrease in the climbing ability of *sod3* mutants at 4 weeks of age suggests that this fly strain presents an accelerated ageing phenotype in terms of locomotor performance, whilst the permanent reduction in climbing velocity in these ageing flies implies a continuous underlying pathology contributing to this accelerated ageing. As described in the introduction, there is increasing evidence for the role of oxidative stress in the pathology of a number of neurological disorders including FALS, Alzheimer's disease and Parkinson's disease. Studies in mammals have revealed one of the primary functional roles of SOD3 to be protection of the brain from oxidative damage, and SOD3 dysfunction has been shown to be important in memory formation (Levin et al. 1998;Levin et al. 2000), neurological recovery from brain injury (Pineda et al. 2001) and in the pathology amyloid associated diseases (Sakashita et al. 1998). Furthermore, reduced climbing

ability is a feature of *Drosophila* models of Parkinson's disease (Feany and Bender 2000). Since climbing is one of *Drosophila's* most natural motor behaviors, it is possible that this decreased climbing performance in $Sod3^{06029}$ flies results from impaired neurological function due to *sod3* absence, possibly by a mechanism of increased oxidative stress. Interestingly, while climbing velocity was reduced at young age (2 weeks) compared to controls, significantly so in females, the ability of flies to climb was in fact enhanced in the *sod3* mutant line. This suggests that although disturbed *sod3* expression impairs climbing performance throughout life, in early life the deleterious effects are insufficient to prevent flies climbing, and in fact there maybe compensatory mechanisms at work to promote fitness and performance earlier in life in $Sod3^{06029}$ flies.

It should be noted that $Sod3^{06029}$ line was only compared to the backcrossed $yw^{c\text{-}iso}$ controls in these experiments. Thus, without comparable studies using the $yw^{c}$ line, one cannot make any conclusions about the function of heritable modifiers with respect locomotor geotaxis function.

# CHAPTER 6

# 6. General discussion

Having first been discovered approximately 10 years after the two intracellular SODs (SOD1 and SOD2), (Marklund et al. 1982) SOD3 is the least well characterised of the SOD family. This lag in functional characterisation has been further exacerbated by the lack of short-lived invertebrate models in which to study the protein. The identification of an extracellular *sod* gene (*sod3*) in insects (Parker et al. 2004a) therefore represented an exciting development in the oxidative stress and ageing fields of biology. Whilst considerable evidence exists highlighting the importance of the cytoplasmic (SOD1) and mitochondrial (SOD2) SOD isoforms in maintaining oxidative protection and survival in various model species (described in Chapter 1), the absence of SOD3's identification in short lived insects models meant that comparably little work has been carried to characterise this protein in mammalian systems and furthermore, to date, no (published) work has been carried out to assess it role within insects. Therefore, the aim of this thesis was to present the novel work carried out to characterise some of the genetic and functional features of the *sod3* gene in a *Drosophila* model system.

## 6.1 Synopsis of results and primary conclusions

Through cDNA cloning the presence of two splice variants of the *sod3* gene, termed *sod3v1* and *sod3v2*, have been confirmed in *Drosophila* (Chapter 2). This finding is analogous to *C. elegans*, where alternative splicing of the extracellular *sod* gene was found to encode membrane bound and extracellular forms of the SOD protein (Fujii et al. 1998), but distinct from mammals, where SOD3 localisation depends upon electrostatic interactions of the C-terminal region of the protein with heparin-sulfate present on cell surfaces and the extracellular matrix (Karlsson et al. 1988).

*Sod3* gene expression profiling (Chapter 3) and SOD activity measurements (Chapter 4) in a *sod3* hypomorph mutant line ($Sod3^{06029}$), generated by transposon insertion,

revealed some interesting findings. Firstly, excision of the *P*-element transposon in the *sod3* hypomorph line was found not only to restore *sod3* gene expression, but was also coupled to increased *sod1* and *sod2* expression in both male and female adult flies. Secondly, Cu Zn SOD activity measurements of the *sod3* hypomorph line showed this strain to have more significantly reduced activity than expected, whilst knocking out the *sod1* gene in another fly strain (*n108*) was found to almost completely abolish all Cu Zn SOD activity. These findings suggest that SOD1 and SOD3 may be co-dependent for maintaining Cu Zn SOD activity, either by transcriptional regulation or by interacting, possibly by forming heterodimers or heterotetramers. The proposal of a mutual dependence becomes more reasonable due to the findings of accumulated intracellular pools of SOD3 in mammalian models (Fattman et al. 2001;Loenders et al. 1998;Ookawara et al. 2002). Furthermore, sequencing of the *Drosophila sod3* gene revealed an ATG site in both variants which corresponds with the *sod1* gene, and is also found to be conserved in mice (see figure 1 in (Parker et al. 2004a)), and this could act as an alternative start site for translational initiation leading to intracellular targeting of *sod3*. A mutual dependence for functional activity might explain one of the key questions surrounding *sod3* in *Drosophila*, that being why did the gene remain undiscovered for so long despite the magnitude of research into the SOD isoforms in this model (discussed in Chapter 1)? The complete absence of SOD activity found in the original *sod1* null research by Phillips *et al*. (1989) would thus be explained by this co-dependency.

Studies of *sod* gene expression, SOD activity and also functional characterisation of $Sod3^{06029}$ flies (Chapter 5) highlights the influence that genetic background and modifiers may play when assessing *sod3's* role. In this study three different control lines were used to assay the $Sod3^{06029}$ mutant: an *Oregon R* line (*WT*), a non-backcrossed *yellow white* line ($yw^{c}$) and a *yellow white* line backcrossed with the $Sod3^{06029}$ line through one generation ($yw^{c\text{-}iso}$). The key findings of $Sod3^{06029}$ flies compared to non-backcrossed controls ($yw^{c}$) were:

i) a significant knockdown of *sod3* gene expression
ii) minimal changes in *sod1* and *sod2* gene expression
iii) a significant decrease in Cu Zn SOD activity

iv) a significant decrease in paraquat resistance in male flies (no change in females)

The key findings of *Sod3*$^{06029}$ flies compared to backcrossed controls (*yw* $^{c\text{-}iso}$) were:

i) a minimal downregulation of *sod3* gene expression
ii) upregulated *sod1* and *sod2* gene expression (significant in males)
iii) a significant increase in Cu Zn SOD activity
iv) a significant increase in paraquat resistance
v) an increase in age-related climbing degeneration

These variations in results found after just one generation of backcrossing have been discussed in the respective chapters and serve to highlight the role that genetic modifiers in the fly backgrounds may play in controlling heritable and phenotypic traits. Although recently studies in the oxidative stress fields of biology have been published in which the genetic background of the *Drosophila* strains tested was ignored (Taghli-Lamallem et al. 2008;Walker et al. 2006), the importance of backcrossing repeatedly into control lines to limit background effects has been acknowledged (Dworkin et al. 2009;Toivonen et al. 2007). In the oxidative stress and ageing fields of biology currently the standard practice is to backcross through a minimum of six generations, leading to 98% homogenisation of the backgrounds (Poon et al. 2010;Slack et al. 2010). Therefore one of the main limitations of this study is the lack of adequate backcrossing. The results discussed demonstrate clear differences in genetic and functional outputs when flies were backcrossed by just one generation, thus additional backcrossing should be carried out to assess how *sod3* deficiency traits might change further upon background homogenisation. Moreover, in addition to backcrossing *Sod3*$^{06029}$ into the *yw* $^{c}$ line, it would also be useful to outcross the *Sod3*$^{06029}$ line to a number of wild caught populations. Inbred laboratory strains are typically short lived and can propagate deleterious alleles meaning that over-expression of longevity extending genes, for example, may serve only to restore lifespan to its natural level (Spencer et al. 2003). Assessing the function of *sod3* in wild caught backgrounds should therefore provide information about the gene which is not influenced by adaptation to the artificial laboratory environment

Discussed below is some of the preliminary work undertaken and future work to be carried out as a result of the findings of this report.

## 6.2 Preliminary and future work

Several questions have been raised off the back of the current study. Firstly, what effect will further backcrossing of the $Sod3^{06029}$ line into the $yw^{c}$ background have on *sod* gene expression, SOD activity and oxidative stress resistance? To assess this, backcrossing of the $Sod3^{06029}$ strain into the $yw^{c}$ line has been started, which will continue for a minimum of six generations to homogenise the backgrounds. After backcrossing, as well as repeating the experiments detailed in this report, *sod3's* influence on lifespan can be assessed in longevity assays.

A second question concerns the localisation of the SOD proteins. Although the scope of this study did not extend to determine protein localisation, sequence analysis suggests that the SOD3 enzymes will localise extracellularly (Landis & Tower 2005;Parker et al. 2004a). In absence of a verified *Drosophila* SOD3 antibody, streptavidin tagged SOD3v1 and SOD3v2 (along with SOD1) fusion constructs have been created for expression in HEK293 human embryonic kidney cells, with western blots being carried out on the cellular and extracellular fractions to preliminarily confirm protein location. Furthermore, available purified recombinant SOD3 proteins could also be used as antigens to synthesis more specific polyclonal *Drosophila* antibodies to SOD3.

A further finding of the work presented in this thesis is the suggestion that SOD1 and SOD3 my share an interdependence for *in vivo* activity. In preparation to test this, bait and prey constructs for each of SOD1, SOD3v1 and SOD3v2 have been generated which can be tested for interactions by two-hybrid analysis (Chien et al. 1991;Fields and Song 1989).

Described below are the methods used and preliminary results of the work described.

## 6.3 Materials and methods

### 6.3.1 Backcrossing of the *Sod3*$^{06029}$ line into the *yw* $^{c}$ background

The *Sod3*$^{06029}$ line is to be backcrossed into the *yw* $^{c}$ line for a minimum of six generations according to the crossing scheme shown in Figure 6.1. Firstly, approximately 30 virgin female *yw* $^{c}$ flies are to be mated with 25 – 30 male *Sod3*$^{06029}$ flies. Males and females of the resulting F1 generation, heterozygous for the *P*-element insertion (selected for by the $w^{+}$ phenotype), will then be crossed with *yw* $^{c}$ flies of the opposite sex to complete the first generation of backcrossing ((1) in Figure 6.1.).

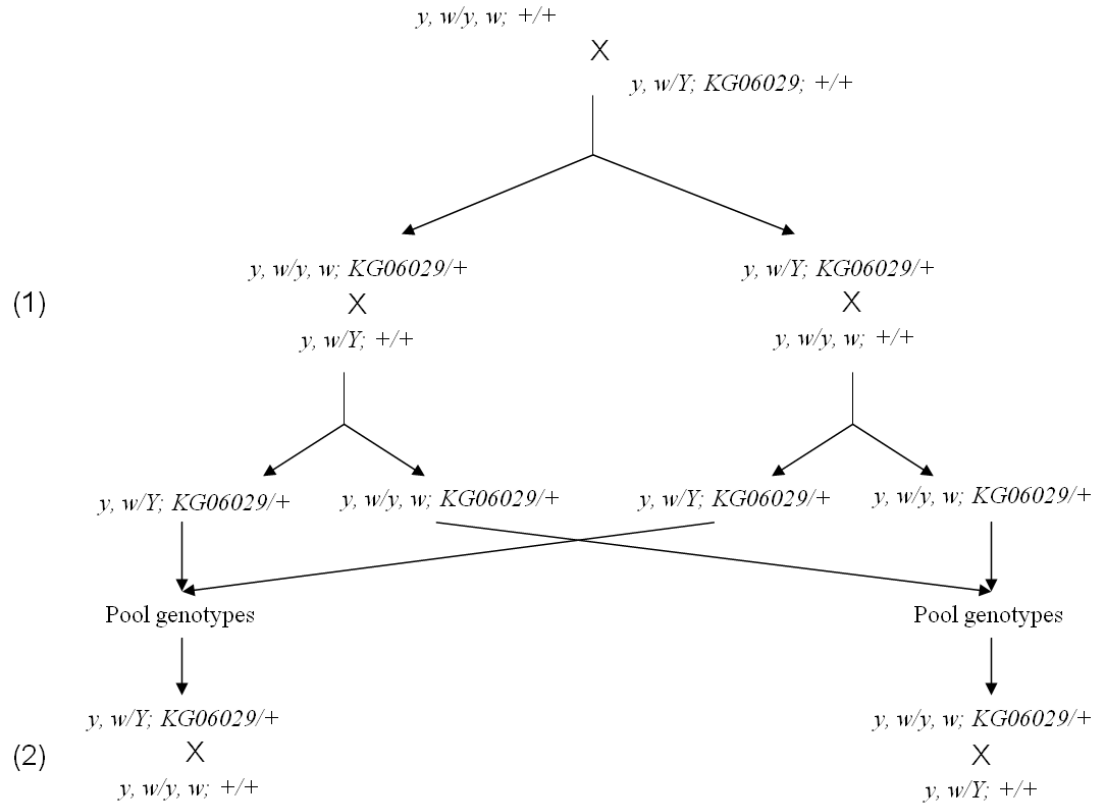


**Figure 6.1. The crossing scheme being carried out to backcross the *Sod3*$^{06029}$ line into the *yw* $^{c}$ background.** *Sod3*$^{06029}$ flies will be backcrossed through six generations, with (1) representing the first generation cross and (2) being the second generation.

Heterozygous males and females from the F1 cross will be pooled by sex and crossed with the *yw* $^{c}$ stock to commence the second generation of backcrossing ((2) in Figure 6.1.). This procedure will be repeated through a minimum of six generations. To recover homozygous *Sod3*$^{06029}$ flies after backcrossing, brother and sister crosses (20 – 30 flies of each sex) of heterozygous *P*-element lines will be mated after pooling by sex. Twenty single pair matings of resulting male and virgin female flies with red eyes (carrying the *P*-element insert) and wild type bodies will then be made and those progeny where only red eyed and wild type bodied flies resulted will be crossed together to recover the *Sod3*$^{06029}$ strain. PCR with primers that bind internally to the *P*-element (Table 3.3) should be carried out on *Sod3*$^{06029}$ flies after backcrossing to ensure the *P*-element has been retained. The original and backcrossed stocks should be maintained in large populations in culture bottles to minimise the effect of inbreeding and genetic drift.

## 6.3.2 Generation of SOD1, SOD3v1 and SOD3v2 bait and prey plasmids for detecting protein-protein interactions using the two-hybrid system

### 6.3.2.1 Cloning into pCR®8/GW/TOPO® entry vectors

First strand cDNA was synthesised from 0.565µg/µL adult poly($A^+$) RNA (Clontech) according to the methods in Chapter 3 Section 3.3.9.

PCR reactions were performed using the primers listed in Table 6.1 in the combinations detailed in Table 6.2, as follows: 1µL genomic DNA was mixed with 2µL 10X PCR Buffer (Qiagen), 1µL 10µM primer 1, 1µL 10µM primer 2, 0.4µL 10mM dNTP mix (Qiagen), 0.4µL 25mM $MgCl_2$ (Qiagen), 0.1µL 5U/µL Taq DNA polymerase (Qiagen) and made up to 20µL with nuclease-free $H_2O$. The reaction was mixed, spun briefly and then subjected to PCR using the DNA Engine tetrad 2® thermocycler (MJ Research). Thermocycling conditions used are shown in Table 6.3.

**Table 6.1. Primer sequences for amplification of adult cDNA.**

| Primer name | Primer sequences |
|---|---|
| F SOD1 GW | 5'-ATCACCATGGTGGTTAAAGCTG-3' |
| F SOD3 GW | 5'-ACCACCATGCAATATCTTGTTGTTAGCC-3' |
| R SOD1 Y2 | 5'-CGACATCGGAATAGATTATCGC-3' |
| R SOD3v1 Y2 | 5'-TGGCTGACACGTTGGAAG-3' |
| R SOD3v2 Y2 | 5'-CCACATGCGTGCATTCGAT-3' |

**Table 6.2. PCR product sizes with specific primer combinations.**

| Primer combinations used | Predicted PCR product size (bp) |
|---|---|
| F SOD1 GW + R SOD1 Y2 | 489 |
| F SOD3 GW + R SOD3v1 Y2 | 572 |
| F SOD3 GW + R SOD3v2 Y2 | 698 |

**Table 6.3. Thermocycling conditions for amplification of adult cDNA with primers listed in Table 1.**

| Steps | Incubation time | Temperature (°C) |
|---|---|---|
| **1. Hot start** | - | 94 |
| **2. Initial denaturation** | 3 mins | 94 |
| **3. 3 step cycling** | - | - |
| Denaturation | 30 sec | 94 |
| Annealing | 30 sec | 60 |
| Extension | 30 sec | 72 |
| **4. 34 more cycles to step 3** | - | - |
| **5. Final extension** | 7 mins | 72 |

PCR products were revealed on 1-2% (w/v) agarose gels according the methods in section 2.3.6 and were subsequently purified and quantified according to the protocols of section 2.3.7.

The purified DNA was subcloned by ligation into pCR®8/GW/TOPO® entry vectors (Figure 6.2.) (Invitrogen), to allow for downstream DNA insert transfer via the Gateway® system, as follows: 2µL DNA was mixed gently with 1µL salt solution (Invitrogen), 0.4µL pCR®8/GW/TOPO® vector and made up to 6µL with nuclease-free $H_2O$. Reactions were incubated for approximately 5 mins at room temperature and transferred to ice. One shot® TOP10 competent *E. coli* cells (≥1 x $10^9$ cfu/µg DNA) (Invitrogen) were transformed with the ligated vectors, as follows: 2µL of cloning reaction was mixed with 25µL of TOP10 cells and incubated on ice for 5 – 30 mins. The cells were heat shocked at 42°C for 30 secs and immediately placed back on ice. Two hundred and fifty microlitres of SOC medium (Invitrogen) was added and

the reactions were incubated at 37°C for 1 hour with constant shaking. Fifty microlitres of each transformation reaction was transferred to pre-made, duplicate LBA plates, supplemented with 100µg/mL spectinomycin (Sigma) (LBA/spec). Plates were incubated overnight at 37°C, with colonies appearing presumed to contain DNA inserts.

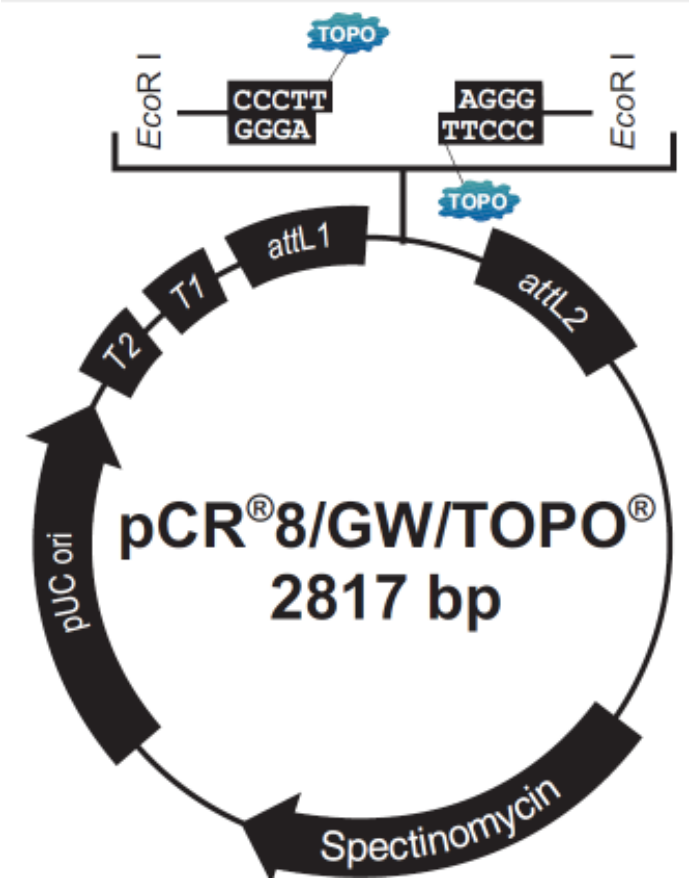


**Figure 6.2. pCR®8/GW/TOPO® entry vector map.** Image taken from the Invitrogen pCR®8/GW/TOPO® TA Cloning® Kit technical manual.

Selected single colonies were cultured by streaking onto a new LBA/spec plate and incubated overnight at 37°C. PCR reactions were run of each colony to confirm the presence of inserts. After overnight incubation colonies were cultured in 4mL LB medium with spectinomycin added to a final concentration of 100µg/mL. The bacterial cells were harvested by centrifugation at 10,000 rpm for 3 mins at room temperature. The DNA plasmids were purified according to the QIAprep spin mini prep protocol (Qiagen). One microlitre of the resulting purified plasmid DNA was quantified on the NanoDrop spectrophotometer and PCRs were run again to confirm

the presence of correct inserts following purification. DNA inserts were sequenced by Microsynth AG, Switzerland. Thirty microlitres of purified plasmid DNA was supplied at a concentration of 100mg/μL and plasmids were sequenced in both directions from the M13 forward and reverse priming sites present on the pCR®8/GW/TOPO® entry vector.

### 6.3.2.2 Creating bait and prey plasmids by LR recombination

Bait (pDEST™32) (Figure 6.3A.) and prey (pDEST™22) (Figure 6.3B.) plasmids for each pCR®8/GW/TOPO® clone (SOD1, SOD3v1 and SOD3v2) were constructed according to the ProQuest™ Two Hybrid System manufacturers instructions (Invitrogen). Reactions were prepared as detailed in Table 6.4.

**Table 6.4. Reaction components for generation of bait and prey plasmids.**

| Component | Forming Bait Plasmid | | | Forming Prey Plasmid | | |
|---|---|---|---|---|---|---|
| | Samples (μL) | | | Samples (μL) | | |
| | SOD1 | SOD3v1 | SOD3v2 | SOD1 | SOD3v1 | SOD3v2 |
| pCR®8/GW/TOPO® clone for bait (130ng/reaction) | 0.69 | 0.66 | 0.96 | - | - | - |
| pCR®8/GW/TOPO® clone for prey (130ng/reaction) | - | - | - | 0.69 | 0.66 | 0.96 |
| PDEST™32 (150ng/uL) | 1 | 1 | 1 | - | - | - |
| PDEST™22 (150ng/uL) | - | - | - | 1 | 1 | 1 |
| TE buffer, pH 8.0 | 6.31 | 6.34 | 6.04 | 6.31 | 6.34 | 6.04 |

Two microlitres of LR Clonase™ enzyme mix was added to each reaction which were subsequently incubated at 25°C for 1 hour. One microlitre of proteinase K solution was added and reactions were incubated for a further 10 mins at 37°C.

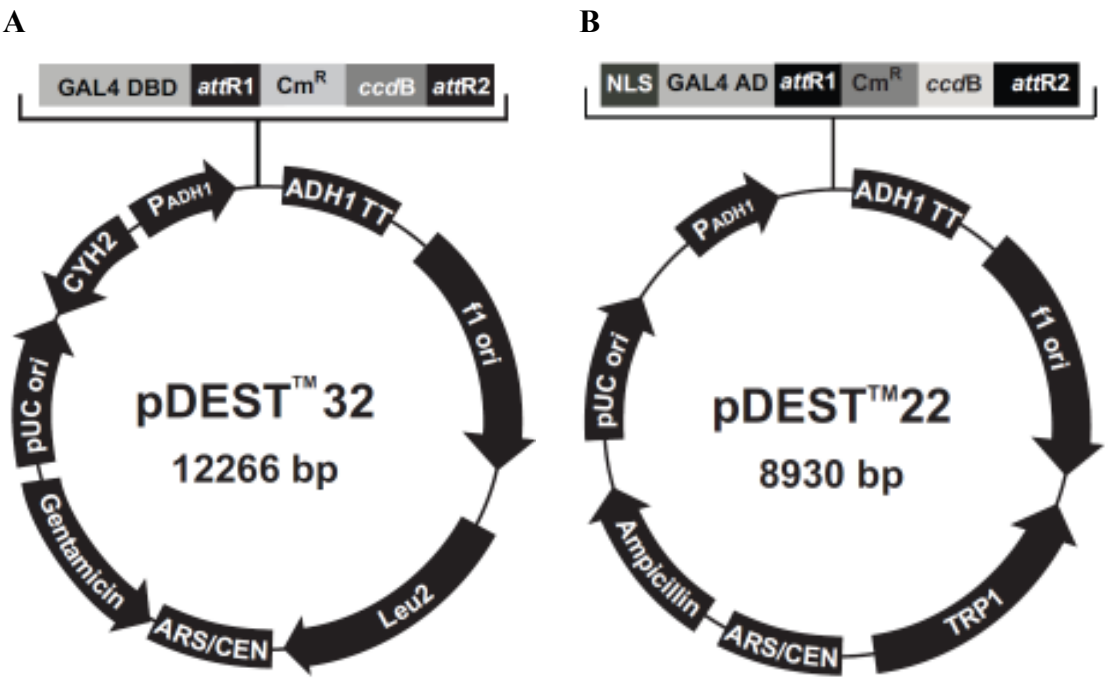


**Figure 6.3. (A) pDEST™32 (bait) and (B) pDEST™22 (prey) vector maps.**
Images taken from the Invitrogen ProQuest™ Two Hybrid System technical manual.

One shot® TOP10 competent *E. coli* cells were transformed with each bait and prey construct as described above. Fifty microlitres of each transformation reaction was transferred to pre-made, duplicate LBA plates, supplemented with either 10µg/mL gentamicin (Sigma) (LBA/gent) for bait plamids, or 100µg/mL ampicillin (Sigma (LBA/amp) for prey plasmids. Plates were incubated at 37°C over night. Selected single colonies were cultured in 4mL LB medium (plus appropriate antibiotic), harvested and the DNA plasmids were purified as described previously. One microlitre of the resulting purified plasmid DNA was quantified on the NanoDrop spectrophotometer.

PCR reactions were performed on each prey and bait construct as described above, with primers annealing to regions of the respective plasmid shown in Table 6.5. DNA inserts were sequenced by Microsynth AG, Switzerland as described previously, with the sequencing primers being those listed in Table 6.5. After confirmation of correct DNA insertion by sequencing, the original colonies were re-streaked onto appropriate LBA/gent or LBA/amp plates and incubated at 37°C over night. A single colony of each construct was subsequently isolated and used to inoculate 2mL of LB medium containing the appropriate antibiotic. Each culture was incubated at 37°C for 12 hours

with constant shaking. After incubation, 0.85mL of culture was mixed with 0.15mL of sterile glycerol (Sigma) and transferred to a cryovial for long term storage at -80°C.

**Table 6.5. Plasmid specific and sequencing primers.**

| Primer name | Primer sequences |
|---|---|
| Bait F | 5'-AACCGAAGTGCGCCAAGTGTCTG-3' |
| Prey F | 5'-TATAACGCGTTTGGAATCACT-3' |
| B&P R | 5'-AGCCGACAACCTTGATTGGAGAC-3' |

## 6.3.3 SOD1, SOD3v1 and SOD3v2 expression in HEK293 cells

### 6.3.3.1 Cloning into pCR®8/GW/TOPO® entry vectors

First strand cDNA was synthesised from 0.565µg/µL adult poly($A^+$) RNA (Clontech) according to section 3.3.9. PCRs were carried out according to the methods of section 6.2.1.2.1 of this chapter using the primers listed in Table 6.6. The predicted sizes of the PCR products for the primer pairs used are listed in Table 6.7. PCR products were cloned into pCR®8/GW/TOPO® entry vectors, purified and sequenced as described previously.

**Table 6.6. Primer sequences for amplification of adult cDNA.**

| Primer name | Primer sequences |
|---|---|
| F SOD1 GW | 5'-ATCACCATGGTGGTTAAAGCTG-3' |
| F SOD3 GW | 5'-ACCACCATGCAATATCTTGTTGTTAGCC-3' |
| R SOD1 GW-1 | 5'-GACCTTGGCAATGCCAAT-3' |
| R SOD3v1 GW | 5'-CTTGATGCCAATAACACCACAG-3' |
| R SOD3v2 GW | 5'-GTCAAGGCTGCGGGCCATGAT-3' |

**Table 6.7. PCR product sizes with specific primer combinations.**

| Primer combinations used | Predicted PCR product size (bp) |
|---|---|
| F SOD1 GW + R SOD1 GW-1 | 464 |
| F SOD3 GW + R SOD3v1 GW | 545 |
| F SOD3 GW + R SOD3v2 GW | 653 |

### 6.3.3.2 Creation of SOD1, SOD3v1 and SOD3v2 expression constructs

Each pCR®8/GW/TOPO® clone (SOD1, SOD3v1 and SOD3v2) was subjected to PCR with the primers listed in Table 6.8. PCR reaction volumes were the same as those described in section 6.2.1.2.1 of this chapter, and thermocycling conditions used are listed in Table 6.9.

**Table 6.8. Primer sequences for PCRs of pCR®8/GW/TOPO® clones.**

| Primer name | Primer sequences |
|---|---|
| F SOD1 inc H111 | 5'-AATTAAGCTTTCACCATGGTGGTTAAAGC-3' |
| F SOD3v1&2 inc H111 | 5'-AATTAAGCTTCCACCATGATGCAATATCTTG TTGT-3' |
| R SOD1 inc BH1 | 5'-AATTGGATCCGACCTTGGCAATGCCAATA-3' |
| R SOD3v1 inc BH1 | 5'-ATTTGGATCCCTTGATGCCAATAACACCA-3' |
| R SOD3v2 inc BH1 | 5'-TAATTGGATCCGTCAAGGCTGCGGGCCAT-3' |

**Table 6.9. Thermocycling conditions for PCRs of pCR®8/GW/TOPO® clones.**

| Steps | Incubation time | Temperature (°C) |
|---|---|---|
| **1. Hot start** | - | 94 |
| **2. Initial denaturation** | 3 mins | 94 |
| **3. 3 step cycling** | - | - |
| Denaturation | 30 sec | 94 |
| Annealing | 30 sec | 67 |
| Extension | 30 sec | 72 |
| **4. 34 more cycles to step 3** | - | - |
| **5. Final extension** | 7 mins | 72 |

PCR products were gel extracted, purified and quantified as detailed previously.

Products were subcloned into the pDRIVE cloning vector (Qiagen) (Figure 6.4.) as follows: 1µL pDRIVE vector (50ng/µL) was combined with 3µL PCR product, 5µL 2X ligation master mix (Qiagen) and 1µL nuclease-free $H_2O$. Mixtures were incubated for 2 hours at 8°C and subsequently one shot® TOP10 cells were transformed as described above. Cultures were plated on duplicate LBA/amp/IPTG/X-Gal plates and incubated at 37°C overnight. Single colonies were selected and subjected to PCR to confirm the presence of insets. Subsequently colonies were cultured in 4mL LB medium (plus appropriate antibiotic), harvested and the DNA plasmids were purified as described previously. One microlitre of the

resulting purified plasmid DNA was quantified on the NanoDrop spectrophotometer. Plasmid DNA inserts were sequenced by Microsynth AG, Switzerland, in both directions form the T7 and SP6 promoters as described previously.

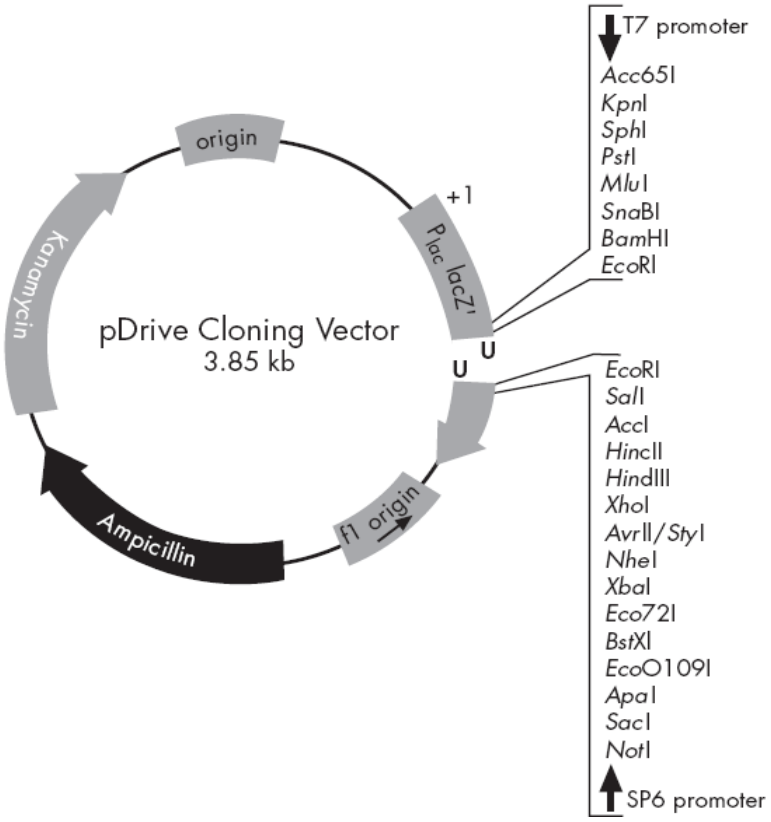


**Figure 6.4. pDRIVE cloning vector map.** Image taken from the Qiagen PCR Cloning Plus Kit manual.

Four micrograms of each pDRIVE clone (SOD1, SOD3v1 and SOD3v2) and the V152 expression vector (a kind gift from Dr Neil Smyth, University of Southampton) (Figure 6.5.), were linearised by restriction digests according to Table 6.10. Restriction digests were incubated for a minimum of 1 hour at 37°C, after which 1.5µL of CIP (Ambion) was added and digests were re-incubated at 37°C for a further hour. Five microlitres of each restriction digest reaction were run on agarose gels, with appropriate products being extracted, purified and quantified as described previously.

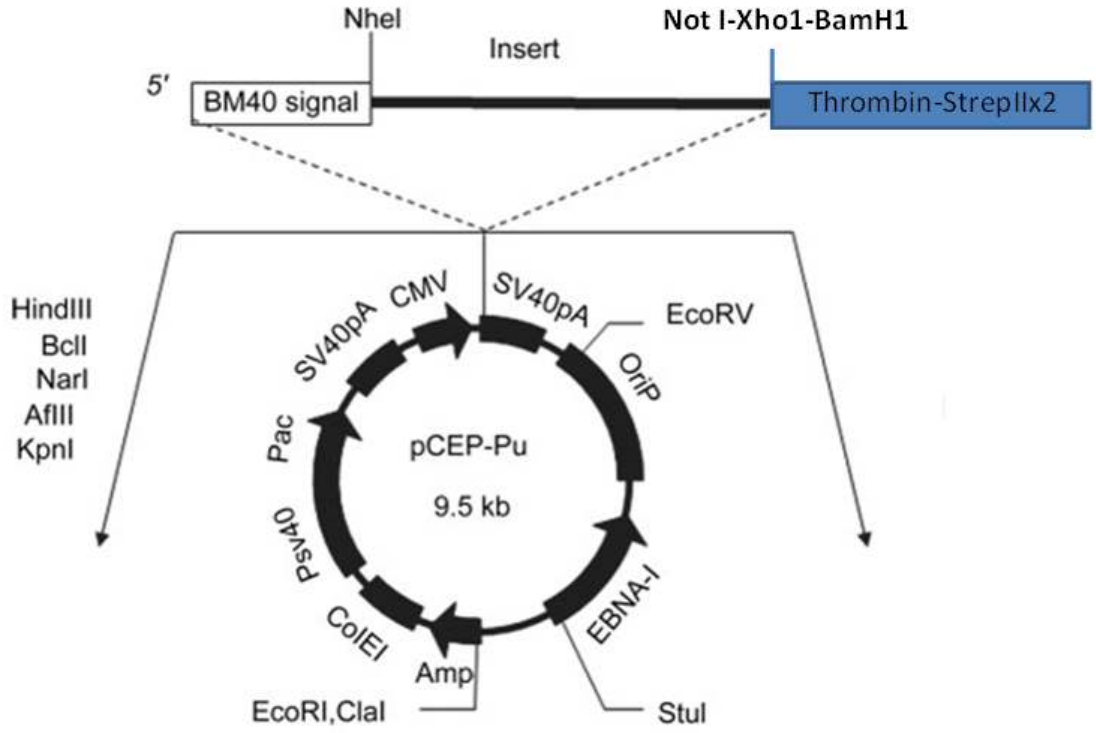


**Figure 6.5. V152 expression vector map.** The vector was a kind gift from Dr N Smyth (University of Southampton) and contains a cDNA insert site flanked by a BM40 signal peptide sequence and a thrombin sequence attached to two *Strep*-tag II.

**Table 6.10. Components and reaction volumes of restriction digests.**

| Component | Samples (µL) | | | |
|---|---|---|---|---|
| | SOD1 in pDRIVE | SOD3v1 in pDRIVE | SOD3v2 in pDRIVE | V152 |
| DNA | 12.74 | 13.44 | 14.41 | - |
| V152 (0.1µg/mL) | - | - | - | 20 |
| 10X Buffer E | 4 | 4 | 4 | 3 |
| Bam H1 | 1 | 1 | 1 | 0.75 |
| Hind III | 1 | 1 | 1 | 0.75 |
| Nuclease-free $H_2O$ | 21.26 | 20.56 | 19.59 | 5.5 |

Approximately 50ng of each DNA insert digested from each pDRIVE plasmid was ligated with approximately 20ng of the linear V152 expression vector according to Table 6.11. Ligation reactions were incubated overnight at 12°C.

**Table 6.11. DNA/V152 vector ligation reaction volumes.**

| Component | Samples (µL) | | |
|---|---|---|---|
| | SOD1 | SOD3v1 | SOD3v2 |
| Linear V152 | 1.17 | 1.17 | 1.17 |
| DNA insert | 5.16 | 3.98 | 3.34 |
| T4 ligase | 0.5 | 0.5 | 0.5 |
| 10X Buffer | 2 | 2 | 2 |
| Nuclease-free $H_2O$ | 11.17 | 12.35 | 12.99 |

One shot® TOP10 cells were transformed with each ligation reaction as described previously and cultures were plated on duplicate LBA/amp plates. After overnight incubation at 37°C, single colonies were selected, cultured in 4mL LB medium (plus appropriate antibiotic), harvested and the DNA plasmids were purified as described previously. One microlitre of the resulting purified plasmid DNA was quantified on the NanoDrop spectrophotometer. Inserts were checked for correct size by digesting 3µg of plasmid DNA according to Table 6.10, incubating reactions at 37°C for 1 hour and then running 5µL of each restriction digest on agarose gels. Resulting purified expression constructs are termed: SOD1-*StrepII*, SOD3v1-*StrepII* and SOD3v2-*StrepII*. Cultures of correct SOD-*StrepII* constructs were grown in 2mL of LB medium (plus antibiotic) and mixed with glycerol, as described previously, for long term storage at -80°C.

### 6.3.4 Tissue culture

HEK293 cells in DMEM media (Invitrogen) (supplemented with 10% heat inactivated fetal bovine serum (Invitrogen), 2mM L-glutamine (Invitrogen), 100U/mL penicillin with 100µg/mL streptomycin (Invitrogen)) were supplied in a 90 mm tissue culture disc (Greiner Bio One) by Dr. Neil Smyth (University of Southampton). Cells were split as follows: supplemented DMEM medium was removed by aspiration and cells were gently washed twice with 5mL of PBS (Invitrogen). Six hundred microlitres of 0.05% trypsin/EDTA (Invitrogen) was added and the plate was incubated for 1 min at 37°C. Cells were checked for dissociation from the bottom of the plate and 10mL of supplemented DMEM was subsequently added. Cells were transferred to a 15mL falcon tube and spun at 1,500 rpm for 5 mins at room temperature. The supernatant was discarded and the cell pellet was resuspended in 1mL of supplemented DMEM.

Five hundred microlitres of cell suspension was added to 20mL of supplemented DMEM in a new tissue culture disc, which was subdivided equally into each well of a 12 well tissue culture plate (Greiner One Bio). The plate was incubated at 37°C with 95% humidity and 5% $CO_2$ for 24 hours.

After 24 hours, cells were transfected with each SOD-*StrepII* expression construct as follows: 100µL of fetal bovine serum-free supplemented DMEM medium was combined with 4µL of FuGENE6 transfection reagent (Roche) and 2µg of DNA construct in a microtube, gently mixed and incubated at room temperature for 30 mins. Fifty microlitres of each transfection mixture was added to a well of cells in duplicate. The plate was gently agitated and incubated at 37°C with 95% humidity and 5% $CO_2$.

Cells were allowed to grow for 2-3 days and were subsequently split as described above, with one of each duplicate construct being transferred to fresh supplemented DMEM media and the other being transferred to serum free supplemented DMEM. Cells transferred to supplemented DMEM were maintained and assessed for puromycin resistance throughout generations to establish stable SOD1, SOD3v1 and SOD3v2 construct expression (carried out by Dr. Neil Smyth). Cells transferred to serum free DMEM were allowed to grow for 2-3 days after which culture medium and cell fractions were isolated for determination of transiently transfected construct expression as detailed below. For culture medium, media was removed from the culture plate by pipette, transferred to a microtube and centrifuged at 1,500 rpm for 3 mins, with the supernatant being retained and stored at -20°C for subsequent western blots. For the cell fraction, cells were pipetted from the culture plate and lysed by mixing with an equal volume of 2X sample buffer. Cell lysates were stored at -20°C and sonicated prior to use in western blots.

### 6.3.5 Ethanol precipitation

Protein samples from the culture medium were concentrated by standard ethanol precipitation techniques as follows: one volume of protein sample was mixed with nine volumes of ice cold 100% ethanol (Sigma) and incubated at -20°C for a

minimum of 1 hour. The protein/ethanol mixture was centrifuged at 15,000 x g at 4°C for 15 mins and the supernatant was discarded. The protein pellet was resuspended in ice cold 90% ethanol, vortexed and re-pelleted after centrifugation at 15,000 x g at 4°C for 15 mins. The supernatant was discarded and the protein pellet was allowed to air dry. The pellet was resuspended in a minimal volume of 1X sample buffer, stored at -20°C and sonicated prior to use in western blots.

### 6.3.6 Western Blots

Western blots of the cell lysates, culture medium and concentrated culture mediums of each SOD-*StrepII* construct were carried out as described in section 4.3.10. Blots were probed with a 1:1000 - 1:10,000 dilution of *Strep*MAB-classic (IBA, Germany) anti *Strep*-tag II® monoclonal primary antibody, followed by a 1:10,000 dilution of an Alexa Fluor 680 anti-mouse secondary antibody (Invitrogen). Western blots visualised using the Li-Cor Odyssey Infrared Imaging System (Li-Cor Biosciences).

## 6.4 Preliminary results

### 6.4.1 Backcrosses of the *Sod3$^{06029}$* line into the *yw $^{c}$* background

Backcrosses of the *Sod3$^{06029}$* line have been initiated and at the time of writing the third generation of backcrossing is underway.

### 6.4.2 Sequencing of bait and prey plasmids

Sequenced bait and prey plasmids are listed in the appendices detailed in Table 6.12.

**Table 6.12. Appendices list for bait and prey constructs.**

| Construct sequenced | Appendix number |
|---|---|
| SOD1 bait | 4 |
| SOD1 prey | 5 |
| SOD3v1 bait | 6 |
| SOD3v1 prey | 7 |
| SOD3v2 bait | 8 |
| SOD3v2 prey | 9 |

### 6.4.3 Expression of SOD-*StrepII* constructs in HEK293 cells

Initially transiently transfected cells and culture medium were assessed for expression of each construct (Figure 6.6). As expected, SOD1-*StrepII* levels were found to be high in the cell fraction but undetectable in the culture medium. SOD3v1-*StrepII* was also detected in the cell fraction, although at considerably lower levels than SOD1-*StrepII*, but was not detected in the extracellular material, while SOD3v2-*StrepII* was not detected in either the cellular component or the culture medium.

Stable SOD1-*StrepII* and SOD3v1-*StrepII* construct HEK293 cells lines were established, however cells could not be propagated that incorporated SOD3v2-*StrepII* (4 individual SOD3v2-*StrepII* constructs were transfected). Western blots of the stable construct lines (Figure 6.7) again showed SOD1-*StrepII* to be found only in the cellular fraction, whilst SOD3v1-*StrepII* was found to be highly expressed within cells, but detectable levels were also found in the concentrated extracellular medium.

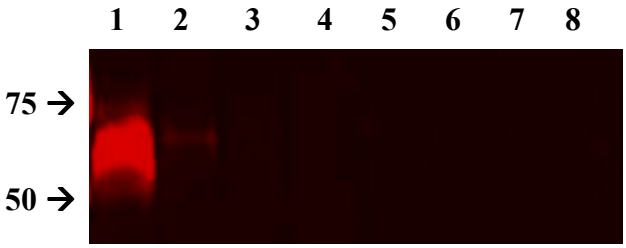


**Figure 6.6. Western blot (10% gel) probing transiently transfected cell fractions with 1:1000 *Strep*MAB-classic primary antibody.** Primary antibody probed against SOD1-*StrepII* cellular fraction (lane 1); SOD3v1-*StrepII* cellular fraction (lane2); SOD3v2-*StrepII* cellular fraction (lane 3); untransfected cells cellular fraction (lane 4); SOD1-*StrepII* media fraction (lane 5); SOD3v1-*StrepII* media fraction (lane 6); SOD3v2-*StrepII* media fraction (lane 7); untransfected cells media fraction (lane 8). Blocking solution = 3% BSA tPBS and secondary antibody = Alexa Fluor 780 at 1:10,000 dilution.

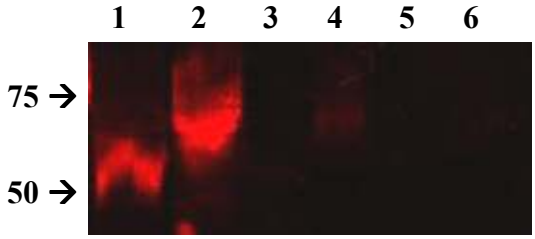


**Figure 6.7. Western blot (10% gel) probing stably transfected cell fractions with 1:5000 *Strep*MAB-classic primary antibody.** Primary antibody probed against SOD1-*StrepII* cellular fraction (lane 1); SOD3v1-*StrepII* cellular fraction (lane2); SOD1-*StrepII* media fraction (post ethanol precipitation) (lane 3); SOD3v1-*StrepII* media fraction (post ethanol precipitation) (lane 4); SOD1-*StrepII* media fraction (unconcentrated) (lane 5); SOD3v1-*StrepII* media fraction (unconcentrated) (lane 6). Blocking solution = 3% BSA tPBS and secondary antibody = Alexa Fluor 780 at 1:10,000 dilution.

## 6.5 Discussion of preliminary work

### 6.5.1 Expression of SOD-*StrepII* constructs in HEK293 cells

SOD expression constructs were assayed by western blots of both transiently transfected cells and stable lines. Interestingly, stable SOD3v2 construct in HEK293

cell lines were not viable, suggesting that either the construct was toxic or that genomic construct integration was occurring at sites critical for cell survival. It seems, however, that lethal genomic insertion is unlikely since transfection was tried on multiple occasions, and additionally with four individual constructs. The basis of SOD3v2 construct toxicity is unknown, however, if, as is found in *C. elegans* (Fujii et al. 1998) and is predicted from hydrophobicity plots of the SOD3v2, the C-terminal region of the protein encodes a membrane binding domain, then the large thrombin tag (MW 37 kDa) transferred from the expression vector, together with the two *StrepII* tags (MW 1 kDa each), may serve to disrupt correct functioning of the SOD3v2 C-terminal region causing toxicity.

Western blots of transiently transfected cells revealed: high SOD1 expression in the cellular fraction, but no extracellular expression; cellular expression of SOD3v1 but no detectable expression in the extracellular fraction and no SOD3v2 expression in either fraction. Cellular, but not extracellular, detection of SOD3v1 suggests that the short version of SOD3 may localise intracellularly, however the relatively low expression level implies that transfection efficiency may have been low for this construct. The absence of any SOD3v2 expression suggests that transfection efficiency may also be low for this construct or as suggested the construct is toxic to cells. Intracellular detection of SOD3v1 was confirmed in stable cell lines, where high levels of expression were observed. Concentration of the extracellular medium revealed SOD3v1 expression also, but at significantly lower levels.

This intracellular labelling of SOD3v1 parallels similar findings of SOD3 in mammalian tissues (Fattman et al. 2001;Loenders et al. 1998;Ookawara et al. 2002) and suggests that either the N-terminal signal peptide identified in Chapter 2 and in SOD3 sequencing (Landis & Tower 2005;Parker et al. 2004a) is cleaved prior to extracellular transport, or that the alternative transcription start site corresponding to SOD1 (Chapter 2) is typically used to initiate gene expression.

## 6.6 Summary of project and SOD3 perspectives

Whilst the role of *sod3* in *Drosophila* has begun to be addressed in this thesis, further work is still required to fully characterise the gene in this insect model. Significant research has demonstrated *sod3's* importance in a number of disease states, including hyperoxia, however its role in ageing, in which the SOD family have been heavily implicated due to the "free radical theory of ageing" (Harman 1956), is still unclear (discussed in Chapter 1). Recently research has begun to focus more on disease pathology through oxidant redox signalling and intracellular signal transduction, rather than molecular damage. Whilst extracellular $O_2^{-}\cdot$ will not easily permeate biological membranes, intracellular signalling and gene transcription can be modulated by signal transducing membrane proteins containing thiol groups, which are particularly sensitive to the extracellular redox state (Moriarty-Craige and Jones 2004). For instance, extracellular thiol oxidation has been shown to activate redox-regulated vasodilation in coronary arteries involving inhibition of extracellular calcium influx (Iesaki and Wolin 2000). As well as having direct affects on signalling through protein oxidation, altered $O_2^{-}\cdot$ levels will affect $ONOO^{-}$ and $NO\cdot$ formation rates, both of which can permeate membranes to influence intracellular signalling (Brzezinska et al. 2000;Rauch et al. 1997). The SOD product $H_2O_2$, although cytotoxic, also acts as a diverse intracellular signalling molecule and is able to inhibit protein tyrosine phosphatases through oxidation of their catalytic cysteine residues (Kamata et al. 2005;Mahadev et al. 2001), leading to activation of signalling pathways causing cell proliferation, differentiation, migration and apoptosis (Veal et al. 2007). It therefore appears likely that distorting *sod* expression will affect cellular signalling since $O_2^{-}\cdot$ is the substrate and $H_2O_2$ the product of SOD activity, and this potential could be at least as important as antioxidant capacity in modulating disease states and ageing. Furthermore, this might explain why *sod* over-expression often appears insufficient to extend lifespan, since down stream components in the signalling cascade will be rate determining and could become saturated.

With respect to *sod3*, a signalling role is emerging with the recent observations of increased blood pressure and vascular inflammation upon *sod3* deletion (Lob et al. 2010), increased $H_2O_2$ induced vascular endothelial growth factor (VEGF) signalling

promoting angiogenesis after *sod3* over-expression (Oshikawa et al. 2010) and, also after *sod3* over-expression, activation of mitogenic Ras-Erk1/2 and PI3 kinase–Akt signalling pathways, resulting in cell proliferation (Laurila et al. 2009). These studies therefore highlight the importance of SOD3 levels and the extracellular $O_2^{-}\cdot/H_2O_2$ balance in regulating essential signalling cascades. One of the main conclusions from the work presented in this thesis is the proposal of a SOD1-SOD3 co-dependency in *Drosophila*. This co-dependency could arise from the physical interaction of the proteins (such through the formation of heterodimers), which could be confirmed by yeast 2-hybrid analysis (the constructs for which have been described in this chapter) or co-immunoprecipitation methods. However, the interaction between SOD1 and SOD3 might also occur through downstream transcriptional events resulting from activated signalling cascades in which the proteins participate. Interestingly Laurila and colleagues found that overexpression of *sod3* resulted in the activation of the serine/threonine kinase Akt, presumable through the $H_2O_2$-mediated inactivation of signal quenching phosphatases (Laurila et al. 2009). Akt is a key constituent of the conserved longevity-influencing insulin signalling pathway in *Drosophila* and is proposed to function by phosphorylating transcription factors that regulate the expression of intracellular SODs (Longo and Fabrizio 2002). Thus it appears that SOD3-derived signalling may influence *sod1* expression. This proposal is further supported by the gene expression data for the *sod1* and *sod3* mutant alleles presented in chapter 3 which found that these genes were influencing each others expression. I would therefore suggest that whilst work to characterise *sod3* and directly assess its importance as an antioxidant and in lifespan regulation remains important, investigating its potential role in redox signalling would also be a worthy avenue of research.

**Appendix 1. Alignment of the two sequences with the *Drosophila* genomic sequence for chromosome 2R.**

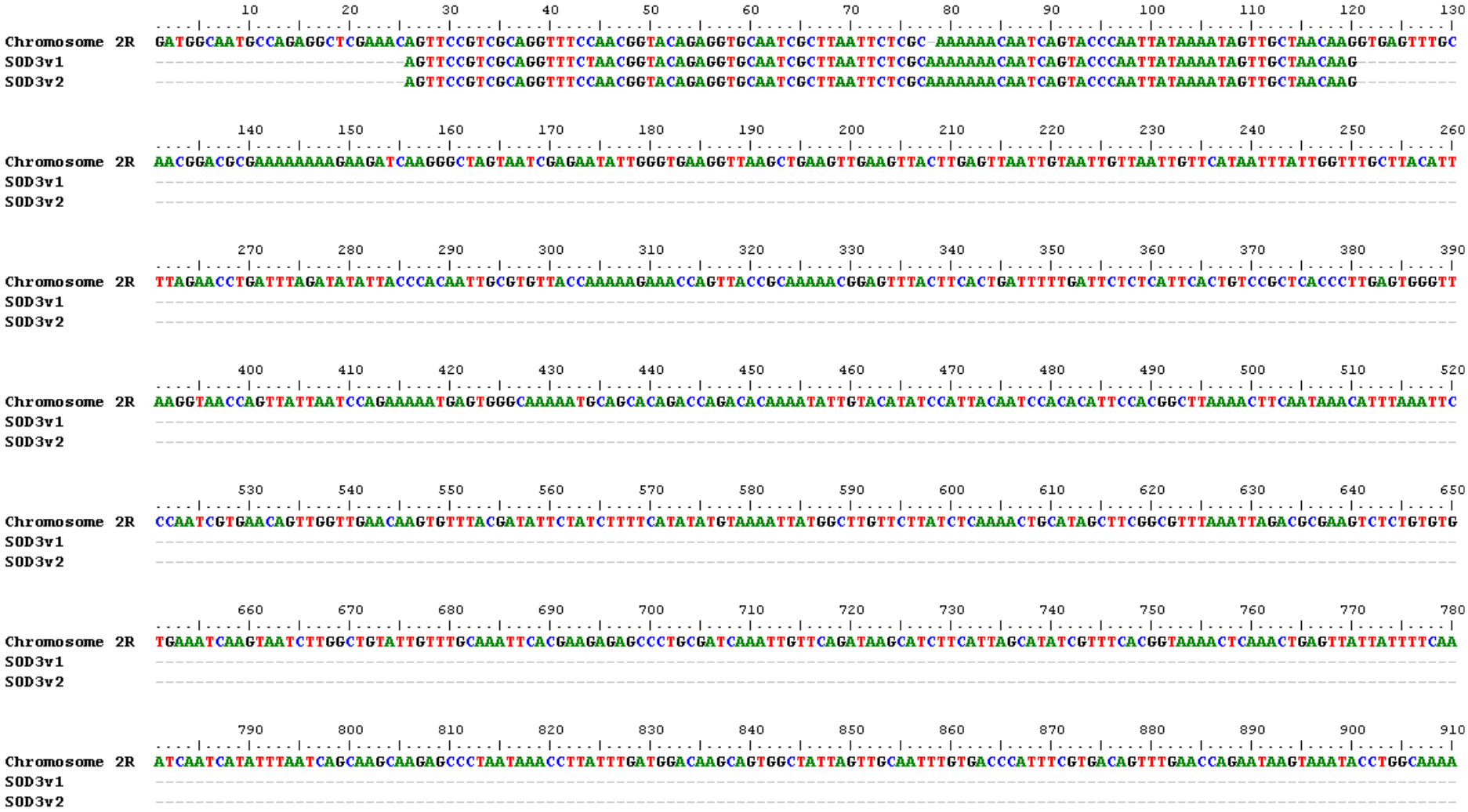


790 800 810 820 830 840 850 860 870 880 890 900 910
Chromosome 2R ATCAATCATATTTAATCAGCAAGCAAGAGCCCTAATAAACCTTATTTGATGGACAAGCAGTGGCTATTAGTTGCAATTTGTGACCCATTTCGTGACAGTTTGAACCAGAATAAGTAAATACCTGGCAAAA
SOD3v1
SOD3v2
920 930 940 950 960 970 980 990 1000 1010 1020 1030 1040
Chromosome 2R AACAGATTAAAATACTTATACGTAATGACAATGGCATTTTTAGTTCCGAAATTCAGTCGCTCTACGAGCGTGAGAATCGTAAATTATGGGACCGATTCCAAGTGCAGATAAGGATACGTGTGTAGAGCAG
SOD3v1
SOD3v2
1050 1060 1070 1080 1090 1100 1110 1120 1130 1140 1150 1160 1170
Chromosome 2R GTACTGACCGCGTTTGAAGATCGTTTCAGAACTCGAGCGTGCAAGATCGCCAGCATATCGCAGACACATTGATAAGACCGTAAGGAAACCGGACCCATAAACAAATATTGCCCCGATAAAGTGTGACACC
SOD3v1
SOD3v2
1180 1190 1200 1210 1220 1230 1240 1250 1260 1270 1280 1290 1300
Chromosome 2R CATCCATTTCATTTGTGGAACTTTGGAAGCGAAGTGCGTACGAAAAAGAGATTGTTGATTGACCTTCCCGCAGCCGCACTTAACCCTGTGAAAAAGGCTGTTTGCATTTAGTTTCGTTTGGGTATCGCTC
SOD3v1
SOD3v2
1310 1320 1330 1340 1350 1360 1370 1380 1390 1400 1410 1420 1430
Chromosome 2R ATTATTCACACACATAAATAATAATACCCGTTCGCACATCATATATGACCCACAAATCGTTTCATAAATTGAGGCTAGGCGCTTCAATTCCGCACACAACTGTCCGTTTAAATGGAATCAAGAGAATGTA
SOD3v1
SOD3v2
1440 1450 1460 1470 1480 1490 1500 1510 1520 1530 1540 1550 1560
Chromosome 2R CACCTGATGACGTCCAAGCCAGAGATGAGCTGGAATTCAAGTGCCAGAGATGAGTTGGCATCACGGAATTTGAGATTACAAGACATAAACCCTCCTAGCATTTCCCAAAACTGAAAGTATTTGGTTCCAA
SOD3v1
SOD3v2
1570 1580 1590 1600 1610 1620 1630 1640 1650 1660 1670 1680 1690
Chromosome 2R ATCATTTAAAGCTTTACTATAAAGCATTATATAAATAGTTTTGGAAGATGTTTTTAATATTGAGTCCATATCAATTATCGAAATTTCAGGATTATCATTTAGTTCATTTTTAGCTATGTCCAGTAGATCA
SOD3v1
SOD3v2

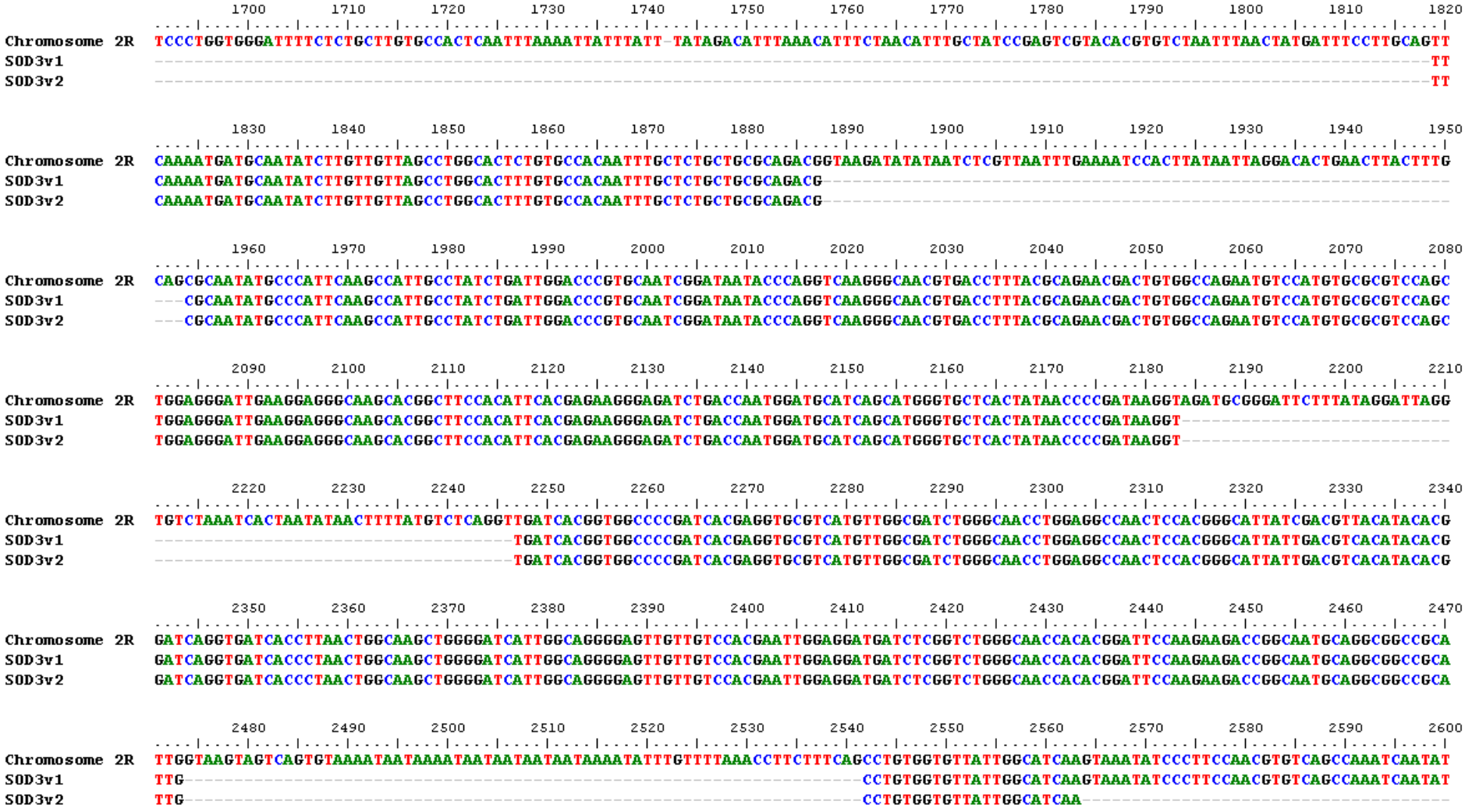
1700 1710 1720 1730 1740 1750 1760 1770 1780 1790 1800 1810 1820
Chromosome 2R TCCCTGGTGGGATTTTCTCTGCTTGTGCCACTCAATTTAAAATTATTTATT-TATAGACATTTAAACATTTCTAACATTTGCTATCCGAGTCGTACACGTGTCTAATTTAACTATGATTTCCTTGCAGTT
SOD3v1 TT
SOD3v2 TT
1830 1840 1850 1860 1870 1880 1890 1900 1910 1920 1930 1940 1950
Chromosome 2R CAAAATGATGCAATATCTTGTTGTTAGCCTGGCACTCTGTGCCACAATTTGCTCTGCTGCGCAGACGGTAAGATATATAATCTCGTTAATTTGAAAATCCACTTATAATTAGGACACTGAACTTACTTTG
SOD3v1 CAAAATGATGCAATATCTTGTTGTTAGCCTGGCACTTTGTGCCACAATTTGCTCTGCTGCGCAGACG
SOD3v2 CAAAATGATGCAATATCTTGTTGTTAGCCTGGCACTTTGTGCCACAATTTGCTCTGCTGCGCAGACG
1960 1970 1980 1990 2000 2010 2020 2030 2040 2050 2060 2070 2080
Chromosome 2R CAGCGCAATATGCCCATTCAAGCCATTGCCTATCTGATTGGACCCGTGCAATCGGATAATACCCAGGTCAAGGGCAACGTGACCTTTACGCAGAACGACTGTGGCCAGAATGTCCATGTGCGCGTCCAGC
SOD3v1 ---CGCAATATGCCCATTCAAGCCATTGCCTATCTGATTGGACCCGTGCAATCGGATAATACCCAGGTCAAGGGCAACGTGACCTTTACGCAGAACGACTGTGGCCAGAATGTCCATGTGCGCGTCCAGC
SOD3v2 ---CGCAATATGCCCATTCAAGCCATTGCCTATCTGATTGGACCCGTGCAATCGGATAATACCCAGGTCAAGGGCAACGTGACCTTTACGCAGAACGACTGTGGCCAGAATGTCCATGTGCGCGTCCAGC
2090 2100 2110 2120 2130 2140 2150 2160 2170 2180 2190 2200 2210
Chromosome 2R TGGAGGGATTGAAGGAGGGCAAGCACGGCTTCCACATTCACGAGAAGGGAGATCTGACCAATGGATGCATCAGCATGGGTGCTCACTATAACCCCGATAAGGTAGATGCGGGATTCTTTATAGGATTAGG
SOD3v1 TGGAGGGATTGAAGGAGGGCAAGCACGGCTTCCACATTCACGAGAAGGGAGATCTGACCAATGGATGCATCAGCATGGGTGCTCACTATAACCCCGATAAGGT
SOD3v2 TGGAGGGATTGAAGGAGGGCAAGCACGGCTTCCACATTCACGAGAAGGGAGATCTGACCAATGGATGCATCAGCATGGGTGCTCACTATAACCCCGATAAGGT
2220 2230 2240 2250 2260 2270 2280 2290 2300 2310 2320 2330 2340
Chromosome 2R TGTCTAAATCACTAATATAACTTTTATGTCTCAGGTTGATCACGGTGGCCCCGATCACGAGGTGCGTCATGTTGGCGATCTGGGCAACCTGGAGGCCAACTCCACGGGCATTATCGACGTTACATACACG
SOD3v1 TGATCACGGTGGCCCCGATCACGAGGTGCGTCATGTTGGCGATCTGGGCAACCTGGAGGCCAACTCCACGGGCATTATTGACGTCACATACACG
SOD3v2 TGATCACGGTGGCCCCGATCACGAGGTGCGTCATGTTGGCGATCTGGGCAACCTGGAGGCCAACTCCACGGGCATTATTGACGTCACATACACG
2350 2360 2370 2380 2390 2400 2410 2420 2430 2440 2450 2460 2470
Chromosome 2R GATCAGGTGATCACCTTAACTGGCAAGCTGGGGATCATTGGCAGGGGAGTTGTTGTCCACGAATTGGAGGATGATCTCGGTCTGGGCAACCACACGGATTCCAAGAAGACCGGCAATGCAGGCGGCCGCA
SOD3v1 GATCAGGTGATCACCCTAACTGGCAAGCTGGGGATCATTGGCAGGGGAGTTGTTGTCCACGAATTGGAGGATGATCTCGGTCTGGGCAACCACACGGATTCCAAGAAGACCGGCAATGCAGGCGGCCGCA
SOD3v2 GATCAGGTGATCACCCTAACTGGCAAGCTGGGGATCATTGGCAGGGGAGTTGTTGTCCACGAATTGGAGGATGATCTCGGTCTGGGCAACCACACGGATTCCAAGAAGACCGGCAATGCAGGCGGCCGCA
2480 2490 2500 2510 2520 2530 2540 2550 2560 2570 2580 2590 2600
Chromosome 2R TTGGTAAGTAGTCAGTGTAAAATAATAAAATAATAATAATAATAAAATATTTGTTTTAAACCTTCTTTCAGCCTGTGGTGTTATTGGCATCAAGTAAATATCCCTTCCAACGTGTCAGCCAAATCAATAT
SOD3v1 TTG CCTGTGGTGTTATTGGCATCAAGTAAATATCCCTTCCAACGTGTCAGCCAAATCAATAT
SOD3v2 TTG CCTGTGGTGTTATTGGCATCAA

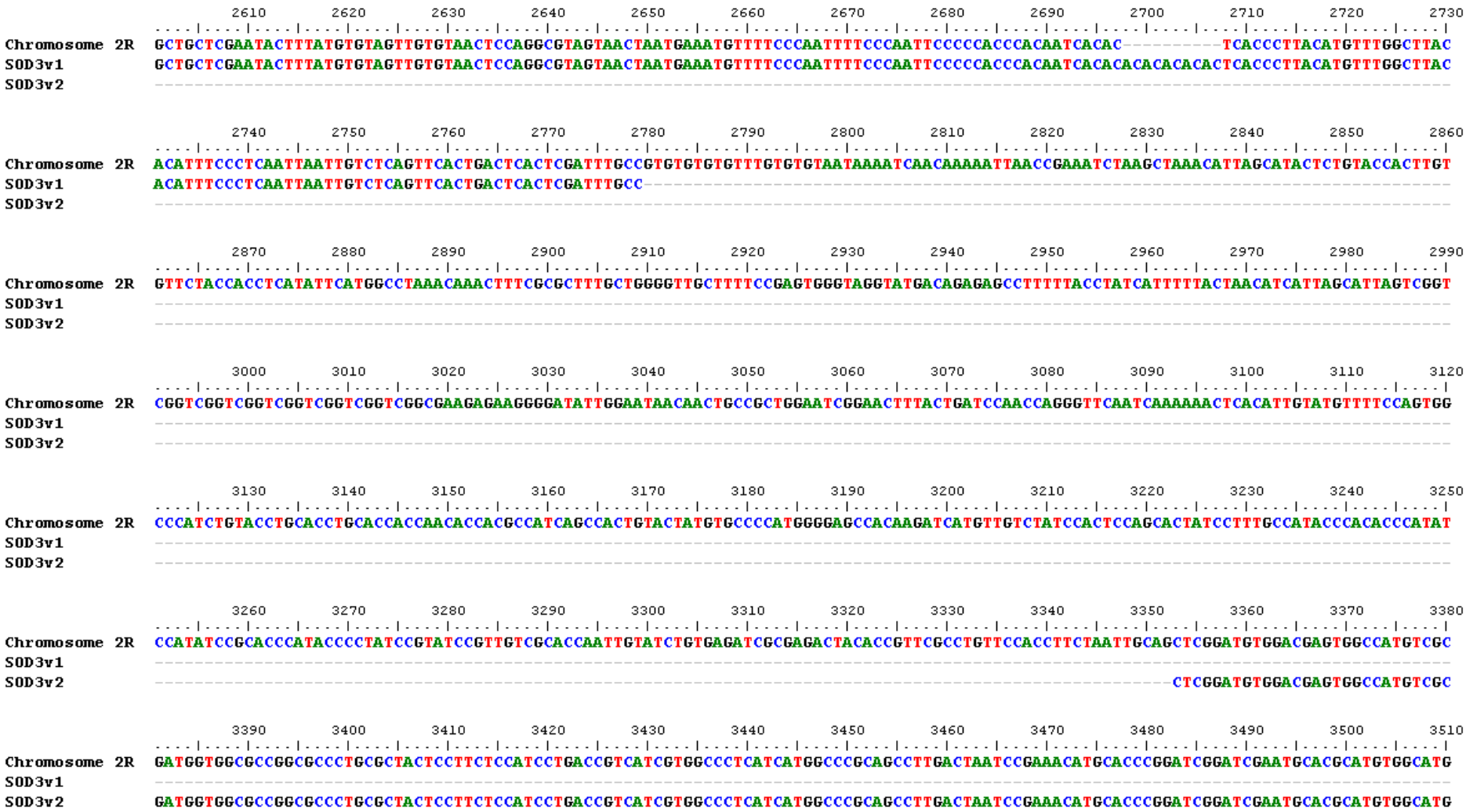
2610 2620 2630 2640 2650 2660 2670 2680 2690 2700 2710 2720 2730
Chromosome 2R GCTGCTCGAATACTTTATGTGTAGTTGTGTAACTCCAGGCGTAGTAACTAATGAAATGTTTTCCCAATTTTCCCAATTCCCCCACCCACAATCACAC----------TCACCCTTACATGTTTGGCTTAC
SOD3v1 GCTGCTCGAATACTTTATGTGTAGTTGTGTAACTCCAGGCGTAGTAACTAATGAAATGTTTTCCCAATTTTCCCAATTCCCCCACCCACAATCACACACACACACACTCACCCTTACATGTTTGGCTTAC
SOD3v2
2740 2750 2760 2770 2780 2790 2800 2810 2820 2830 2840 2850 2860
Chromosome 2R ACATTTCCCTCAATTAATTGTCTCAGTTCACTGACTCACTCGATTTGCCGTGTGTGTGTTTGTGTGTAATAAAATCAACAAAAATTAACCGAAATCTAAGCTAAACATTAGCATACTCTGTACCACTTGT
SOD3v1 ACATTTCCCTCAATTAATTGTCTCAGTTCACTGACTCACTCGATTTGCC----------
SOD3v2
2870 2880 2890 2900 2910 2920 2930 2940 2950 2960 2970 2980 2990
Chromosome 2R GTTCTACCACCTCATATTCATGGCCTAAACAAACTTTCGCGCTTTGCTGGGGTTGCTTTTCCGAGTGGGTAGGTATGACAGAGAGCCTTTTTACCTATCATTTTTACTAACATCATTAGCATTAGTCGGT
SOD3v1
SOD3v2
3000 3010 3020 3030 3040 3050 3060 3070 3080 3090 3100 3110 3120
Chromosome 2R CGGTCGGTCGGTCGGTCGGTCGGTCGGCGAAGAGAAGGGGATATTGGAATAACAACTGCCGCTGGAATCGGAACTTTACTGATCCAACCAGGGTTCAATCAAAAAACTCACATTGTATGTTTTCCAGTGG
SOD3v1
SOD3v2
3130 3140 3150 3160 3170 3180 3190 3200 3210 3220 3230 3240 3250
Chromosome 2R CCCATCTGTACCTGCACCTGCACCACCAACACCACGCCATCAGCCACTGTACTATGTGCCCCATGGGGAGCCACAAGATCATGTTGTCTATCCACTCCAGCACTATCCTTTGCCATACCCACACCCATAT
SOD3v1
SOD3v2
3260 3270 3280 3290 3300 3310 3320 3330 3340 3350 3360 3370 3380
Chromosome 2R CCATATCCGCACCCATACCCCTATCCGTATCCGTTGTCGCACCAATTGTATCTGTGAGATCGCGAGACTACACCGTTCGCCTGTTCCACCTTCTAATTGCAGCTCGGATGTGGACGAGTGGCCATGTCGC
SOD3v1
SOD3v2 CTCGGATGTGGACGAGTGGCCATGTCGC
3390 3400 3410 3420 3430 3440 3450 3460 3470 3480 3490 3500 3510
Chromosome 2R GATGGTGGCGCCGGCGCCCTGCGCTACTCCTTCTCCATCCTGACCGTCATCGTGGCCCTCATCATGGCCCGCAGCCTTGACTAATCCGAAACATGCACCCGGATCGGATCGAATGCACGCATGTGGCATG
SOD3v1
SOD3v2 GATGGTGGCGCCGGCGCCCTGCGCTACTCCTTCTCCATCCTGACCGTCATCGTGGCCCTCATCATGGCCCGCAGCCTTGACTAATCCGAAACATGCACCCGGATCGGATCGAATGCACGCATGTGGCATG

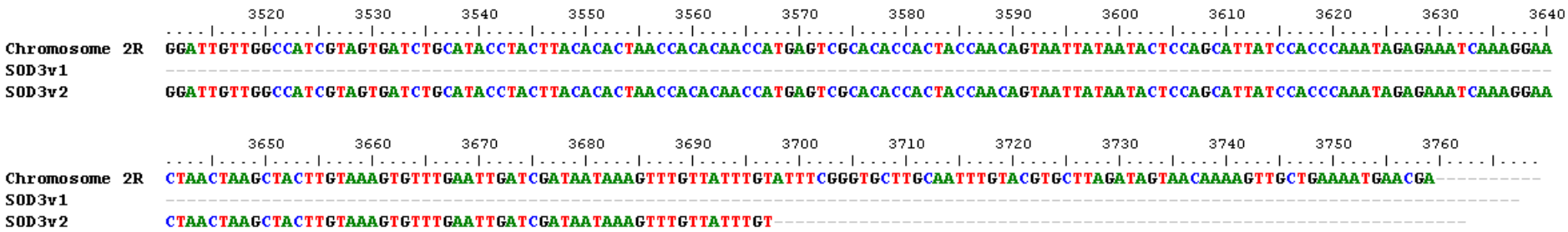
3520 3530 3540 3550 3560 3570 3580 3590 3600 3610 3620 3630 3640
Chromosome 2R GGATTGTTGGCCATCGTAGTGATCTGCATACCTACTTACACACTAACCACACAACCATGAGTCGCACACCACTACCAACAGTAATTATAATACTCCAGCATTATCCACCCAAATAGAGAAATCAAAGGAA
SOD3v1
SOD3v2 GGATTGTTGGCCATCGTAGTGATCTGCATACCTACTTACACACTAACCACACAACCATGAGTCGCACACCACTACCAACAGTAATTATAATACTCCAGCATTATCCACCCAAATAGAGAAATCAAAGGAA
3650 3660 3670 3680 3690 3700 3710 3720 3730 3740 3750 3760
Chromosome 2R CTAACTAAGCTACTTGTAAAGTGTTTGAATTGATCGATAATAAAGTTTGTTATTTGTATTTCGGGTGCTTGCAATTTGTACGTGCTTAGATAGTAACAAAAGTTGCTGAAAATGAACGA
SOD3v1
SOD3v2 CTAACTAAGCTACTTGTAAAGTGTTTGAATTGATCGATAATAAAGTTTGTTATTTGT

## Appendix 2

### Drosophila medium

6g Agar

17.5g Yeast

10g Soya flour

73.1g yellow maize meal

46.2g Light malt extract

48g Sucrose

1080mL Distilled $H_2O$

5mL Propionic acid

### Egg lay plates

22g Agar

500mL Blackcurrant juice

500mL Distilled $H_2O$

**Appendix 3. PCR screen of each excision line for small genomic DNA deletions.**


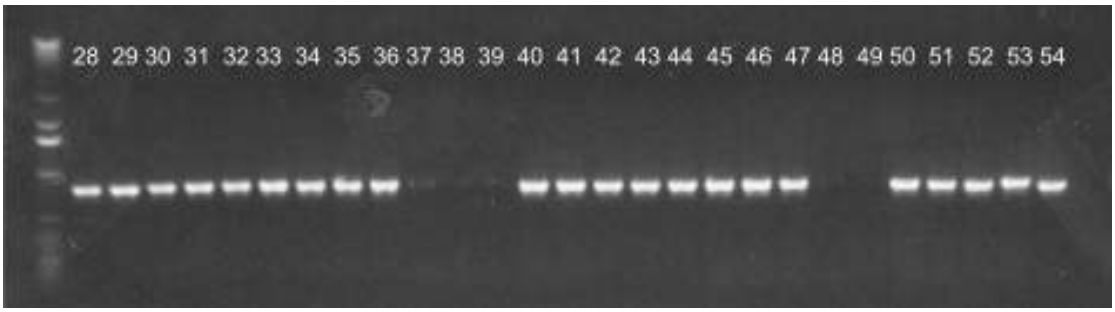


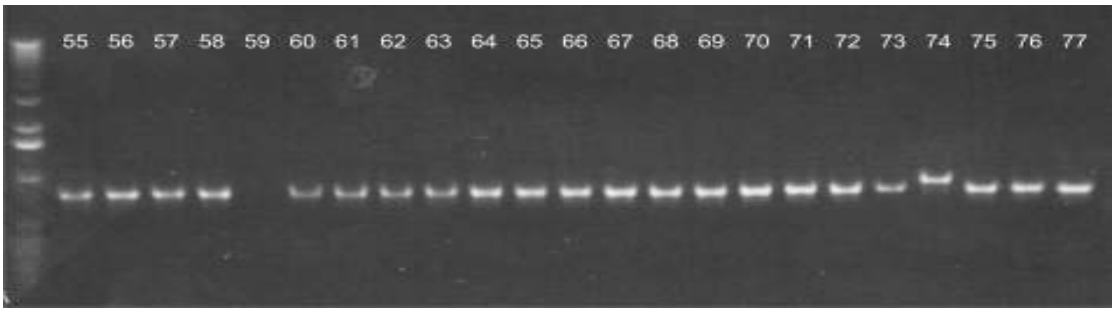


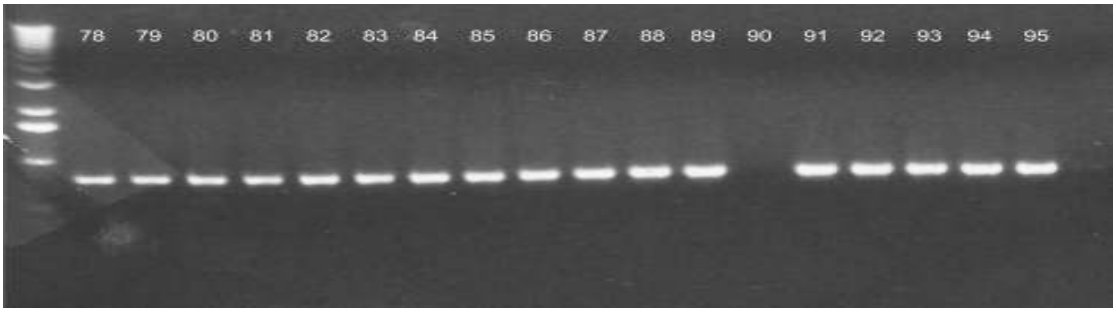


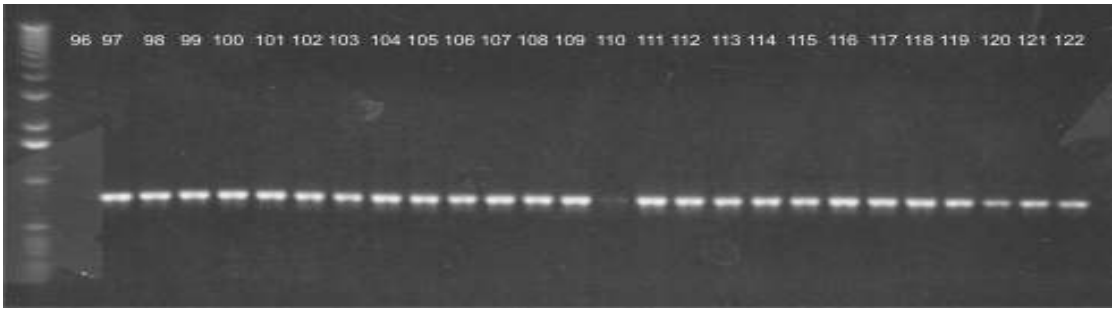

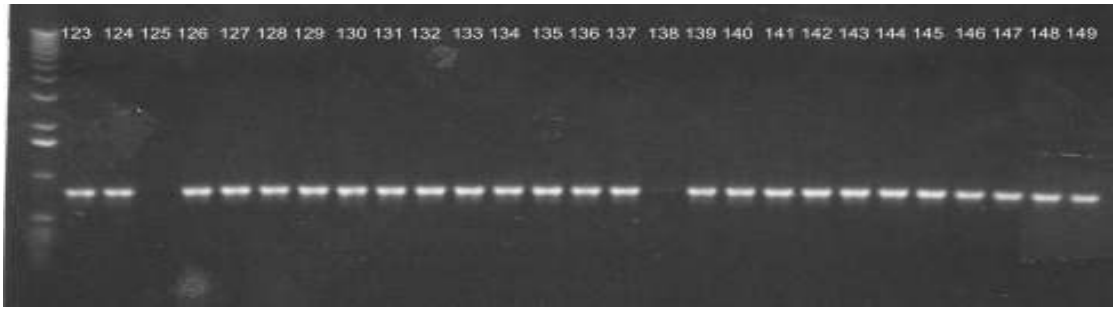
123 124 125 126 127 128 129 130 131 132 133 134 135 136 137 138 139 140 141 142 143 144 145 146 147 148 149

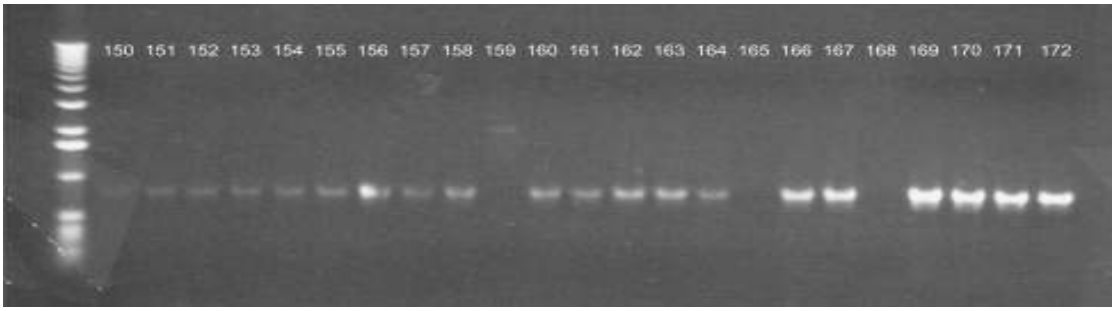
150 151 152 153 154 155 156 157 158 159 160 161 162 163 164 165 166 167 168 169 170 171 172

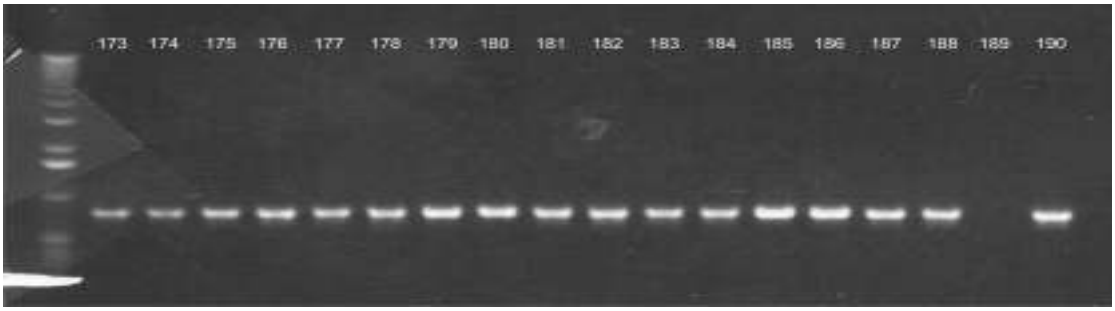
173 174 175 176 177 178 179 180 181 182 183 184 185 186 187 188 189 190

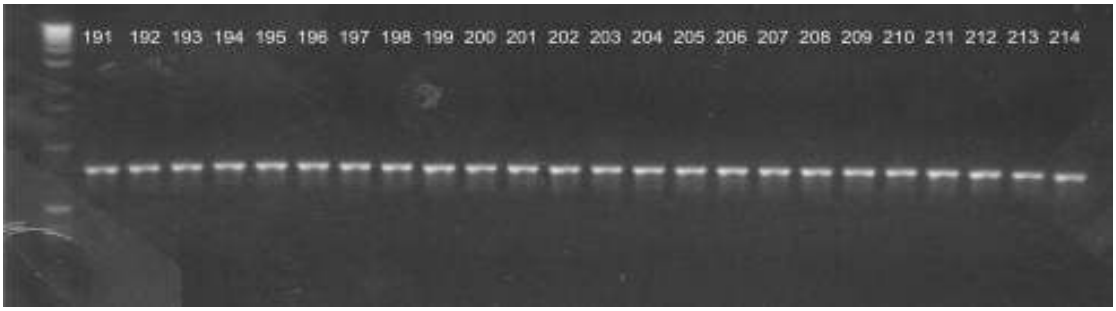
191 192 193 194 195 196 197 198 199 200 201 202 203 204 205 206 207 208 209 210 211 212 213 214


215 216 217 218 219 220 221 222 223 224 225 226 227 228 229 230 231 232 233 234 235 236

## Appendix 4. Sequencing of the SOD1 Bait construct.

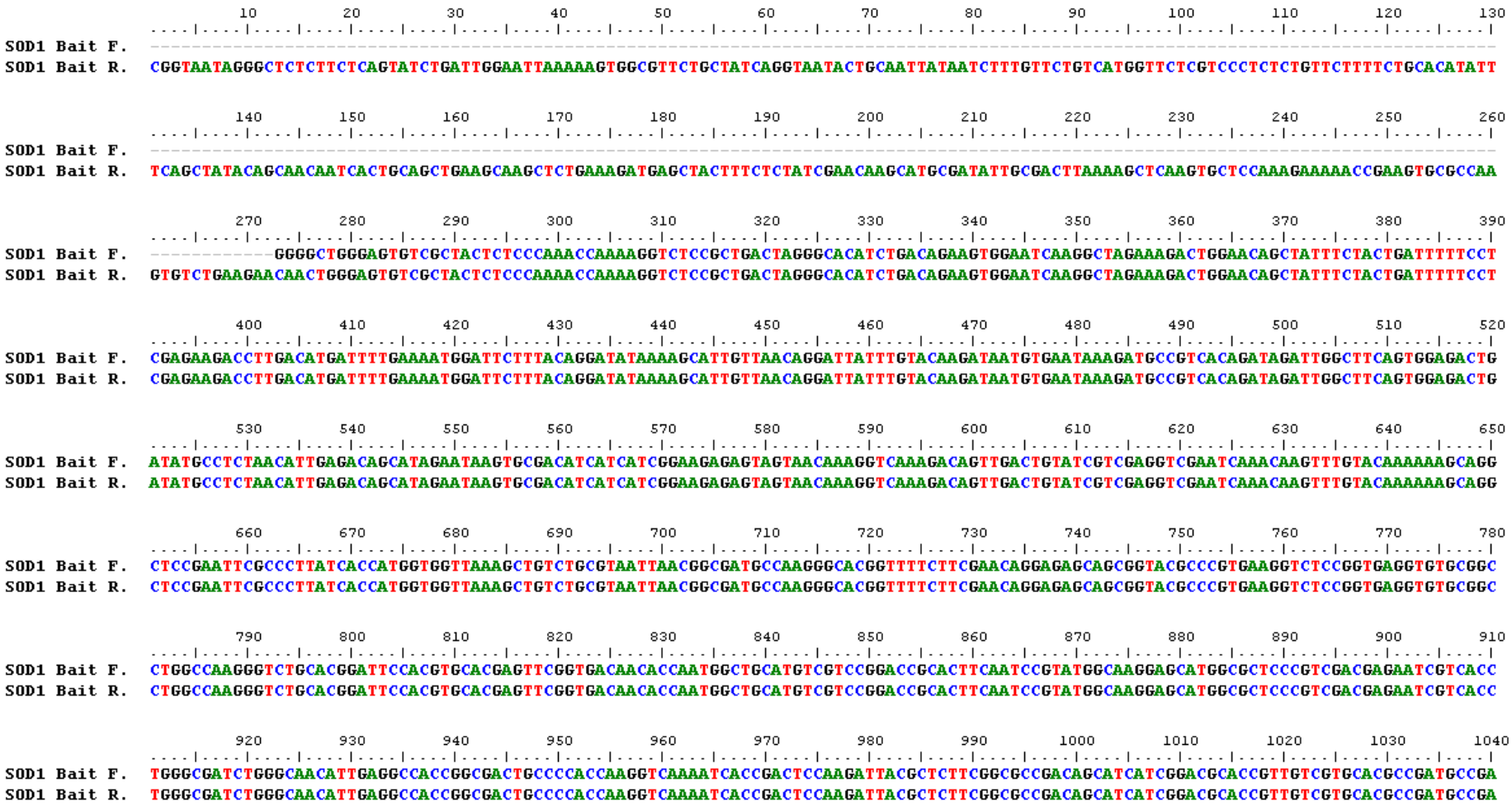

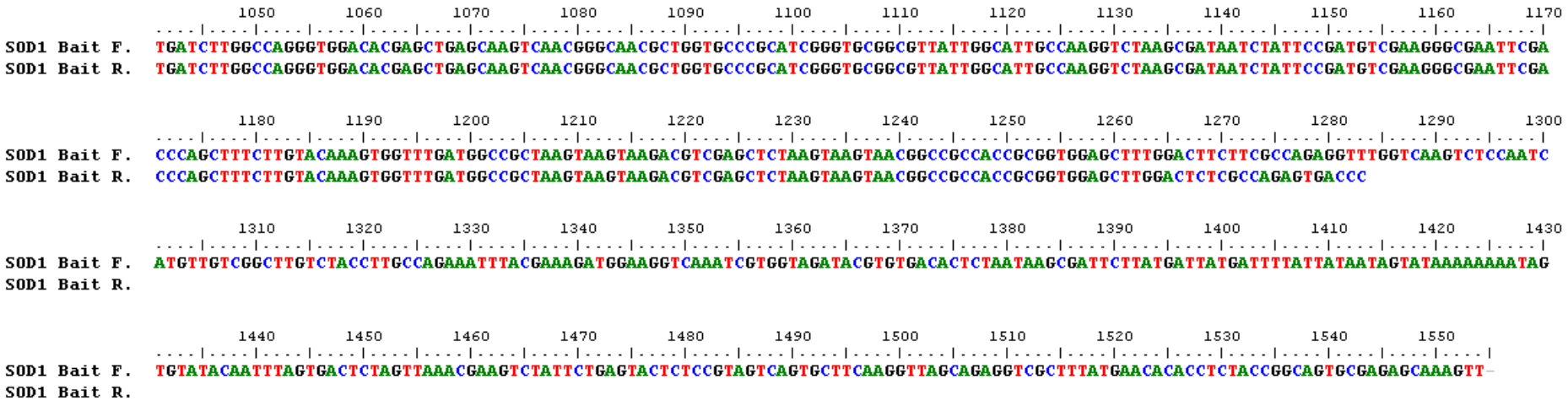
1050 1060 1070 1080 1090 1100 1110 1120 1130 1140 1150 1160 1170
SOD1 Bait F. TGATCTTGGCCAGGGTGGACACGAGCTGAGCAAGTCAACGGGCAACGCTGGTGCCCGCATCGGGTGCGGCGTTATTGGCATTGCCAAGGTCTAAGCGATAATCTATTCCGATGTCGAAGGGCGAATTCGA
SOD1 Bait R. TGATCTTGGCCAGGGTGGACACGAGCTGAGCAAGTCAACGGGCAACGCTGGTGCCCGCATCGGGTGCGGCGTTATTGGCATTGCCAAGGTCTAAGCGATAATCTATTCCGATGTCGAAGGGCGAATTCGA
1180 1190 1200 1210 1220 1230 1240 1250 1260 1270 1280 1290 1300
SOD1 Bait F. CCCAGCTTTCTTGTACAAAGTGGTTTGATGGCCGCTAAGTAAGTAAGACGTCGAGCTCTAAGTAAGTAACGGCCGCCACCGCGGTGGAGCTTTGGACTTCTTCGCCAGAGGTTTGGTCAAGTCTCCAATC
SOD1 Bait R. CCCAGCTTTCTTGTACAAAGTGGTTTGATGGCCGCTAAGTAAGTAAGACGTCGAGCTCTAAGTAAGTAACGGCCGCCACCGCGGTGGAGCTTGGACTCTCGCCAGAGTGACCC
1310 1320 1330 1340 1350 1360 1370 1380 1390 1400 1410 1420 1430
SOD1 Bait F. ATGTTGTCGGCTTGTCTACCTTGCCAGAAATTTACGAAAGATGGAAGGTCAAATCGTGGTAGATACGTGTGACACTCTAATAAGCGATTCTTATGATTATGATTTTATTATAATAGTATAAAAAAAAATAG
SOD1 Bait R.
1440 1450 1460 1470 1480 1490 1500 1510 1520 1530 1540 1550
SOD1 Bait F. TGTATACAATTTAGTGACTCTAGTTAAACGAAGTCTATTCTGAGTACTCTCCGTAGTCAGTGCTTCAAGGTTAGCAGAGGTCGCTTTATGAACACACCTCTACCGGCAGTGCGAGAGCAAAGTT-
SOD1 Bait R.

## Appendix 5. Sequencing of the SOD1 Prey construct.

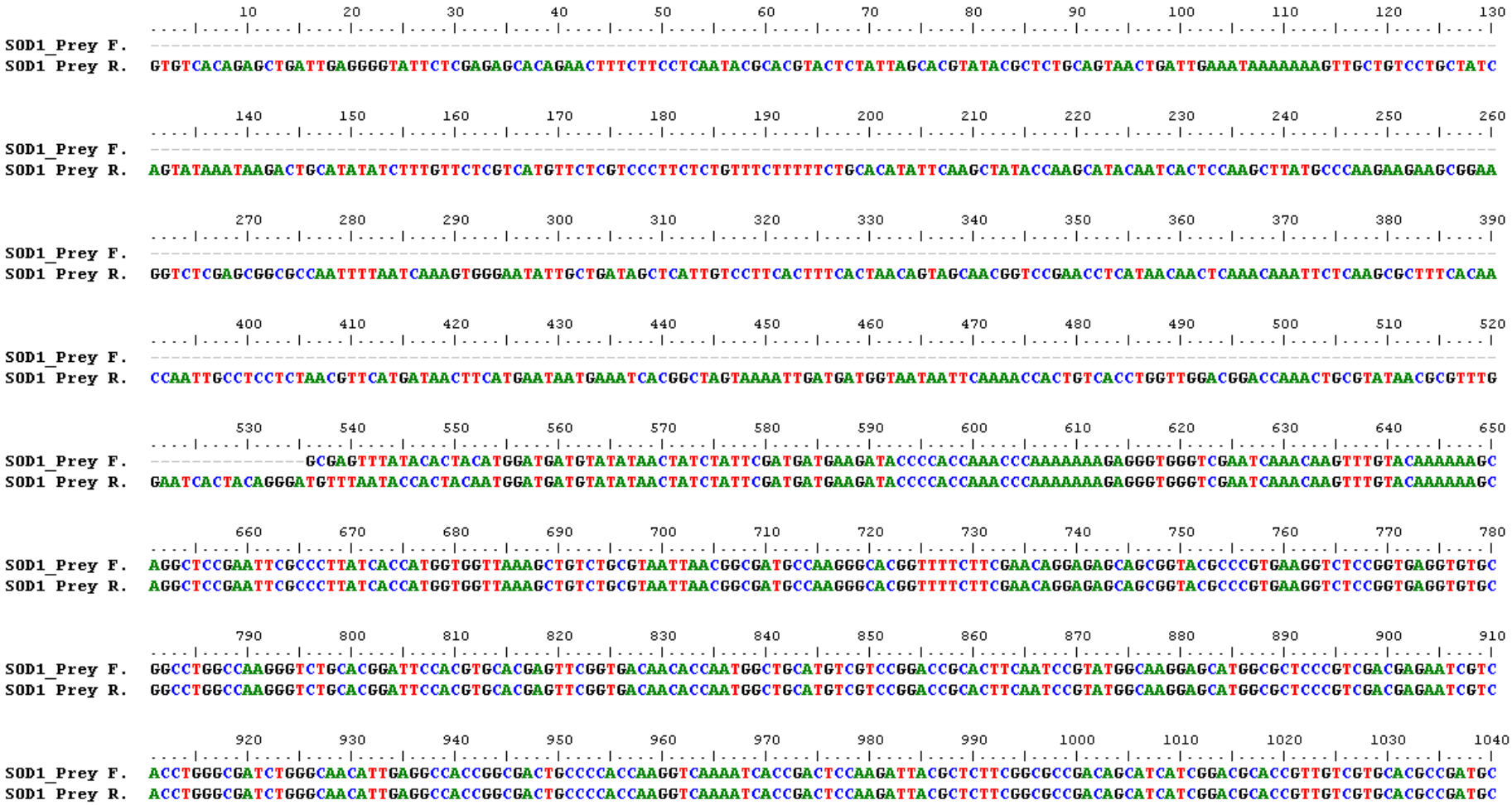

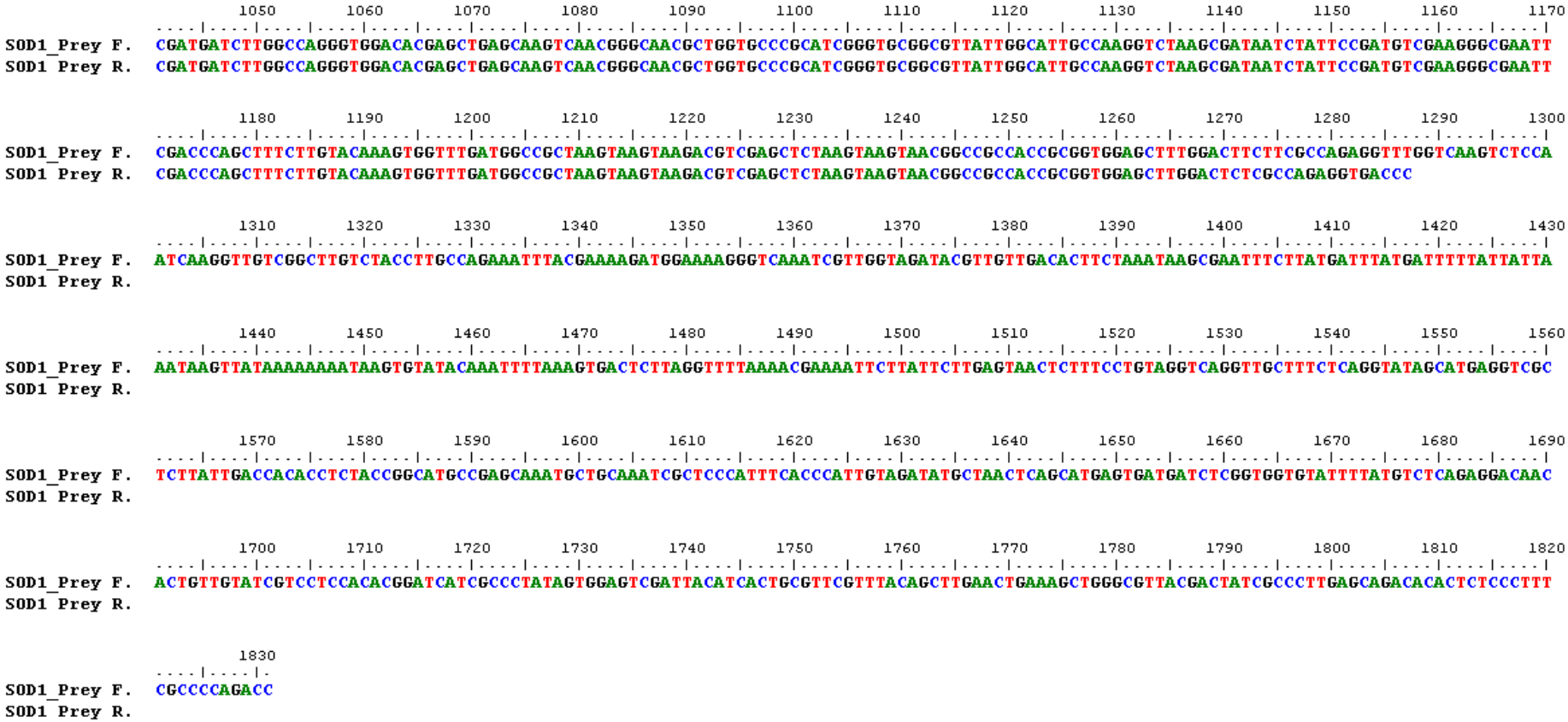
1050 1060 1070 1080 1090 1100 1110 1120 1130 1140 1150 1160 1170
SOD1_Prey F. CGATGATCTTGGCCAGGGTGGACACGAGCTGAGCAAGTCAACGGGCAACGCTGGTGCCCGCATCGGGTGCGGCGTTATTGGCATTGCCAAGGTCTAAGCGATAATCTATTCCGATGTCGAAGGGCGAATT
SOD1 Prey R. CGATGATCTTGGCCAGGGTGGACACGAGCTGAGCAAGTCAACGGGCAACGCTGGTGCCCGCATCGGGTGCGGCGTTATTGGCATTGCCAAGGTCTAAGCGATAATCTATTCCGATGTCGAAGGGCGAATT
1180 1190 1200 1210 1220 1230 1240 1250 1260 1270 1280 1290 1300
SOD1_Prey F. CGACCCAGCTTTCTTGTACAAAGTGGTTTGATGGCCGCTAAGTAAGTAAGACGTCGAGCTCTAAGTAAGTAACGGCCGCCACCGCGGTGGAGCTTTGGACTTCTTCGCCAGAGGTTTGGTCAAGTCTCCA
SOD1 Prey R. CGACCCAGCTTTCTTGTACAAAGTGGTTTGATGGCCGCTAAGTAAGTAAGACGTCGAGCTCTAAGTAAGTAACGGCCGCCACCGCGGTGGAGCTTGGACTCTCGCCAGAGGTGACCC
1310 1320 1330 1340 1350 1360 1370 1380 1390 1400 1410 1420 1430
SOD1_Prey F. ATCAAGGTTGTCGGCTTGTCTACCTTGCCAGAAATTTACGAAAAGATGGAAAAGGGTCAAATCGTTGGTAGATACGTTGTTGACACTTCTAAATAAGCGAATTTCTTATGATTTATGATTTTTATTATTA
SOD1 Prey R.
1440 1450 1460 1470 1480 1490 1500 1510 1520 1530 1540 1550 1560
SOD1_Prey F. AATAAGTTATAAAAAAAATAAGTGTATACAAATTTTAAAGTGACTCTTAGGTTTTAAAACGAAAATTCTTATTCTTGAGTAACTCTTTCCTGTAGGTCAGGTTGCTTTCTCAGGTATAGCATGAGGTCGC
SOD1 Prey R.
1570 1580 1590 1600 1610 1620 1630 1640 1650 1660 1670 1680 1690
SOD1_Prey F. TCTTATTGACCACACCTCTACCGGCATGCCGAGCAAATGCTGCAAATCGCTCCCATTTCACCCATTGTAGATATGCTAACTCAGCATGAGTGATGATCTCGGTGGTGTATTTTATGTCTCAGAGGACAAC
SOD1 Prey R.
1700 1710 1720 1730 1740 1750 1760 1770 1780 1790 1800 1810 1820
SOD1_Prey F. ACTGTTGTATCGTCCTCCACACGGATCATCGCCCTATAGTGGAGTCGATTACATCACTGCGTTCGTTTACAGCTTGAACTGAAAGCTGGGCGTTACGACTATCGCCCTTGAGCAGACACACTCTCCCTTT
SOD1 Prey R.
1830
SOD1_Prey F. CGCCCCAGACC
SOD1 Prey R.

## Appendix 6. Sequencing of the SOD3v1 Bait construct.

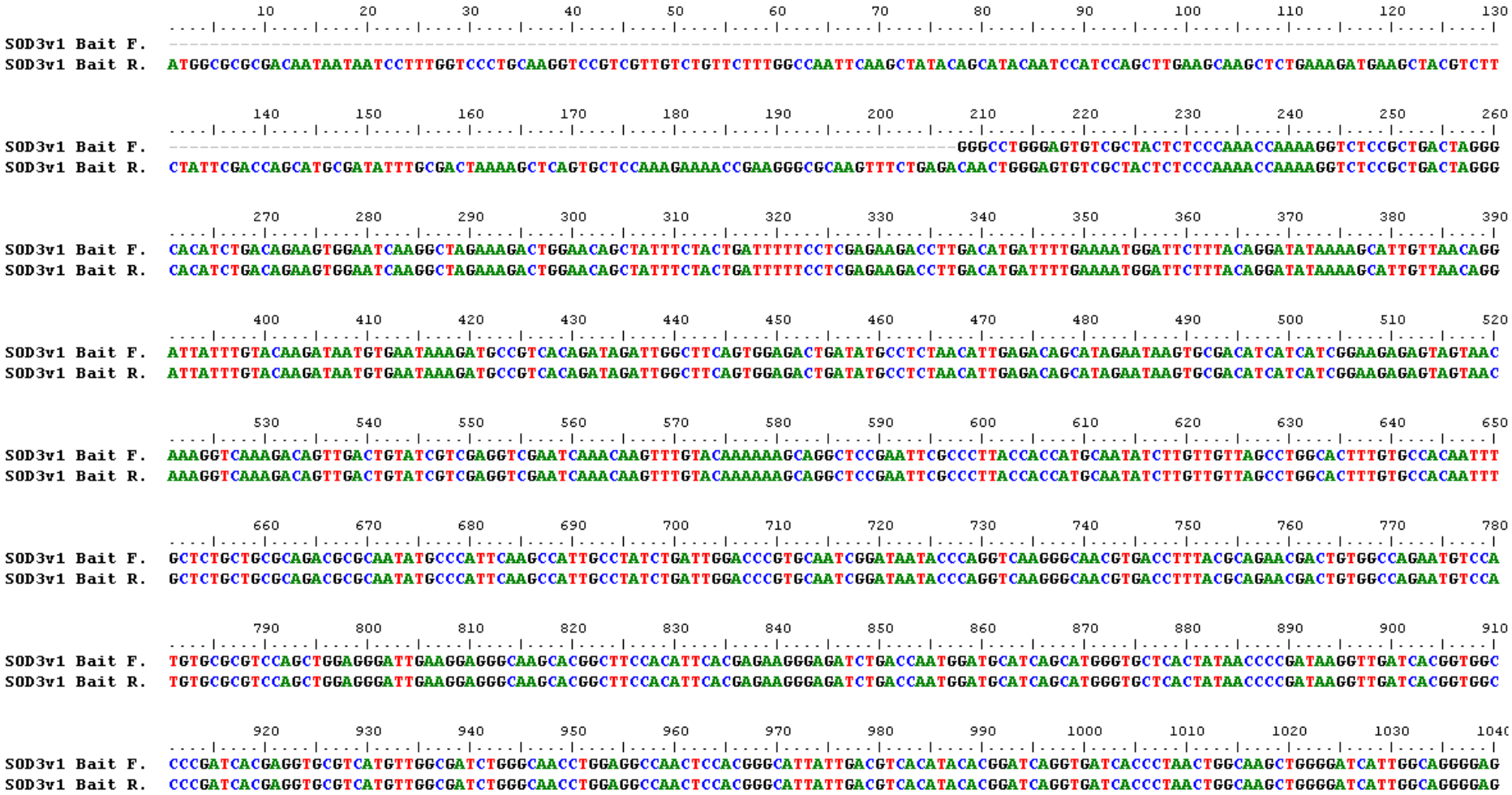

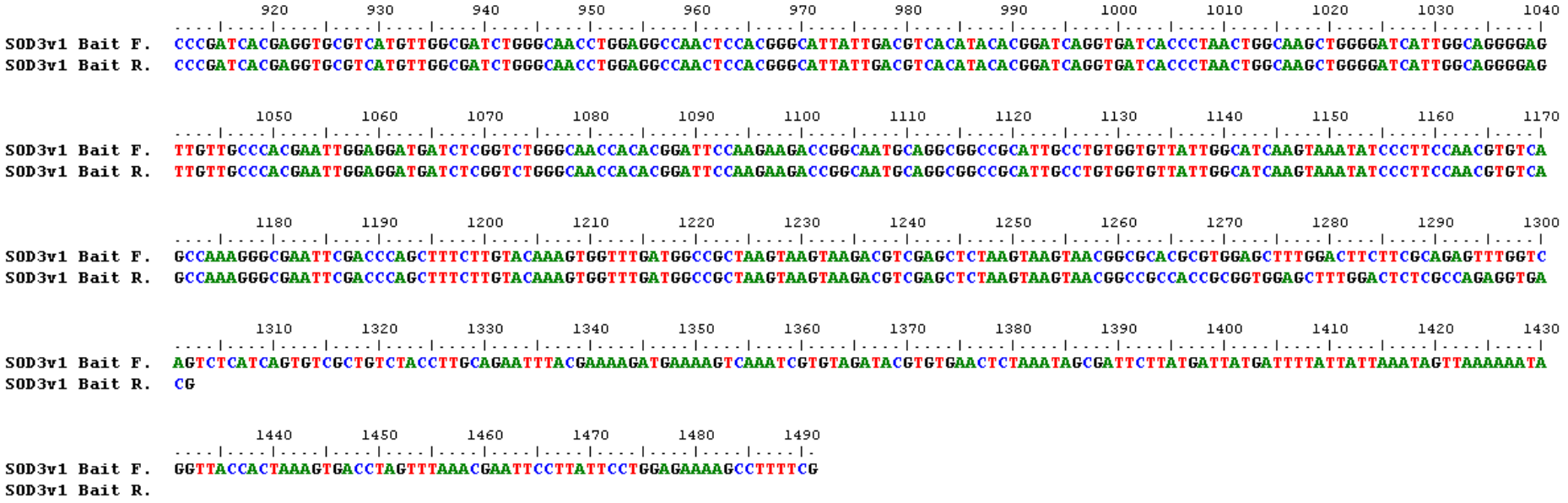
920 930 940 950 960 970 980 990 1000 1010 1020 1030 1040
SOD3v1 Bait F. CCCGATCACGAGGTGCGTCATGTTGGCGATCTGGGCAACCTGGAGGCCAACTCCACGGGCATTATTGACGTCACATACACGGATCAGGTGATCACCCTAACTGGCAAGCTGGGGATCATTGGCAGGGGAG
SOD3v1 Bait R. CCCGATCACGAGGTGCGTCATGTTGGCGATCTGGGCAACCTGGAGGCCAACTCCACGGGCATTATTGACGTCACATACACGGATCAGGTGATCACCCTAACTGGCAAGCTGGGGATCATTGGCAGGGGAG
1050 1060 1070 1080 1090 1100 1110 1120 1130 1140 1150 1160 1170
SOD3v1 Bait F. TTGTTGCCCACGAATTGGAGGATGATCTCGGTCTGGGCAACCACACGGATTCCAAGAAGACCGGCAATGCAGGCGGCCGCATTGCCTGTGGTGTTATTGGCATCAAGTAAATATCCCTTCCAACGTGTCA
SOD3v1 Bait R. TTGTTGCCCACGAATTGGAGGATGATCTCGGTCTGGGCAACCACACGGATTCCAAGAAGACCGGCAATGCAGGCGGCCGCATTGCCTGTGGTGTTATTGGCATCAAGTAAATATCCCTTCCAACGTGTCA
1180 1190 1200 1210 1220 1230 1240 1250 1260 1270 1280 1290 1300
SOD3v1 Bait F. GCCAAAGGGCGAATTCGACCCAGCTTTCTTGTACAAAGTGGTTTGATGGCCGCTAAGTAAGTAAGACGTCGAGCTCTAAGTAAGTAACGGCGCACGCGTGGAGCTTTGGACTTCTTCGCAGAGTTTGGTC
SOD3v1 Bait R. GCCAAAGGGCGAATTCGACCCAGCTTTCTTGTACAAAGTGGTTTGATGGCCGCTAAGTAAGTAAGACGTCGAGCTCTAAGTAAGTAACGGCCGCCACCGCGGTGGAGCTTTGGACTCTCGCCAGAGGTGA
1310 1320 1330 1340 1350 1360 1370 1380 1390 1400 1410 1420 1430
SOD3v1 Bait F. AGTCTCATCAGTGTCGCTGTCTACCTTGCAGAATTTACGAAAAGATGAAAAGTCAAATCGTGTAGATACGTGTGAACTCTAAATAGCGATTCTTATGATTATGATTTTATTATTAAATAGTTAAAAAATA
SOD3v1 Bait R. CG
1440 1450 1460 1470 1480 1490
SOD3v1 Bait F. GGTTACCACTAAAGTGACCTAGTTTAAACGAATTCCTTATTCCTGGAGAAAAGCCTTTTCG
SOD3v1 Bait R.

**Appendix 7. Sequencing of the SOD3v1 Prey construct.**

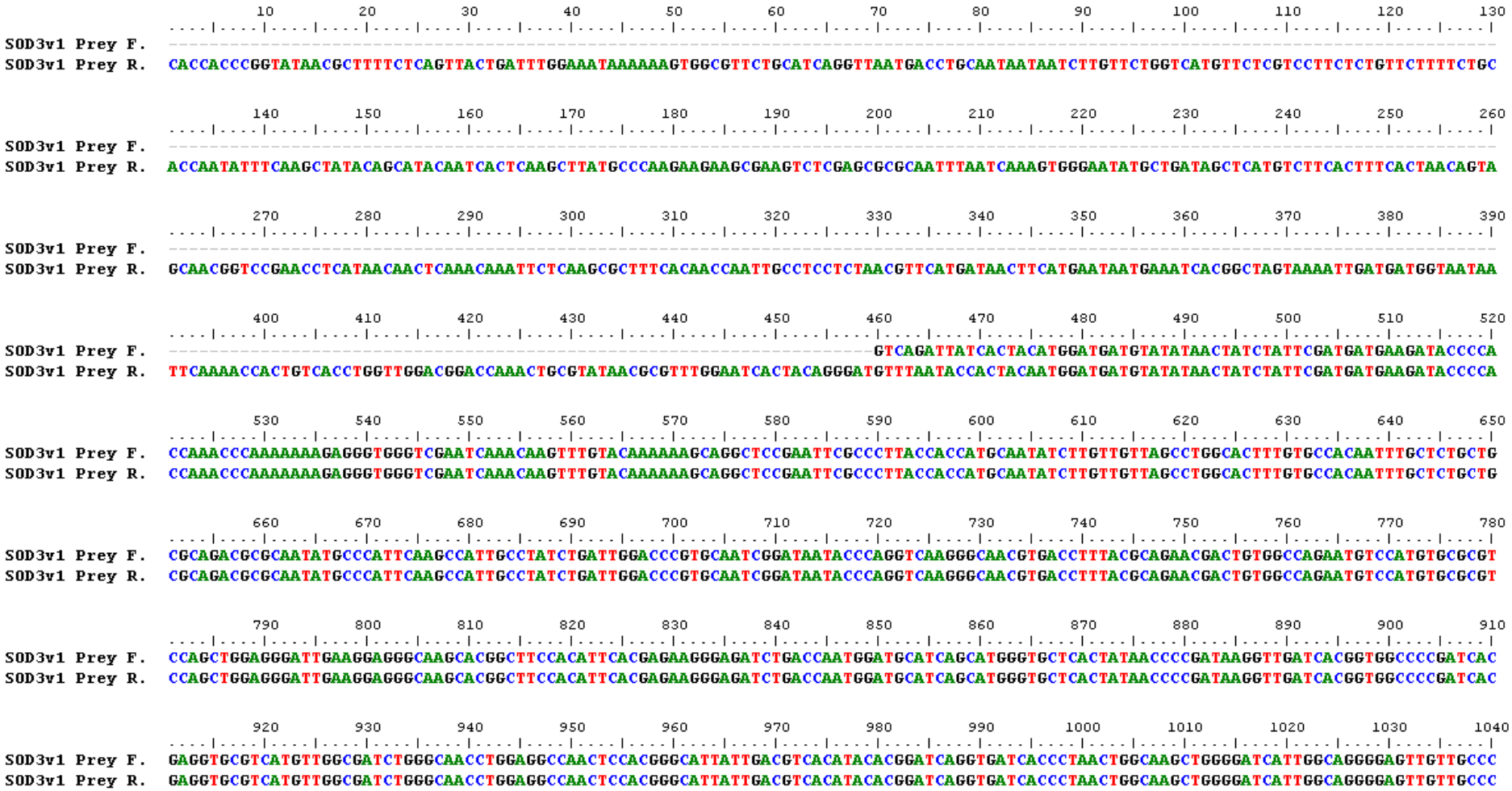

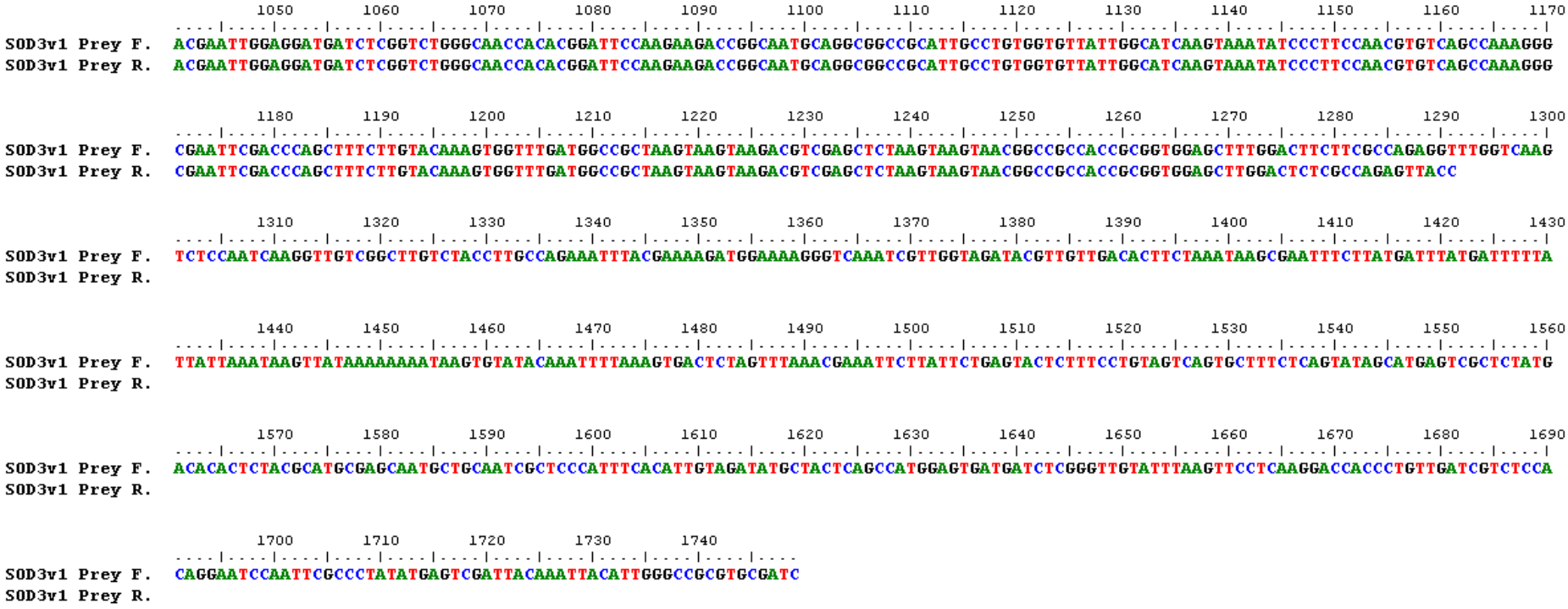
1050 1060 1070 1080 1090 1100 1110 1120 1130 1140 1150 1160 1170
SOD3v1 Prey F. ACGAATTGGAGGATGATCTCGGTCTGGGCAACCACACGGATTCCAAGAAGACCGGCAATGCAGGCGGCCGCATTGCCTGTGGTGTTATTGGCATCAAGTAAATATCCCTTCCAACGTGTCAGCCAAAGGG
SOD3v1 Prey R. ACGAATTGGAGGATGATCTCGGTCTGGGCAACCACACGGATTCCAAGAAGACCGGCAATGCAGGCGGCCGCATTGCCTGTGGTGTTATTGGCATCAAGTAAATATCCCTTCCAACGTGTCAGCCAAAGGG
1180 1190 1200 1210 1220 1230 1240 1250 1260 1270 1280 1290 1300
SOD3v1 Prey F. CGAATTCGACCCAGCTTTCTTGTACAAAGTGGTTTGATGGCCGCTAAGTAAGTAAGACGTCGAGCTCTAAGTAAGTAACGGCCGCCACCGCGGTGGAGCTTTGGACTTCTTCGCCAGAGGTTTGGTCAAG
SOD3v1 Prey R. CGAATTCGACCCAGCTTTCTTGTACAAAGTGGTTTGATGGCCGCTAAGTAAGTAAGACGTCGAGCTCTAAGTAAGTAACGGCCGCCACCGCGGTGGAGCTTGGACTCTCGCCAGAGTTACC
1310 1320 1330 1340 1350 1360 1370 1380 1390 1400 1410 1420 1430
SOD3v1 Prey F. TCTCCAATCAAGGTTGTCGGCTTGTCTACCTTGCCAGAAATTTACGAAAAGATGGAAAAGGGTCAAATCGTTGGTAGATACGTTGTTGACACTTCTAAATAAGCGAATTTCTTATGATTTATGATTTTTA
SOD3v1 Prey R.
1440 1450 1460 1470 1480 1490 1500 1510 1520 1530 1540 1550 1560
SOD3v1 Prey F. TTATTAAATAAGTTATAAAAAAAAATAAGTGTATACAAATTTTAAAGTGACTCTAGTTTAAACGAAATTCTTATTCTGAGTACTCTTTCCTGTAGTCAGTGCTTTCTCAGTATAGCATGAGTCGCTCTATG
SOD3v1 Prey R.
1570 1580 1590 1600 1610 1620 1630 1640 1650 1660 1670 1680 1690
SOD3v1 Prey F. ACACACTCTACGCATGCGAGCAATGCTGCAATCGCTCCCATTTCACATTGTAGATATGCTACTCAGCCATGGAGTGATGATCTCGGGTTGTATTTAAGTTCCTCAAGGACCACCCTGTTGATCGTCTCCA
SOD3v1 Prey R.
1700 1710 1720 1730 1740
SOD3v1 Prey F. CAGGAATCCAATTCGCCCTATATGAGTCGATTACAAATTACATTGGGCCGCGTGCGATC
SOD3v1 Prey R.

## Appendix 8. Sequencing of the SOD3v2 Bait construct.

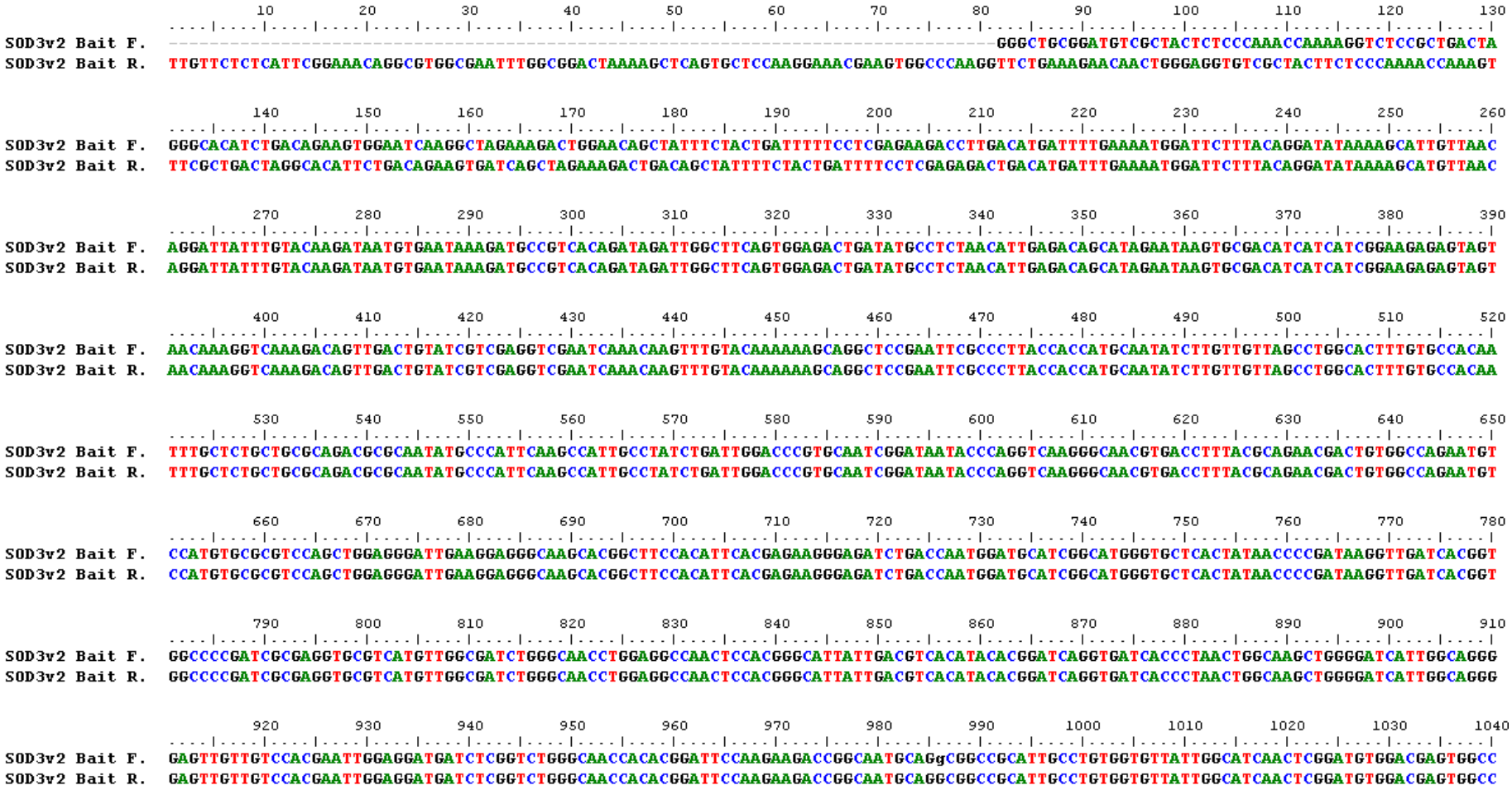

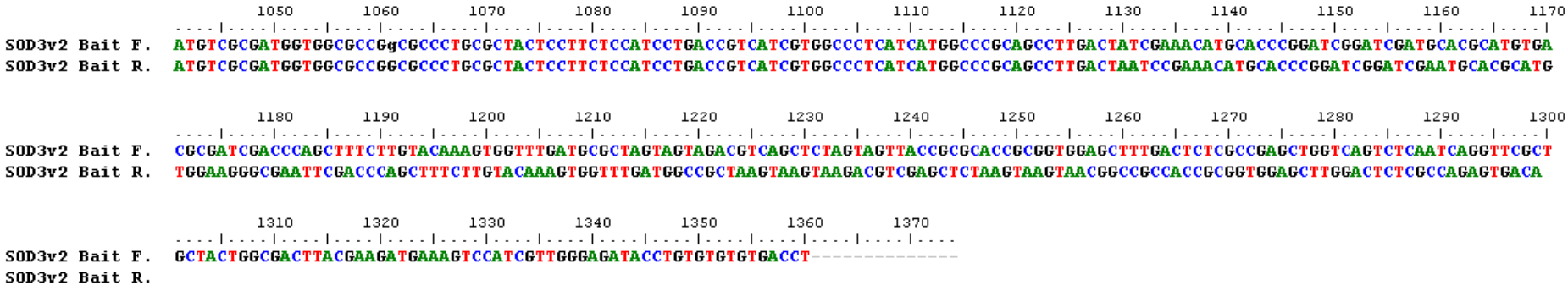
1050 1060 1070 1080 1090 1100 1110 1120 1130 1140 1150 1160 1170
SOD3v2 Bait F. ATGTCGCGATGGTGGCGCCGgCGCCCTGCGCTACTCCTTCTCCATCCTGACCGTCATCGTGGCCCTCATCATGGCCCGCAGCCTTGACTATCGAAACATGCACCCGGATCGGATCGATGCACGCATGTGA
SOD3v2 Bait R. ATGTCGCGATGGTGGCGCCGGCGCCCTGCGCTACTCCTTCTCCATCCTGACCGTCATCGTGGCCCTCATCATGGCCCGCAGCCTTGACTAATCCGAAACATGCACCCGGATCGGATCGAATGCACGCATG
1180 1190 1200 1210 1220 1230 1240 1250 1260 1270 1280 1290 1300
SOD3v2 Bait F. CGCGATCGACCCAGCTTTCTTGTACAAAGTGGTTTGATGCGCTAGTAGTAGACGTCAGCTCTAGTAGTTACCGCGCACCGCGGTGGAGCTTTGACTCTCGCCGAGCTGGTCAGTCTCAATCAGGTTCGCT
SOD3v2 Bait R. TGGAAGGGCGAATTCGACCCAGCTTTCTTGTACAAAGTGGTTTGATGGCCGCTAAGTAAGTAAGACGTCGAGCTCTAAGTAAGTAACGGCCGCCACCGCGGTGGAGCTTGGACTCTCGCCAGAGTGACA
1310 1320 1330 1340 1350 1360 1370
SOD3v2 Bait F. GCTACTGGCGACTTACGAAGATGAAAGTCCATCGTTGGGAGATACCTGTGTGTGTGACCT
SOD3v2 Bait R.

## Appendix 9. Sequencing of the SOD3v2 Prey construct.

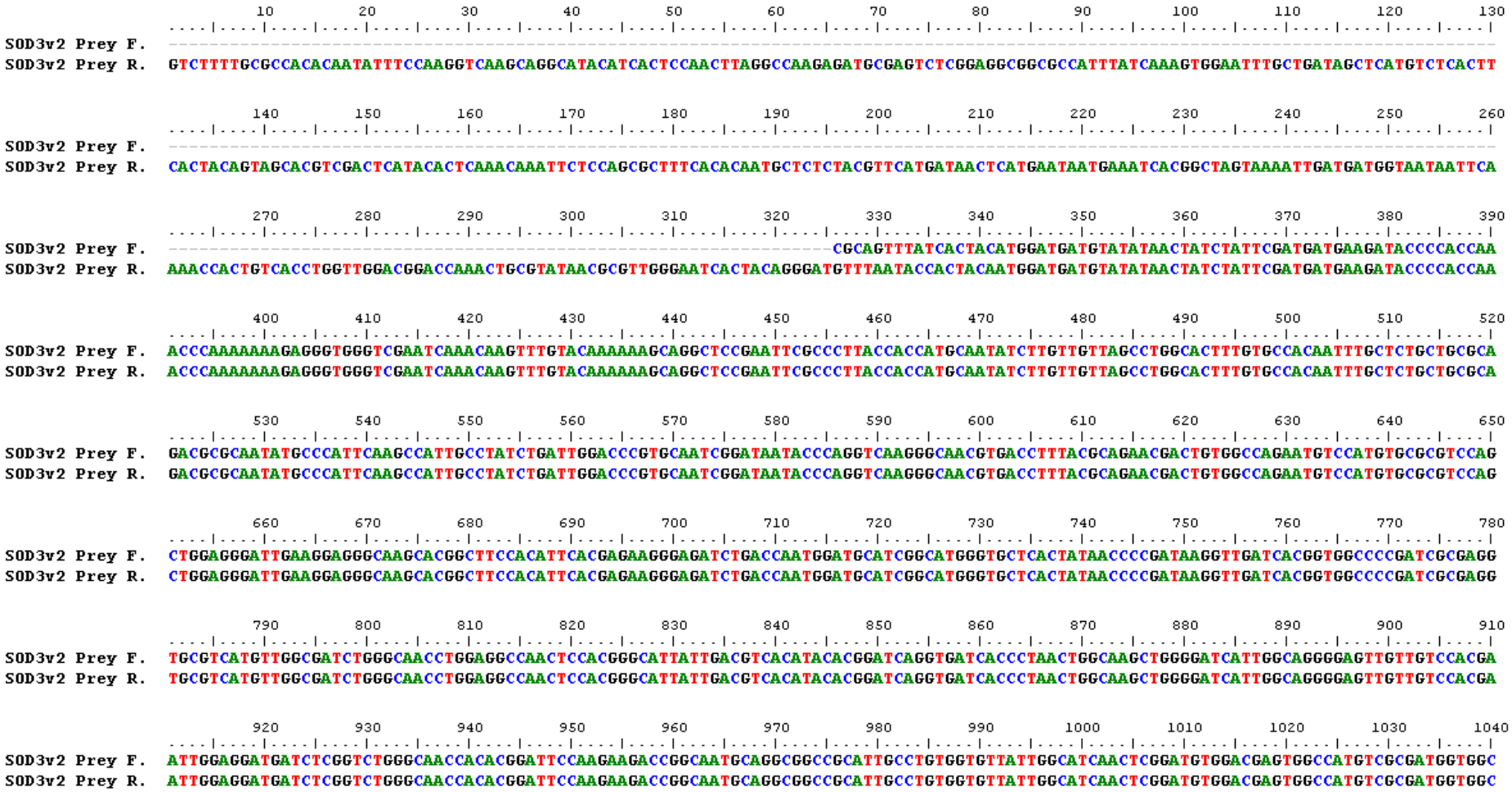

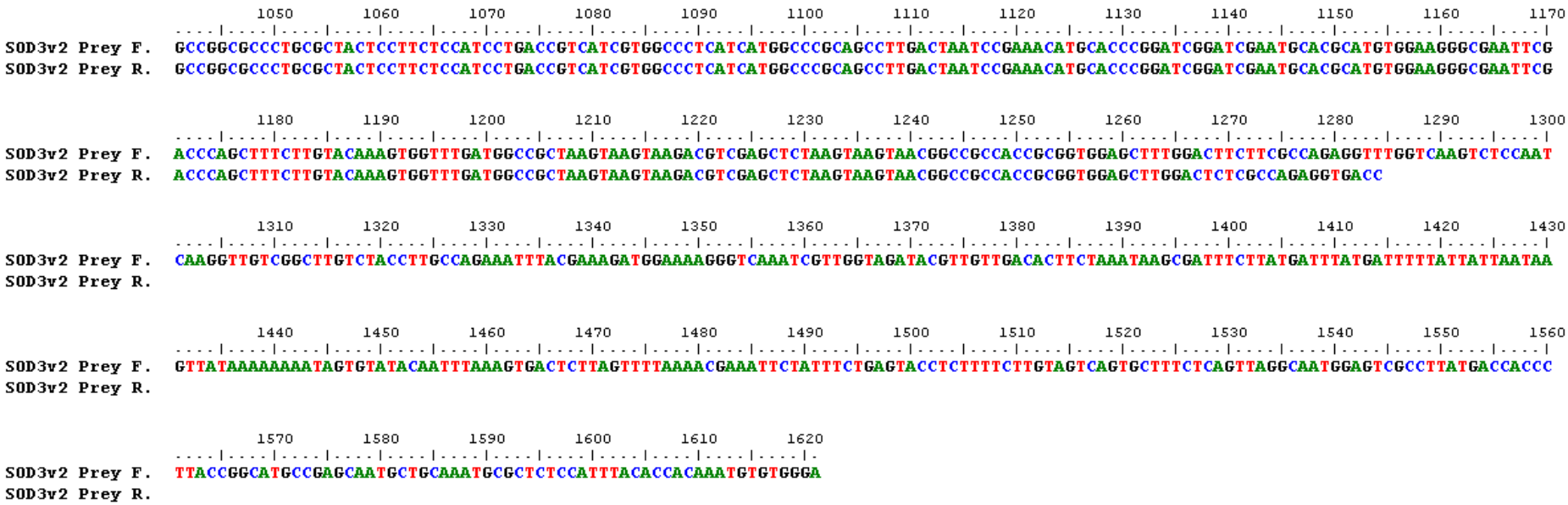
1050 1060 1070 1080 1090 1100 1110 1120 1130 1140 1150 1160 1170
SOD3v2 Prey F. GCCGGCGCCCTGCGCTACTCCTTCTCCATCCTGACCGTCATCGTGGCCCTCATCATGGCCCGCAGCCTTGACTAATCCGAAACATGCACCCGGATCGGATCGAATGCACGCATGTGGAAGGGCGAATTCG
SOD3v2 Prey R. GCCGGCGCCCTGCGCTACTCCTTCTCCATCCTGACCGTCATCGTGGCCCTCATCATGGCCCGCAGCCTTGACTAATCCGAAACATGCACCCGGATCGGATCGAATGCACGCATGTGGAAGGGCGAATTCG
1180 1190 1200 1210 1220 1230 1240 1250 1260 1270 1280 1290 1300
SOD3v2 Prey F. ACCCAGCTTTCTTGTACAAAGTGGTTTGATGGCCGCTAAGTAAGTAAGACGTCGAGCTCTAAGTAAGTAACGGCCGCCACCGCGGTGGAGCTTTGGACTTCTTCGCCAGAGGTTTGGTCAAGTCTCCAAT
SOD3v2 Prey R. ACCCAGCTTTCTTGTACAAAGTGGTTTGATGGCCGCTAAGTAAGTAAGACGTCGAGCTCTAAGTAAGTAACGGCCGCCACCGCGGTGGAGCTTGGACTCTCGCCAGAGGTGACC
1310 1320 1330 1340 1350 1360 1370 1380 1390 1400 1410 1420 1430
SOD3v2 Prey F. CAAGGTTGTCGGCTTGTCTACCTTGCCAGAAATTTACGAAAGATGGAAAAGGGTCAAATCGTTGGTAGATACGTTGTTGACACTTCTAAATAAGCGATTTCTTATGATTTATGATTTTTATTATTAATAA
SOD3v2 Prey R.
1440 1450 1460 1470 1480 1490 1500 1510 1520 1530 1540 1550 1560
SOD3v2 Prey F. GTTATAAAAAAAATAGTGTATACAATTTAAAGTGACTCTTAGTTTTAAAACGAAATTCTATTTCTGAGTACCTCTTTTCTTGTAGTCAGTGCTTTCTCAGTTAGGCAATGGAGTCGCCTTATGACCACCC
SOD3v2 Prey R.
1570 1580 1590 1600 1610 1620
SOD3v2 Prey F. TTACCGGCATGCCGAGCAATGCTGCAAATGCGCTCTCCATTTACACCACAAATGTGTGGGA
SOD3v2 Prey R.

References

Adachi, T., Nakamura, M., Yamada, H., Futenma, A., kato, K., & Hirano, K. 1994. Quantitative and qualitative changes of extracellular-superoxide dismutase in patients with various diseases. *Clin.Chim.Acta*, 229, (1-2) 123-131

Adams, M.D., Celniker, S.E., Holt, R.A., Evans, C.A., Gocayne, J.D., Amanatides, P.G., Scherer, S.E., Li, P.W., Hoskins, R.A., Galle, R.F., George, R.A., Lewis, S.E., Richards, S., Ashburner, M., Henderson, S.N., Sutton, G.G., Wortman, J.R., Yandell, M.D., Zhang, Q., Chen, L.X., Brandon, R.C., Rogers, Y.H., Blazej, R.G., Champe, M., Pfeiffer, B.D., Wan, K.H., Doyle, C., Baxter, E.G., Helt, G., Nelson, C.R., Gabor, G.L., Abril, J.F., Agbayani, A., An, H.J., Andrews-Pfannkoch, C., Baldwin, D., Ballew, R.M., Basu, A., Baxendale, J., Bayraktaroglu, L., Beasley, E.M., Beeson, K.Y., Benos, P.V., Berman, B.P., Bhandari, D., Bolshakov, S., Borkova, D., Botchan, M.R., Bouck, J., Brokstein, P., Brottier, P., Burtis, K.C., Busam, D.A., Butler, H., Cadieu, E., Center, A., Chandra, I., Cherry, J.M., Cawley, S., Dahlke, C., Davenport, L.B., Davies, P., de, P.B., Delcher, A., Deng, Z., Mays, A.D., Dew, I., Dietz, S.M., Dodson, K., Doup, L.E., Downes, M., Dugan-Rocha, S., Dunkov, B.C., Dunn, P., Durbin, K.J., Evangelista, C.C., Ferraz, C., Ferriera, S., Fleischmann, W., Fosler, C., Gabrielian, A.E., Garg, N.S., Gelbart, W.M., Glasser, K., Glodek, A., Gong, F., Gorrell, J.H., Gu, Z., Guan, P., Harris, M., Harris, N.L., Harvey, D., Heiman, T.J., Hernandez, J.R., Houck, J., Hostin, D., Houston, K.A., Howland, T.J., Wei, M.H., Ibegwam, C., Jalali, M., Kalush, F., Karpen, G.H., Ke, Z., Kennison, J.A., Ketchum, K.A., Kimmel, B.E., Kodira, C.D., Kraft, C., Kravitz, S., Kulp, D., Lai, Z., Lasko, P., Lei, Y., Levitsky, A.A., Li, J., Li, Z., Liang, Y., Lin, X., Liu, X., Mattei, B., McIntosh, T.C., McLeod, M.P., McPherson, D., Merkulov, G., Milshina, N.V., Mobarry, C., Morris, J., Moshrefi, A., Mount, S.M., Moy, M., Murphy, B., Murphy, L., Muzny, D.M., Nelson, D.L., Nelson, D.R., Nelson, K.A., Nixon, K., Nusskern, D.R., Pacleb, J.M., Palazzolo, M., Pittman, G.S., Pan, S., Pollard, J., Puri, V., Reese, M.G., Reinert, K., Remington, K., Saunders, R.D., Scheeler, F., Shen, H., Shue, B.C., Siden-Kiamos, I., Simpson, M., Skupski, M.P., Smith, T., Spier, E., Spradling, A.C., Stapleton, M., Strong, R., Sun, E., Svirskas, R., Tector, C., Turner, R., Venter, E., Wang, A.H., Wang, X., Wang, Z.Y., Wassarman, D.A., Weinstock, G.M., Weissenbach, J., Williams, S.M., WoodageT, Worley, K.C., Wu, D., Yang, S., Yao,

Q.A., Ye, J., Yeh, R.F., Zaveri, J.S., Zhan, M., Zhang, G., Zhao, Q., Zheng, L., Zheng, X.H., Zhong, F.N., Zhong, W., Zhou, X., Zhu, S., Zhu, X., Smith, H.O., Gibbs, R.A., Myers, E.W., Rubin, G.M., & Venter, J.C. 2000. The genome sequence of *Drosophila melanogaster*. *Science*, 287, (5461) 2185-2195

Adams, M.D. & Sekelsky, J.J. 2002. From sequence to phenotype: reverse genetics in Drosophila melanogaster. *Nat.Rev.Genet.*, 3, (3) 189-198

Aksenov, M.Y., Aksenova, M.V., Butterfield, D.A., Geddes, J.W., & Markesbery, W.R. 2001. Protein oxidation in the brain in Alzheimer's disease. *Neuroscience*, 103, (2) 373-383

Al-Chalabi, A., Andersen, P.M., Chioza, B., Shaw, C., Sham, P.C., Robberecht, W., Matthijs, G., Camu, W., Marklund, S.L., Forsgren, L., Rouleau, G., Laing, N.G., Hurse, P.V., Siddique, T., Leigh, P.N., & Powell, J.F. 1998. Recessive amyotrophic lateral sclerosis families with the D90A SOD1 mutation share a common founder: evidence for a linked protective factor. *Hum.Mol.Genet.*, 7, (13) 2045-2050

Allen, R.G., Farmer, K.J., Newton, R.K., & Sohal, R.S. 1984. Effects of paraquat administration on longevity, oxygen consumption, lipid peroxidation, superoxide dismutase, catalase, glutathione reductase, inorganic peroxides and glutathione in the adult housefly. *Comp.Biochem.Phys C*, 78, (2) 283-288

Ames, B.N., Cathcart, R., Schwiers, E., & Hochstein, P. 1981. Uric acid provides an antioxidant defense in humans against oxidant- and radical-caused aging and cancer: a hypothesis. *Proc.Natl.Acad.Sci.U.S.A*, 78, (11) 6858-6862

Amici, A., Levine, R.L., Tsai, L., & Stadtman, E.R. 1989. Conversion of amino acid residues in proteins and amino acid homopolymers to carbonyl derivatives by metal-catalyzed oxidation reactions. *J.Biol.Chem.*, 264, (6) 3341-3346

Andziak, B., O'connor, T.P., & Buffenstein, R. 2005. Antioxidants do not explain the disparate longevity between mice and the longest-living rodent, the naked mole-rat. *Mech.Ageing Dev.*, 126, (11) 1206-1212

Antunes, F., Han, D., & Cadenas, E. 2002. Relative contributions of heart mitochondria glutathione peroxidise and catalase to $H_2O_2$ detoxification in *in vivo* conditions. *Free Radic.Biol.Med*., 33, (9) 1260-1267

Aratani, Y., Koyama, H., Nyui, S., Suzuki, K., Kura, F., & Maeda, N. 1999. Severe impairment in early host defense against Candida albicans in mice deficient in myeloperoxidase. *Infect.Immun.*, 67, (4) 1828-1836

Aratani, Y., Kura, F., Watanabe, H., Akagawa, H., Takano, Y., Suzuki, K., Maeda, N., & Koyama, H. 2000. Differential host susceptibility to pulmonary infections with bacteria and fungi in mice deficient in myeloperoxidase. *J.Infect.Dis.*, 182, (4) 1276-1279

Arking, R. 1987. Successful selection for increased longevity in *Drosophila*: analysis of the survival data and presentation of a hypothesis on the genetic regulation of longevity. *Exp.Gerontol*., 22, (3) 199-220

Arking, R., Buck, S., Berrios, A., Dwyer, S., & Baker, G.T. 1991. Elevated paraquat resistance can be used as a bioassay for longevity in a genetically based long-lived strain of *Drosophila*. *Dev.Genet.*, 12, (5) 362-370

Arking, R., Burde, V., Graves, K., Hari, R., Feldman, E., Zeevi, A., Soliman, S., Saraiya, A., Buck, S., Vettraino, J., Sathrasala, K., Wehr, N., & Levine, R.L. 2000. Forward and reverse selection for longevity in *Drosophil*a is characterized by alteration of antioxidant gene expression and oxidative damage patterns. *Exp.Gerontol*., 35, (2) 167-185

Asikainen, T.M., Huang, T.T., Taskinen, E., Levonen, A.L., Carlson, E., Lapatto, R., Epstein, C.J., & Raivio, K.O. 2002. Increased sensitivity of homozygous Sod2 mutant mice to oxygen toxicity. *Free Radic.Biol Med*., 32, (2) 175-186

Auten, R.L., O'Reilly, M.A., Oury, T.D., Nozik-Grayck, E., & Whorton, M.H. 2006. Transgenic extracellular superoxide dismutase protects postnatal alveolar epithelial

proliferation and development during hyperoxia. *Am.J Physiol Lung Cell Mol.Physiol*., 290, (1) L32-L40

Babior, B.M., Kipnes, R.S., & Curnutte, J.T. 1973. Biological defense mechanisms. The production by leukocytes of superoxide, a potential bactericidal agent. *J.Clin.Invest.*, 52, (3) 741-744

Back, P., Matthijssens, F., Vlaeminck, C., Braeckman, B.P., & Vanfleteren, J. 2010. Effects of sod gene overexpression and deletion mutation on the expression profiles of reporter genes of major detoxification pathways in *Caenorhabditis elegans*. *Exp.Gerontol.*, 45, (7-8) 603-610

Bae, Y.S., Kang, S.W., Seo, M.S., Baines, I.C., Tekle, E., Chock, P.B., & Rhee, S.G. 1997. Epidermal Growth Factor (EGF)-induced generation of hydrogen peroxide. *J.Biol.Chem.*, 272, (1) 217-221

Barra, D., Schinina, M.E., Simmaco, M., Bannister, J.V., Bannister, W.H., Rotilio, G., & Bossa, F. 1984. The primary structure of human liver manganese superoxide dismutase. *J.Biol.Chem.*, 259, (20) 12595-12601

Bates, T.E., Loesch, A., Burnstock, G., & Clark, J.B. 1995. Immunocytochemical evidence for a mitochondrially located nitric oxide synthase in brain and liver. *Biochem.Biophys.Res.Co.*, 213, (3) 896-900

Bayne, A.C., Mockett, R.J., Orr, W.C., & Sohal, R.S. 2005. Enhanced catabolism of mitochondrial superoxide/hydrogen peroxide and aging in transgenic *Drosophila*. *Biochem.J.*, 391, (Pt 2) 277-284

Beauchamp, C. & Fridovich, I. 1971. Superoxide dismutase: improved assays and an assay applicable to acrylamide gels. *Anal.Biochem*., 44, (1) 276-287

Beckman, K.B. & AMES, B.N. 1998. The Free Radical Theory of Aging Matures. *Physiol.Rev.*, 78, (2) 547-581

Bellen, H.J., Levis, R.W., Liao, G., He, Y., Carlson, J.W., Tsang, G., Evans-Holm, M., Hiesinger, P.R., Schulze, K.L., Rubin, G.M., Hoskins, R.A., & Spradling, A.C. 2004a. The BDGP gene disruption project: single transposon insertions associated with 40% of *Drosophila* genes. *Genetics*, 167, (2) 761-781

Benjamin, I.J. & McMillan, D.R. 1998. Stress (heat shock) proteins: molecular chaperones in cardiovascular biology and disease. *Circ.Res.*, 83, (2) 117-132

Best, C.J., Gillespie, J.W., Yi, Y., Chandramouli, G.V., Perlmutter, M.A., Gathright, Y., Erickson, H.S., Georgevich, L., Tangrea, M.A., Duray, P.H., Gonzalez, S., Velasco, A., Linehan, W.M., Matusik, R.J., Price, D.K., Figg, W.D., Emmert-Buck, M.R., & Chuaqui, R.F. 2005. Molecular alterations in primary prostate cancer after androgen ablation therapy. *Clin.Cancer Res.*, 11, (19 Pt 1) 6823-6834

Biswas, D.K., Shi, Q., Baily, S., Strickland, I., Ghosh, S., Pardee, A.B., & Iglehart, J.D. 2004. NF-kappa B activation in human breast cancer specimens and its role in cell proliferation and apoptosis. *Proc.Natl.Acad.Sci.U.S.A*, 101, (27) 10137-10142

Brand, A.H. & Perrimon, N. 1993. Targeted gene expression as a means of altering cell fates and generating dominant phenotypes. *Development*, 118, (2) 401-415

Brown, G.C. & Borutaite, V. 2004. Inhibition of mitochondrial respiratory complex I by nitric oxide, peroxynitrite and S-nitrosothiols. *Biochim.Biophys.Acta*, 1658, (1-2) 44-49

Brownlee, M. 2001. Biochemistry and molecular cell biology of diabetic complications. *Nature*, 414, (6865) 813-820

Brzezinska, A.K., Gebremedhin, D., Chilian, W.M., Kalyanaraman, B., & Elliott, S.J. 2000. Peroxynitrite reversibly inhibits Ca(2+)-activated K(+) channels in rat cerebral artery smooth muscle cells. *Am.J Physiol Heart Circ.Physiol.*, 278, (6) H1883-H1890

Burney, S., Caulfield, J.L., Niles, J.C., Wishnok, J.S., & Tannenbaum, S.R. 1999. The chemistry of DNA damage from nitric oxide and peroxynitrite. *Mutat.Res.*, 424, (1-2) 37-49

Busuttil, R.A., Garcia, A.M., Cabrera, C., Rodriguez, A., Suh, Y., Kim, W.H., Huang, T.T., & Vijg, J. 2005. Organ-specific increase in mutation accumulation and apoptosis rate in CuZn-superoxide dismutase-deficient mice. *Cancer Res.*, 65, (24) 11271-11275

Butterfield, D.A., Castegna, A., Lauderback, C.M., & Drake, J. 2002. Evidence that amyloid beta-peptide-induced lipid peroxidation and its sequelae in Alzheimer's disease brain contribute to neuronal death. *Neurobiol.Aging*, 23, (5) 655-664

Cadenas, E. & Davies, K.J.A. 2000. Mitochondrial free radical generation, oxidative stress, and aging. *Free Radic.Biol.Med.*, 29, (3-4) 222-230

Callio, J., Oury, T.D., & Chu, C.T. 2005. Manganese superoxide dismutase protects against 6-hydroxydopamine injury in mouse brains. *J.Biol.Chem.*, 280, (18) 18536-18542

Campbell, S.D., Hilliker, A.J., & Phillips, J.P. 1986. Cytogenetic analysis of the cSOD microregion in *Drosophila melanogaster*. *Genetics*, 112, (2) 205-215

Carlsson, L.M., Jonsson, J., Edlund, T., & Marklund, S.L. 1995. Mice lacking extracellular superoxide dismutase are more sensitive to hyperoxia. *Proc.Natl.Acad.Sci.U.S.A*, 92, (14) 6264-6268

Catarzi, S., Degl'Innocenti, D., Iantomasi, T., Favilli, F., & Vincenzini, M.T. 2002. The role of $H_2O_2$ in the platelet-derived growth factor-induced transcription of the gamma-glutamylcysteine synthetase heavy subunit. *Cell.Mol.Life.Sci.*, 59, (8) 1388-1394

Cayirlioglu, P., Bonnette, P.C., Dickson, M.R., & Duronio, R.J. 2001. *Drosophila* E2f2 promotes the conversion from genomic DNA replication to gene amplification in ovarian follicle cells. *Development*, 128, (24) 5085-5098

Chance, B., Sies, H., & Boveris, A. 1979. Hydroperoxide metabolism in mammalian organs. *Physiol.Rev.*, 59, (3) 527-605

Chang, L.Y., Slot, J.W., Geuze, H.J., & Crapo, J.D. 1988. Molecular immunocytochemistry of the CuZn superoxide dismutase in rat hepatocytes. *J.Cell Biol.*, 107, (6 Pt 1) 2169-2179

Chen, E.P., Bittner, H.B., Davis, R.D., Van, T.P., & Folz, R.J. 1998. Physiologic effects of extracellular superoxide dismutase transgene overexpression on myocardial function after ischemia and reperfusion injury. *J.Thorac.Cardiovasc.Surg.*, 115, (2) 450-458

Chien, C.T., Bartel, P.L., Sternglanz, R., & Fields, S. 1991. The two-hybrid system: a method to identify and clone genes for proteins that interact with a protein of interest. *Proc.Natl.Acad.Sci.U.S.A*, 88, (21) 9578-9582

Choi, Y.S., Lee, K.S., Yoon, H.J., Kim, I., Sohn, H.D., & Jin, B.R. 2006. *Bombus ignitus* Cu,Zn superoxide dismutase (SOD1): cDNA cloning, gene structure, and up-regulation in response to paraquat, temperature stress, or lipopolysaccharide stimulation. *Comp.Biochem.Phys.B*, 144, (3) 365-371

Clare, M. 1925. A study of oxygen metabolism in *Drosophila melanogaster*. The Biological Bulletin, 49, (6) 440-460

Clark, M.E., Anderson, C.L., Cande, J., & Karr, T.L. 2005. Widespread prevalence of wolbachia in laboratory stocks and the implications for *Drosophila* research. *Genetics*, 170, (4) 1667-1675

Corona, M., Velarde, R.A., Remolina, S., Moran-Lauter, A., Wang, Y., Hughes, K.A., & Robinson, G.E. 2007. Vitellogenin, juvenile hormone, insulin signaling, and queen honey bee longevity. *Proc.Natl.Acad.Sci U.S.A*, 104, (17) 7128-7133

Crapo, J.D., Oury, T., Rabouille, C., Slot, J.W., & Chang, L.Y. 1992. Copper,zinc superoxide dismutase is primarily a cytosolic protein in human cells. *Proc.Natl.Acad.Sci.U.S.A*, 89, (21) 10405-10409

Csiszar, A., Labinskyy, N., Zhao, X., Hu, F., Serpillon, S., Huang, Z., Ballabh, P., Levy, R.J., Hintze, T.H., Wolin, M.S., Austad, S.N., Podlutsky, A., & Ungvari, Z. 2007. Vascular superoxide and hydrogen peroxide production and oxidative stress resistance in two closely related rodent species with disparate longevity. *Aging Cell*, 6, (6) 783-797

Cullen, J.J., Weydert, C., Hinkhouse, M.M., Ritchie, J., Domann, F.E., Spitz, D., & Oberley, L.W. 2003. The role of manganese superoxide dismutase in the growth of pancreatic adenocarcinoma. *Cancer Res*., 63, (6) 1297-1303

Culotta, V.C., Yang, M., & O'Halloran, T.V. 2006. Activation of superoxide dismutases: putting the metal to the pedal. *Biochim.Biophys.Acta*, 1763, (7) 747-758

Culotta, V.C., Klomp, L.W., Strain, J., Casareno, R.L., Krems, B., & Gitlin, J.D. 1997. The copper chaperone for superoxide dismutase. *J.Biol.Chem.*, 272, (38) 23469-23472

Dean, M.D. 2006. A Wolbachia-associated fitness benefit depends on genetic background in *Drosophila simulans*. *Proc.Biol.Sci*., 273, (1592) 1415-1420

Dean, R.T., Fu, S., Stocker, R., & Davies, M.J. 1997. Biochemistry and pathology of radical-mediated protein oxidation. *Biochem.J*, 324 ( Pt 1), 1-18

Demchenko, I.T., Gutsaeva, D.R., Moskvin, A.N., & Zhilyaev, S.Y. 2010. Involvement of extracellular superoxide dismutase in regulating brain blood flow. *Neurosci.Behav.Physiol.*, 40, (2) 173-178

Dizdaroglu, M., Jaruga, P., Birincioglu, M., & Rodriguez, H. 2002. Free radical-induced damage to DNA: mechanisms and measurement. *Free Radic.Biol Med.*, 32, (11) 1102-1115

Doonan, R., McElwee, J.J., Matthijssens, F., Walker, G.A., Houthoofd, K., Back, P., Matscheski, A., Vanfleteren, J.R., & Gems, D. 2008. Against the oxidative damage theory of aging: superoxide dismutases protect against oxidative stress but have little or no effect on life span in *Caenorhabditis elegans*. *Gene Dev.*, 22, (23) 3236-3241

Dougall, W.C. & Nick, H.S. 1991. Manganese superoxide dismutase: a hepatic acute phase protein regulated by interleukin-6 and glucocorticoids. *Endocrinology*, 129, (5) 2376-2384

Droge, W. 2002. Free radicals in the physiological control of cell function. *Physiol.Rev.*, 82, (1) 47-95

Dubrac, S. & Touati, D. 2002. Fur-mediated transcriptional and post-transcriptional regulation of FeSOD expression in *Escherichia coli*. *Microbiology*, 148, (Pt 1) 147-156

Dudas, S.P. & Arking, R. 1995. A coordinate upregulation of antioxidant gene activities is associated with the delayed onset of senescence in a long-lived strain of *Drosophila*. *J.Gerontol.A Biol.Sci.Med.Sci.*, 50, (3) B117-B127

Duttaroy, A., Paul, A., Kundu, M., & Belton, A. 2003. A Sod2 null mutation confers severely reduced adult life span in *Drosophila*. *Genetics*, 165, (4) 2295-2299

Dworkin, I., Kennerly, E., Tack, D., Hutchinson, J., Brown, J., Mahaffey, J., & Gibson, G. 2009. Genomic consequences of background effects on scalloped mutant expressivity in the wing of *Drosophila melanogaster. Genetics*, 181, (3) 1065-1076

Elam, J.S., Taylor, A.B., Strange, R., Antonyuk, S., Doucette, P.A., Rodriguez, J.A., Hasnain, S.S., Hayward, L.J., Valentine, J.S., Yeates, T.O., & Hart, P.J. 2003.

Amyloid-like filaments and water-filled nanotubes formed by SOD1 mutant proteins linked to familial ALS. *Nat.Struct.Biol.*, 10, (6) 461-467

Elchuri, S., Oberley, T.D., Qi, W., Eisenstein, R.S., Jackson Roberts, L., Van Remmen, H., Epstein, C.J., & Huang, T.T. 2004. CuZnSOD deficiency leads to persistent and widespread oxidative damage and hepatocarcinogenesis later in life. *Oncogene*, 24, (3) 367-380

Elfering, S.L., Sarkela, T.M., & Giulivi, C. 2002. Biochemistry of mitochondrial nitric-oxide synthase. *J.Biol.Chem.*, 277, (41) 38079-38086

Elia, A.J., Parkes, T.L., Kirby, K., St George-Hyslop, P., Boulianne, G.L., Phillips, J.P., & Hilliker, A.J. 1999. Expression of human FALS SOD in motorneurons of *Drosophila*. *Free Radic.Biol.Med.*, 26, (9-10) 1332-1338

Farrington, J.A., Ebert, M., Land, E.J., & Fletcher, K. 1973. Bipyridylium quaternary salts and related compounds. V. Pulse radiolysis studies of the reaction of paraquat radical with oxygen. Implications for the mode of action of bipyridyl herbicides. *Biochim.Biophys.Acta*, 314, (3) 372-381

Fattman, C.L., Chu, C.T., Kulich, S.M., Enghild, J.J., & Oury, T.D. 2001. Altered expression of extracellular superoxide dismutase in mouse lung after bleomycin treatment. *Free Radic.Biol Med.*, 31, (10) 1198-1207

Fattman, C.L., Schaefer, L.M., & Oury, T.D. 2003. Extracellular superoxide dismutase in biology and medicine. *Free Radic.Biol.Med.*, 35, (3) 236-256

Feany, M.B. & Bender, W.W. 2000. A *Drosophila* model of Parkinson's disease. *Nature*, 404, (6776) 394-398

Field, L.S., Furukawa, Y., O'Halloran, T.V., & Culotta, V.C. 2003. Factors controlling the uptake of yeast copper/zinc superoxide dismutase into mitochondria. *J.Biol.Chem.*, 278, (30) 28052-28059

Fields, S. & Song, O. 1989. A novel genetic system to detect protein-protein interactions. *Nature*, 340, (6230) 245-246

Fink, S.P., Reddy, G.R., & Marnett, L.J. 1997. Mutagenicity in *Escherichia coli* of the major DNA adduct derived from the endogenous mutagen malondialdehyde. *Proc.Natl.Acad.Sci.U.S.A*, 94, (16) 8652-8657

Folz, R.J., Abushamaa, A.M., & Suliman, H.B. 1999. Extracellular superoxide dismutase in the airways of transgenic mice reduces inflammation and attenuates lung toxicity following hyperoxia. *J.Clin.Invest.*, 103, (7) 1055-1066

Folz, R.J. & Crapo, J.D. 1994. Extracellular superoxide dismutase (SOD3): tissue-specific expression, genomic characterization, and computer-assisted sequence analysis of the human EC SOD gene. *Genomics*, 22, (1) 162-171

Folz, R.J., Guan, J., Seldin, M.F., Oury, T.D., Enghild, J.J., & Crapo, J.D. 1997. Mouse extracellular superoxide dismutase: primary structure, tissue-specific gene expression, chromosomal localization, and lung in situ hybridization. *Am.J.Respir.Cell Mol.Biol.*, 17, (4) 393-403

Force, A.G., Staples, T., Soliman, S., & Arking, R. 1995. Comparative biochemical and stress analysis of genetically selected *Drosophila* strains with different longevities. *Dev.Genet.*, 17, (4) 340-351

Frank, S., Kampfer, H., Podda, M., Kaufmann, R., & Pfeilschifter, J. 2000. Identification of copper/zinc superoxide dismutase as a nitric oxide-regulated gene in human (HaCaT) keratinocytes: implications for keratinocyte proliferation. *Biochem.J*, 346 Pt 3, 719-728

Frohman, M.A., Dush, M.K., & Martin, G.R. 1988. Rapid production of full-length cDNAs from rare transcripts: amplification using a single gene-specific oligonucleotide primer. *Proc.Natl.Acad.Sci.U.S.A*, 85, (23) 8998-9002

Frost, M.T., Wang, Q., Moncada, S., & Singer, M. 2005. Hypoxia accelerates nitric oxide-dependent inhibition of mitochondrial complex I in activated macrophages. *Am.J.Physiol.Regul.Integr.Comp.Physiol.*, 288, (2) R394-R400

Fujii, M., Ishii, N., Joguchi, A., Yasuda, K., & Ayusawa, D. 1998. A novel superoxide dismutase gene encoding membrane-bound and extracellular isoforms by alternative splicing in *Caenorhabditis elegans*. *DNA Res.*, 5, (1) 25-30

Fukai, T., Galis, Z.S., Meng, X.P., Parthasarathy, S., & Harrison, D.G. 1998. Vascular expression of extracellular superoxide dismutase in atherosclerosis. *J.Clin.Invest.*, 101, (10) 2101-2111

Fukai, T., Siegfried, M.R., Ushio-Fukai, M., Cheng, Y., Kojda, G., & Harrison, D.G. 2000. Regulation of the vascular extracellular superoxide dismutase by nitric oxide and exercise training. *J.Clin.Invest*, 105, (11) 1631-1639

Fukushima, T., Tanaka, K., Lim, H., & Moriyama, M. 2002. Mechanism of cytotoxicity of paraquat. *Environ.Health Prev.Med.*, 7, (3) 89-94

Furukawa, Y., Fu, R., Deng, H.X., Siddique, T., & O'Halloran, T.V. 2006. From the Cover: Disulfide cross-linked protein represents a significant fraction of ALS-associated Cu, Zn-superoxide dismutase aggregates in spinal cords of model mice. *Proc.Natl.Acad.Sci.U.S.A*, 103, (18) 7148-7153

Gabbianelli, R., Battistoni, A., Polizio, F., Carri, M.T., De, M.A., Meier, B., Desideri, A., & Rotilio, G. 1995. Metal uptake of recombinant cambialistic superoxide dismutase from Propionibacterium shermanii is affected by growth conditions of host *Escherichia coli* cells. *Biochem.Biophys.Res Commun.*, 216, (3) 841-847

Ganetzky, B. & Flanagan, J.R. 1978. On the relationship between senescence and age-related changes in two wild-type strains of *Drosophila melanogaster*. *Exp.Gerontol.*, 13, (3-4) 189-196

Gauhar, Z., Ghanim, M., Herreman, T., Lambert, J. D., Li, T. R., Mason, C., Rifkin, S., Sun, L., White, K. P., Costello, J. C., & Andrews, J. R. *Drosophila melanogaster* life-cycle gene expression dataset and microarray normalisation protocols. 2008. Ref Type: Personal Communication

Gems, D., Sutton, A.J., Sundermeyer, M.L., Albert, P.S., King, K.V., Edgley, M.L., Larsen, P.L., & Riddle, D.L. 1998. Two pleiotropic classes of daf-2 mutation affect larval arrest, adult behavior, reproduction and longevity in *Caenorhabditis elegans*. *Genetics*, 150, (1) 129-155

Ghafourifar, P. & Cadenas, E. 2005. Mitochondrial nitric oxide synthase. *Trends Pharmacol.Sci*., 26, (4) 190-195

Gibb, H.J., Lees, P.S., Pinsky, P.F., & Rooney, B.C. 2000. Lung cancer among workers in chromium chemical production. *Am.J Ind.Med.*, 38, (2) 115-126

Good, P.F., Hsu, A., Werner, P., Perl, D.P., & Olanow, C.W. 1998. Protein nitration in Parkinson's disease. *J.Neuropathol.Exp Neurol.*, 57, (4) 338-342

Gracy, R.W., Talent, J.M., Kong, Y., & Conrad, C.C. 1999. Reactive oxygen species: the unavoidable environmental insult? *Mutat.Res.*, 428, (1-2) 17-22

Groner, Y., Elroy-Stein, O., Avraham, K.B., Schickler, M., Knobler, H., Minc-Golomb, D., Bar-Peled, O., Yarom, R., & Rotshenker, S. 1994. Cell damage by excess CuZnSOD and Down's syndrome. *Biomed.Pharmacother.*, 48, (5-6) 231-240

Gu, W. & Hecht, N.R. 1996. Translation of a testis-specific Cu/Zn superoxide dismutase (SOD-1) mRNA is regulated by a 65-kilodalton protein which binds to its 5' untranslated region. *Mol.Cell Biol.*, 16, (8) 4535-4543

Gus'kova, R.A., Ivanov, I.I., Kol'tover, V.K., Akhobadze, V.V., & Rubin, A.B. 1984. Permeability of bilayer lipid membranes for superoxide (O2-.) radicals. *Biochim.Biophys.Acta*, 778, (3) 579-585

Hagglof, C., Hammarsten, P., Josefsson, A., Stattin, P., Paulsson, J., Bergh, A., & Ostman, A. 2010. Stromal PDGFRbeta expression in prostate tumors and non-malignant prostate tissue predicts prostate cancer survival. *PLoS One.*, 5, (5) e10747

Halfon, M.S., Gisselbrecht, S., Lu, J., Estrada, B., Keshishian, H., & Michelson, A.M. 2002. New fluorescent protein reporters for use with the *Drosophila* Gal4 expression system and for vital detection of balancer chromosomes. *Genesis.*, 34, (1-2) 135-138

Halliwell, B. & Gutteridge, J. 2007. Free Radicals in Biology and Medicine, 4 ed. Oxford University Press.

Hari, R., Burde, V., & Arking, R. 1998. Immunological confirmation of elevated levels of CuZn superoxide dismutase protein in an artificially selected long-lived strain of *Drosophila melanogaster*. *Exp.Gerontol.*, 33, (3) 227-237

Harman, D. 1956. Aging: a theory based on free radical and radiation chemistry. *J.Gerontol.*, 11, (3) 298-300

Hass, M.A. & Massaro, D. 1988. Regulation of the synthesis of superoxide dismutases in rat lungs during oxidant and hyperthermic stresses. *J.Biol.Chem.*, 263, (2) 776-781

Hevel, J.M., White, K.A., & Marletta, M.A. 1991. Purification of the inducible murine macrophage nitric oxide synthase. Identification as a flavoprotein. *J.Biol.Chem.*, 266, (34) 22789-22791

Hibbs, J.B., Jr., Vavrin, Z., & Taintor, R.R. 1987. L-arginine is required for expression of the activated macrophage effector mechanism causing selective metabolic inhibition in target cells. *J.Immunol.*, 138, (2) 550-565

Hiesinger, P.R. & Bellen, H.J. 2004. Flying in the face of total disruption. *Nat.Genet.*, 36, (3) 211-212

Hirsch, F.R., Scagliotti, G.V., Langer, C.J., Varella-Garcia, M., & Franklin, W.A. 2003. Epidermal growth factor family of receptors in preneoplasia and lung cancer: perspectives for targeted therapies. *Lung Cancer*, 41 Suppl 1, S29-S42

Hitchler, M.J., Wikainapakul, K., Yu, L., Powers, K., Attatippaholkun, W., & Domann, F.E. 2006. Epigenetic regulation of manganese superoxide dismutase expression in human breast cancer cells. *Epigenetics*, 1, (4) 163-171

Hitchler, M.J., Oberley, L.W., & Domann, F.E. 2008. Epigenetic silencing of SOD2 by histone modifications in human breast cancer cells. *Free Radic.Biol.Med.*, 45, (11) 1573-1580

Ho, Y.S., Gargano, M., Cao, J., Bronson, R.T., Heimler, I., & Hutz, R.J. 1998. Reduced fertility in female mice lacking copper-zinc superoxide dismutase. *J.Biol.Chem.*, 273, (13) 7765-7769

Ho, Y.S. 2002. Transgenic and knockout models for studying the role of lung antioxidant enzymes in defense against hyperoxia. *Am.J.Respir.Crit.Care Med.*, 166, (12) 51S-556

Hollstein, M., Sidransky, D., Vogelstein, B., & Harris, C.C. 1991. p53 mutations in human cancers. *Science*, 253, (5015) 49-53

Honda, Y., Tanaka, M., & Honda, S. 2008. Modulation of longevity and diapause by redox regulation mechanisms under the insulin-like signaling control in *Caenorhabditis elegans*. *Exp.Gerontol.*, 43, (6) 520-529

Hool, L.C. 2006. Reactive oxygen species in cardiac signalling: from mitochondria to plasma membrane ion channels. *Clin.Exp.Pharmacol.Physiol.*, 33, (1-2) 146-151

Hough, M.A., Grossmann, J.G., Antonyuk, S.V., Strange, R.W., Doucette, P.A., Rodriguez, J.A., Whitson, L.J., Hart, P.J., Hayward, L.J., Valentine, J.S., & Hasnain, S.S. 2004. Dimer destabilization in superoxide dismutase may result in disease-

causing properties: structures of motor neuron disease mutants. *Proc.Natl.Acad.Sci.U.S.A*, 101, (16) 5976-5981

Houthoofd, K., Braeckman, B.P., Johnson, T.E., & Vanfleteren, J.R. 2003. Life extension via dietary restriction is independent of the Ins/IGF-1 signalling pathway in *Caenorhabditis elegans*. *Exp.Gerontol.*, 38, (9) 947-954

Hu, D., Cao, P., Thiels, E., Chu, C.T., Wu, G.Y., Oury, T.D., & Klann, E. 2007. Hippocampal long-term potentiation, memory, and longevity in mice that overexpress mitochondrial superoxide dismutase. *Neurobiol.Learn.Mem.*, 87, (3) 372-384

Huang, T.T., Carlson, E.J., Gillespie, A.M., Shi, Y., & Epstein, C.J. 2000. Ubiquitous overexpression of CuZn superoxide dismutase does not extend life span in mice. *J.Gerontol.A Biol.Sci.Med.Sci.*, 55, (1) B5-B9

Iesaki, T. & Wolin, M.S. 2000. Thiol oxidation activates a novel redox-regulated coronary vasodilator mechanism involving inhibition of $Ca^{2+}$ influx. *Arterioscler.Thromb.Vasc.Biol*., 20, (11) 2359-2365

Jaarsma, D., Haasdijk, E.D., Grashorn, J.A., Hawkins, R., van, D.W., Verspaget, H.W., London, J., & Holstege, J.C. 2000. Human Cu/Zn superoxide dismutase (SOD1) overexpression in mice causes mitochondrial vacuolization, axonal degeneration, and premature motoneuron death and accelerates motoneuron disease in mice expressing a familial amyotrophic lateral sclerosis mutant SOD1. *Neurobiol.Dis.*, 7, (6 Pt B) 623-643

Jackson, R.M., Parish, G., & Ho, Y.S. 1996. Effects of hypoxia on expression of superoxide dismutases in cultured ATII cells and lung fibroblasts. *Am.J Physiol*., 271, (6 Pt 1) L955-L962

Jackson, S.M. & Cooper, J.B. 1998. An analysis of structural similarity in the iron and manganese superoxide dismutases based on known structures and sequences. *Biometals*, 11, (2) 159-173

Jaworska, A. & Rosiek, O. 1991. Paraquat increases superoxide dismutase activity and radiation resistance in two mouse lymphoma L5178Y cell strains of different radiosensitivities. *Int.J.Radiat.Biol.*, 60, (6) 899-906

Jeney, V., Itoh, S., Wendt, M., Gradek, Q., Ushio-Fukai, M., Harrison, D.G., & Fukai, T. 2005. Role of antioxidant-1 in extracellular superoxide dismutase function and expression. *Circ.Res.*, 96, (7) 723-729

Jenner, P. 1998. Oxidative mechanisms in nigral cell death in Parkinson's disease. *Mov.Disord.*, 13 Suppl 1, 24-34

Jenner, P. 2003. Oxidative stress in Parkinson's disease. *Ann.Neurol.*, 53 Suppl 3, S26-S36

Johnson, F. & Giulivi, C. 2005. Superoxide dismutases and their impact upon human health. *Mol.Aspects Med.*, 26, (4-5) 340-352

Jones, S.A., O'Donnell, V.B., Wood, J.D., Broughton, J.P., Hughes, E.J., & Jones, O.T. 1996. Expression of phagocyte NADPH oxidase components in human endothelial cells. *Am.J.Physiol.*, 271, (4 Pt 2) H1626-H1634

Kamata, H. & Hirata, H. 1999. Redox regulation of cellular signalling. *Cell Signal.*, 11, (1) 1-14

Kamata, H., Honda, S., Maeda, S., Chang, L., Hirata, H., & Karin, M. 2005. Reactive oxygen species promote TNFalpha-induced death and sustained JNK activation by inhibiting MAP kinase phosphatases. *Cell*, 120, (5) 649-661

Karlin, S. & McGregor, J. 1972. The evolutionary development of modifier genes. *Proc.Natl.Acad.Sci.U.S.A*, 69, (12) 3611-3614

Karlsson, K., Lindahl, U., & Marklund, S.L. 1988. Binding of human extracellular superoxide dismutase C to sulphated glycosaminoglycans. *Biochem.J*, 256, (1) 29-33

Karlsson, K. & Marklund, S.L. 1988a. Extracellular superoxide dismutase in the vascular system of mammals. *Biochem.J*, 255, (1) 223-228

Karlsson, K. & Marklund, S.L. 1988b. Plasma clearance of human extracellular-superoxide dismutase C in rabbits. *J.Clin.Invest*, 82, (3) 762-766

Kasahara, Y., Iwai, K., Yachie, A., Ohta, K., Konno, A., Seki, H., Miyawaki, T., & Taniguchi, N. 1997. Involvement of reactive oxygen intermediates in spontaneous and CD95(Fas/APO-1)-mediated apoptosis of neutrophils. *Blood*, 89, (5) 1748-1753

Keaney, M., Matthijssens, F., Sharpe, M., Vanfleteren, J., & Gems, D. 2004. Superoxide dismutase mimetics elevate superoxide dismutase activity *in vivo* but do not retard aging in the nematode *Caenorhabditis elegans*. *Free Radic.Biol.Med*., 37, (2) 239-250

Kim, Y.S., Morgan, M.J., Choksi, S., & Liu, Z.G. 2007. TNF-induced activation of the Nox1 NADPH oxidase and its role in the induction of necrotic cell death. *Mol.Cell*, 26, (5) 675-687

Kimura, K.D., Tissenbaum, H.A., Liu, Y., & Ruvkun, G. 1997. daf-2, an insulin receptor-like gene that regulates longevity and diapause in *Caenorhabditis elegans*. *Science*, 277, (5328) 942-946

Kirby, K., Hu, J., Hilliker, A.J., & Phillips, J.P. 2002. RNA interference-mediated silencing of Sod2 in *Drosophila* leads to early adult-onset mortality and elevated endogenous oxidative stress. *Proc.Natl.Acad.Sci.U.S.A*, 99, (25) 16162-16167

Kita, T., Kume, N., Minami, M., Hayashida, K., Murayama, T., Sano, H., Moriwaki, H., Kataoka, H., Nishi, E., Horiuchi, H., Arai, H., & Yokode, M. 2001. Role of oxidized LDL in atherosclerosis. *Ann.N.Y.Acad.Sci.*, 947, 199-205

Kyte, J. & Doolittle, R.F. 1982. A simple method for displaying the hydropathic character of a protein. *J.Mol.Biol*., 157, (1) 105-132

Lambert, A.J. & Brand, M.D. 2004. Superoxide production by NADH:ubiquinone oxidoreductase (complex I) depends on the pH gradient across the mitochondrial inner membrane. *Biochem.J*, 382, (Pt 2) 511-517

Lambeth, J.D. 2004. NOX enzymes and the biology of reactive oxygen. *Nat.Rev.Immunol*., 4, (3) 181-189

Lancaster, V.L., LoBrutto, R., Selvaraj, F.M., & Blankenship, R.E. 2004. A cambialistic superoxide dismutase in the thermophilic photosynthetic bacterium Chloroflexus aurantiacus. *J.Bacteriol*., 186, (11) 3408-3414

Landis, G.N. & Tower, J. 2005. Superoxide dismutase evolution and life span regulation. *Mech.Ageing Dev*., 126, (3) 365-379

Larsen, P.L. 1993. Aging and resistance to oxidative damage in *Caenorhabditis elegans*. *Proc.Natl.Acad.Sci.U.S.A*, 90, (19) 8905-8909

Laurila, J.P., Castellone, M.D., Curcio, A., Laatikainen, L.E., Haaparanta-Solin, M., Gronroos, T.J., Marjamaki, P., Martikainen, S., Santoro, M., & Laukkanen, M.O. 2009. Extracellular superoxide dismutase is a growth regulatory mediator of tissue injury recovery. *Mol.Ther*., 17, (3) 448-454

Lebovitz, R.M., Zhang, H., Vogel, H., Cartwright, J., Jr., Dionne, L., Lu, N., Huang, S., & Matzuk, M.M. 1996. Neurodegeneration, myocardial injury, and perinatal death in mitochondrial superoxide dismutase-deficient mice. *Proc.Natl.Acad.Sci*. U.S.A, 93, (18) 9782-9787

Lee, B.M., Jang, J.J., & Kim, H.S. 1998. Benzopyrene diol-epoxide-I-DNA and oxidative DNA adducts associated with gastric adenocarcinoma. *Cancer Lett.*, 125, (1-2) 61-68

Levanon, D., Lieman-Hurwitz, J., Dafni, N., Wigderson, M., Sherman, L., Bernstein, Y., Laver-Rudich, Z., Danciger, E., Stein, O., & Groner, Y. 1985. Architecture and

anatomy of the chromosomal locus in human chromosome 21 encoding the Cu/Zn superoxide dismutase. *EMBO J.*, 4, (1) 77-84

Levin, E.D., Brady, T.C., Hochrein, E.C., Oury, T.D., Jonsson, L.M., Marklund, S.L., & Crapo, J.D. 1998. Molecular manipulations of extracellular superoxide dismutase: functional importance for learning. *Behav.Genet.*, 28, (5) 381-390

Levin, E.D., Brucato, F.H., & Crapo, J.D. 2000. Molecular overexpression of extracellular superoxide dismutase increases the dependency of learning and memory performance on motivational state. *Behav.Genet.*, 30, (2) 95-100

Levin, E.D., Christopher, N.C., & Crapo, J.D. 2005. Memory decline of aging reduced by extracellular superoxide dismutase overexpression. *Behav.Genet.*, 35, (4) 447-453

Li, Y., Huang, T.T., Carlson, E.J., Melov, S., Ursell, P.C., Olson, J.L., Noble, L.J., Yoshimura, M.P., Berger, C., Chan, P.H., Wallace, D.C., & Epstein, C.J. 1995. Dilated cardiomyopathy and neonatal lethality in mutant mice lacking manganese superoxide dismutase. *Nat.Genet.*, 11, (4) 376-381

Lindberg, M.J., Bystrom, R., Boknas, N., Andersen, P.M., & Oliveberg, M. 2005. Systematically perturbed folding patterns of amyotrophic lateral sclerosis (ALS)-associated SOD1 mutants. *Proc.Natl.Acad.Sci.U.S.A*, 102, (28) 9754-9759

Linnen, C., Tatar, M., & Promislow, D.E. 2001. Cultural artifacts: a comparison of senescence in natural, lab-adapted and artificially selected lines of *Drosophila melanogaster*. *Evol.Ecol.Res.*, 3, 877-888

Liochev, S.I. & Fridovich, I. 1994. The role of $O_2^{\cdot-}$ in the production of HO·: in vitro and in vivo. *Free Radic.Biol.Med.*, 16, (1) 29-33

Liu, X.F., Elashvili, I., Gralla, E.B., Valentine, J.S., Lapinskas, P., & Culotta, V.C. 1992. Yeast lacking superoxide dismutase. Isolation of genetic suppressors. *J.Biol.Chem.*, 267, (26) 18298-18302

Liu, X. & Gorovsky, M.A. 1993. Mapping the 5' and 3' ends of Tetrahymena thermophila mRNAs using RNA ligase mediated amplification of cDNA ends (RLM-RACE). *Nucleic Acids Res.*, 21, (21) 4954-4960

Liu, Y., Brooks, B.R., Taniguchi, N., & Hartmann, H.A. 1998. CuZnSOD and MnSOD immunoreactivity in brain stem motor neurons from amyotrophic lateral sclerosis patients. *Acta Neuropathol.*, 95, (1) 63-70

Lo, Y.Y. & Cruz, T.F. 1995. Involvement of reactive oxygen species in cytokine and growth factor induction of c-fos expression in chondrocytes. *J.Biol.Chem*., 270, (20) 11727-11730

Lo, Y.Y., Wong, J.M., & Cruz, T.F. 1996. Reactive oxygen species mediate cytokine activation of c-Jun NH2-terminal kinases. *J.Biol.Chem*., 271, (26) 15703-15707

Lob, H.E., Marvar, P.J., Guzik, T.J., Sharma, S., McCann, L.A., Weyand, C., Gordon, F.J., & Harrison, D.G. 2010. Induction of hypertension and peripheral inflammation by reduction of extracellular superoxide dismutase in the central nervous system. *Hypertension*, 55, (2) 277-83, 6p

Loenders, B., Van, M.E., Nicolai, S., Buyssens, N., Van, O.N., Jorens, P.G., Willems, J., Herman, A.G., & Slegers, H. 1998. Localization of extracellular superoxide dismutase in rat lung: neutrophils and macrophages as carriers of the enzyme. *Free Radic.Biol.Med.*, 24, (7-8) 1097-1106

Longo, V.D. & Fabrizio, P. 2002. Regulation of longevity and stress resistance: a molecular strategy conserved from yeast to humans? *Cell Mol.Life Sci*., 59, (6) 903-908

Longo, V.D., Gralla, E.B., & Valentine, J.S. 1996. Superoxide dismutase activity is essential for stationary phase survival in *Saccharomyces cerevisiae*. Mitochondrial production of toxic oxygen species in vivo. *J.Biol.Chem.*, 271, (21) 12275-12280

Longo, V.D., Liou, L.L., Valentine, J.S., & Gralla, E.B. 1999. Mitochondrial superoxide decreases yeast survival in stationary phase. *Arch.Biochem.Biophys*., 365, (1) 131-142

Loschen, G., Azzi, A., Richter, C., & Flohq, L. 1974. Superoxide radicals as precursors of mitochondrial hydrogen peroxide. *FEBS Letts.*, 42, (1) 68-72

Lovell, M.A., Gabbita, S.P., & Markesbery, W.R. 1999. Increased DNA oxidation and decreased levels of repair products in Alzheimer's disease ventricular CSF. *J.Neurochem*., 72, (2) 771-776

Lovell, M.A., Robertson, J.D., Teesdale, W.J., Campbell, J.L., & Markesbery, W.R. 1998. Copper, iron and zinc in Alzheimer's disease senile plaques. *J.Neurol.Sci.*, 158, (1) 47-52

Lowry, O., Rosebrough, N., Farr, A., & Randall, R. 1951. Protein measurement with the Folin phenol reagent. *J.Biol.Chem.*, 193, (1) 265-275

Luckinbill, L.S., Arking, R., Clare, M., Cirocco, W., & Buck, S. 1984. Selection for delayed senescence in *Drosophila melanogaster*. *Evolution*, 38, (5) 996-1003

Lui, S.-L., Zhang, X., Zhu, W., Lo, C., Chan, T., Fung, P., & Lai, K. 1999. Demonstration of nitric oxide generation during renal ischemia reperfusion injury using paramagnetic resonance spectroscopy. *Transplant.Proc.*, 31, (1-2) 1020-1021

Luk, E., Yang, M., Jensen, L.T., Bourbonnais, Y., & Culotta, V.C. 2005. Manganese activation of superoxide dismutase 2 in the mitochondria of *Saccharomyces cerevisiae*. *J.Biol.Chem.*, 280, (24) 22715-22720

Magliaro, B.C. & Saldanha, C.J. 2009. Clozapine protects PC-12 cells from death due to oxidative stress induced by hydrogen peroxide via a cell-type specific mechanism involving inhibition of extracellular signal-regulated kinase phosphorylation. *Brain Res.*, In Press, Uncorrected Proof,

Mahadev, K., Zilbering, A., Zhu, L., & Goldstein, B.J. 2001. Insulin-stimulated hydrogen peroxide reversibly inhibits protein-tyrosine phosphatase 1b in vivo and enhances the early insulin action cascade. *J.Biol.Chem.*, 276, (24) 21938-21942

Maragos, W.F., Jakel, R., Chesnut, D., Pocernich, C.B., Butterfield, D.A., St, C.D., & Cass, W.A. 2000. Methamphetamine toxicity is attenuated in mice that overexpress human manganese superoxide dismutase. *Brain Res*., 878, (1-2) 218-222

Marklund, S.L. 1984a. Extracellular superoxide dismutase and other superoxide dismutase isoenzymes in tissues from nine mammalian species. *Biochem.J*., 222, (3) 649-655

Marklund, S.L. 1984b. Extracellular superoxide dismutase in human tissues and human cell lines. *J.Clin.Invest*., 74, (4) 1398-1403

Marklund, S.L. 1992. Regulation by cytokines of extracellular superoxide dismutase and other superoxide dismutase isoenzymes in fibroblasts. *J.Biol.Chem.*, 267, (10) 6696-6701

Marklund, S.L., Holme, E., & Hellner, L. 1982. Superoxide dismutase in extracellular fluids. *Clin.Chim.Acta*, 126, (1) 41-51

Marklund, S.L. 1982. Human copper-containing superoxide dismutase of high molecular weight. *Proc.Natl.Acad.Sci.U.S.A*, 79, (24) 7634-7638

Marnett, L.J. 1999. Lipid peroxidation-DNA damage by malondialdehyde. *Mutat.Res*., 424, (1-2) 83-95

Martinez, V.G., Javadi, C.S., Ngo, E., Ngo, L., Lagow, R.D., & Zhang, B. 2007. Age-related changes in climbing behavior and neural circuit physiology in *Drosophila*. *Dev.Neurobiol*., 67, (6) 778-791

Massie, H.R., Aiello, V.R., & Williams, T.R. 1980. Changes in superoxide dismutase activity and copper during development and ageing in the fruit fly *Drosophila melanogaster*. *Mech.Ageing Dev.*, 12, (3) 279-286

Matters, G.L. & Scandalios, J.G. 1986. Effect of the free radical-generating herbicide paraquat on the expression of the superoxide dismutase (Sod) genes in maize. *Biochim.Biophys.Acta*, 882, (1) 29-38

McCord, J.M. & Fridovich, I. 1969. Superoxide dismutase. An enzymic function for erythrocuprein (hemocuprein). *J.Biol.Chem.*, 244, (22) 6049-6055

McEachern, G., Kassovska-Bratinova, S., Raha, S., Tarnopolsky, M.A., Turnbull, J., Bourgeois, J., & Robinson, B. 2000. Manganese superoxide dismutase levels are elevated in a proportion of amyotrophic lateral sclerosis patient cell lines. *Biochem.Biophys.Res.Commun.*, 273, (1) 359-363

McElroy, J.A., Shafer, M.M., Trentham-Dietz, A., Hampton, J.M., & Newcomb, P.A. 2006. Cadmium exposure and breast cancer risk. *J.Natl.Cancer Inst.*, 98, (12) 869-873

Meier, B., Cross, A.R., Hancock, J.T., Kaup, F.J., & Jones, O.T. 1991. Identification of a superoxide-generating NADPH oxidase system in human fibroblasts. *Biochem.J.*, 275 ( Pt 1), 241-245

Mele, J., Remmen, H.V., Vijg, J., & Richardson, A. 2006. Characterization of transgenic mice that overexpress both copper zinc superoxide dismutase and catalase. *Antioxid.Redox Signal.*, 8, (3-4) 628-638

Melov, S., Ravenscroft, J., Malik, S., Gill, M.S., Walker, D.W., Clayton, P.E., Wallace, D.C., Malfroy, B., Doctrow, S.R., & Lithgow, G.J. 2000. Extension of life-span with superoxide dismutase/catalase mimetics. *Science*, 289, (5484) 1567-1569

Melov, S., Coskun, P., Patel, M., Tuinstra, R., Cottrell, B., Jun, A.S., Zastawny, T.H., Dizdaroglu, M., Goodman, S.I., Huang, T.T., Miziorko, H., Epstein, C.J., & Wallace,

D.C. 1999. Mitochondrial disease in superoxide dismutase 2 mutant mice. *Proc.Natl.Acad.Sci.U.S.A*, 96, (3) 846-851

Melov, S., Schneider, J.A., Day, B.J., Hinerfeld, D., Coskun, P., Mirra, S.S., Crapo, J.D., & Wallace, D.C. 1998. A novel neurological phenotype in mice lacking mitochondrial manganese superoxide dismutase. *Nat.Genet*., 18, (2) 159-163

Mihaly, J., Hogga, I., Gausz, J., Gyurkovics, H., & Karch, F. 1997. In situ dissection of the Fab-7 region of the bithorax complex into a chromatin domain boundary and a Polycomb-response element. *Development*, 124, (9) 1809-1820

Millar, T.M., Phan, V., & Tibbles, L.A. 2007. ROS generation in endothelial hypoxia and reoxygenation stimulates MAP kinase signaling and kinase-dependent neutrophil recruitment. *Free Radic.Biol.Med.*, 42, (8) 1165-1177

Miller, A.F. 2004. Superoxide dismutases: active sites that save, but a protein that kills. *Curr.Opin.Chem.Biol*., 8, (2) 162-168

Miwa, S., St-Pierre, J., Partridge, L., & Brand, M.D. 2003. Superoxide and hydrogen peroxide production by *Drosophila mitochondria*. *Free Radic.Biol.Med.*, 35, (8) 938-948

Mockett, R.J., Bayne, A.C., Sohal, B.H., & Sohal, R.S. 2002. Biochemical assay of superoxide dismutase activity in *Drosophila*. *Methods Enzymol.*, 349, 287-292

Mockett, R.J., Radyuk, S.N., Benes, J.J., Orr, W.C., & Sohal, R.S. 2003. Phenotypic effects of familial amyotrophic lateral sclerosis mutant Sod alleles in transgenic *Drosophila*. *Proc.Natl.Acad.Sci.U.S.A*, 100, (1) 301-306

Mockett, R.J., Orr, W.C., Rahmandar, J.J., Benes, J.J., Radyuk, S.N., Klichko, V.I., & Sohal, R.S. 1999. Overexpression of Mn-containing superoxide dismutase in transgenic *Drosophila melanogaster*. *Arch.Biochem.Biophys.*, 371, (2) 260-269

Moore, S.F. & MacKenzie, A.B. 2009. NADPH oxidase NOX2 mediates rapid cellular oxidation following ATP stimulation of endotoxin-primed macrophages. *J.Immunol*., 183, (5) 3302-3308

Moriarty-Craige, S.E. & Jones, D.P. 2004. Extracellular thiols and thiol/disulfide redox in metabolism. *Annu.Rev.Nutr.*, 24, 481-509

Mugge, A., Brandes, R.P., Boger, R.H., Dwenger, A., Bode-Boger, S., Kienke, S., Frolich, J.C., & Lichtlen, P.R. 1994. Vascular release of superoxide radicals is enhanced in hypercholesterolemic rabbits. *J.Cardiovasc.Pharmacol*., 24, (6) 994-998

Muller, F.L., Lustgarten, M.S., Jang, Y., Richardson, A., & Van Remmen, H. 2007. Trends in oxidative aging theories. *Free Radic.Biol.Med.*, 43, (4) 477-503

Nestler, E. & Hyman, S. 2002, "Regulation of Gene Expression," In Neuropsychopharmacology: The Fifth Generation of Progress, 5 ed. K. Davis et al., eds., American College of Neuropsychopharmacology, pp. 217-228.

Nickla, H., Anderson, J., & Palzkill, T. 1983. Enzymes involved in oxygen detoxification during development of *Drosophila melanogaster*. *Experientia*, 39, (6) 610-612

Nohl, H. & Hegner, D. 1978. Do mitochondria produce oxygen radicals *in vivo*? *Eur.J.Biochem*., 82, (2) 563-567

Nozik-Grayck, E., Suliman, H.B., Majka, S., Albietz, J., Van, R.Z., Roush, K., & Stenmark, K.R. 2008. Lung EC-SOD overexpression attenuates hypoxic induction of Egr-1 and chronic hypoxic pulmonary vascular remodeling. *Am.J.Physiol.Lung Cell Mol.Physiol*., 295, (3) L422-L430

O'Brien, K.M., Dirmeier, R., Engle, M., & Poyton, R.O. 2004. Mitochondrial protein oxidation in yeast mutants lacking manganese-(MnSOD) or copper- and zinc-containing superoxide dismutase (CuZnSOD): evidence that MnSOD and CuZnSOD

have both unique and overlapping functions in protecting mitochondrial proteins from oxidative damage. *J.Biol.Chem.*, 279, (50) 51817-51827

O'hara, Y., Peterson, T.E., & Harrison, D.G. 1993. Hypercholesterolemia increases endothelial superoxide anion production. *J.Clin.Invest*., 91, (6) 2546-2551

Okado-Matsumoto, A. & Fridovich, I. 2002. Amyotrophic lateral sclerosis: A proposed mechanism. *Proc.Natl.Acad.Sci.U.S.A*., 99, (13) 9010-9014

Oliva, M.R., Ripoll, F., Muniz, P., Iradi, A., Trullenque, R., Valls, V., Drehmer, E., & Saez, G.T. 1997. Genetic alterations and oxidative metabolism in sporadic colorectal tumors from a Spanish community. *Mol.Carcinog*., 18, (4) 232-243

Ookawara, T., Kizaki, T., Takayama, E., Imazeki, N., Matsubara, O., Ikeda, Y., Suzuki, K., Li, J.L., Tadakuma, T., Taniguchi, N., & Ohno, H. 2002. Nuclear translocation of extracellular superoxide dismutase. *Biochem.Biophys.Res.Commun.*, 296, (1) 54-61

Orr, W.C., Mockett, R.J., Benes, J.J., & Sohal, R.S. 2003. Effects of overexpression of copper-zinc and manganese superoxide dismutases, catalase, and thioredoxin reductase genes on longevity in *Drosophila melanogaster*. *J.Biol.Chem.*, 278, (29) 26418-26422

Orr, W.C. & Sohal, R.S. 1993. Effects of Cu-Zn superoxide dismutase overexpression of life span and resistance to oxidative stress in transgenic *Drosophila melanogaster*. *Arch.Biochem.Biophys*., 301, (1) 34-40

Orr, W.C. & Sohal, R.S. 1994. Extension of life-span by overexpression of superoxide dismutase and catalase in *Drosophila melanogaster*. *Science*, 263, (5150) 1128-1130

Orr, W.C. & Sohal, R.S. 2003. Does overexpression of Cu,Zn-SOD extend life span in *Drosophila melanogaster*? *Exp.Gerontol*., 38, (3) 227-230

Oshikawa, J., Urao, N., Kim, H.W., Kaplan, N., Razvi, M., McKinney, R., Poole, L.B., Fukai, T., & Ushio-Fukai, M. 2010. Extracellular SOD-derived $H_2O_2$ promotes VEGF signaling in caveolae/lipid rafts and post-ischemic angiogenesis in mice. *PLoS One.*, 5, (4) e10189

Oury, T.D., Day, B.J., & Crapo, J.D. 1996. Extracellular superoxide dismutase in vessels and airways of humans and baboons. *Free Radic.Biol Med*., 20, (7) 957-965

Oury, T.D., Schaefer, L.M., Fattman, C.L., Choi, A., Weck, K.E., & Watkins, S.C. 2002. Depletion of pulmonary EC-SOD after exposure to hyperoxia. *Am.J.Physiol. Lung Cell Mol.Physiol*., 283, (4) L777-L784

Ow, S.Y., Salim, M., Noirel, J., Evans, C., Rehman, I., & Wright, P.C. 2009. iTRAQ underestimation in simple and complex mixtures: "the good, the bad and the ugly". *J.Proteome.Res*., 8, (11) 5347-5355

Packer, M.A., Porteous, C.M., & Murphy, M.P. 1996. Superoxide production by mitochondria in the presence of nitric oxide forms peroxynitrite. *Biochem.Mol.Biol.Int*., 40, (3) 527-534

Palmer, R.M.J., Ferrige, A.G., & Moncada, S. 1987. Nitric oxide release accounts for the biological activity of endothelium-derived relaxing factor. *Nature*, 327, (6122) 524-526

Parker, J.D., Parker, K.M., & Keller, L. 2004a. Molecular phylogenetic evidence for an extracellular Cu Zn superoxide dismutase gene in insects. *Insect.Mol.Biol.*, 13, (6) 587-594

Parker, J.D., Parker, K.M., Sohal, B.H., Sohal, R.S., & Keller, L. 2004b. Decreased expression of Cu-Zn superoxide dismutase 1 in ants with extreme lifespan. *Proc.Natl.Acad.Sci.U.S.A*., 101, (10) 3486-3489

Parker, M.W., Blake, C.C., Barra, D., Bossa, F., Schinina, M.E., Bannister, W.H., & Bannister, J.V. 1987. Structural identity between the iron- and manganese-containing superoxide dismutases. *Protein Eng*., 1, (5) 393-397

Parkes, T.L., Elia, A.J., Dickinson, D., Hilliker, A.J., Phillips, J.P., & Boulianne, G.L. 1998. Extension of *Drosophila lifespa*n by overexpression of human SOD1 in motorneurons. *Nat.Genet*., 19, (2) 171-174

Pastori, G.M. & Trippi, V.S. 1992. Oxidative stress induces high rate of glutathione reductase synthesis in a drought-resistant maize strain. *Plant.Cell Physiol.*, 33, (7) 957-961

Pedersen, K.S., Codrea, M.C., Vermeulen, C.J., Loeschcke, V., & Bendixen, E. 2010. Proteomic characterization of a temperature-sensitive conditional lethal in *Drosophila melanogaster*. *Heredity*, 104, (2) 125-134

Perez-Campo, R., Lopez-Torres, M., Cadenas, S., Rojas, C., & Barja, G. 1998. The rate of free radical production as a determinant of the rate of aging: evidence from the comparative approach. *J.Comp.Physiol.B*., 168, (3) 149-158

Phillips, J.P., Campbell, S.D., Michaud, D., Charbonneau, M., & Hilliker, A.J. 1989. Null mutation of copper/zinc superoxide dismutase in *Drosophila* confers hypersensitivity to paraquat and reduced longevity. *Proc.Natl.Acad.Sci.U.S.A*., 86, (8) 2761-2765

Phillips, J.P., Parkes, T.L., & Hilliker, A.J. 2000. Targeted neuronal gene expression and longevity in *Drosophila*. *Exp.Gerontol*., 35, (9-10) 1157-1164

Phillips, J.P., Tainer, J.A., Getzoff, E.D., Boulianne, G.L., Kirby, K., & Hilliker, A.J. 1995. Subunit-destabilizing mutations in *Drosophila* copper/zinc superoxide dismutase: neuropathology and a model of dimer dysequilibrium. *Proc.Natl.Acad.Sci.U.S.A*., 92, (19) 8574-8578

Pineda, J.A., Aono, M., Sheng, H., Lynch, J., Wellons, J.C., Laskowitz, D.T., Pearlstein, R.D., Bowler, R., Crapo, J., & Warner, D.S. 2001. Extracellular superoxide dismutase overexpression improves behavioral outcome from closed head injury in the mouse. *J.Neurotrauma.*, 18, (6) 625-634

Poon, P.C., Kuo, T.H., Linford, N.J., Roman, G., & Pletcher, S.D. 2010. Carbon dioxide sensing modulates lifespan and physiology in *Drosophila*. *PLoS Biol*., 8, (4) e1000356

Potter, S.Z. & Valentine, J.S. 2003. The perplexing role of copper-zinc superoxide dismutase in amyotrophic lateral sclerosis (Lou Gehrig's disease). *J.Biol.Inorg.Chem*., 8, (4) 373-380

Puscas, I., Baican, M., Coltău, M., Puscas, C., & Domuta, G. 1999. Erythrocyte superoxide dismutase activity in patients with digest cancer: adjuvant diagnosis test. *Caner Lett*., 143, (3) 95-98

Radi, R., Peluffo, G., Alvarez, M.N., Naviliat, M., & Cayota, A. 2001. Unraveling peroxynitrite formation in biological systems. *Free Radic.Biol Med*., 30, (5) 463-488

Rae, T.D., Torres, A.S., Pufahl, R.A., & O'Halloran, T.V. 2001. Mechanism of Cu,Zn-superoxide dismutase activation by the human metallochaperone hCCS. *J.Biol.Chem.*, 276, (7) 5166-5176

Rando, T.A., Crowley, R.S., Carlson, E.J., Epstein, C.J., & Mohapatra, P.K. 1998a. Overexpression of copper/zinc superoxide dismutase: a novel cause of murine muscular dystrophy. *Ann.Neurol*., 44, (3) 381-386

Rauch, M., Schmid, H.A., deVente, J., & Simon, E. 1997. Electrophysiological and immunocytochemical evidence for a cGMP-mediated inhibition of subfornical organ neurons by nitric oxide. *J.Neurosci*., 17, (1) 363-371

Reaume, A., Elliott, J.L., Hoffman, E.K., Kowall, N.W., Ferrante, R.J., Siwek, D.R., Wilcox, H.M., Flood, D.G., Beal, M.F., Brown, R.H., Scott, R.W., & Snider, W.D.

1996. Motor neurons in Cu/Zn superoxide dismutase-deficient mice develop normally but exhibit enhanced cell death after axonal injury. *Nat.Genet.*, 13, (1) 43-47

Reveillaud, I., Niedzwiecki, A., Bensch, K.G., & Fleming, J.E. 1991. Expression of bovine superoxide dismutase in *Drosophila melanogaster* augments resistance of oxidative stress. *Mol.Cell Biol.*, 11, (2) 632-640

Rice, R.H., Lee, Y.M., & Brown, W.D. 1983. Interactions of heme proteins with hydrogen peroxide: protein crosslinking and covalent binding of benzo(α)pyrene and 17 β-estradiol. *Arch.Biochem.Biophys.*, 221, (2) 417-427

Richardson, J., Thomas, K.A., Rubin, B.H., & Richardson, D.C. 1975. Crystal structure of bovine Cu,Zn superoxide dismutase at 3 A resolution: chain tracing and metal ligands. *Proc.Natl.Acad.Sci.U.S.A.*, 72, (4) 1349-1353

Richter, C., Park, J.W., & Ames, B.N. 1988. Normal oxidative damage to mitochondrial and nuclear DNA is extensive. *Proc.Natl.Acad.Sci.U.S.A.*, 85, (17) 6465-6467

Robertson, H.M., Preston, C.R., Phillis, R.W., Johnson-Schlitz, D.M., Benz, W.K., & Engels, W.R. 1988. A stable genomic source of P element transposase in *Drosophila melanogaster. Genetics*, 118, (3) 461-470

Rogina, B. & Helfand, S.L. 2000. Cu, Zn superoxide dismutase deficiency accelerates the time course of an age-related marker in *Drosophila melanogaster. Biogerontology.*, 1, (2) 163-169

Rogina, B., Reenan, R.A., Nilsen, S.P., & Helfand, S.L. 2000. Extended life-span conferred by cotransporter gene mutations in *Drosophila. Science*, 290, (5499) 2137-2140

Rommel, C., Camps, M., & Ji, H. 2007. PI3K[delta] and PI3K[gamma]: partners in crime in inflammation in rheumatoid arthritis and beyond? *Nat.Rev.Immunol.*, 7, (3) 191-201

Rosen, D.R., Siddique, T., Patterson, D., Figlewicz, D.A., Sapp, P., Hentati, A., Donaldson, D., Goto, J., O'Regan, J.P., & Deng, H.X. 1993. Mutations in Cu/Zn superoxide dismutase gene are associated with familial amyotrophic lateral sclerosis. *Nature*, 362, (6415) 59-62

Rotruck, J.T., Pope, A.L., Ganther, H.E., Swanson, A.B., Hafeman, D.G., & Hoekstra, W.G. 1973. Selenium: biochemical role as a component of glutathione peroxidase. *Science*, 179, (73) 588-590

Ruan, H., Tang, X.D., Chen, M.L., Joiner, M.L., Sun, G., Brot, N., Weissbach, H., Heinemann, S.H., Iverson, L., Wu, C.F., & Hoshi, T. 2002. High-quality life extension by the enzyme peptide methionine sulfoxide reductase. *Proc.Natl.Acad.Sci.U.S.A.*, 99, (5) 2748-2753

Sakashita, N., Ando, Y., Marklund, S.L., Nilsson, P., Tashima, K., Yamashita, T., & Takahashi, K. 1998. Familial amyloidotic polyneuropathy type I with extracellular superoxide dismutase mutation: a case report. *Hum.Pathol.*, 29, (10) 1169-1172

Salin, M.L. & Bridges, S.M. 1982. Isolation and characterization of an iron-containing superoxide dismutase from water lily, *Nuphar luteum*. *Plant Physiol.*, 69, (1) 161-165

Salz, H.K., Cline, T.W., & Schedl, P. 1987. Functional changes associated with structural alterations induced by mobilization of a P element inserted in the Sex-lethal gene of *Drosophila. Genetics*, 117, (2) 221-231

Sambrook, J., Fritsch, E.F., & Maniatis, T. 1989. Molecular cloning: a laboratory manual volume 2, 2nd. ed. New York : Cold Spring Harbor.

Sayre, L.M., Zelasko, D.A., Harris, P.L., Perry, G., Salomon, R.G., & Smith, M.A. 1997. 4-Hydroxynonenal-derived advanced lipid peroxidation end products are increased in Alzheimer's disease. *J.Neurochem.*, 68, (5) 2092-2097

Schaefer, B.C. 1995. Revolutions in rapid amplification of cDNA ends: New strategies for polymerase chain reaction cloning of full-length cDNA ends. *Anal.Biochem.*, 227, (2) 255-273

Schoneich, C. 1999. Reactive oxygen species and biological aging: a mechanistic approach. *Exp.Gerontol.*, 34, (1) 19-34

Seehuus, S.C., Norberg, K., Gimsa, U., Krekling, T., & Amdam, G.V. 2006. Reproductive protein protects functionally sterile honey bee workers from oxidative stress. *Proc.Natl.Acad.Sci.U.S.A.*, 103, (4) 962-967

Segal, A.W. 2005. How neutrophils kill microbes. *Annu.Rev.Immunol.*, 23, 197-223

Segal, A.W. 1996. The NADPH oxidase and chronic granulomatous disease. *Mol.Med.Today*, 2, (3) 129-135

Selye, H. 1936. A Syndrome produced by diverse nocuous agents. *Nature*, 138, 32

Sentman, M.L., Granstrom, M., Jakobson, H., Reaume, A., Basu, S., & Marklund, S.L. 2006. Phenotypes of mice lacking extracellular superoxide dismutase and copper- and zinc-containing superoxide dismutase. *J.Biol.Chem.*, 281, (11) 6904-6909

Seto, N.O., Hayashi, S., & Tener, G.M. 1990. Overexpression of Cu-Zn superoxide dismutase in *Drosophila* does not affect life-span. *Proc.Natl.Acad.Sci.U.S.A*, 87, (11) 4270-4274

Shao, D., Segal, A.W., & Dekker, L.V. 2003. Lipid rafts determine efficiency of NADPH oxidase activation in neutrophils. *FEBS Lett.*, 550, (1-3) 101-106

Shigenaga, M.K., Gimeno, C.J., & Ames, B.N. 1989. Urinary 8-hydroxy-2'-deoxyguanosine as a biological marker of in vivo oxidative DNA damage. *Proc.Natl.Acad.Sci.U.S.A.*, 86, (24) 9697-9701

Shimoda-Matsubayashi, S., Matsumine, H., Kobayashi, T., Nakagawa-Hattori, Y., Shimizu, Y., & Mizuno, Y. 1996. Structural dimorphism in the mitochondrial targeting sequence in the human manganese superoxide dismutase gene. A predictive evidence for conformational change to influence mitochondrial transport and a study of allelic association in Parkinson's disease. *Biochem.Biophys.Res.Commun.*, 226, (2) 561-565

Simon, A.F., Liang, D.T., & Krantz, D.E. 2006. Differential decline in behavioral performance of *Drosophila melanogaster* with age. *Mech.Ageing Dev.*, 127, (7) 647-651

Slack, C., Werz, C., Wieser, D., Alic, N., Foley, A., Stocker, H., Withers, D.J., Thornton, J.M., Hafen, E., & Partridge, L. 2010. Regulation of lifespan, metabolism, and stress responses by the *Drosophila* SH2B protein, Lnk. *PLoS Genet.*, 6, (3) e1000881

Smith, A.H., Hopenhayn-Rich, C., Bates, M.N., Goeden, H.M., Hertz-Picciotto, I., Duggan, H.M., Wood, R., Kosnett, M.J., & Smith, M.T. 1992. Cancer risks from arsenic in drinking water. *Environ.Health Perspect.*, 97, 259-267

Sohal, R.S. 1988. Effect of hydrogen peroxide administration on life span, superoxide dismutase, catalase, and glutathione in the adult housefly, *Musca domestica*. *Exp.Gerontol.*, 23, (3) 211-216

Soini, Y., Vakkala, M., Kahlos, K., Paakko, P., & Kinnula, V. 2001. MnSOD expression is less frequent in tumour cells of invasive breast carcinomas than in *in situ* carcinomas or non-neoplastic breast epithelial cells. *J.Pathol.*, 195, (2) 156-162

Spencer, C.C., Howell, C.E., Wright, A.R., & Promislow, D.E. 2003. Testing an 'aging gene' in long-lived *Drosophila* strains: increased longevity depends on sex and genetic background. *Aging Cell*, 2, (2) 123-130

Squadrito, G.L. & Pryor, W.A. 1998. Oxidative chemistry of nitric oxide: the roles of superoxide, peroxynitrite, and carbon dioxide. *Free Radic.Biol.Med*., 25, (4-5) 392-403

Stadtman, E.R. 2004. Role of oxidant species in aging. *Curr.Med.Chem*., 11, (9) 1105-1112

Stone, J.R. & Collins, T. 2002. The role of hydrogen peroxide in endothelial proliferative responses. *Endothelium*, 9, (4) 231-238

Stralin, P., Karlsson, K., Johansson, B.O., & Marklund, S.L. 1995. The interstitium of the human arterial wall contains very large amounts of extracellular superoxide dismutase. *Arterioscler.Thromb.Vasc.Biol*., 15, (11) 2032-2036

Stralin, P. & Marklund, S.L. 2001. Vasoactive factors and growth factors alter vascular smooth muscle cell EC-SOD expression. *Am.J.Physiol Heart Circ.Physiol*., 281, (4) H1621-H1629

Stubauer, G., Giuffre, A., & Sarti, P. 1999. Mechanism of S-nitrosothiol formation and degradation mediated by copper ions. *J.Biol.Chem.*, 274, (40) 28128-28133

Sun, J., Folk, D., Bradley, T.J., & Tower, J. 2002. Induced overexpression of mitochondrial Mn-superoxide dismutase extends the life span of adult *Drosophila melanogaster*. *Genetics*, 161, (2) 661-672

Sun, J., Molitor, J., & Tower, J. 2004. Effects of simultaneous over-expression of Cu/ZnSOD and MnSOD on *Drosophila melanogaster* life span. *Mech.Ageing Dev.*, 125, (5) 341-349

Sun, J. & Tower, J. 1999. FLP recombinase-mediated induction of Cu/Zn-superoxide dismutase transgene expression can extend the life span of adult *Drosophila melanogaster* flies. *Mol.Cell Biol*., 19, (1) 216-228

Sundaresan, M., Yu, Z.X., Ferrans, V.J., Sulciner, D.J., Gutkind, J.S., Irani, K., Goldschmidt-Clermont, P.J., & Finkel, T. 1996. Regulation of reactive-oxygen-species generation in fibroblasts by Rac1. *Biochem.J*, 318 ( Pt 2), 379-382

Sunkar, R., Kapoor, A., & Zhu, J.K. 2006. Posttranscriptional induction of two Cu/Zn superoxide dismutase genes in *Arabidopsis* is mediated by downregulation of miR398 and important for oxidative stress tolerance. *Plant Cell*, 18, (8) 2051-2065

Suzanne, M., Irie, K., Glise, B., Agnes, F., Mori, E., Matsumoto, K., & Noselli, S. 1999. The *Drosophila* p38 MAPK pathway is required during oogenesis for egg asymmetric development. *Genes Dev.*, 13, (11) 1464-1474

Suzuki, N., Inokuma, K., Yasuda, K., & Ishii, N. 1996. Cloning, sequencing and mapping of a manganese superoxide dismutase gene of the nematode *Caenorhabditis elegans. DNA Res*., 3, (3) 171-174

Swerdlow, R.H., Parks, J.K., Miller, S.W., Tuttle, J.B., Trimmer, P.A., Sheehan, J.P., Bennett, J.P., Jr., Davis, R.E., & Parker, W.D., Jr. 1996. Origin and functional consequences of the complex I defect in Parkinson's disease. *Ann.Neurol.*, 40, (4) 663-671

Taghli-Lamallem, O., Akasaka, T., Hogg, G., Nudel, U., Yaffe, D., Chamberlain, J.S., Ocorr, K., & Bodmer, R. 2008. Dystrophin deficiency in *Drosophila* reduces lifespan and causes a dilated cardiomyopathy phenotype. *Aging Cell*, 7, (2) 237-249

Takahashi, M.A. & Asada, K. 1983. Superoxide anion permeability of phospholipid membranes and chloroplast thylakoids. *Arch.Biochem.Biophys.*, 226, (2) 558-566

Takatsu, H., Tasaki, H., Kim, H.N., Ueda, S., Tsutsui, M., Yamashita, K., Toyokawa, T., Morimoto, Y., Nakashima, Y., & Adachi, T. 2001. Overexpression of EC-SOD suppresses endothelial-cell-mediated LDL oxidation. *Biochem.Biophys.Res Commun.*, 285, (1) 84-91

Tammariello, S.P., Quinn, M.T., & Estus, S. 2000. NADPH oxidase contributes directly to oxidative stress and apoptosis in nerve growth factor-deprived sympathetic neurons. *J.Neurosci*., 20, (1) RC53:1-5

Thiels, E., Urban, N.N., Gonzalez-Burgos, G.R., Kanterewicz, B.I., Barrionuevo, G., Chu, C.T., Oury, T.D., & Klann, E. 2000. Impairment of long-term potentiation and associative memory in mice that overexpress extracellular superoxide dismutase. *J.Neurosci.*, 20, (20) 7631-7639

Thisse, B., Stoetzel, C., & Perrin-Schmidt, M. 1987. Genes of the *Drosophila* maternal dorsal group control the specific expression of the zygotic gene twist in presumptive mesodermal cells. *Genes Dev.*, 1, 709-715

Toivonen, J.M., Walker, G.A., Martinez-Diaz, P., Bjedov, I., Driege, Y., Jacobs, H.T., Gems, D., & Partridge, L. 2007. No influence of Indy on lifespan in *Drosophila* after correction for genetic and cytoplasmic background effects. *PLoS Genet*., 3, (6) e95

Toma, D.P., White, K.P., Hirsch, J., & Greenspan, R.J. 2002. Identification of genes involved in *Drosophila melanogaster* geotaxis, a complex behavioural trait. *Nat.Genet*., 31, (4) 349-353

Tomita, M., Okuyama, T., Katsuyama, H., Miura, Y., Nishimura, Y., Hidaka, K., Otsuki, T., & Ishikawa, T. 2007. Mouse model of paraquat-poisoned lungs and its gene expression profile. *Toxicology*, 231, (2-3) 200-209

Trachootham, D., Alexandre, J., & Huang, P. 2009. Targeting cancer cells by ROS-mediated mechanisms: a radical therapeutic approach? *Nat.Rev.Drug Discov*., 8, (7) 579-591

Tumurkhuu, G., Koide, N., Dagvadorj, J., Noman, A.S.M., Khuda, I.I.E., Naiki, Y., Komatsu, T., Yoshida, T., & Yokochi, T. 2010. B1 cells produce nitric oxide in response to a series of toll-like receptor ligands. *Cell.Immunol*., 261, (2) 122-127

Turner, B.J., Atkin, J.D., Farg, M.A., Zang, D.W., Rembach, A., Lopes, E.C., Patch, J.D., Hill, A.F., & Cheema, S.S. 2005. Impaired extracellular secretion of mutant superoxide dismutase 1 associates with neurotoxicity in familial amyotrophic lateral sclerosis. *J.Neurosci*., 25, (1) 108-117

Valko, M., Leibfritz, D., Moncol, J., Cronin, M.T., Mazur, M., & Telser, J. 2007. Free radicals and antioxidants in normal physiological functions and human disease. *Int.J.Biochem.Cell Biol*., 39, (1) 44-84

Valko, M., Morris, H., Mazur, M., Rapta, P., & Bilton, R.F. 2001. Oxygen free radical generating mechanisms in the colon: do the semiquinones of vitamin K play a role in the aetiology of colon cancer? *Biochim.Biophys.Acta*, 1527, (3) 161-166

Valko, M., Rhodes, C.J., Moncol, J., Izakovic, M., & Mazur, M. 2006. Free radicals, metals and antioxidants in oxidative stress-induced cancer. *Chem.Biol.Interact.*, 160, (1) 1-40

Van Raamsdonk, J.M. & Hekimi, S. 2009. Deletion of the mitochondrial superoxide dismutase sod-2 extends lifespan in *Caenorhabditis elegans*. *PLoS Genet*., 5, (2) e1000361

Van, R.H., Ikeno, Y., Hamilton, M., Pahlavani, M., Wolf, N., Thorpe, S.R., Alderson, N.L., Baynes, J.W., Epstein, C.J., Huang, T.T., Nelson, J., Strong, R., & Richardson, A. 2003. Life-long reduction in MnSOD activity results in increased DNA damage and higher incidence of cancer but does not accelerate aging. *Physiol.Genomics*, 16, (1) 29-37

Veal, E.A., Day, A.M., & Morgan, B.A. 2007. Hydrogen peroxide sensing and signaling. *Mol.Cell*, 26, (1) 1-14

Venkataraman, S., Jiang, X., Weydert, C., Zhang, Y., Zhang, H.J., Goswami, P.C., Ritchie, J.M., Oberley, L.W., & Buettner, G.R. 2005. Manganese superoxide dismutase overexpression inhibits the growth of androgen-independent prostate cancer cells. *Oncogene*, 24, (1) 77-89

Viner, R. 1999. Putting stress in life: Hans Selye and the making of stress theory. *Soc.Stud.Sci.*, 29, (3) 391-410

Vorbach, C., Harrison, R., & Capecchi, M.R. 2003. Xanthine oxidoreductase is central to the evolution and function of the innate immune system. *Trends Immunol.*, 24, (9) 512-517

Vulimiri, S.V., Wu, X., Baer-Dubowska, W., de, A.M., Detry, M., Spitz, M.R., & DiGiovanni, J. 2000. Analysis of aromatic DNA adducts and 7,8-dihydro-8-oxo- 2'-deoxyguanosine in lymphocyte DNA from a case-control study of lung cancer involving minority populations. *Mol.Carcinog.*, 27, (1) 34-46

Walker, D.W., Hajek, P., Muffat, J., Knoepfle, D., Cornelison, S., Attardi, G., & Benzer, S. 2006. Hypersensitivity to oxygen and shortened lifespan in a *Drosophila* mitochondrial complex II mutant. *Proc.Natl.Acad.Sci.U.S.A.*, 103, (44) 16382-16387

Wallin, I.E. 1923. The mitochondria problem. *Am.Nat.*, 57, (650) 255-261

Wan, X.S., Devalaraja, M.N., & St Clair, D.K. 1994. Molecular structure and organization of the human manganese superoxide dismutase gene. *DNA Cell Biol.*, 13, (11) 1127-1136

Wang, M., Dhingra, K., Hittelman, W.N., Liehr, J.G., de, A.M., & Li, D. 1996. Lipid peroxidation-induced putative malondialdehyde-DNA adducts in human breast tissues. *Cancer Epidemiol.Biomarkers Prev.*, 5, (9) 705-710

Weisiger, R.A. & Fridovich, I. 1973. Mitochondrial superoxide dismutase. Site of synthesis and intramitochondrial localization. *J.Biol.Chem.*, 248, (13) 4793-4796

Wheeler, M.A., Smith, S.D., Garcia-Cardena, G., Nathan, C.F., Weiss, R.M., & Sessa, W.C. 1997. Bacterial infection induces nitric oxide synthase in human neutrophils. *J.Clin.Invest.*, 99, (1) 110-116

White, C.R., Brock, T.A., Chang, L.Y., Crapo, J., Briscoe, P., Ku, D., Bradley, W.A., Gianturco, S.H., Gore, J., Freeman, B.A., & . 1994. Superoxide and peroxynitrite in atherosclerosis. *Proc.Natl.Acad.Sci.U.S.A*., 91, (3) 1044-1048

Wiener, H.W., Perry, R.T., Chen, Z., Harrell, L.E., & Go, R.C. 2007. A polymorphism in SOD2 is associated with development of Alzheimer's disease. *Genes Brain Behav.*, 6, (8) 770-775

Wolsky, A. 1938. The effect of carbon monoxide on the oxygen consumption of *Drosophila melanogaster* pupae. *J.Exp.Biol.*, 15, (2) 225-234

Woodruff, R.C., Phillips, J.P., & Hilliker, A.J. 2004. Increased spontaneous DNA damage in Cu/Zn superoxide dismutase (SOD1) deficient *Drosophila*. *Genome*, 47, (6) 1029-1035

Xun, Z., Sowell, R.A., Kaufman, T.C., & Clemmer, D.E. 2008. Quantitative proteomics of a presymptomatic A53T alpha-synuclein *Drosophila* model of Parkinson disease. *Mol.Cell Proteomics*., 7, (7) 1191-1203

Yoo, H.Y., Chang, M.S., & Rho, H.M. 1999a. Heavy metal-mediated activation of the rat Cu/Zn superoxide dismutase gene via a metal-responsive element. *Mol.Gen.Genet*., 262, (2) 310-313

Yoo, H.Y., Chang, M.S., & Rho, H.M. 1999b. The activation of the rat copper/zinc superoxide dismutase gene by hydrogen peroxide through the hydrogen peroxide-responsive element and by paraquat and heat shock through the same heat shock element. *J.Biol.Chem.*, 274, (34) 23887-23892

Youn, H.D., Kim, E.J., Roe, J.H., Hah, Y.C., & Kang, S.O. 1996. A novel nickel-containing superoxide dismutase from *Streptomyces spp*. *Biochem.J.*, 318 ( Pt 3), 889-896

Zelko, I.N., Mariani, T.J., & Folz, R.J. 2002. Superoxide dismutase multigene family: a comparison of the CuZn-SOD (SOD1), Mn-SOD (SOD2), and EC-SOD (SOD3) gene structures, evolution, and expression. *Free Radic.Biol.Med.*, 33, (3) 337-349

Zhao, Y., Xue, Y., Oberley, T.D., Kiningham, K.K., Lin, S.M., Yen, H.C., Majima, H., Hines, J., & St Clair, D. 2001. Overexpression of manganese superoxide dismutase suppresses tumor formation by modulation of activator protein-1 signalling in a multistage skin carcinogenesis model. *Cancer Res.*, 61, (16) 6082-6088

Zweier, J.L., Wang, P., & Kuppusamy, P. 1995. Direct Measurement of nitric oxide generation in the ischemic heart using electron paramagnetic resonance spectroscopy. *J.Biol.Chem.*, 270, (1) 304-307